Multi-scale modelling of fracture

Pierre KERFRIDEN, Lars BEEX, Olivier GOURY,
Ahmad AKBARI, Jack HALE, Paul Hauseux, Hussein RAPPEL
Stéphane P.A. BORDAS

http://legato-team.eu

CARDIFF UNIVERSITY PRIFYSGOL CAERDYDD
THE UNIVERSITY OF WESTERN AUSTRALIA
erc
uni.lu UNIVERSITÉ DU LUXEMBOURG

Background on the Legato team

USA-Switzerland-Scotland-Wales-Luxembourg

http://legato-team.eu

Acknowledgements

EPSRC
Pioneering research and skills

The Royal Academy of Engineering

THE ROYAL SOCIETY

USIAS
University of Strasbourg Institute for Advanced Study

Inria
INVENTEURS DU MONDE NUMÉRIQUE

hpc CYMRU WALES

SEVENTH FRAMEWORK PROGRAMME

The Leverhulme Trust

European Research Council erc IDEAS

Permanent Researchers


Jack S. Hale


Lars Beex

Legato-team
Luxembourg

Post-docs


Alexandre Bilger

Comp. Sci.


Elisa Schenone

Maths


Georgios Bourantas

Physicist


Huu Phuoc BUI


Kostyantyn Malukhin


Satyendra K. Tomar

Maths

PhD Students


Hussein Rappel

Administrative assistant


Marie Leblanc


Changkye Lee


Chi Hoang

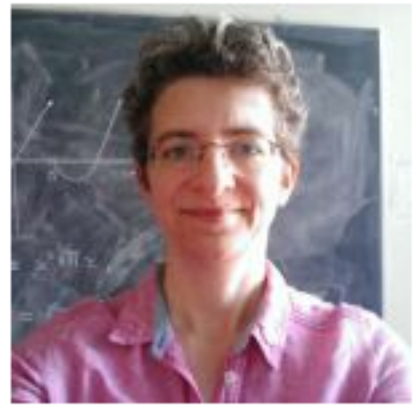
Claire Heaney


Danas Sutula


Daniel Alves Paladim


Hung Nguyen Xuan

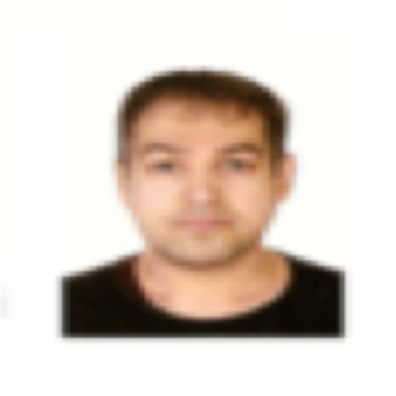
Kevin Bronik


Mohammed Al-Saad


Pedro Bonilla


Peng Yu


Waled Alnaas


Xiaohan Du

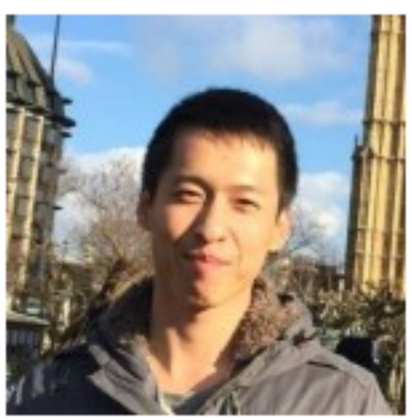
Xiude Lin


Xuan Peng

Legato-team
Cardiff


Table of the Finite Elements
O'NEILL

Chicago, Illinois

IMAM
Institute of Mechanics
& Advanced Materials

Advisor: Brian Moran
Now vice-provost for
faculty affairs at KAUST

1997-2003

MSc Geotechnical Engineering

PhD. Damage Tolerance of Aerospace Structures (XFEM)
and Biofilm Growth

I MAM

Institute of Mechanics
& Advanced Materials

Post-doc 2003-2006 -

Meshless/XFEM Geomechanics

ÉCOLE POLYTECHNIQUE
FÉDÉRALE DE LAUSANNE

IMAM
Institute of Mechanics & Advanced Materials

Lecturer in civil engineering

UNIVERSITY of GLASGOW


4. Glasgow
5. Cardiff
6. Luxembourg
1. Paris
2. Chicago
3. Lausanne
SPAIN
ITALY
TURKEY
ALGERIA
LIBYA
EGYPT
IRAN
IRAQ
SAUDI ARABIA
MALI
NIGER
CHAD
SUDAN
BRAZIL
PERU
COLOMBIA

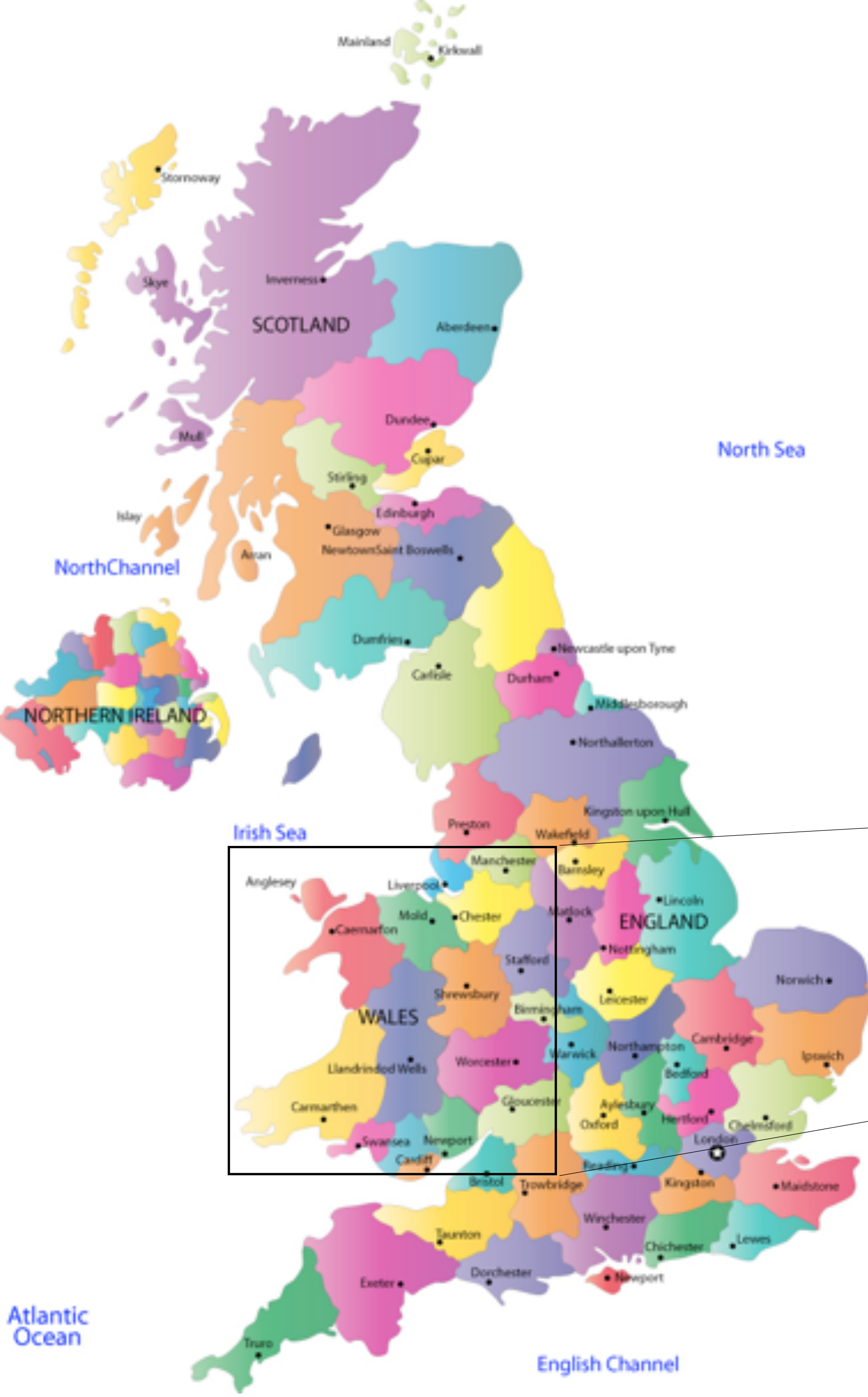
Mainland
Kirkwall
Stornoway
Skye
Inverness
SCOTLAND
Aberdeen
Dundee
Cupar
Mull
Stirling
Edinburgh
Islay
Glasgow
NewtownSaint Boswells
Arran
North Sea
NorthChannel
Dumfries
Carlisle
Newcastle upon Tyne
Durham
Middlesborough
Northallerton
NORTHERN IRELAND
Irish Sea
Preston
Kingston upon Hull
Wakefield
Manchester
Barnsley
Anglesey
Liverpool
Mold
Chester
Caernarfon
Matlock
Lincoln
ENGLAND
Nottingham
Stafford
Norwich
Shrewsbury
Birmingham
Leicester
WALES
Cambridge
Ipswich
Llandrindod Wells
Worcester
Warwick
Northampton
Bedford
Carmarthen
Gloucester
Aylesbury
Hertford
Chelmsford
Oxford
Swansea
Newport
Cardiff
London
Bristol
Trowbridge
Reading
Kingston
Maidstone
Taunton
Winchester
Lewes
Chichester
Exeter
Dorchester
Newport
Truro
Atlantic Ocean
English Channel


Liverpool Bay
Anglesey (Ynys Môn)
Flint
Bangor
Irish Sea
Snowdon
1085
Dee
Wrexham
Barmouth
Cambrian Mts
Welshpool
Cardigan Bay
Severn
England
Wales
Cardigan
Teifi
St George's Channel
Tywi
Usk
Brecon Beacons
Swansea
Newport
Cardiff
Bristol Channel


Mynyddislwyn
Porth
Pontypridd
Caerphilly
Newport
Groeswen
Rudry
Bassaleg
Efail Isaf
Coedkernew
Thornhill
Miskin
St. Mellons
Pontyclun
Peterstone Wentlooge
Blackweir
Pendoylan
CARDIFF
Bonvilston
Penarth
Dinas Powys
BRISTOL CHANNEL
Llanbethery
Barry
Docks
Swanbridge
West Aberthaw
Cardiff Airport (CWL)
Weston Super Mare
©World Guides

CARDIFF
BLUES


AFAT

"Coat of arms of Luxembourg" by en:User:Ssolbergj and authors of source files - Texte coordonné du 16 septembre 1993 de la loi modifiée du 23 juin 1972 sur les emblèmes nationaux.File:Coat of Arms of Sweden.svgFile:Coat of arms of Luxembourg.pngFile:Escudo de la Segunda República Española.svg. Licensed under GFDL via Commons - https://commons.wikimedia.org/wiki/File:Coat_of_arms_of_Luxembourg.svg#/media/File:Coat_of_arms_of_Luxembourg.svg

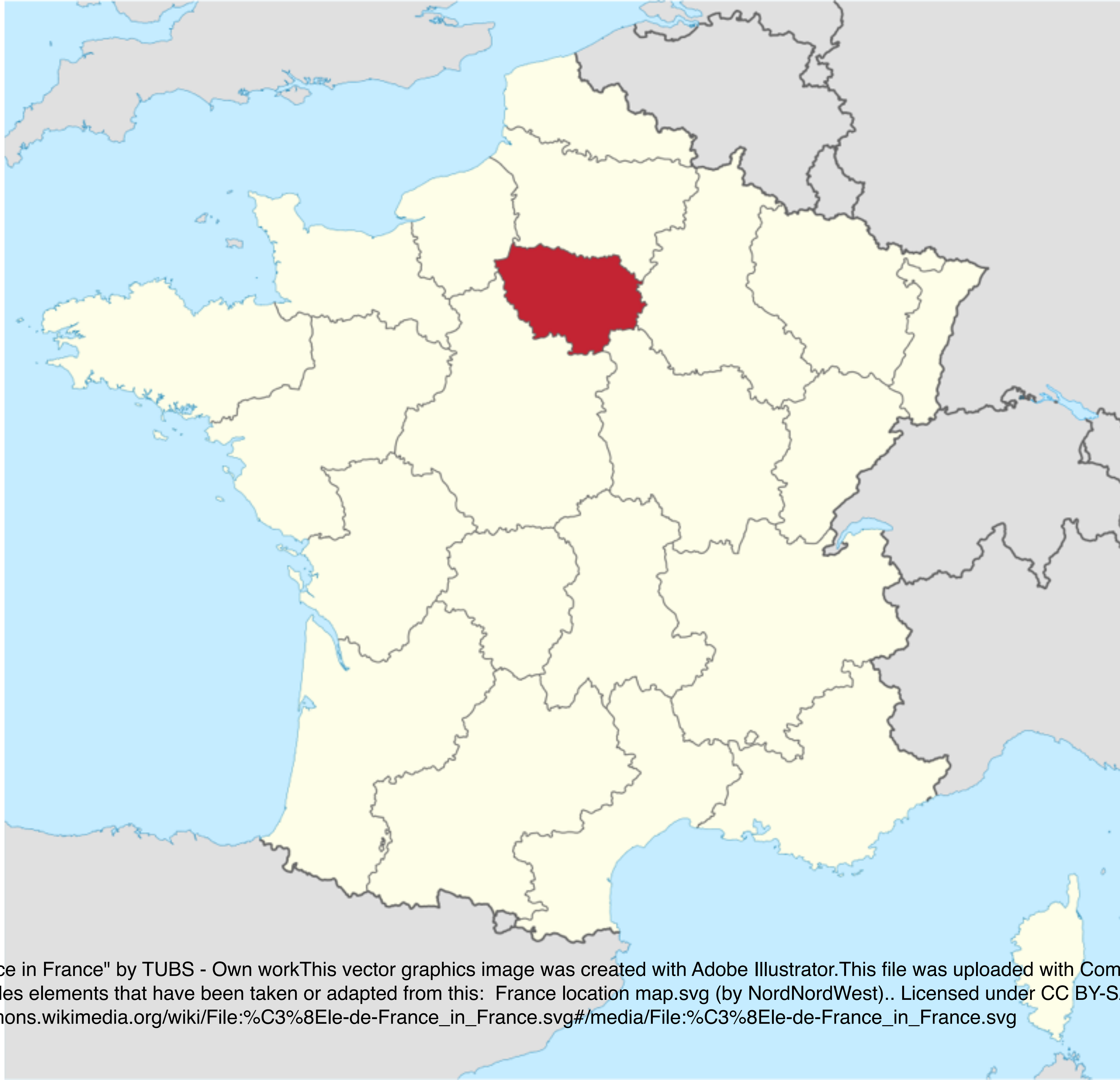

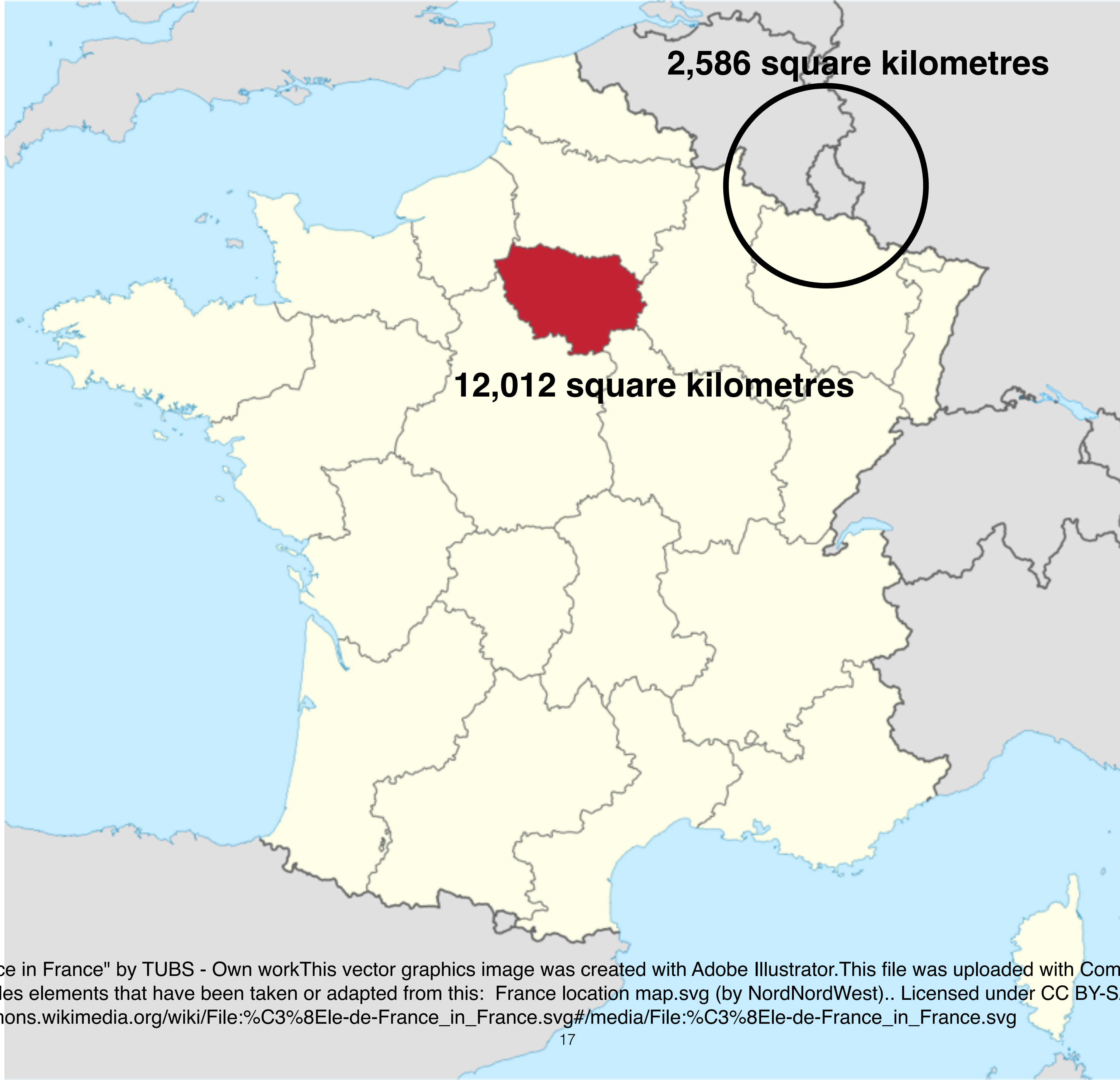

"Île-de-France in France" by TUBS - Own workThis vector graphics image was created with Adobe Illustrator.This file was uploaded with Commonist.This vector image includes elements that have been taken or adapted from this: France location map.svg (by NordNordWest).. Licensed under CC BY-SA 3.0 via Commons https://commons.wikimedia.org/wiki/File:%C3%8Ele-de-France_in_France.svg#/media/File:%C3%8Ele-de-France_in_France.svg

Competences and research focus

Mechanics of interfaces

MECHANICS OF INTERFACES

COMPETENCES

DISCRETISATION
discrete and continuum approaches

STATISTICAL INVERSE PROBLEMS AND UNCERTAINTY QUANTIFICATION

MULTI-SCALE FRACTURE
aerospace composites, polycrystalline materials

COUPLED PROBLEMS
biofilms, liquid crystals, fluid-structure, batteries

QUALITY & ERROR CONTROL
optimise computational time given an accuracy level

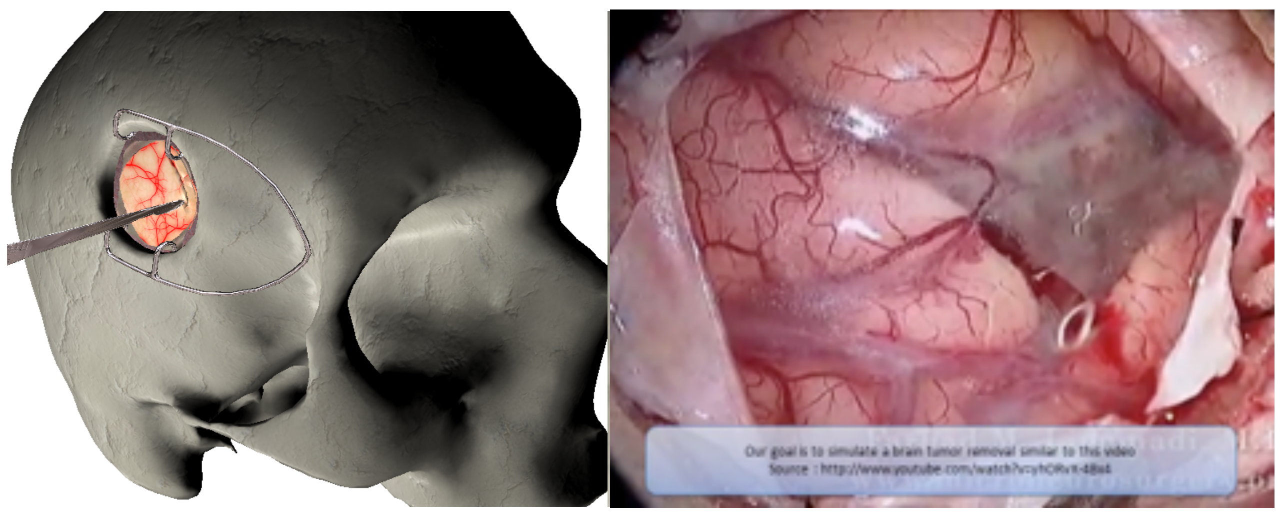

Real-time simulation of cutting during brain surgery, Courtecuisse et al. 2014, Medical Image Analysis

INTERACTIVITY
Reduce computational costs by several orders of magnitude

APPLICATIONS

PERSONALISED MEDICINE

- *Computer-aided surgery*
- *Computer-aided diagnostics*

ENGINEERING

- *Durability & Sustainability*
- *Energy*
- *Aerospace*

Discontinuities

1

Large scale

Small scale

Discontinuities

1

Large scale

Small scale

Discontinuities

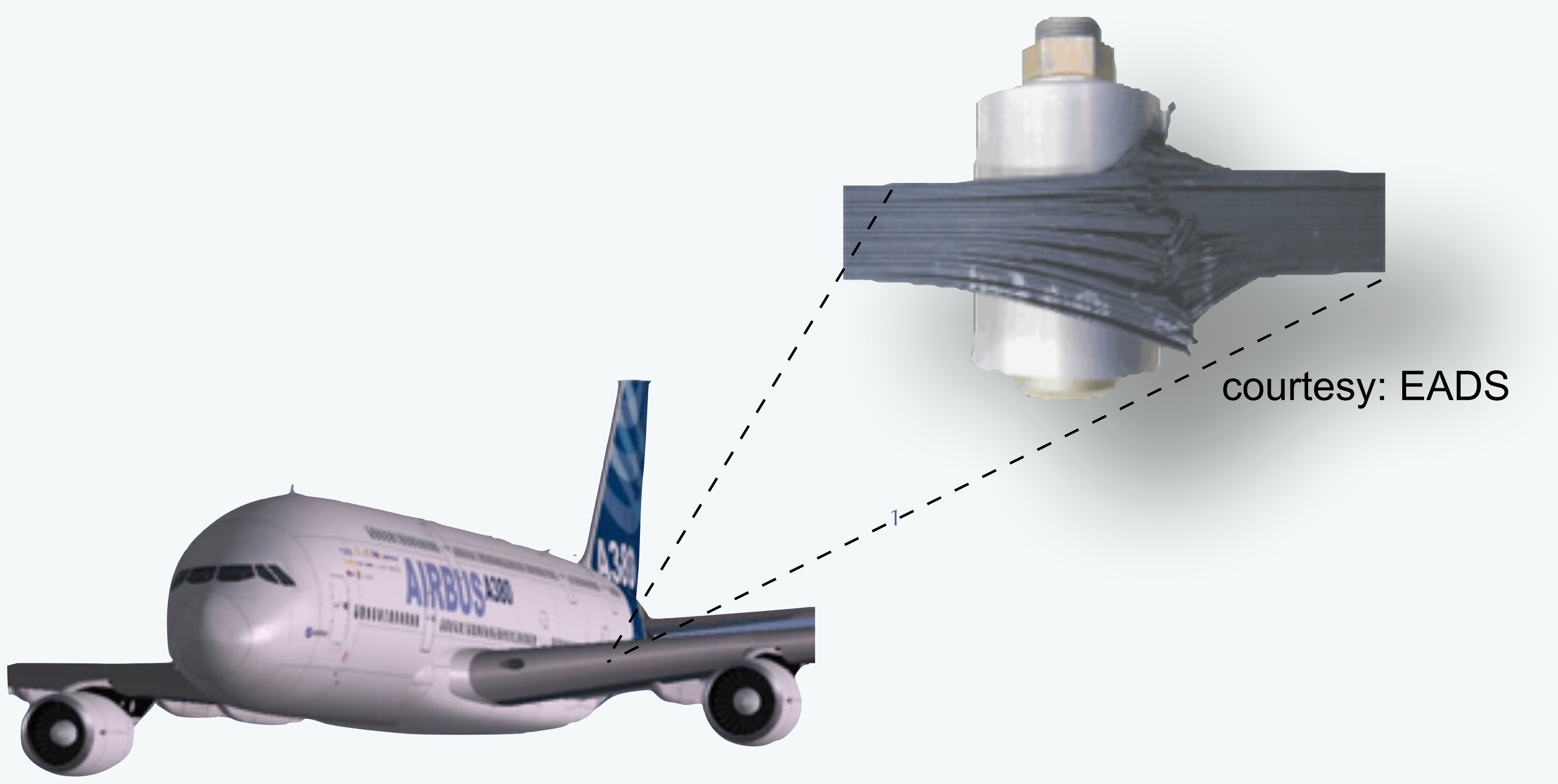

Large scale

Small scale

Discontinuities

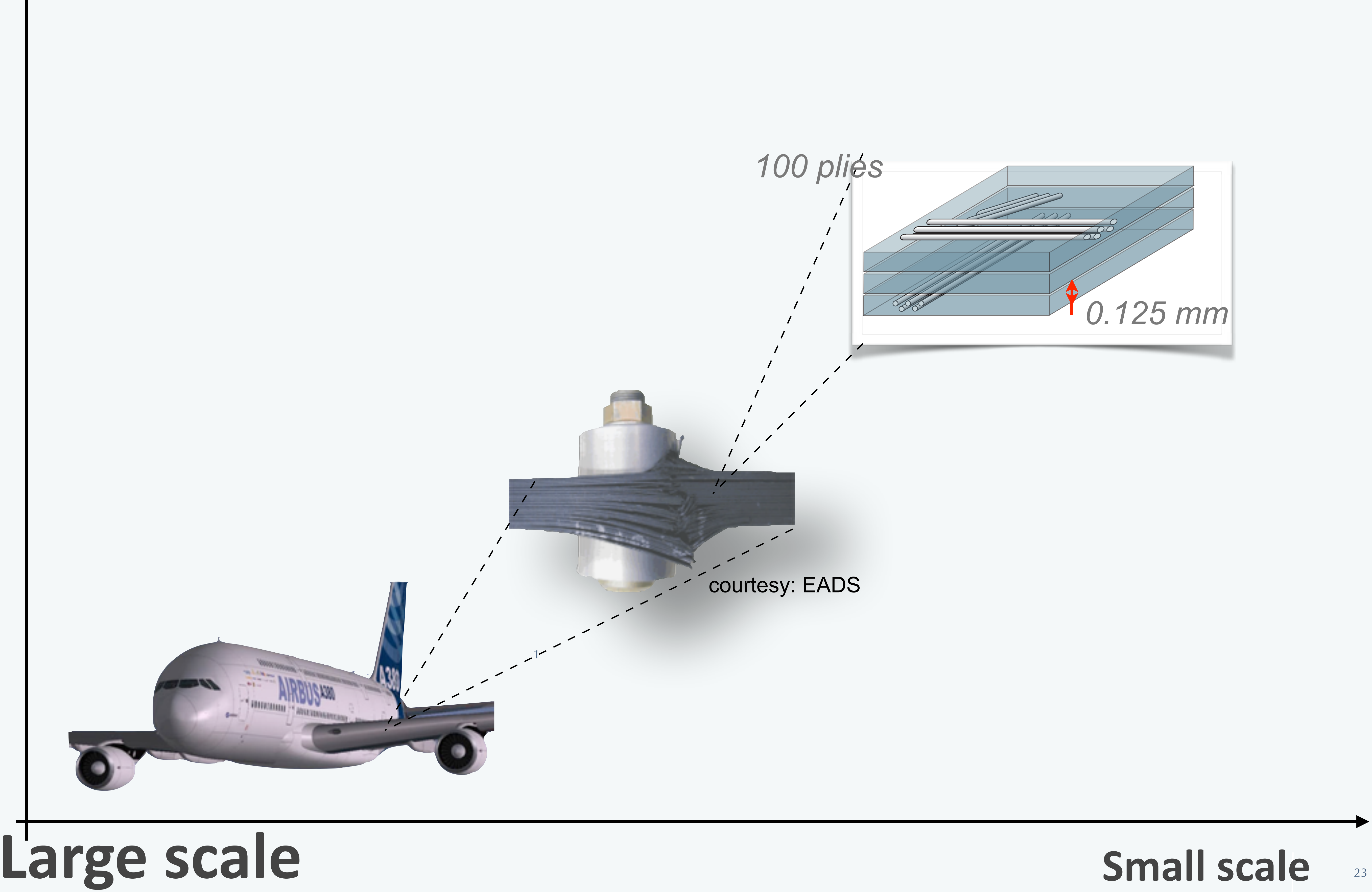

Discontinuities

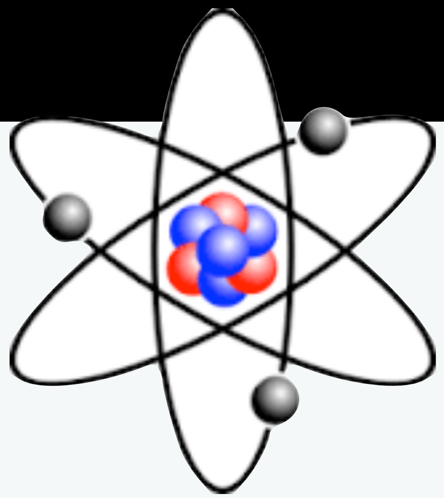

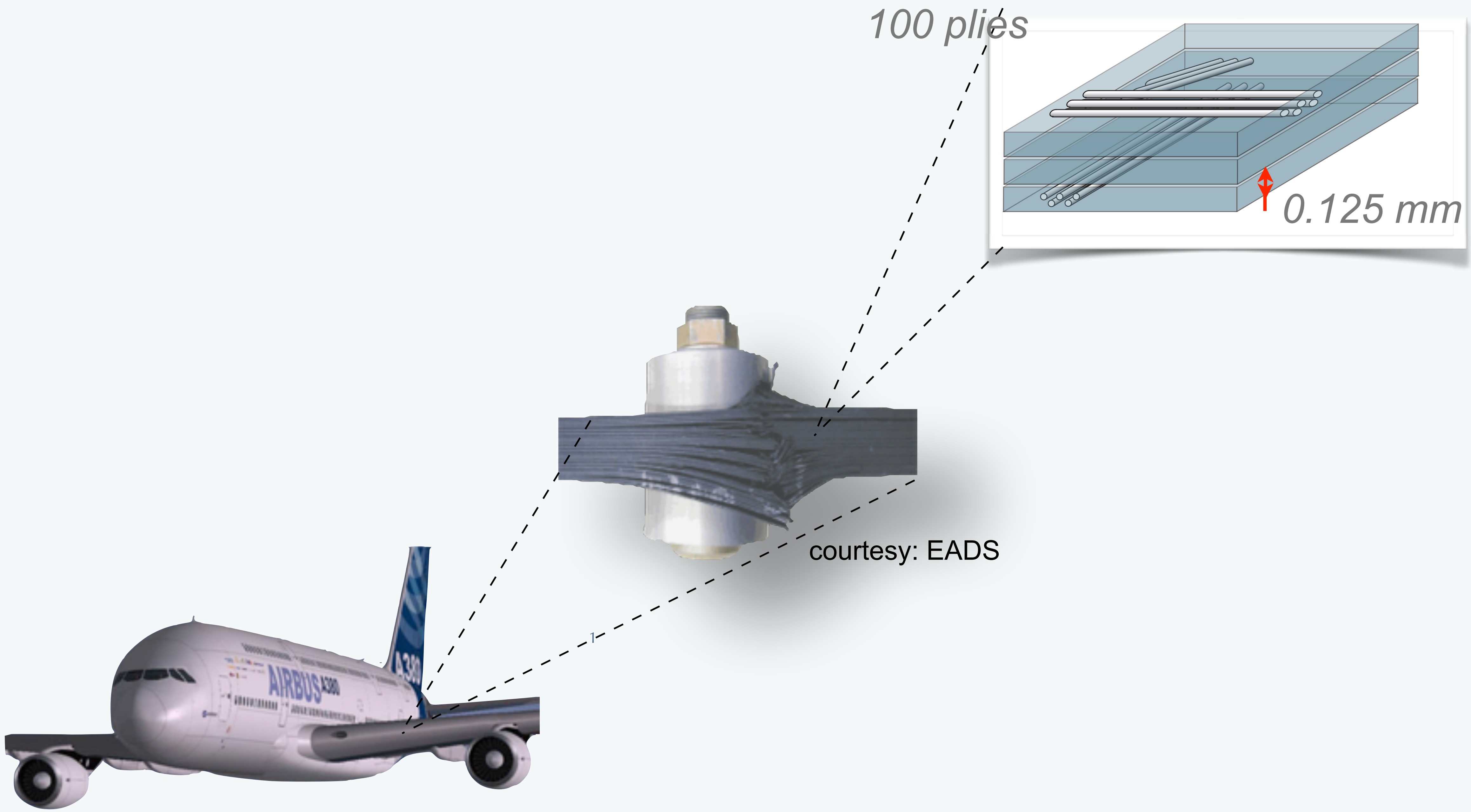

Large scale

Small scale

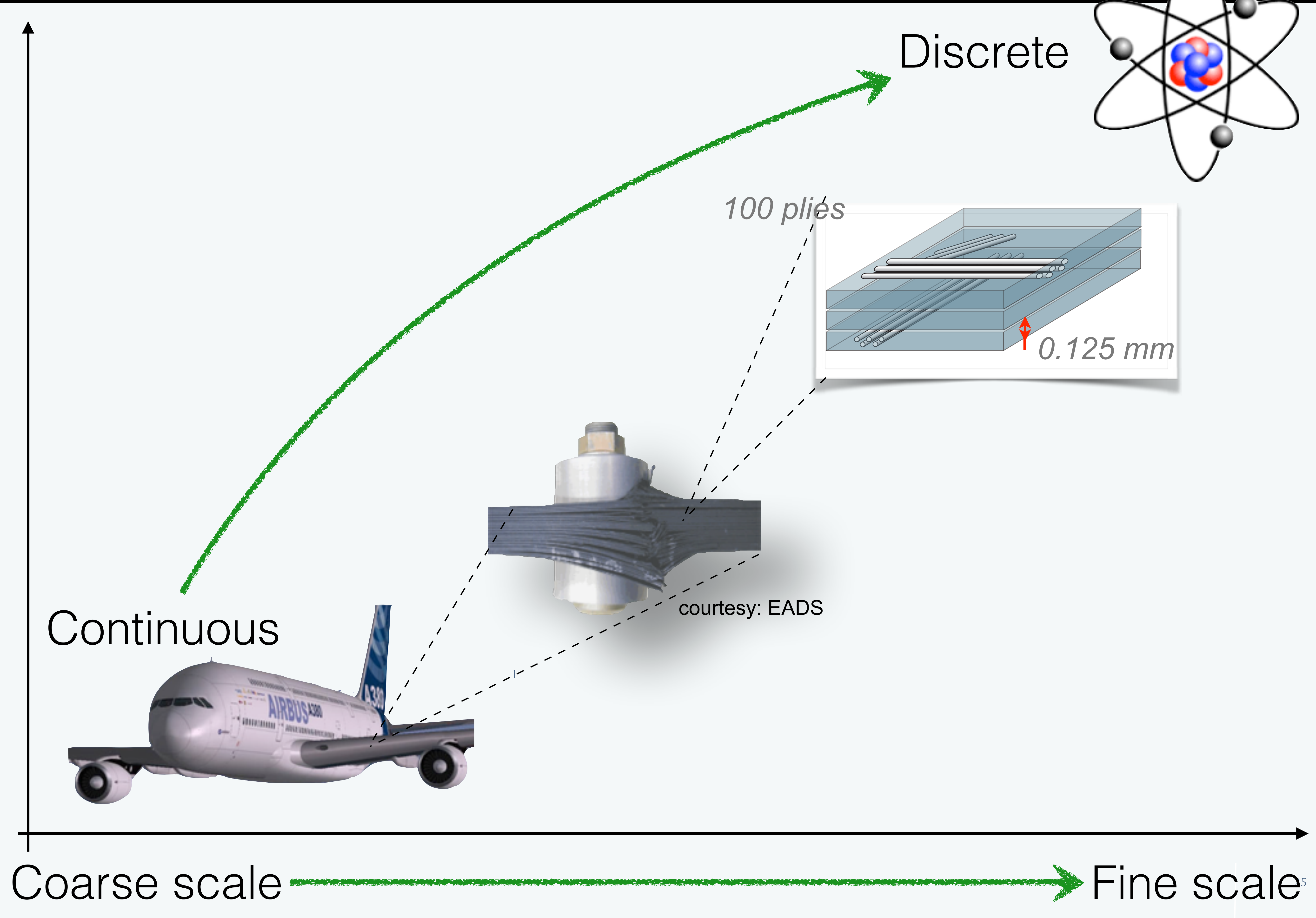
Discrete
100 plies
0.125 mm
courtesy: EADS
Continuous
Coarse scale
Fine scale

FEM

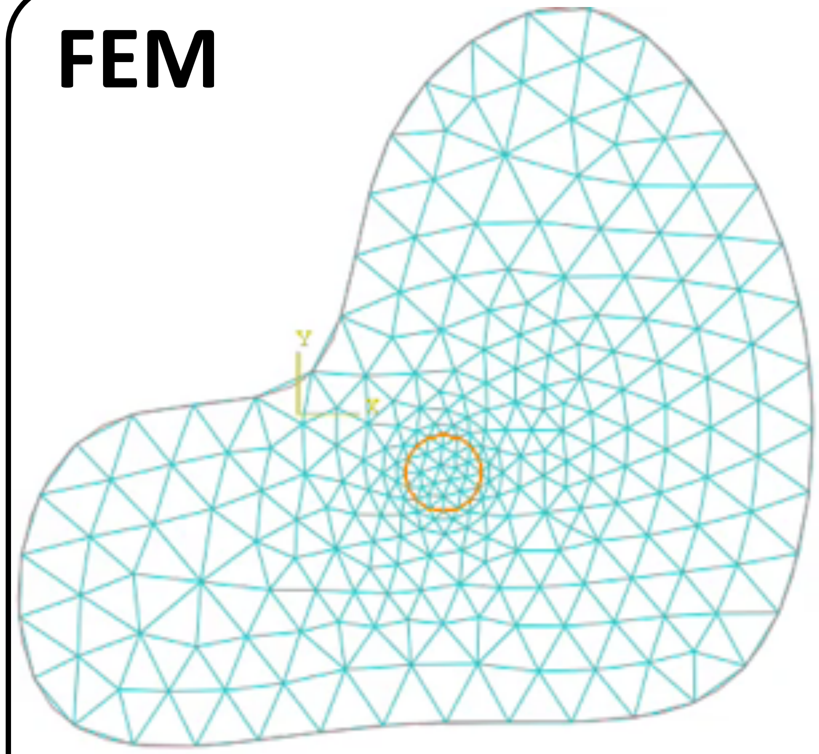

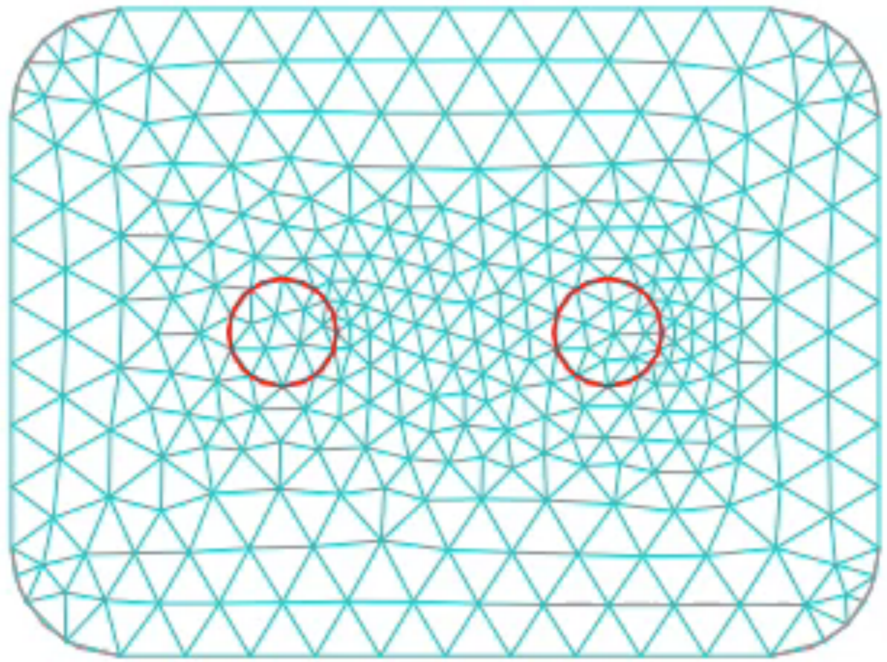

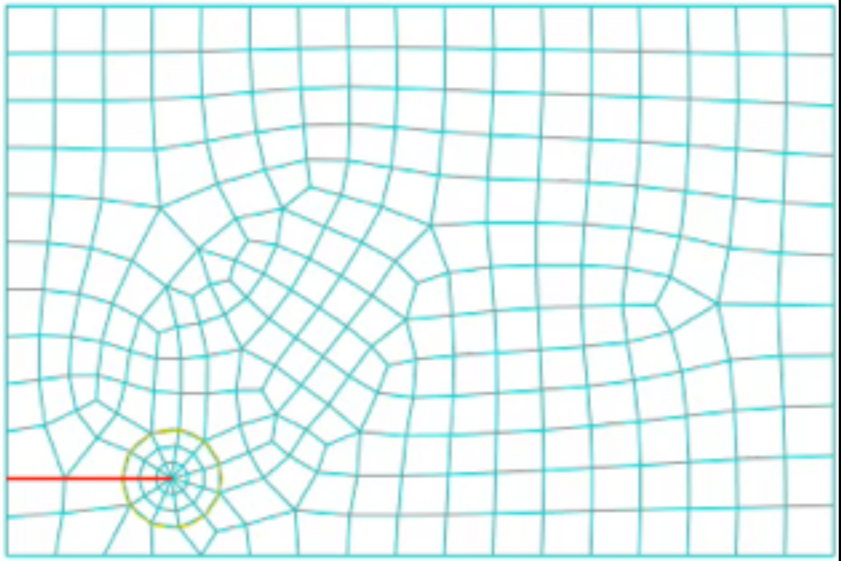

XFEM

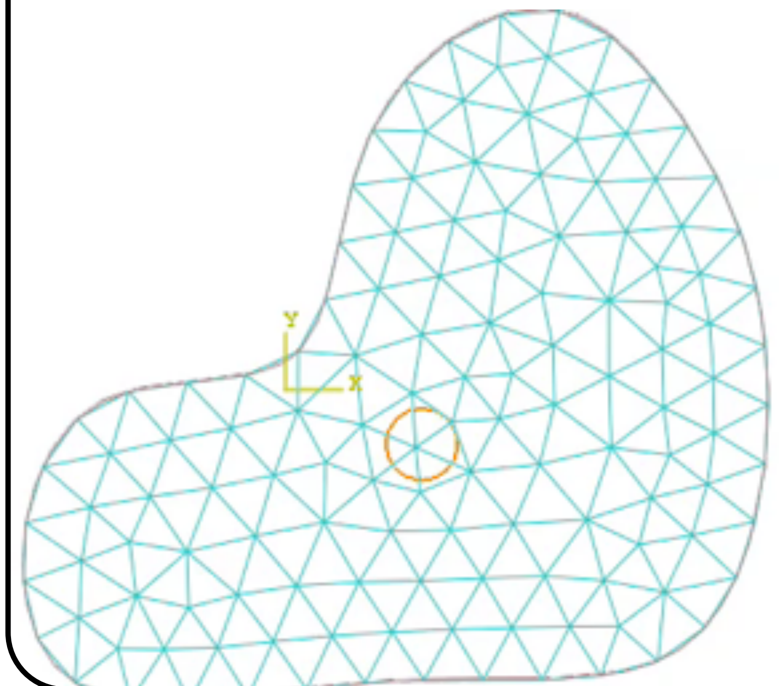

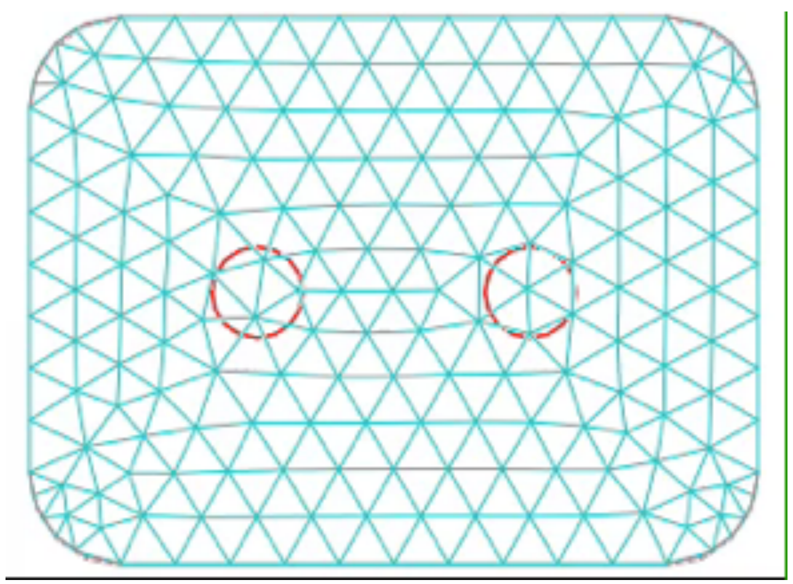

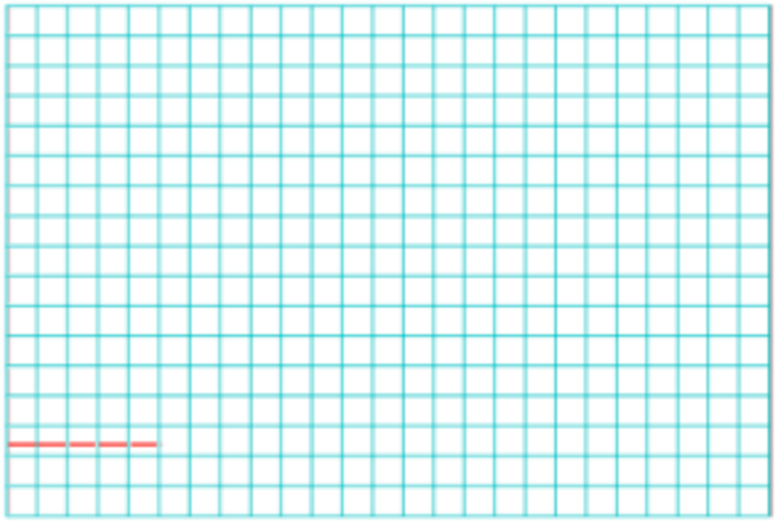

Interfaces in practical engineering simulations

PHASES

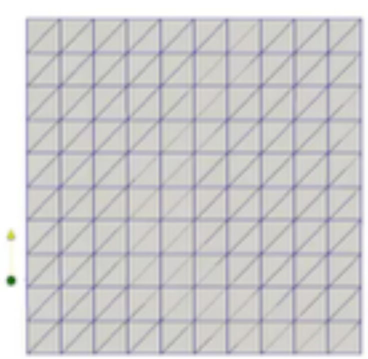

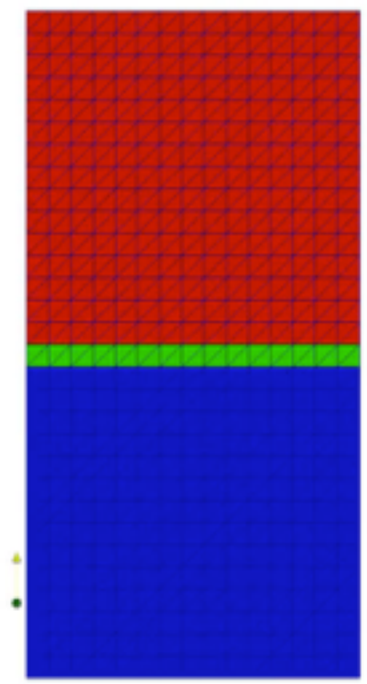

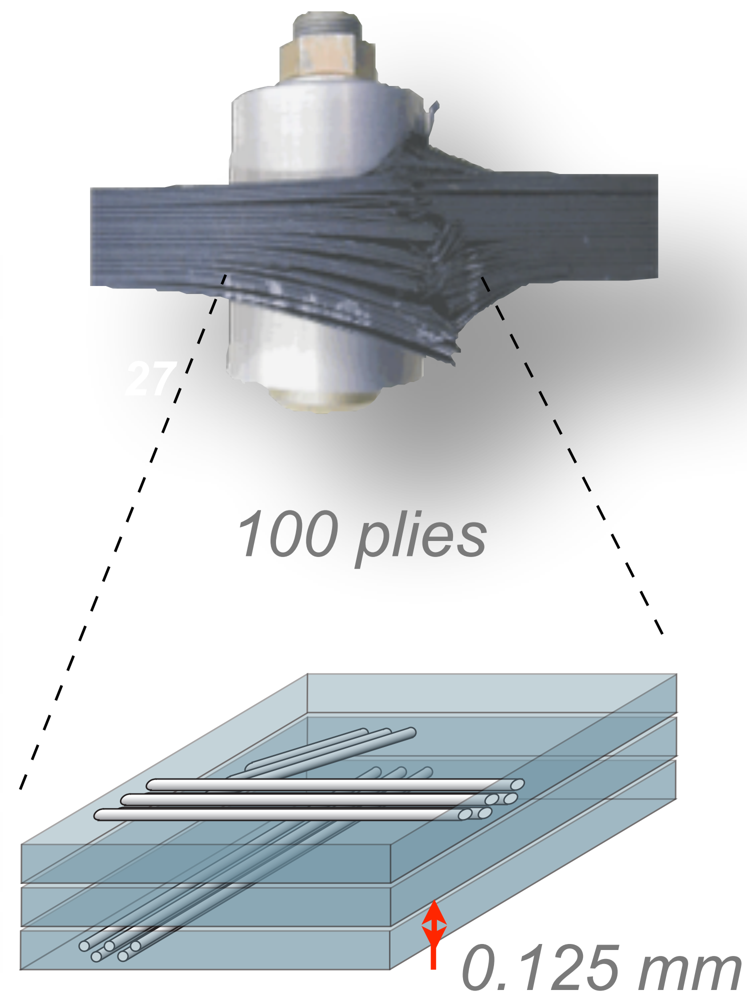

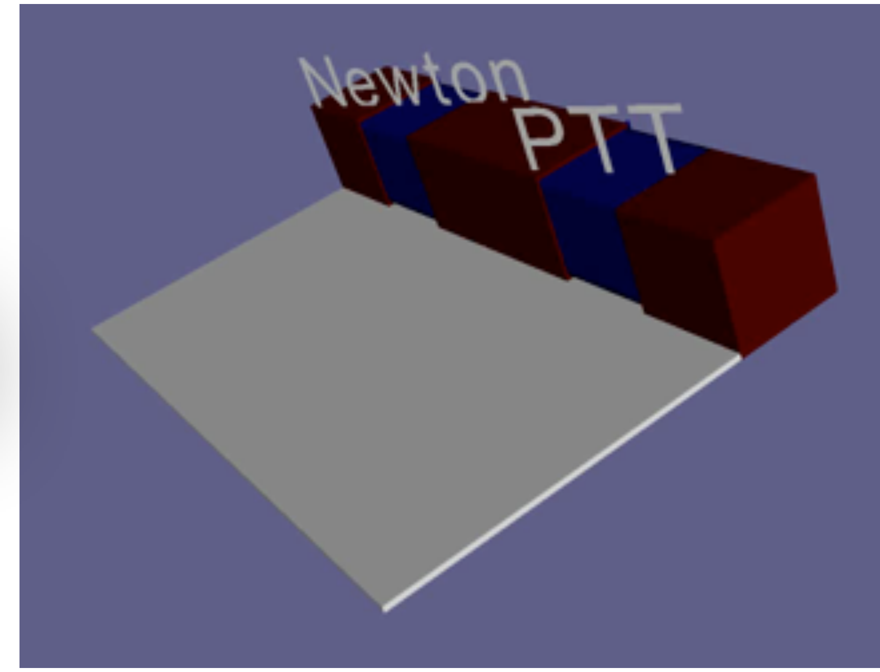

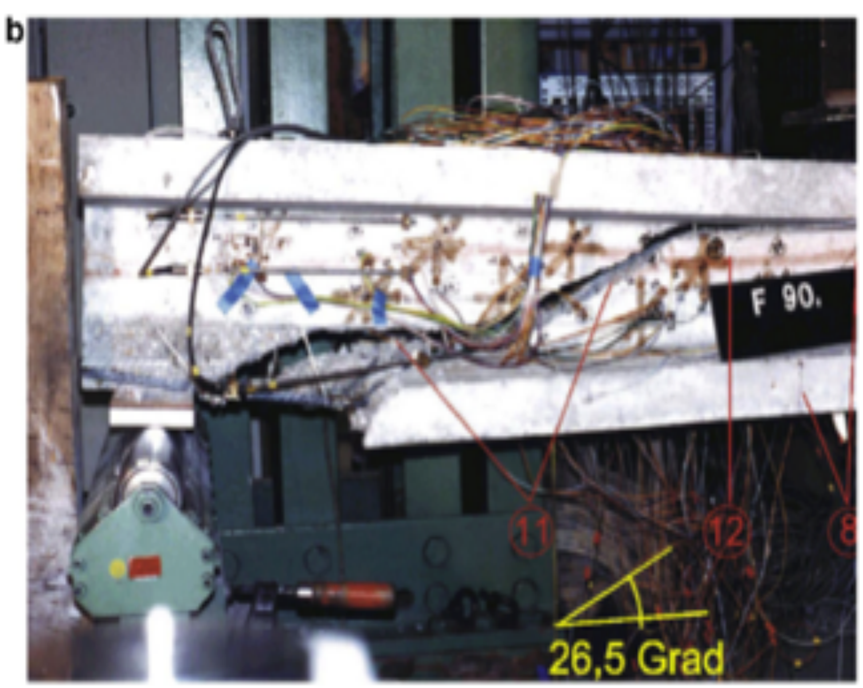

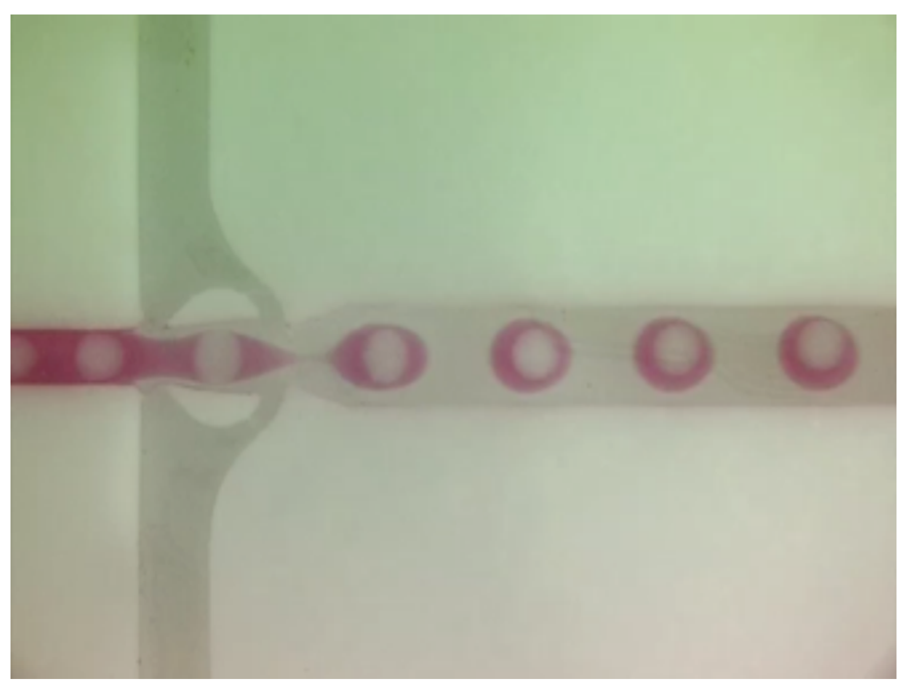

Interfaces in practical engineering simulations

CRACKS & CUTS

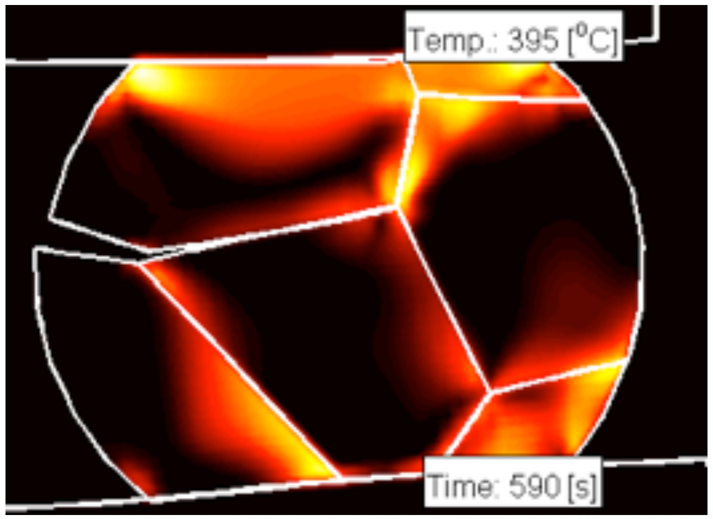

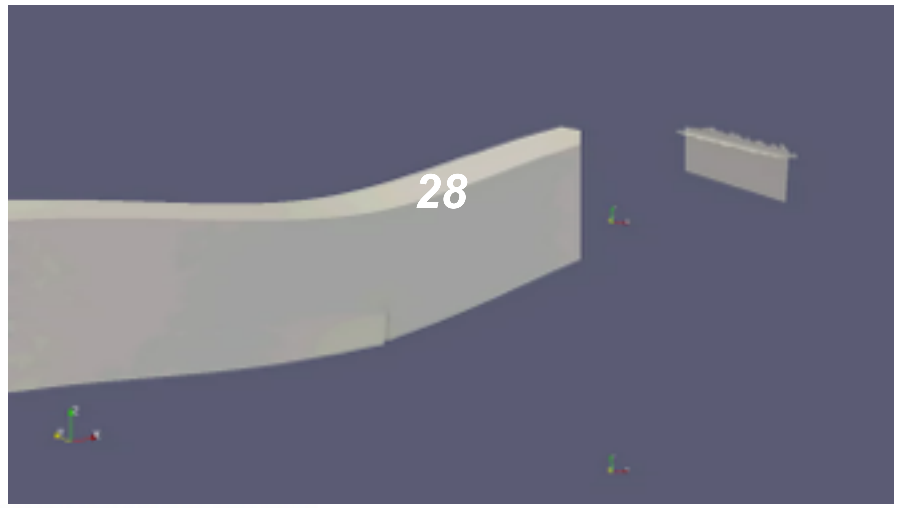

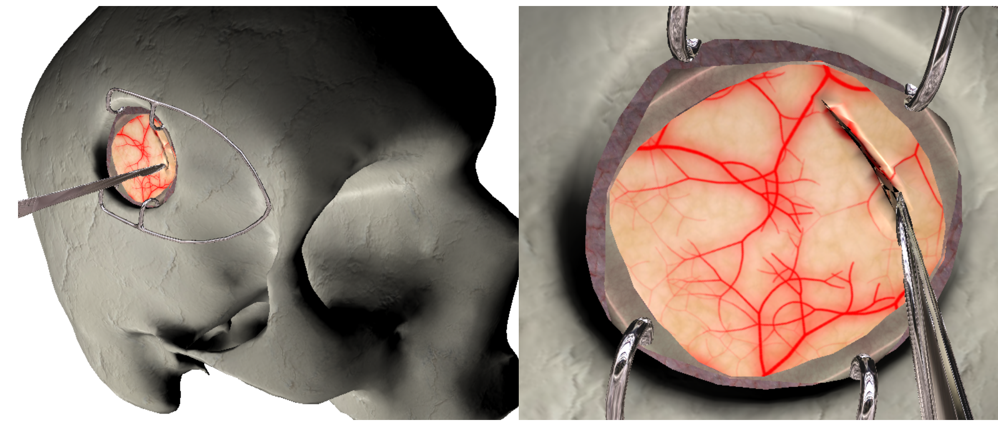

Real-time simulation of cutting during brain surgery

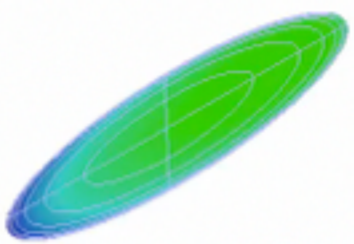

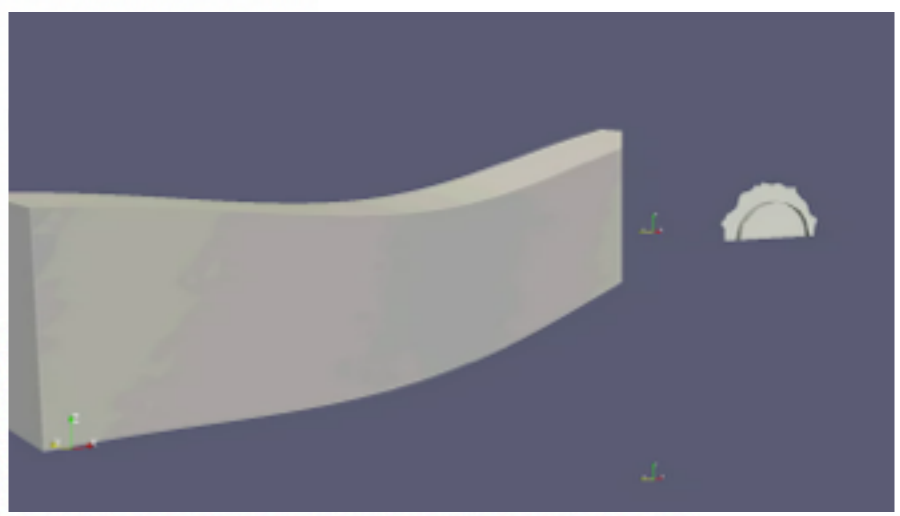

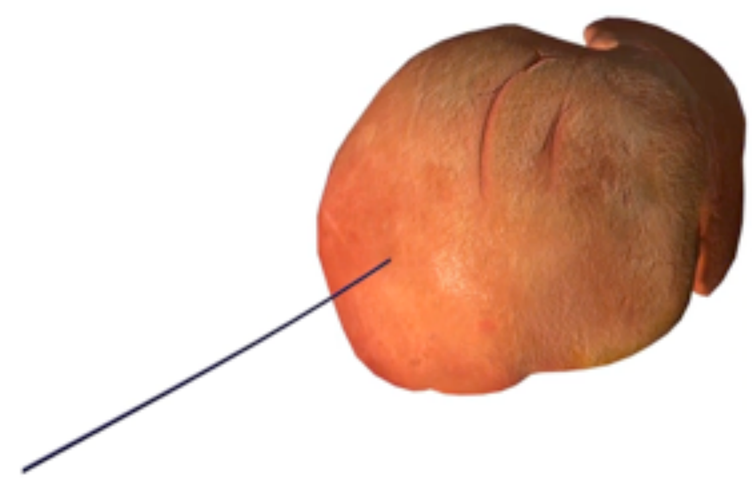

Needle tissue interaction with breathing motion

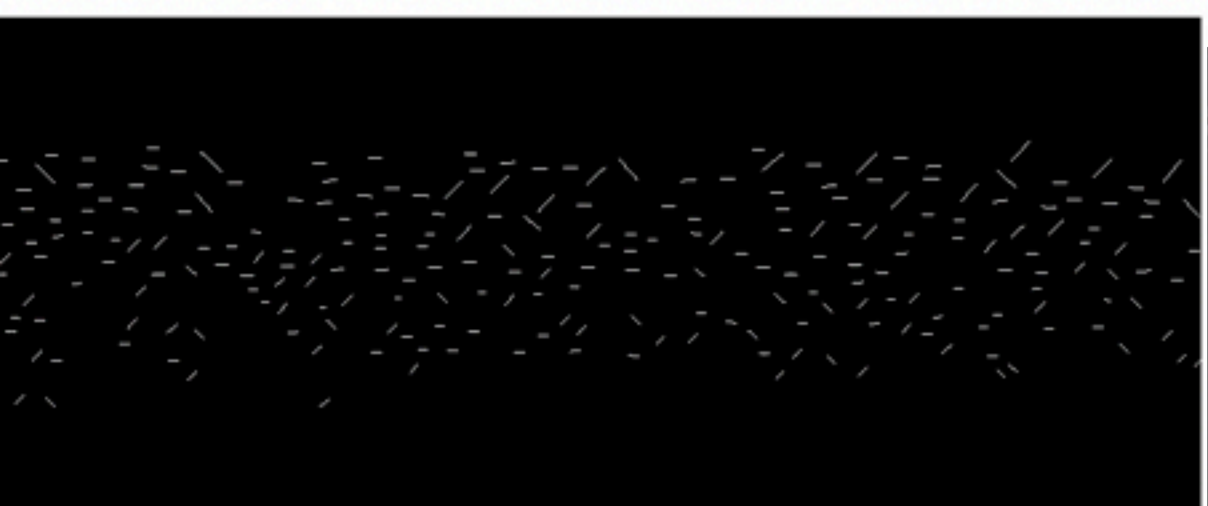

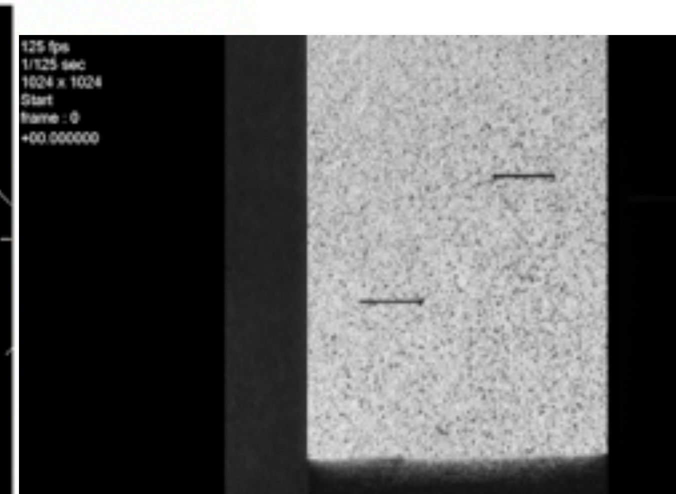

Interfaces in practical engineering simulations

MODELS

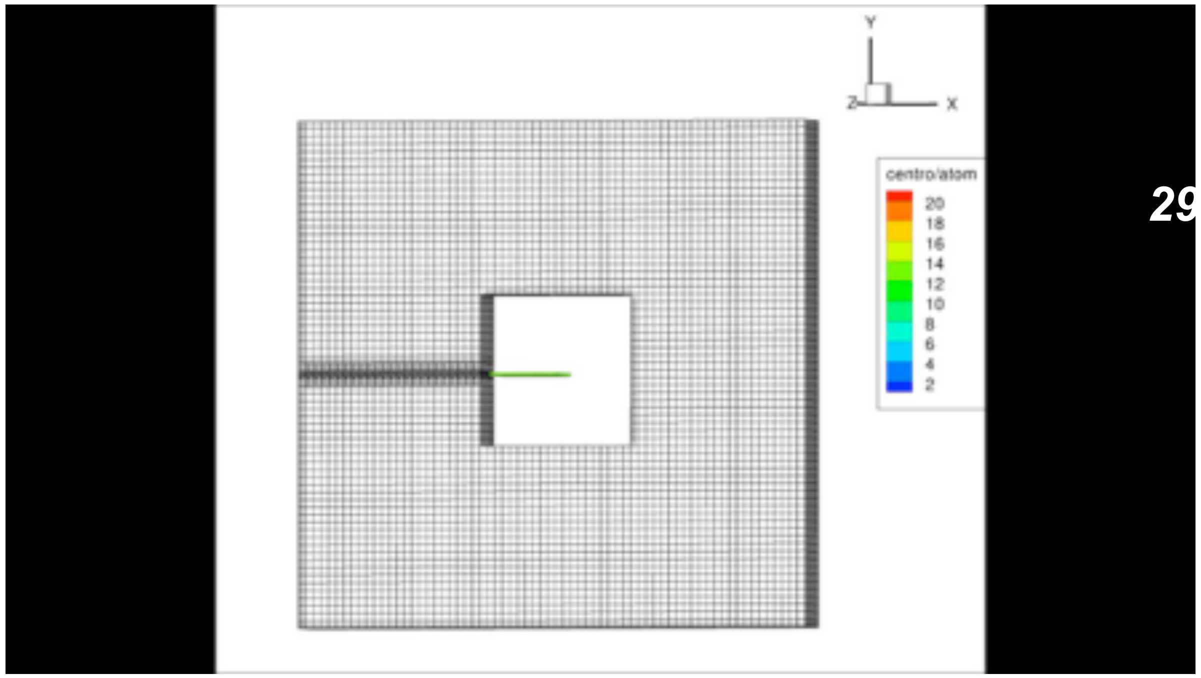

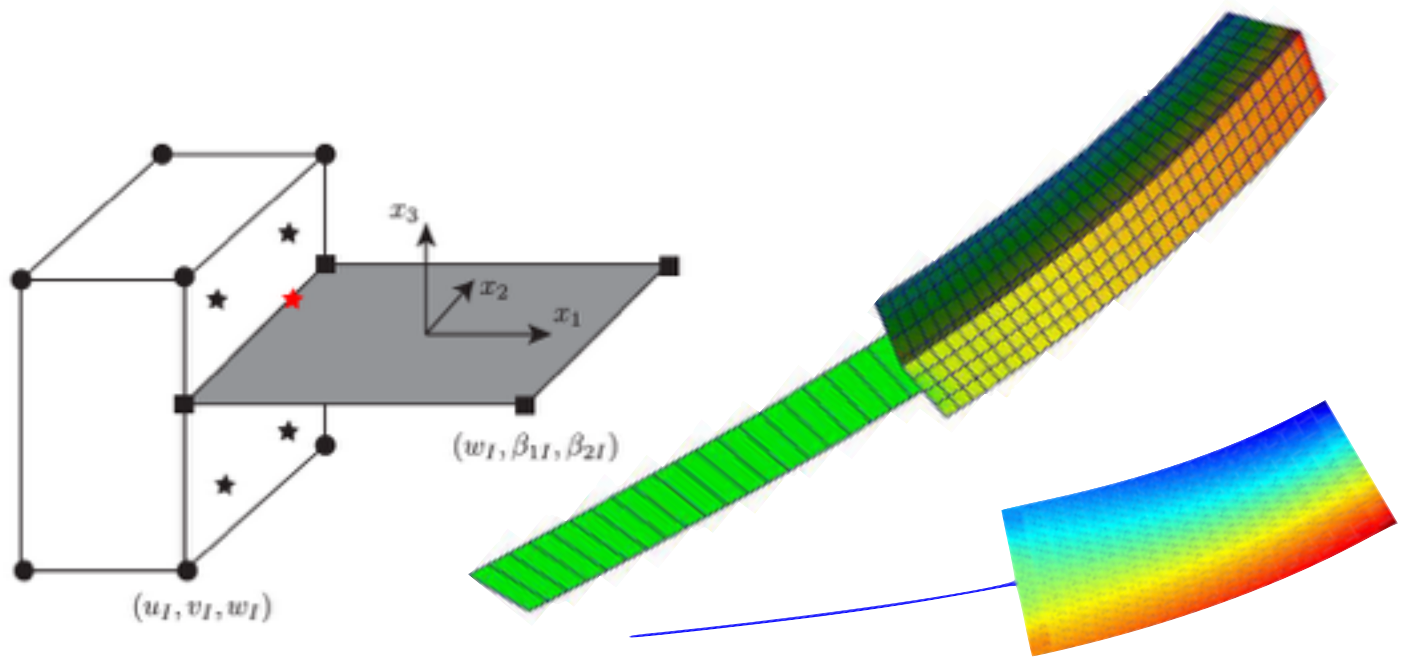

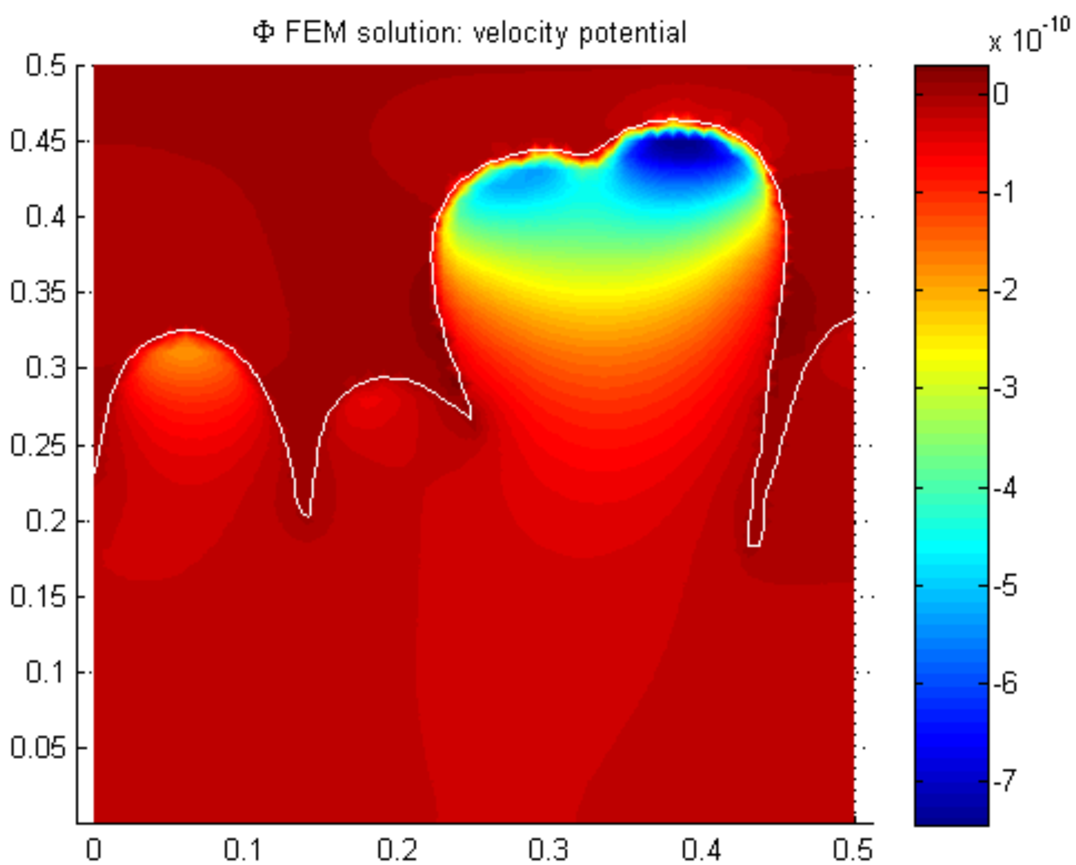

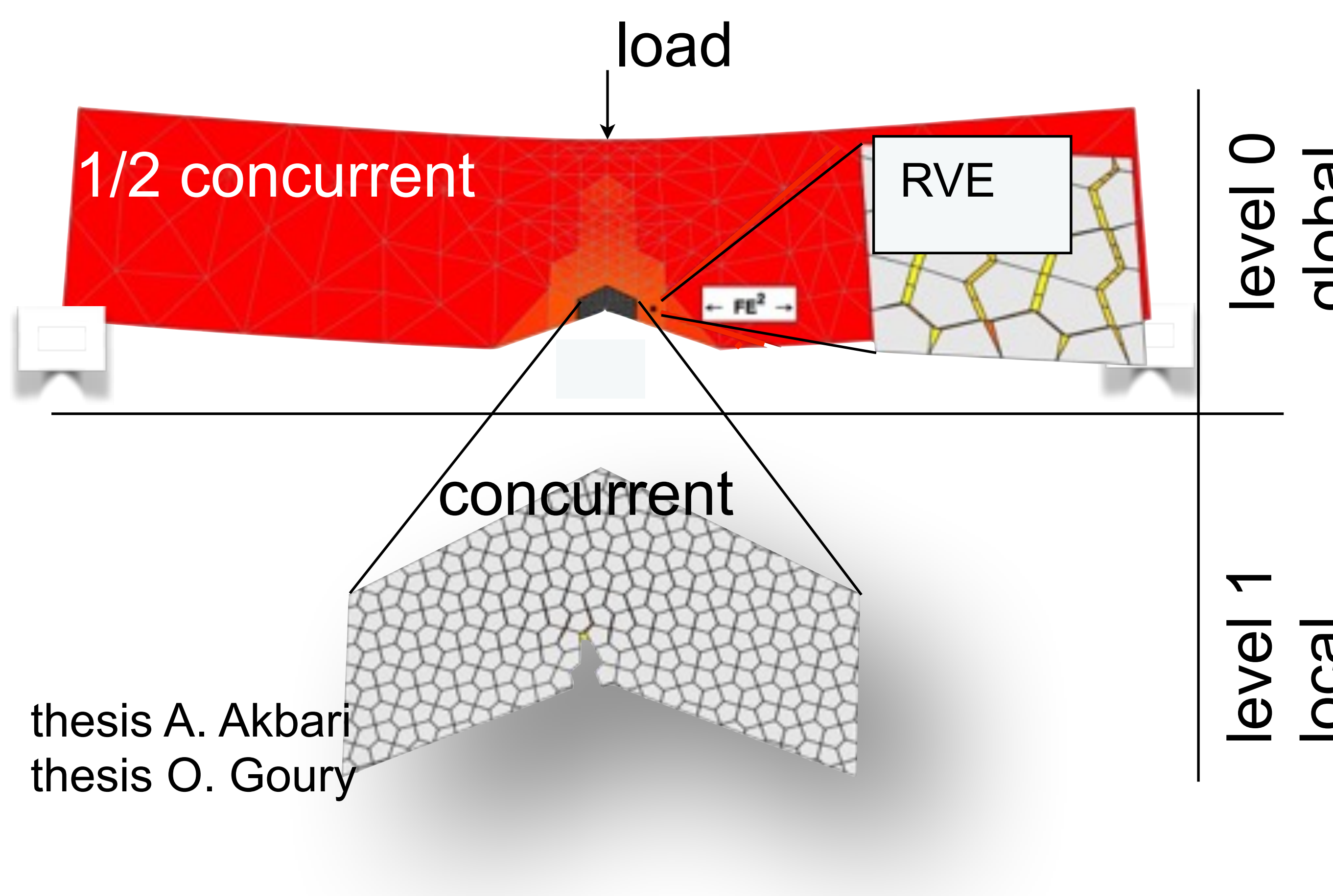

thesis A. Akbari
thesis O. Goury

DISCRETISATION

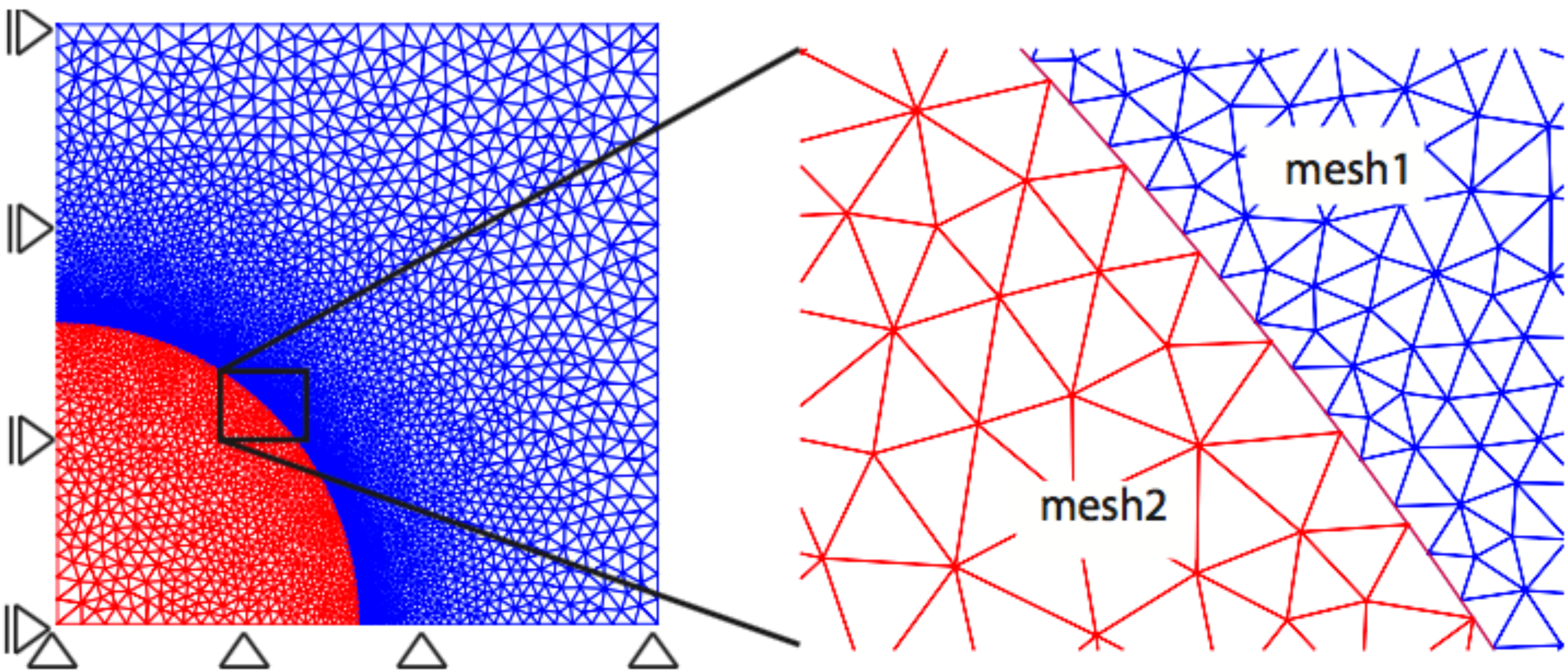

Discretisation

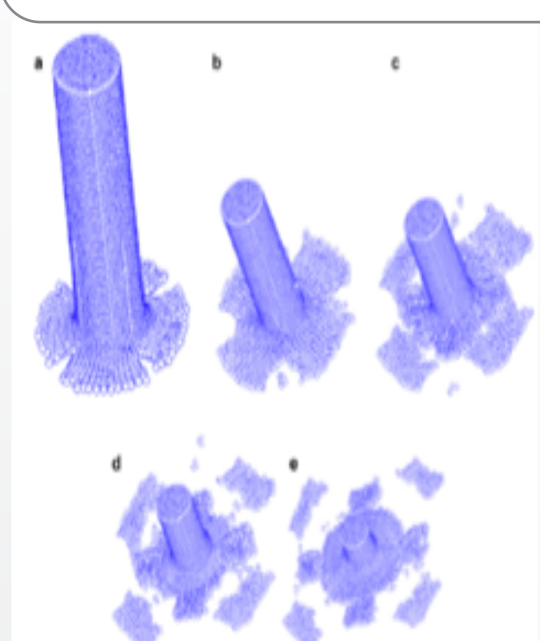

Mesh-free and discrete approaches to fracture

Fracture over multiple scales

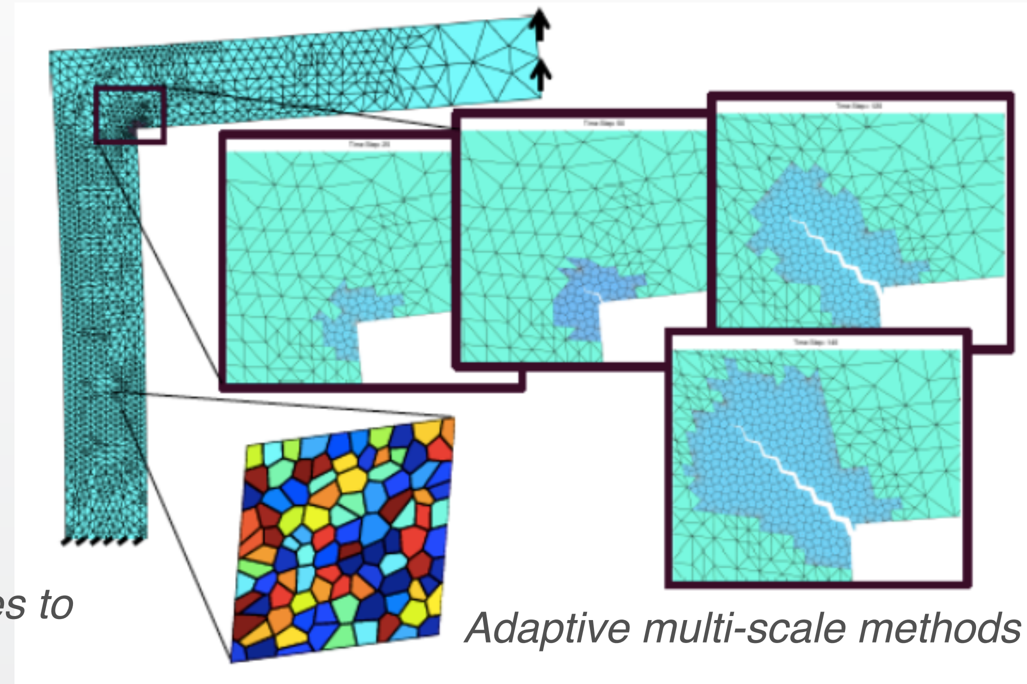

Adaptive multi-scale methods

Coupled problems

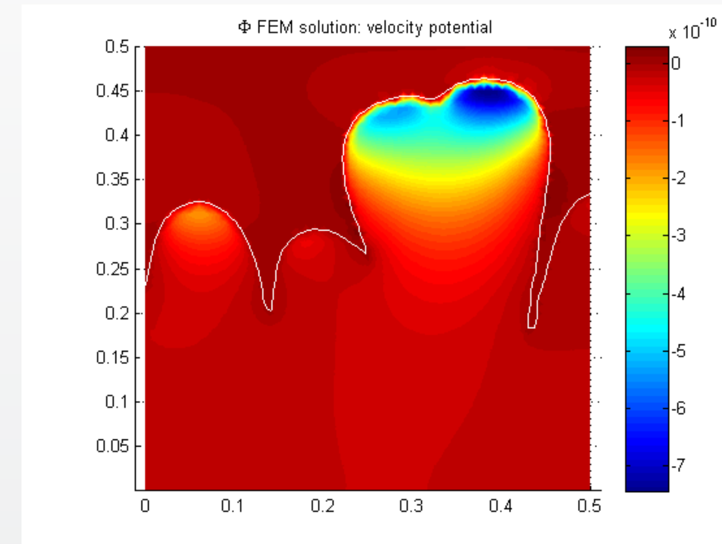

Biofilm growth

Quality and error control

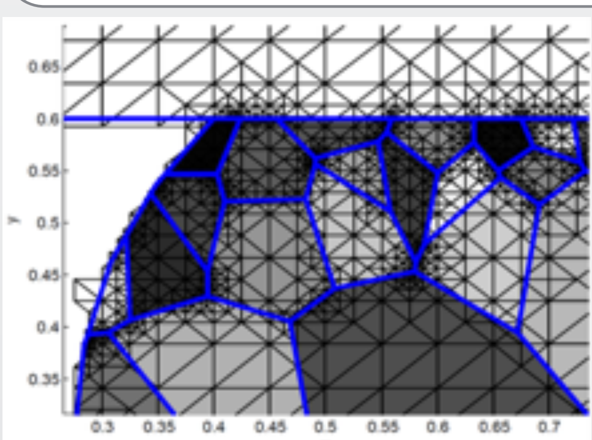

Durability of Pb-free solders

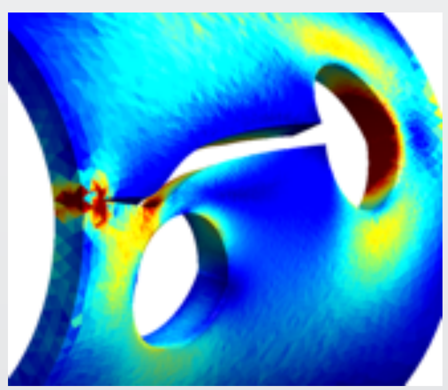

Error estimates for fracture

Interactivity and model order reduction

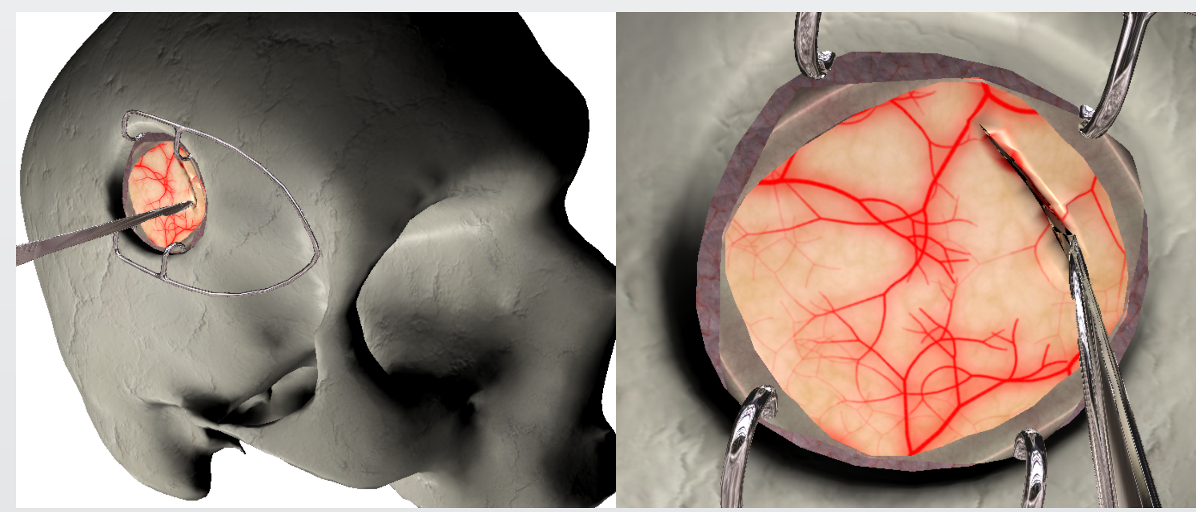

APPLICATIONS

Personalised Medicine

- *Computer-aided surgery*
- *Computer-aided diagnostics*

Engineering

- *Durability & Sustainability*
- *Energy*
- *Aerospace*

Motivation for this talk

Fracture

125 fps
1/125 sec
1024 x 1024
Start
frame : 0
+00.000000

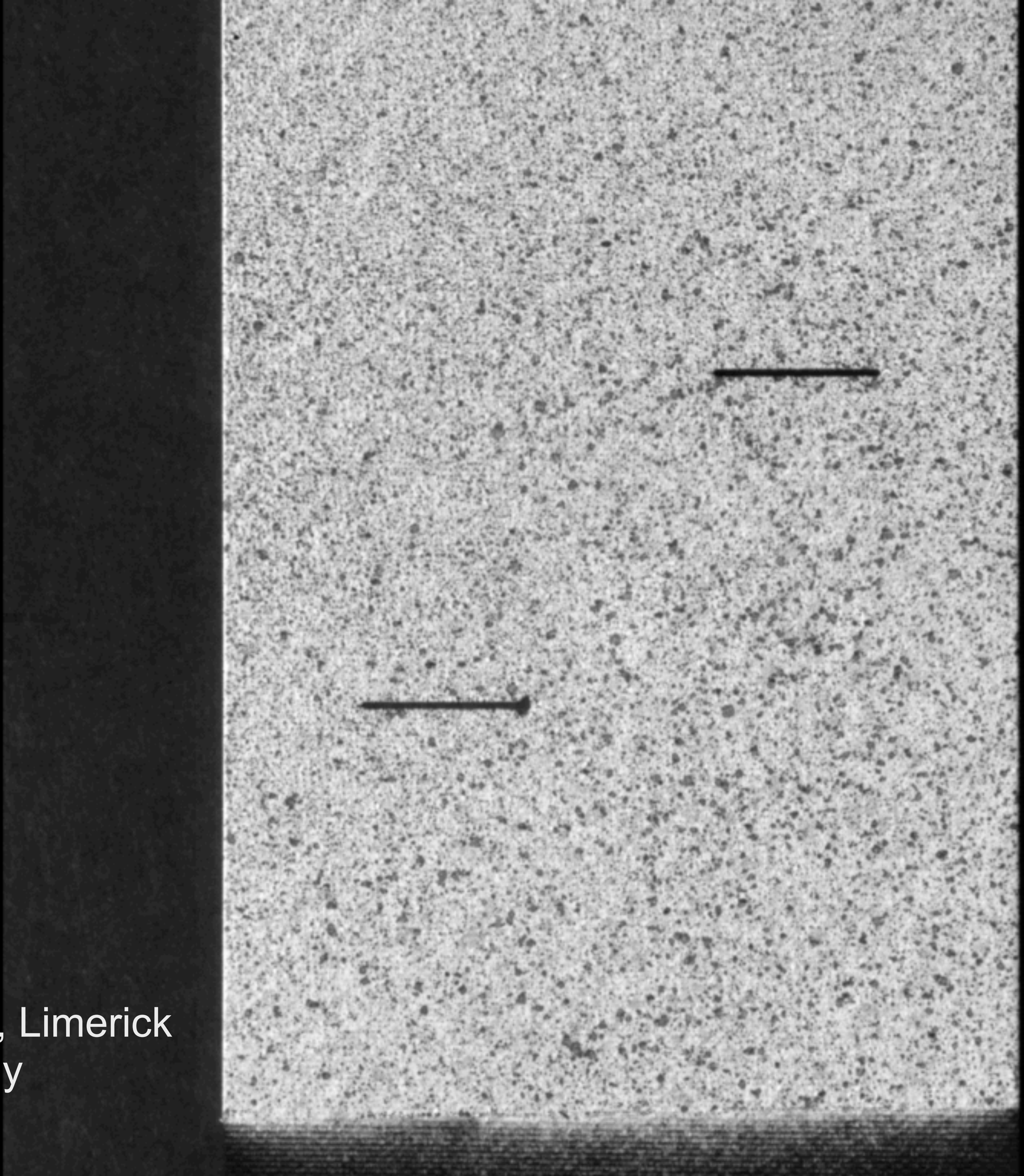

Failure of “heterogeneous” engineering materials

Crack growth in carbon fibre reinforced composites [right]

with the Composite Centre, Limerick
Lisa Cahill, Conor McCarthy

125 fps
1/125 sec
1024 x 1024
Start
frame : 384
+03.072000

Cracks grow along the carbon fibre direction

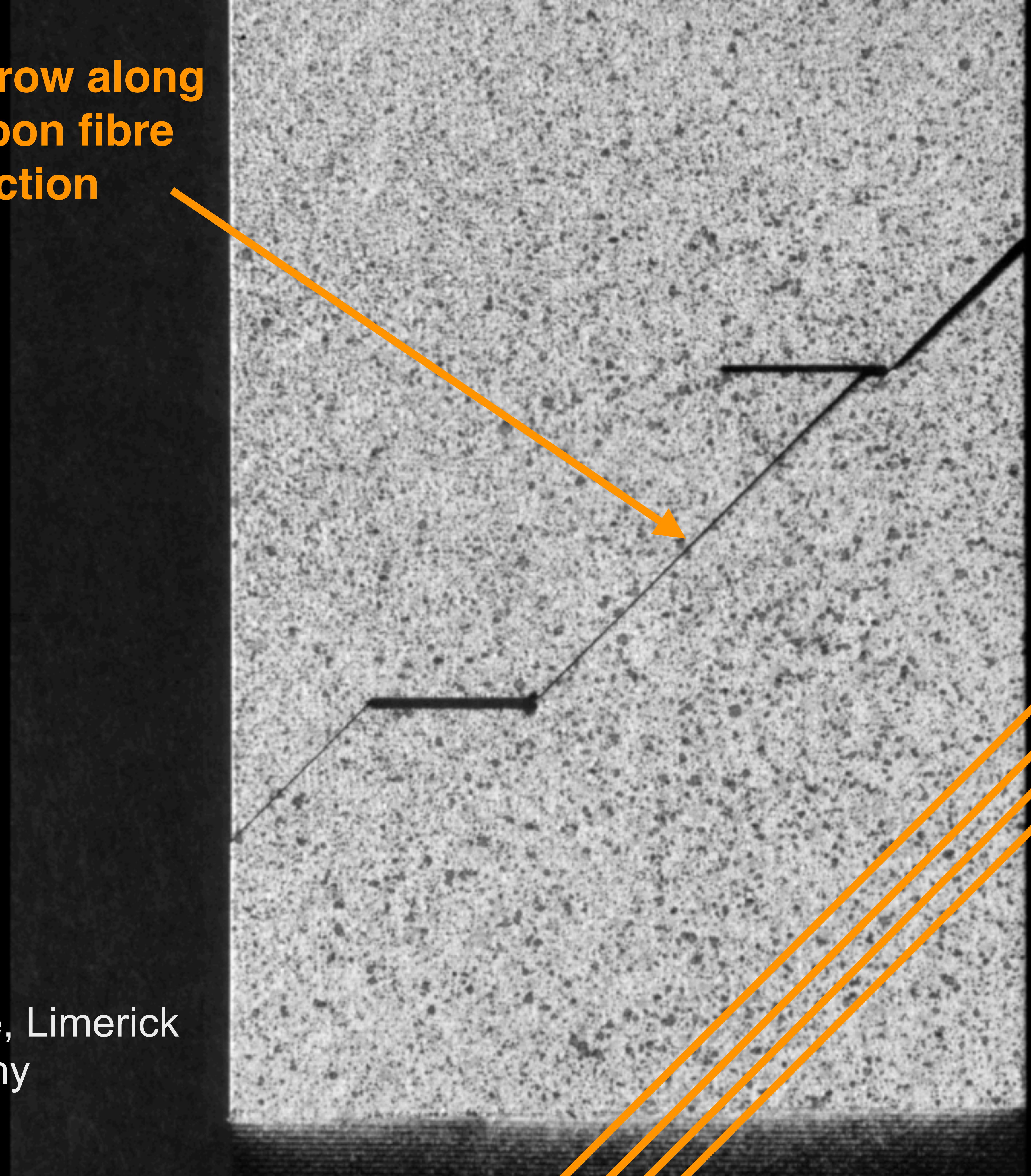

Failure of “heterogeneous” engineering materials

Crack growth in carbon fibre reinforced composites [right]

with the Composite Centre, Limerick
Lisa Cahill, Conor McCarthy

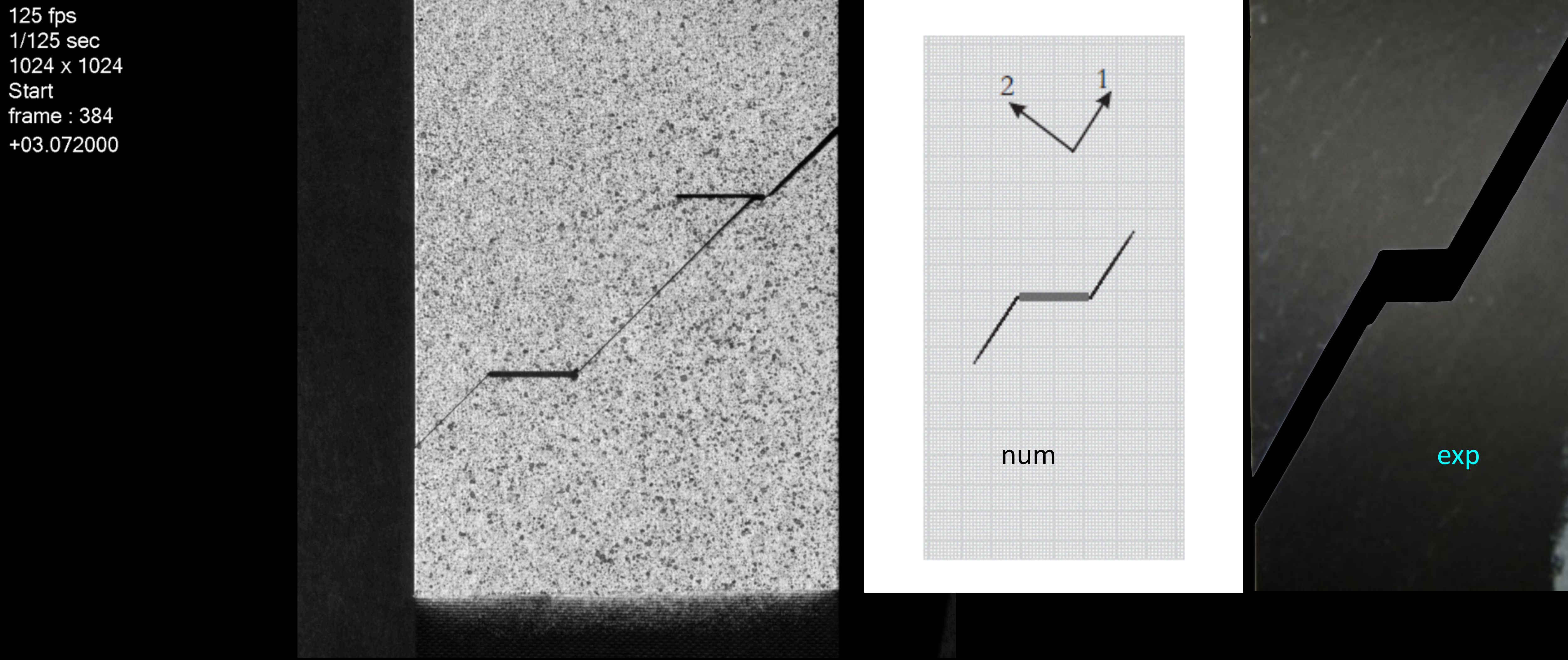

Here, a simple orthotropic phenomenological model suffices

An experimental/numerical investigation into the main driving force for crack propagation in uni-directional fibre-reinforced composite laminae

Cahill, Natarajan, SPAB, O'Higgins, McCarthy,
Composite Structures, 107 (2014) 119-130

Motivation: fracture of engineering structures and materials

- **Limerick**: unidirectional composites

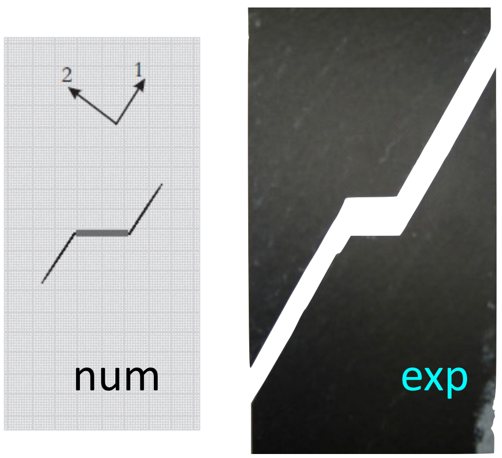

thesis L. Cahill, 2014

- **China/USA**: hydraulic fracturing (shale gas)

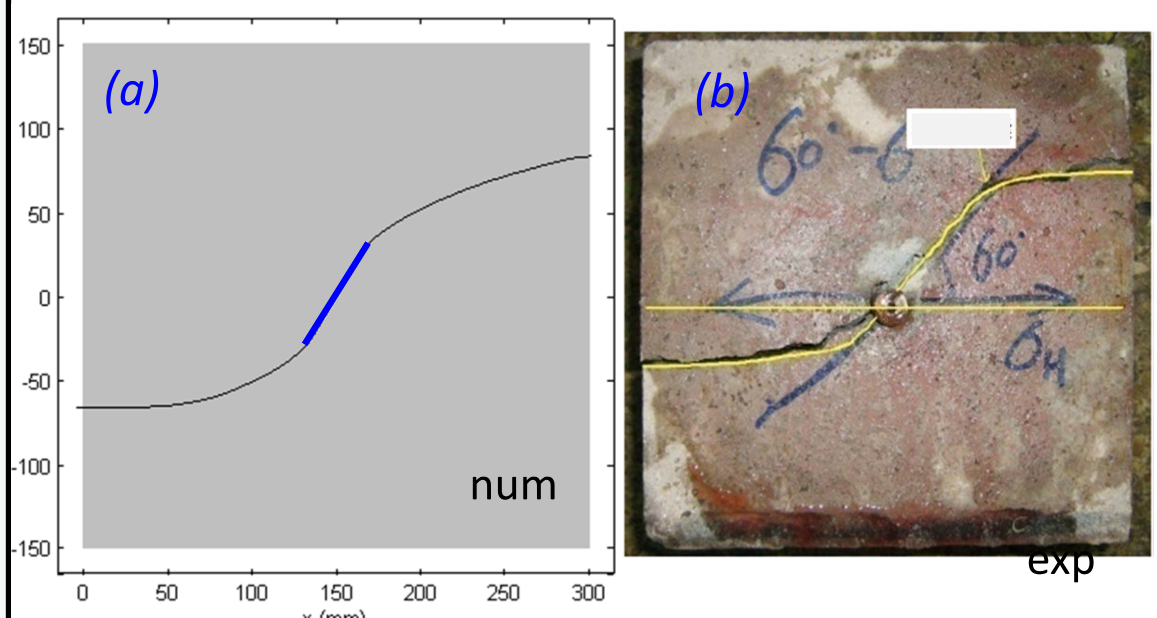

thesis M. Sheng, USA, China, 2016

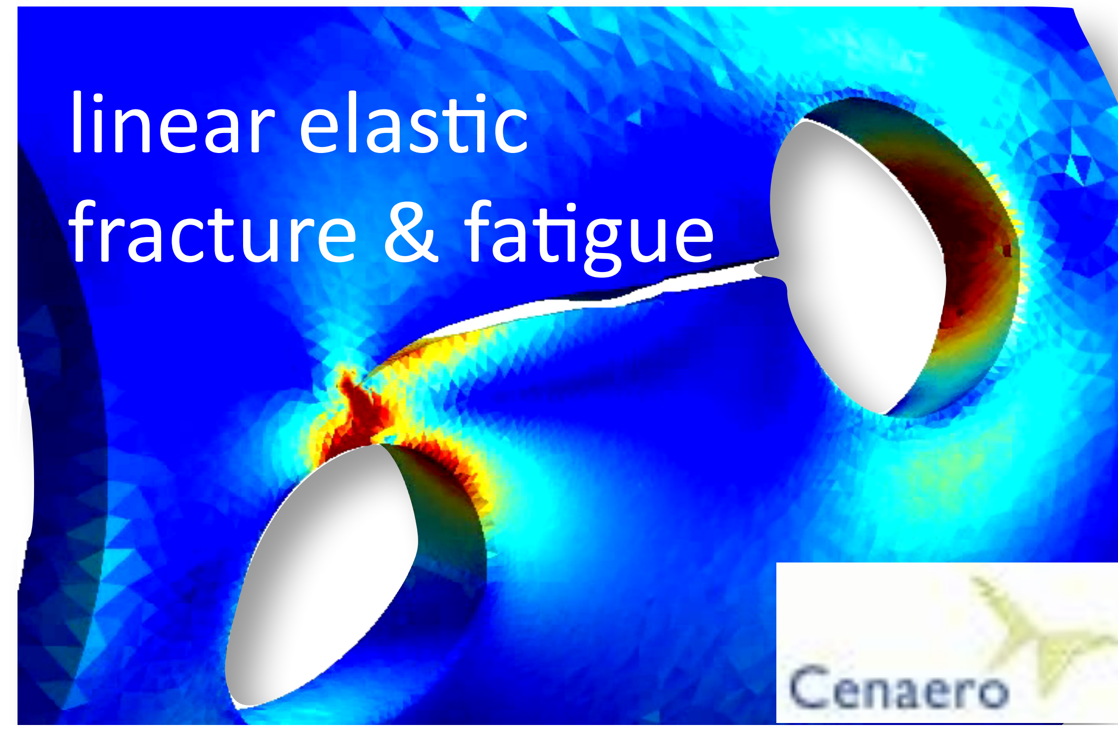

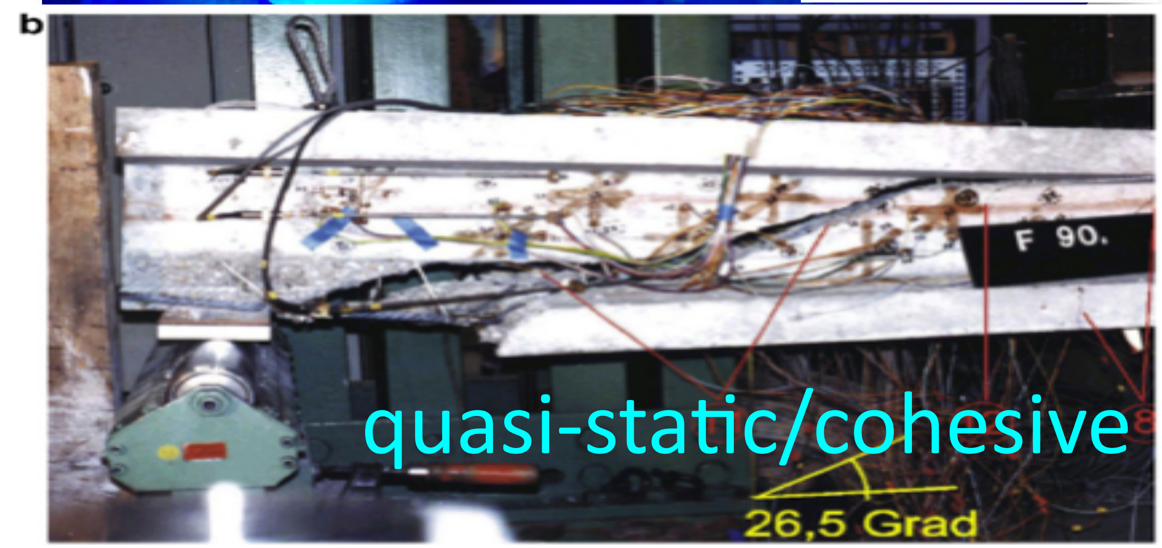

dynamics
ductile

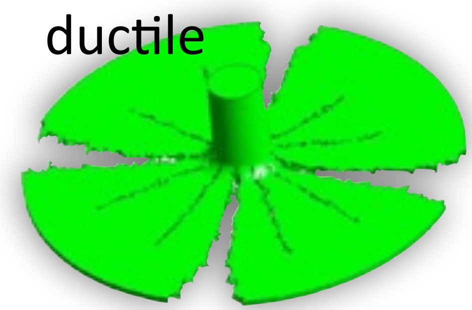

dynamics/brittle

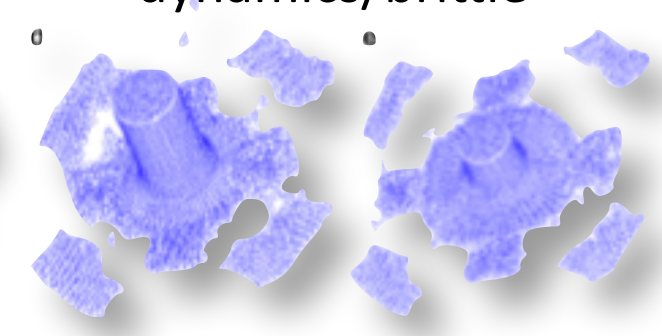

Motivation: multiscale fracture of engineering structures and materials

Solder joint durability (microelectronics), Bosch GmbH

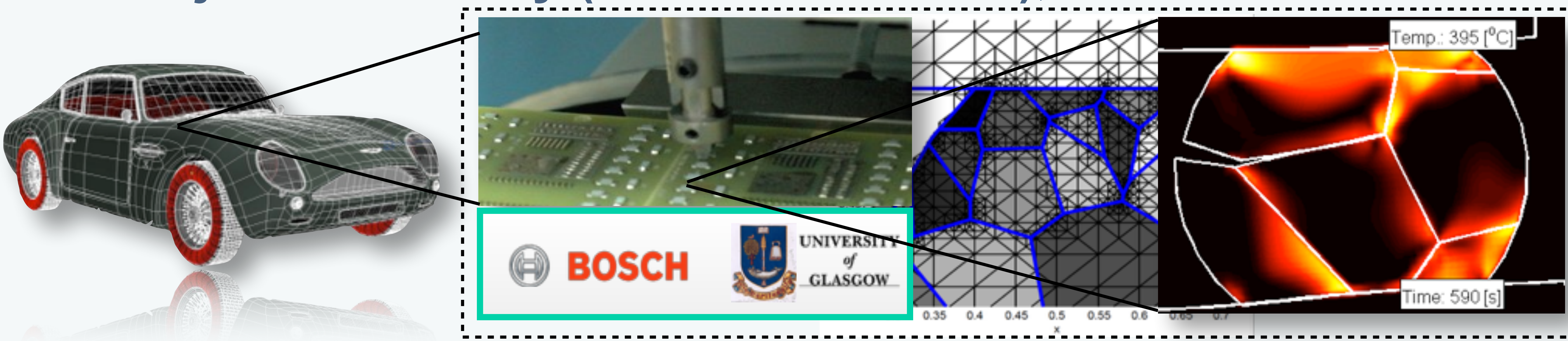

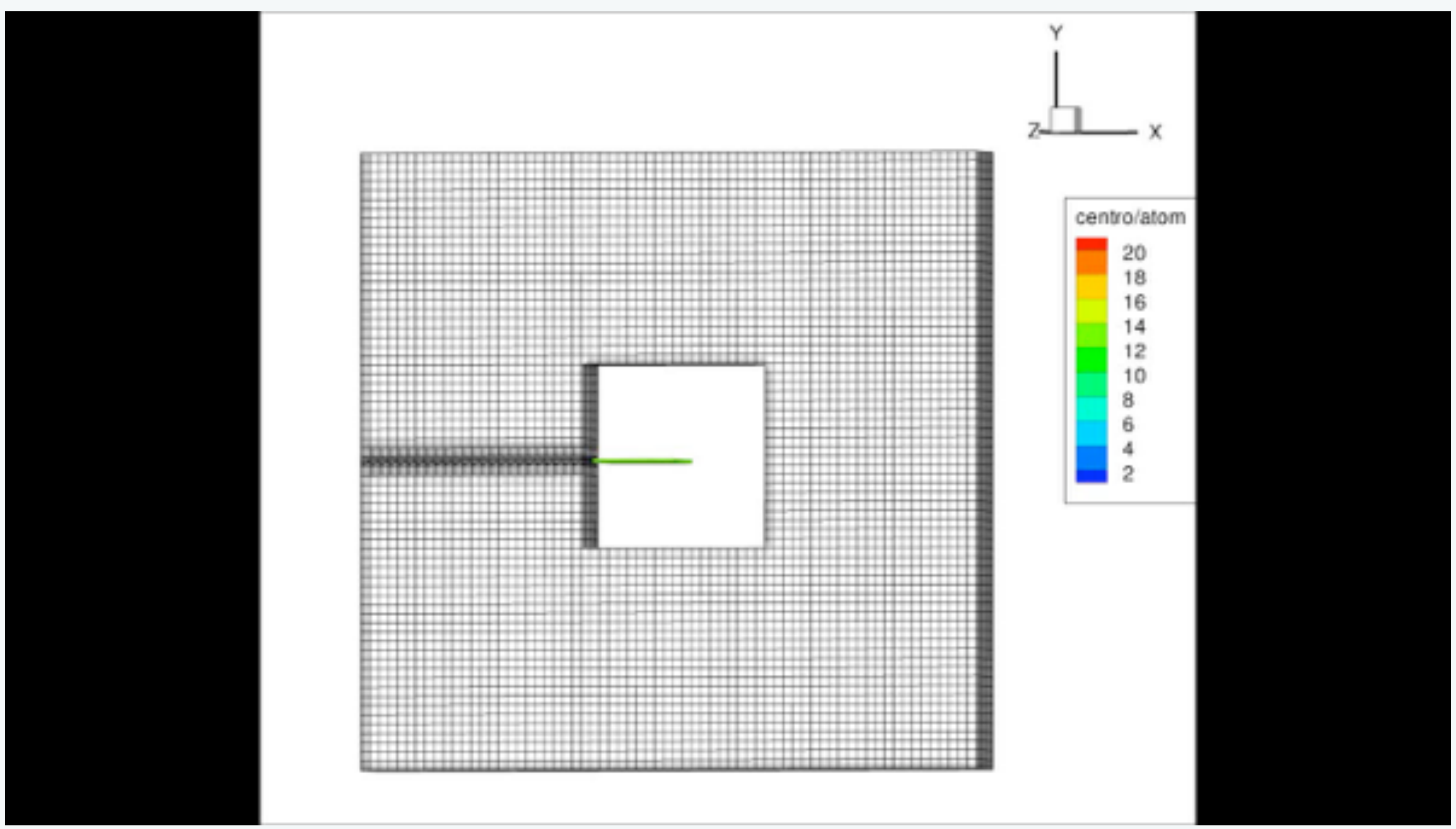

Phenomenological models were impractical

We developed multi-scale models

Adaptive Molecular Dynamics - Continuum coupling

Motivation: multiscale fracture of engineering structures and materials

Practical early-stage design simulations (interactive)

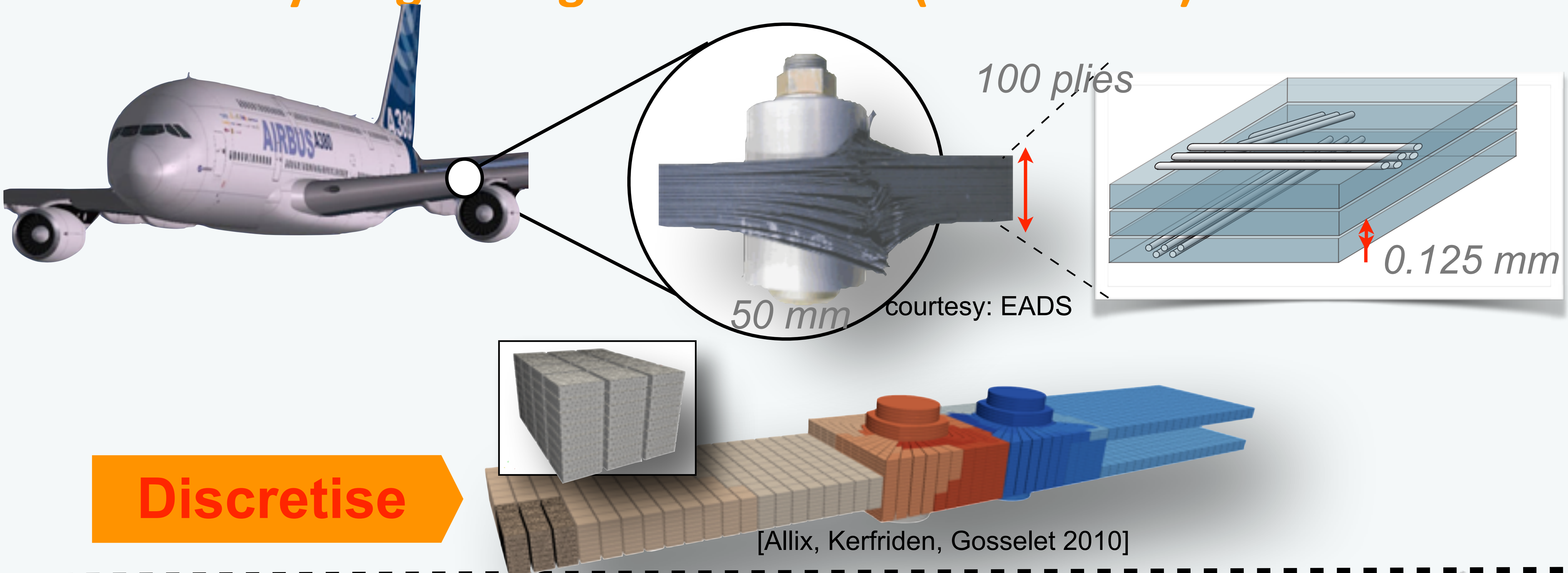

Surgical simulation

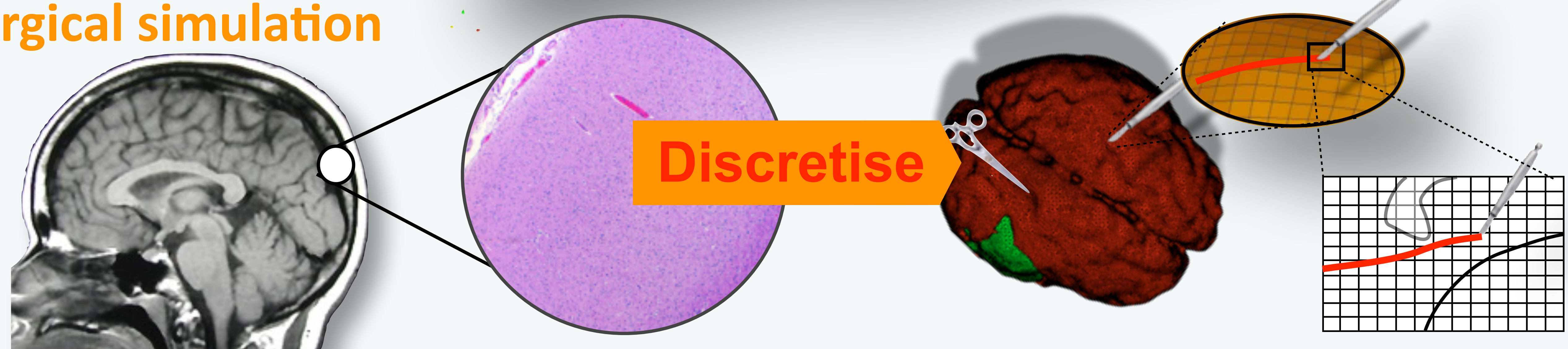

- Reduce the problem size while controlling the error (in QoI) when solving very large (multiscale) mechanics problems

Computational expense reduction in multi-scale fracture fracture

- Homogenisation - Hierarchical, FE^2
- Concurrent and hybrid (bridging domain, ARLEQUIN…)
- Adaptivity Enrichment (PUFEM, XFEM, GFEM…)
- Model reduction (Quasi-Continuum, POD, PGD…)
- Outlook - learning models?

Outline

- Reminders and definitions on multi-scale methods
- An error-controlled adaptive method for fracture
- Model reduction approaches (adaptive POD and Quasi-Continuum)
- Outlook - learning models?

Definitions and Basics

Multi-scale methods

Which model, at what scale?

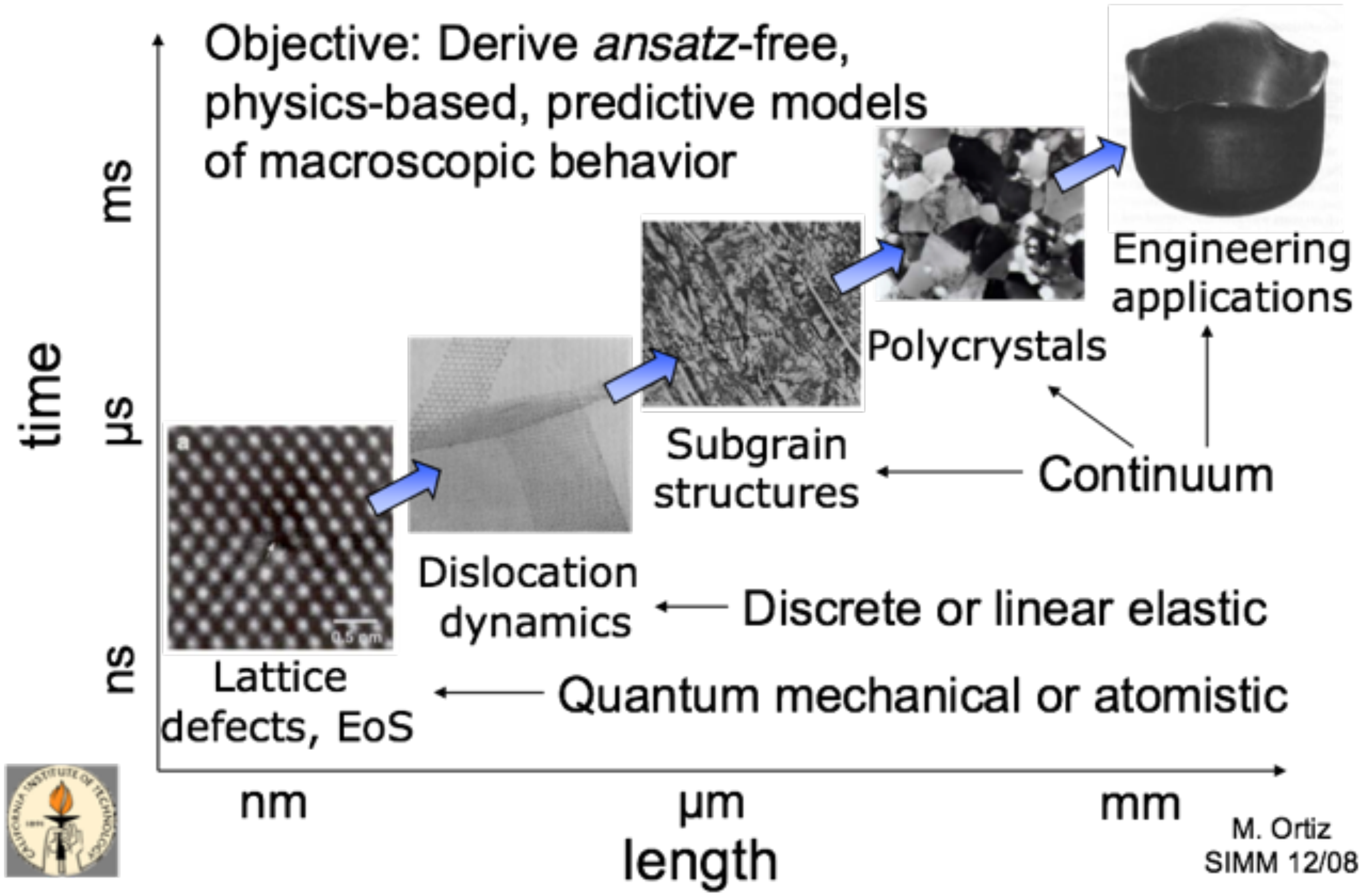

Working scale: scale at which observations/predictions must be made

Length-scale: length of a typical constituent of the structure whose physics can be described in a self-consistent manner

Multiscale modelling

- Top-bottom view: Feed macroscopic model with some information coming subscale modelling

- Bottom-up view: **replace heterogeneous subscale model by an equivalent**, smoother, **model** at the scale where predictions are required (i.e. macroscopic scale)
  - In an ideal world: model subscales directly

    → infeasible in practice
  - Multiscale methods: Use an approximate model s.t. (e.g. [Fish '07]):

Error in QoI macroscopic < Tolerance Cost of solving macromodel << subscale model

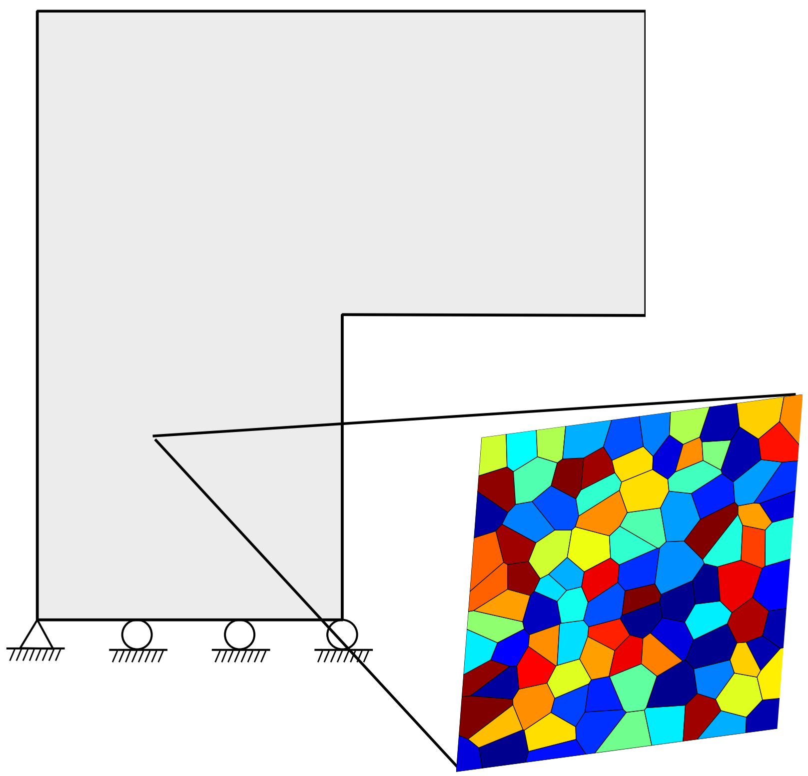

[Chen et al. 2011]

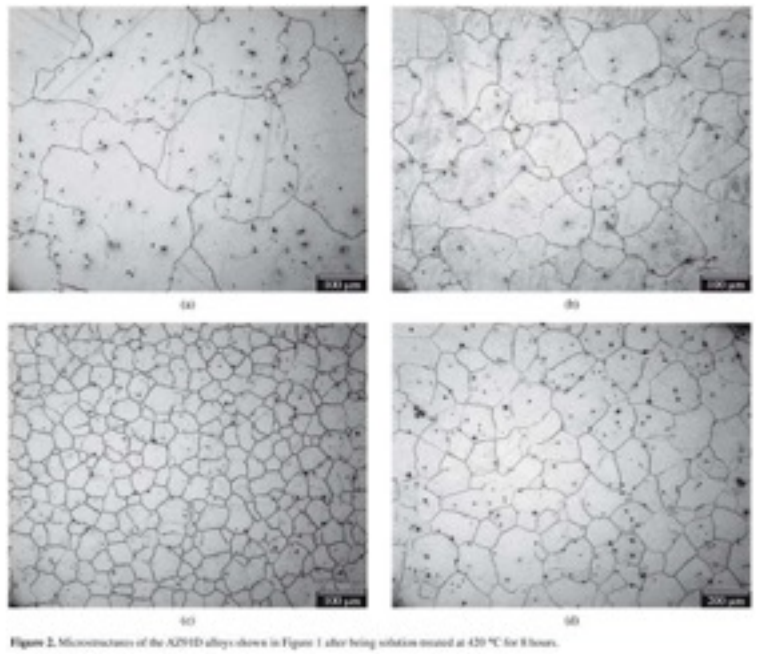

Why scale bridging? (1/3)

- Phenomenological macroscale modelling
  - Assume the “shape” of the governing equations
  - Identify constants from experimental data

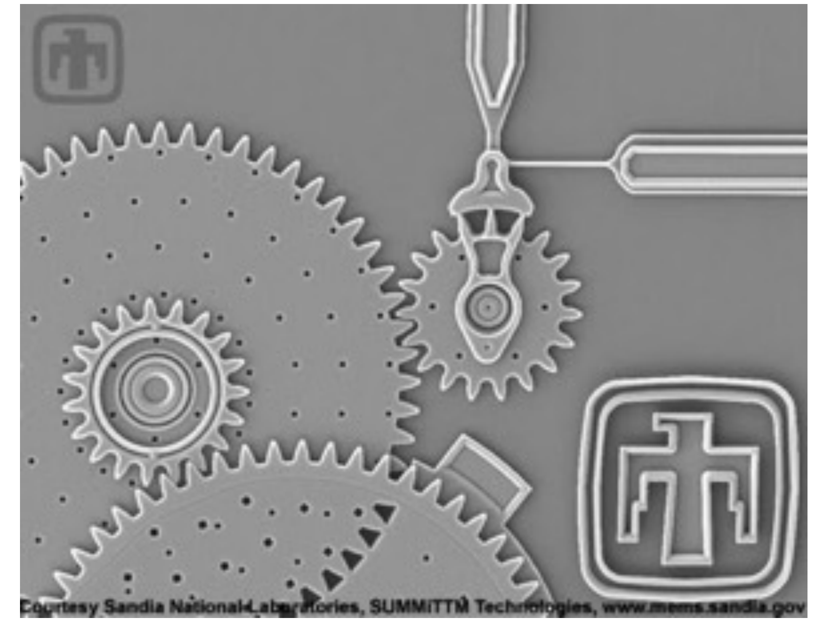

- But, if the first step is not done correctly: **lack of predictivity** (the model cannot fit of overfits the data)

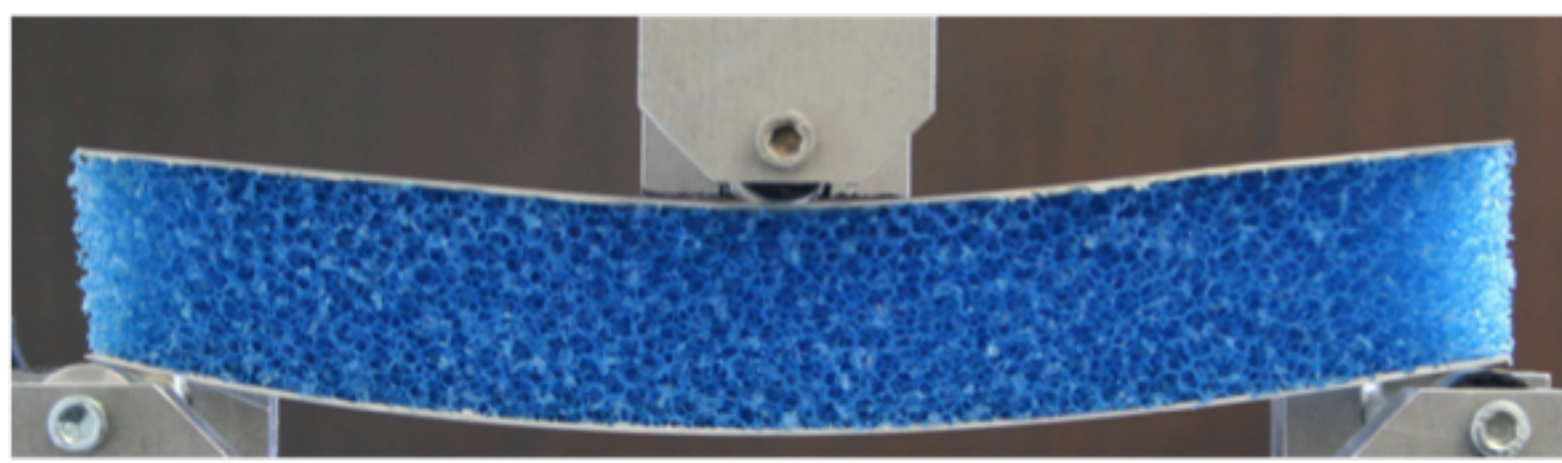

[Janicke et al. 2012]

pierre.kerfriden@gmail.com stephane.bordas@alum.northwestern.edu lars.beex@uni.lu

Why scale bridging? (2/3)

- Modify the microstructure virtually and test the overall response of the structure
  → Need reliable link between of macroscale equations and micro parameters, which would be difficult to identify experimentally

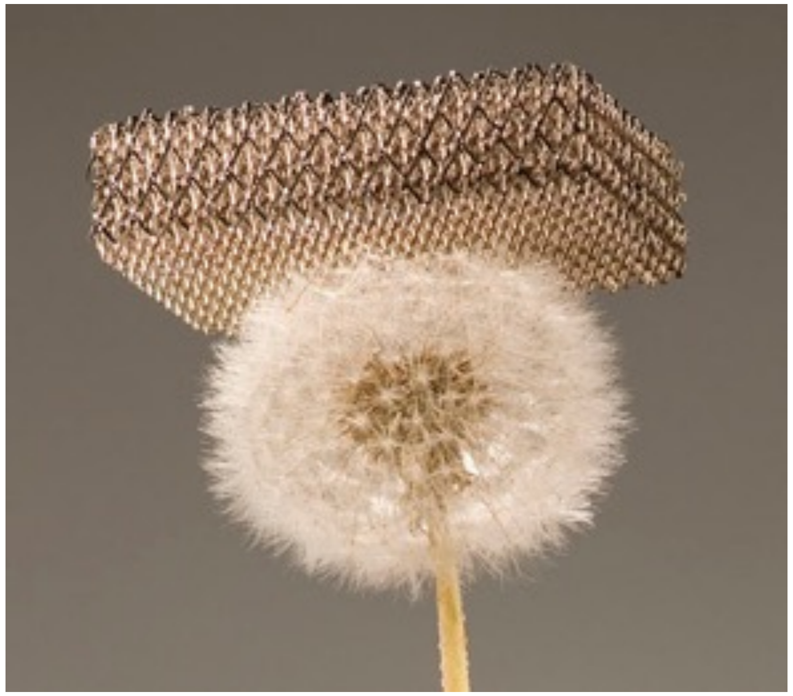

- Virtual optimisation
  - Architectured materials
  - Controlled microstructures

Optimisation of fiber content in sandwich beams to minimise interfacial stress in

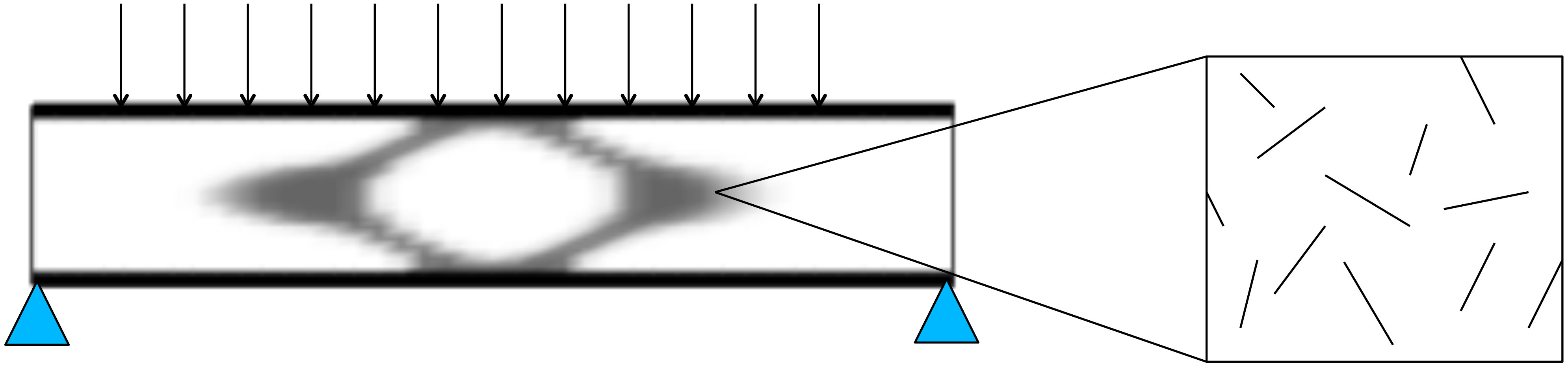

Why scale bridging? (3/3)

- Observations at the microscale but approximations required to propagate the macroscoale load to the regions of interest

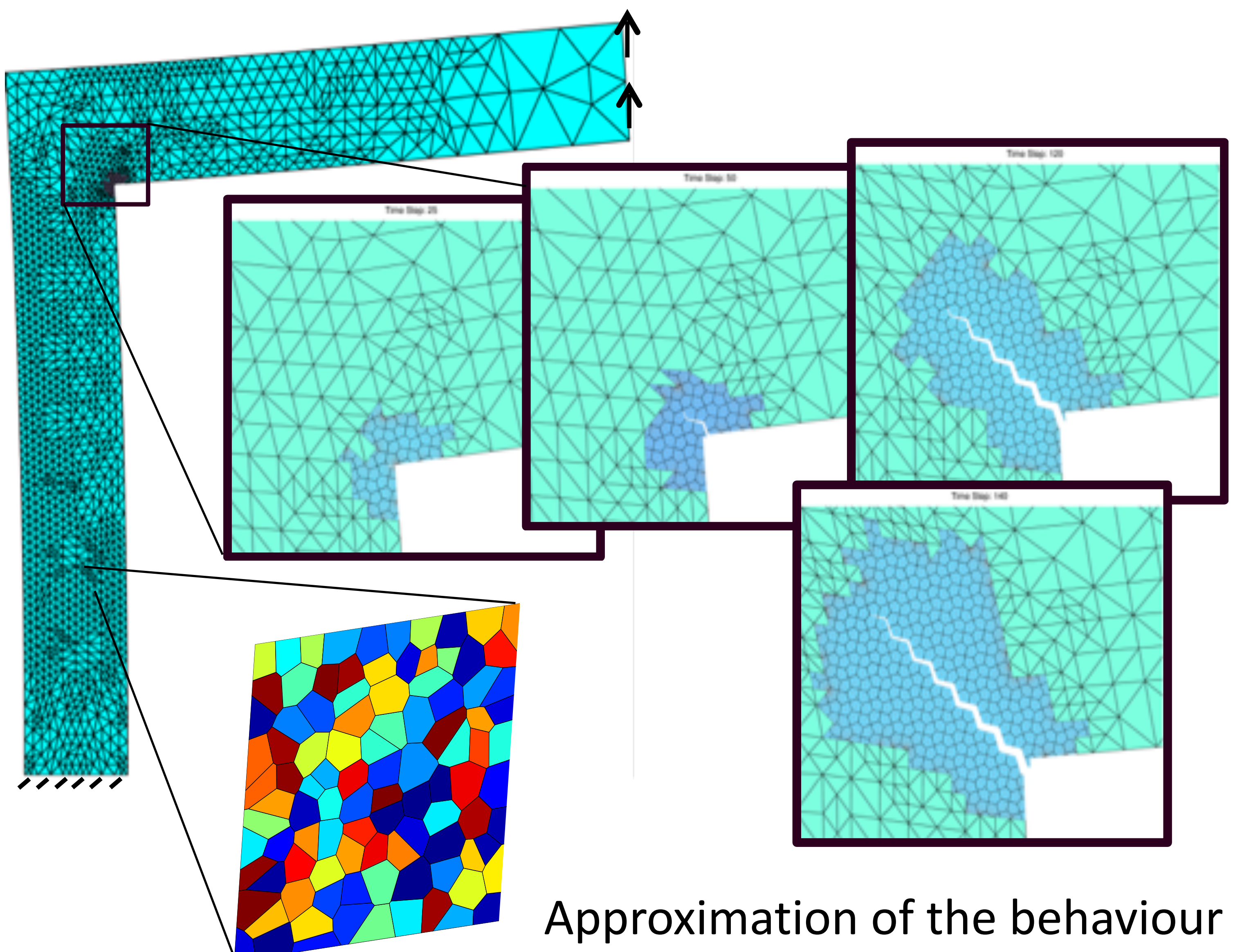

Approximation of the behaviour of polycrystalline materials away from microscopic damage

pierre.kerfriden@gmail.com stephane.bordas@alum.northwestern.edu lars.beex@uni.lu

Multiscale computational strategies: taxonomy

- Information passing strategies
  - → Get macroscale equations from subscale
  - → Post-process (some) microscopic features

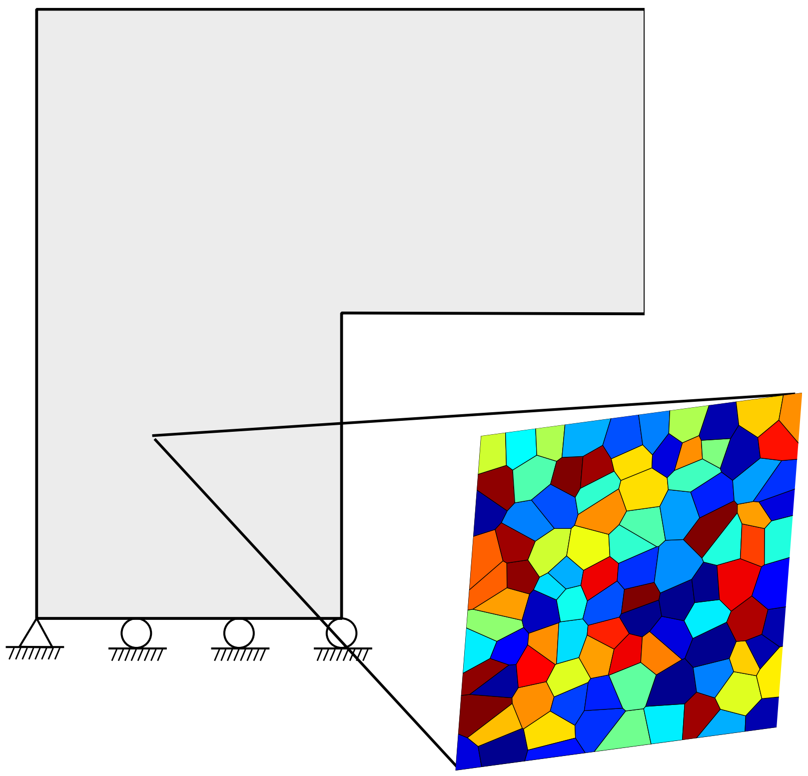

- Concurrent multiscale methods
  - → Strongly couple models at different scales

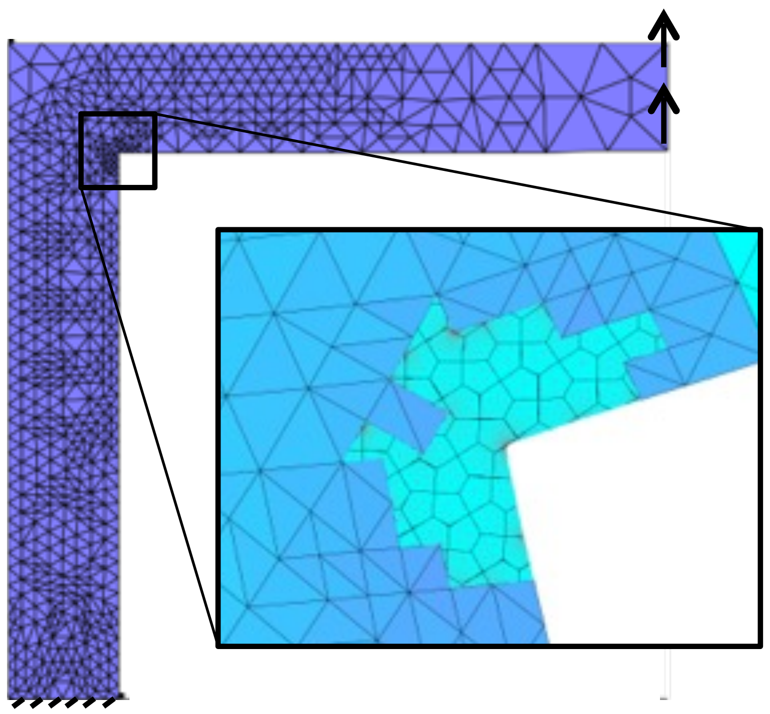

- Multiscale preconditioners: use coarse scales to fasten the direct solution of subscale models (e.g. error estimation, multigrid solvers, domain decomposition)

Basic component: homogenisation

- Knowing the governing equations at the microscale, can we find homogeneous governing equations at the macroscale s. t.:
  - The solution of the macroscale problem converges to the solution of the microscale problem when the scale ratio tends to zero

- *Hopefully*, the solution of the macroscale problem is a good approximation of the solution of the microscale problem (in some sense) even **when the scale ratio is not very small.**

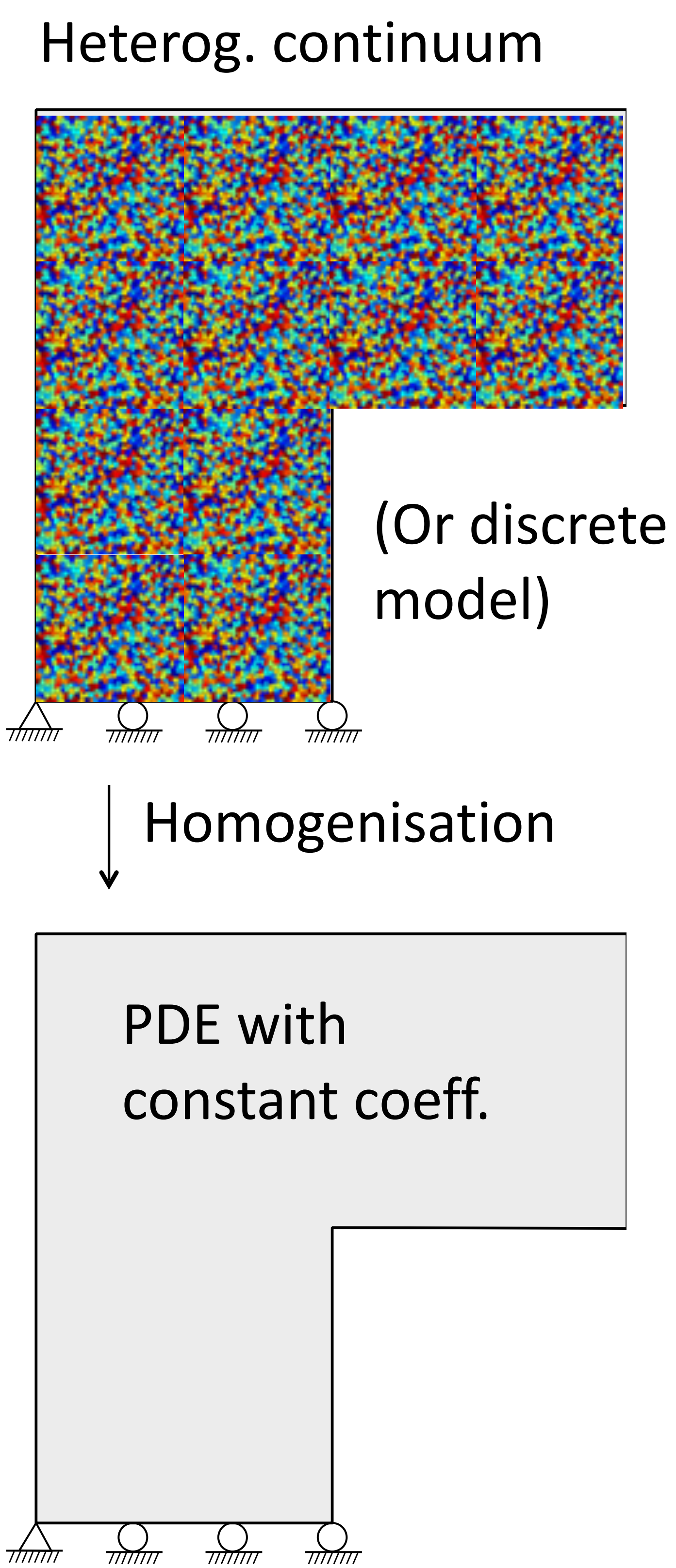

Alternative: micromechanics

- Assume the form of macroscopic laws and attach a representative volume element to the material point

- Assume that the average strain over the RVE is complemented by a well-chosen microscopic fluctuation

- Get the constitutive effective law by enforcing a micro-macro energy equivalence ("macro-energy = average micro-energy in all compatible micro-macro deformations")

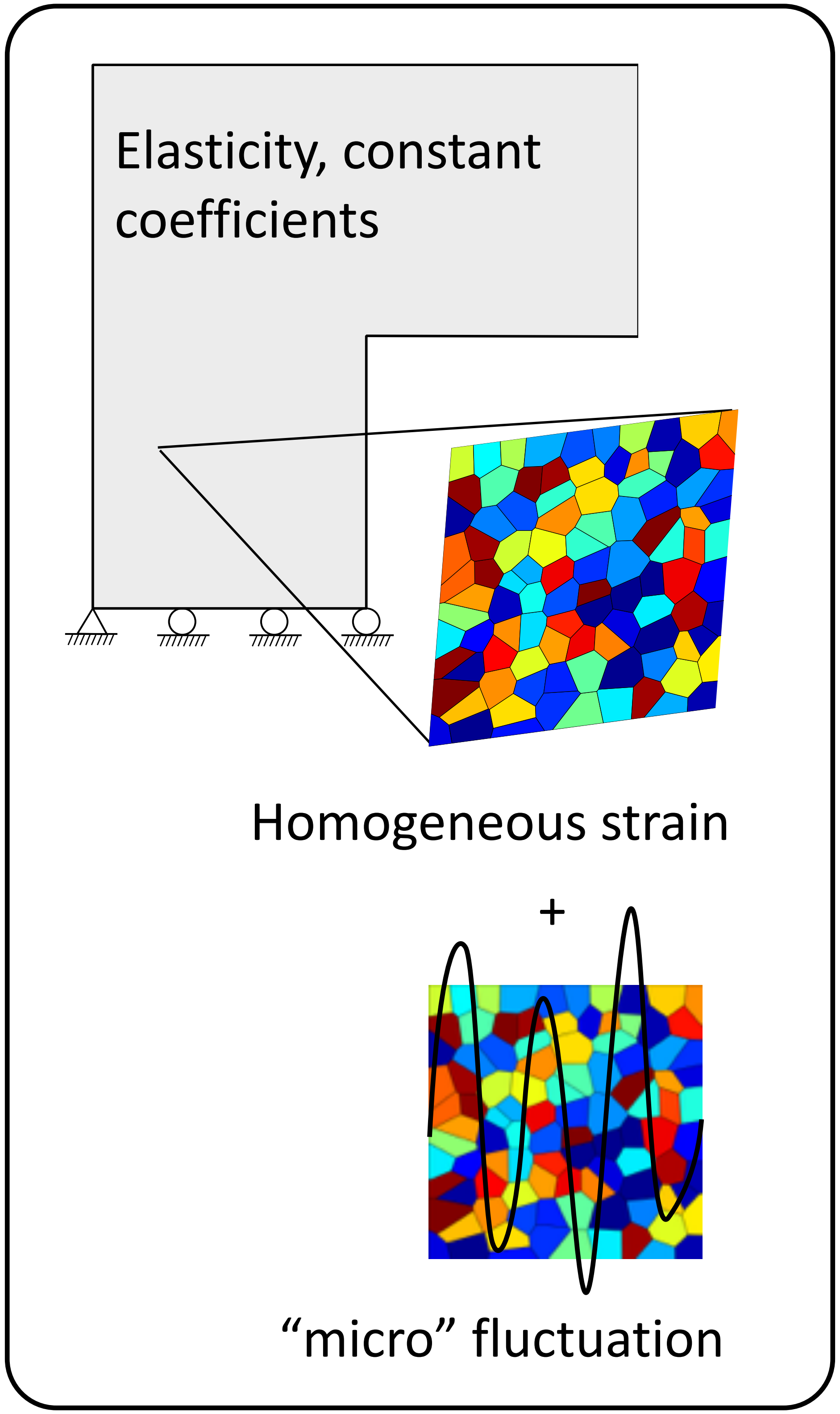

Some key publications

- Chapter on micromechanics by S. Forest in *Nonlinear Mechanics of Materials*, 2009
- Zohdi and Wriggers, *An Introduction to Computational Micromechanics, 2005*
- S. Palencia, *Homogenization in Mechanics: a Survey of Solved and Opend Problems*, 1986
- J. Fish, *Bridging the scales in nano engineering and science*, 2006
- D. Cioranescu, *An introduction to homogenisation*, 1999
- A Romkes., J. T. Oden and K. Vemaganti, *Multi-scale goal-oriented adaptive modeling of random heterogeneous materials*, 2006
- F. Larsson and K. Runesson, *On two-scale adaptive FE analysis of micro-heterogeneous media with seamless scale-bridging*, 2011

pierre.kerfriden@gmail.com stephane.bordas@alum.northwestern.edu lars.beex@uni.lu

An adaptive multi-scale method for fracture

Polycrystalline materials

Error Controlled Adaptive Multiscale Method For Fracture Modelling in Polycrystalline materials

Akbari,A.; Kerfriden P.; SPAB, in *Philosophical Magazine* (2015)

http://orbilu.uni.lu/handle/10993/18262

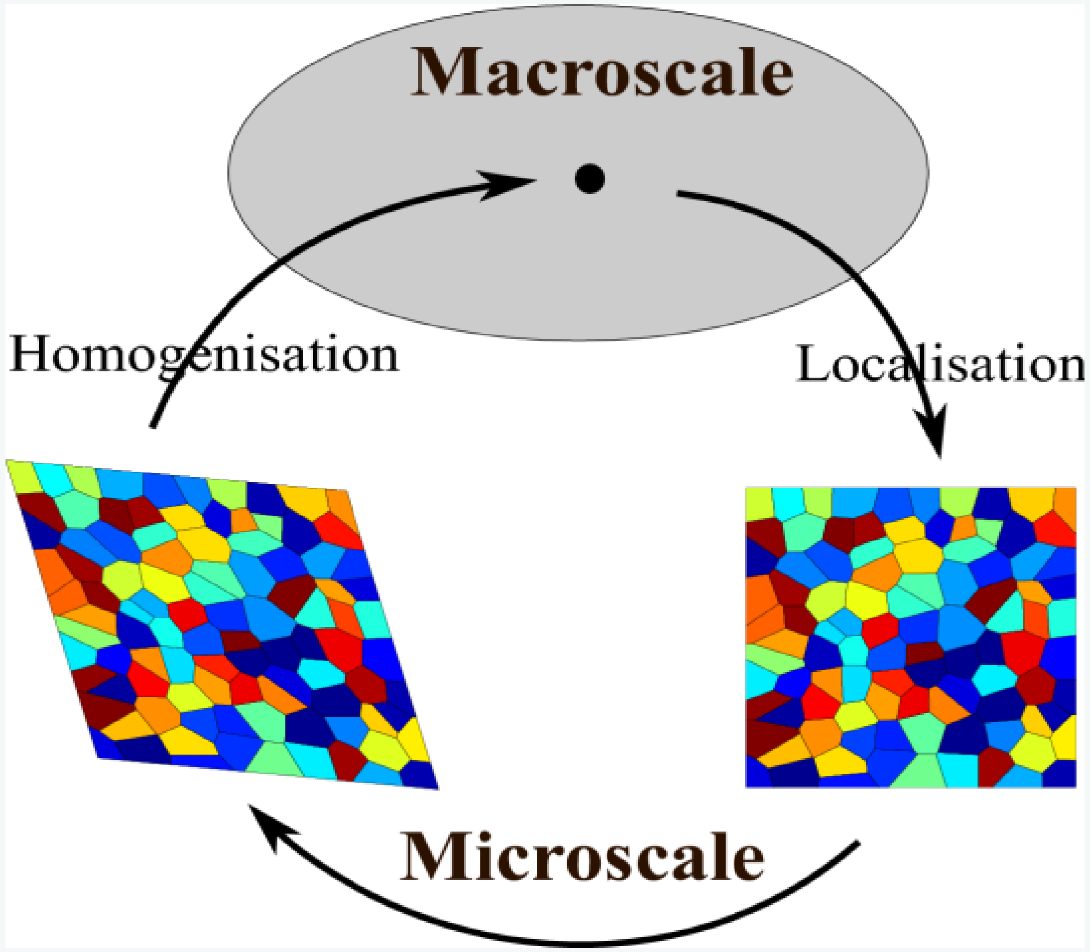

Definition of an RVE

$$l^c \gg l^f \gg l^g$$

Coupling of macroscopic and microscopic levels

The volume averaging theorem is postulated for:

1) Strain tensor:

$$\boldsymbol{\epsilon}^c = \frac{1}{|\Omega(\mathbf{x}^c)|} \int_{\partial\Omega(\mathbf{x}^c)} \mathbf{u}^f \otimes_s \mathbf{n}\, d\Gamma$$

2) Virtual work (Hill-Mandel condition):

$$\boldsymbol{\sigma}^c : \delta\boldsymbol{\epsilon}^c = \frac{1}{|\Omega(\mathbf{x}^c)|} \int_{\partial\Omega(\mathbf{x}^c)} \mathbf{t}^f \cdot \delta\mathbf{u}^f\, d\Gamma$$

3) Stress tensor:

$$\boldsymbol{\sigma}^c = \frac{1}{|\Omega(\mathbf{x}^c)|} \int_{\partial\Omega(\mathbf{x}^c)} \mathbf{t}^f \otimes \mathbf{x}^f\, d\Gamma$$

Akbari,A.; Kerfriden P.; SPAB, in Philosophical Magazine (2015)

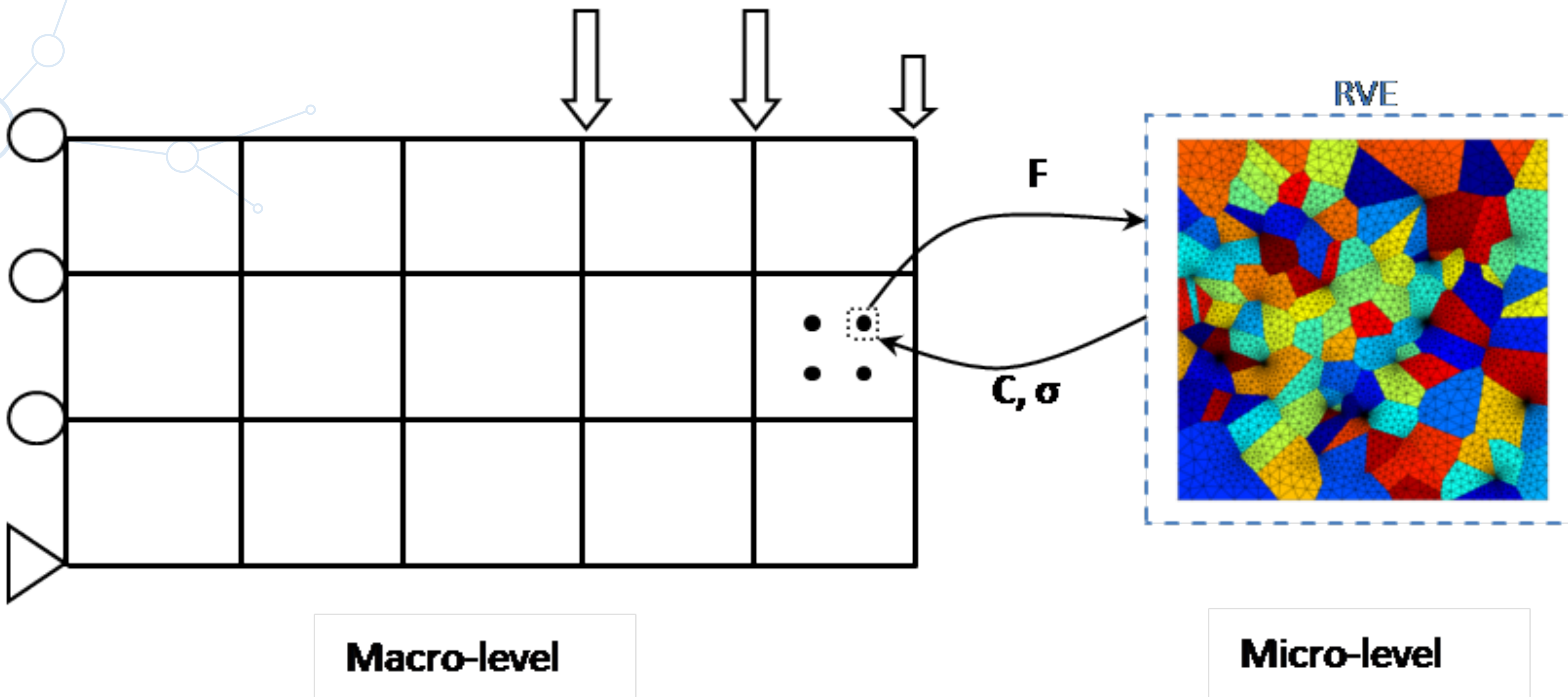

Advantages and abilities:

The macroscopic constitutive law is not required
Non-linear material behaviour can be simulated
Microscale behaviour of material is monitored at each load step

Drawbacks:

In softening regime:

- Lack of scale separation
- Macroscale mesh dependence

Akbari,A.; Kerfriden P.; SPAB, in Philosophical Magazine (2015)

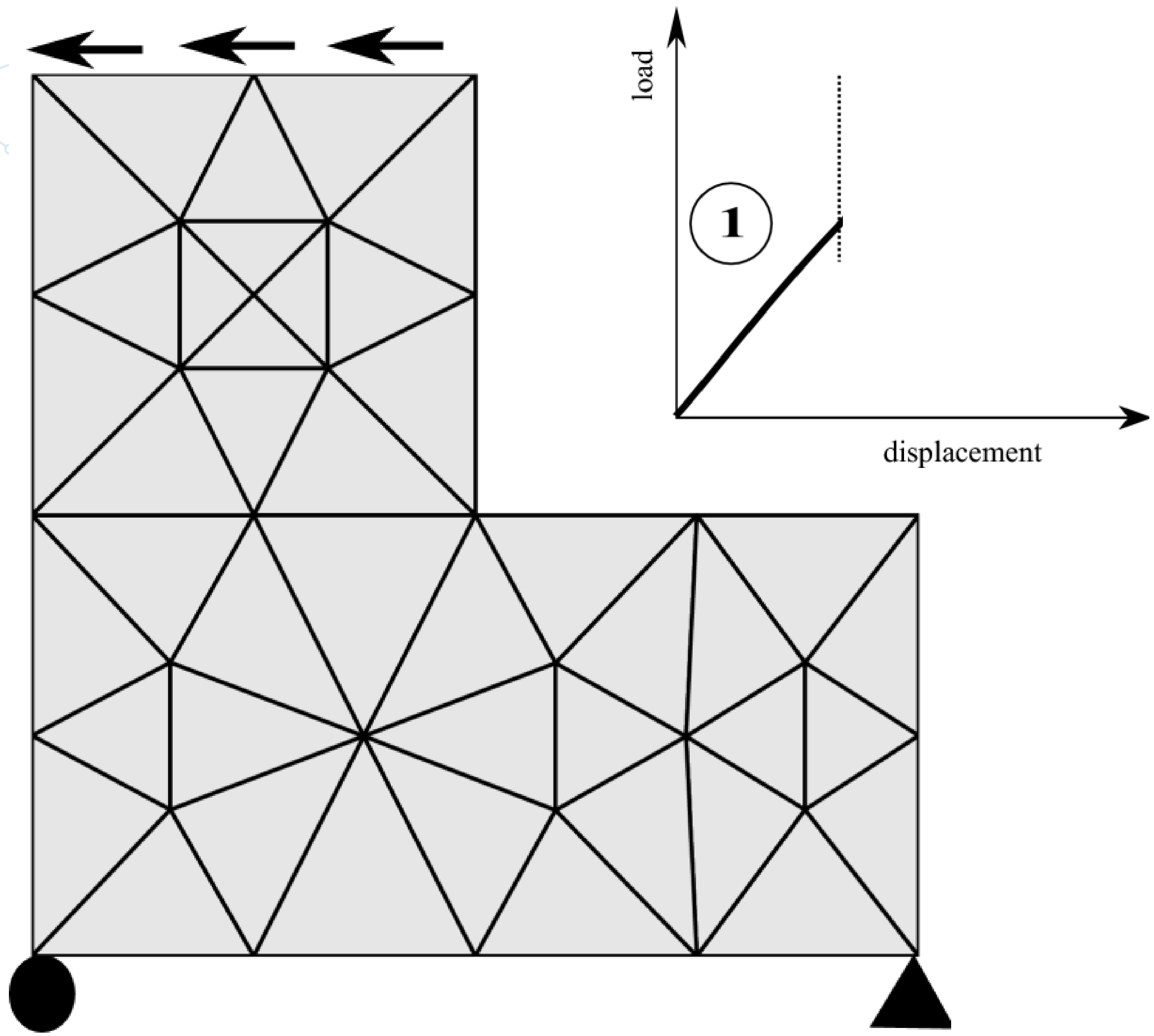

Akbari,A.; Kerfriden P.; SPAB, in Philosophical Magazine (2015)

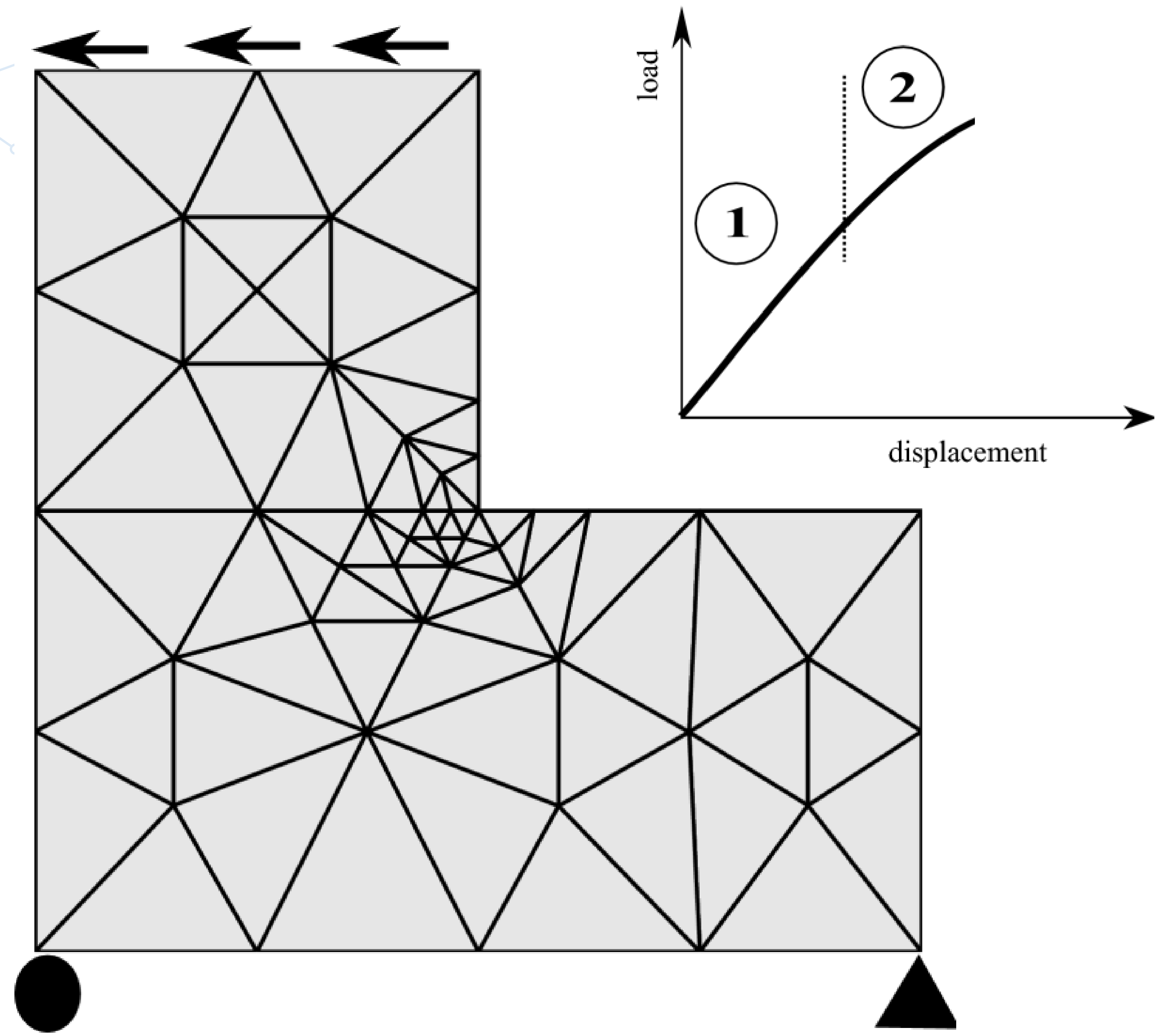

Akbari,A.; Kerfriden P.; SPAB, in Philosophical Magazine (2015)

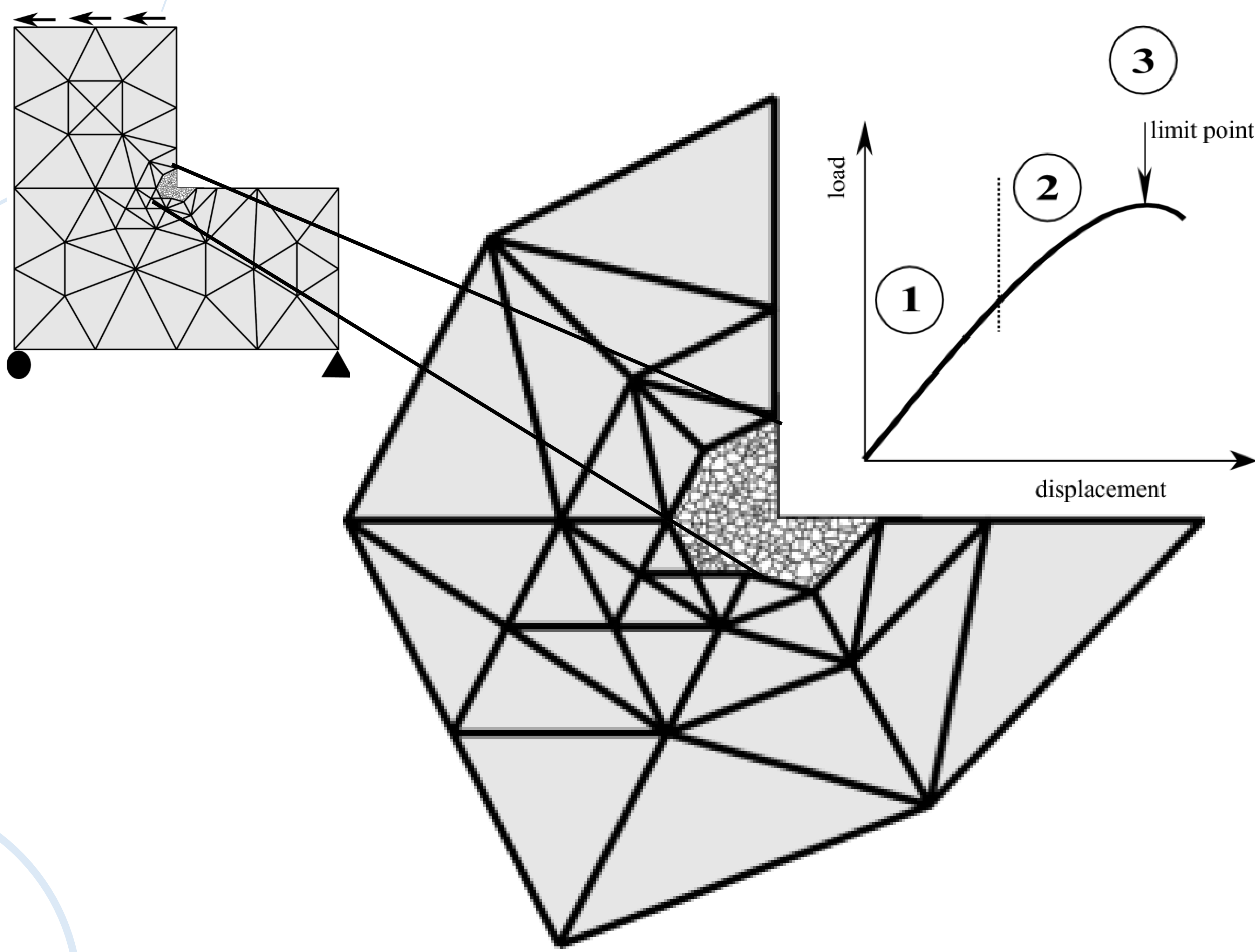

Details in Phil. Magazine, 2015, Akbari, Kerfriden, Bordas

http://orbilu.uni.lu/handle/10993/18262

Akbari,A.; Kerfriden P.; SPAB, in Philosophical Magazine (2015)

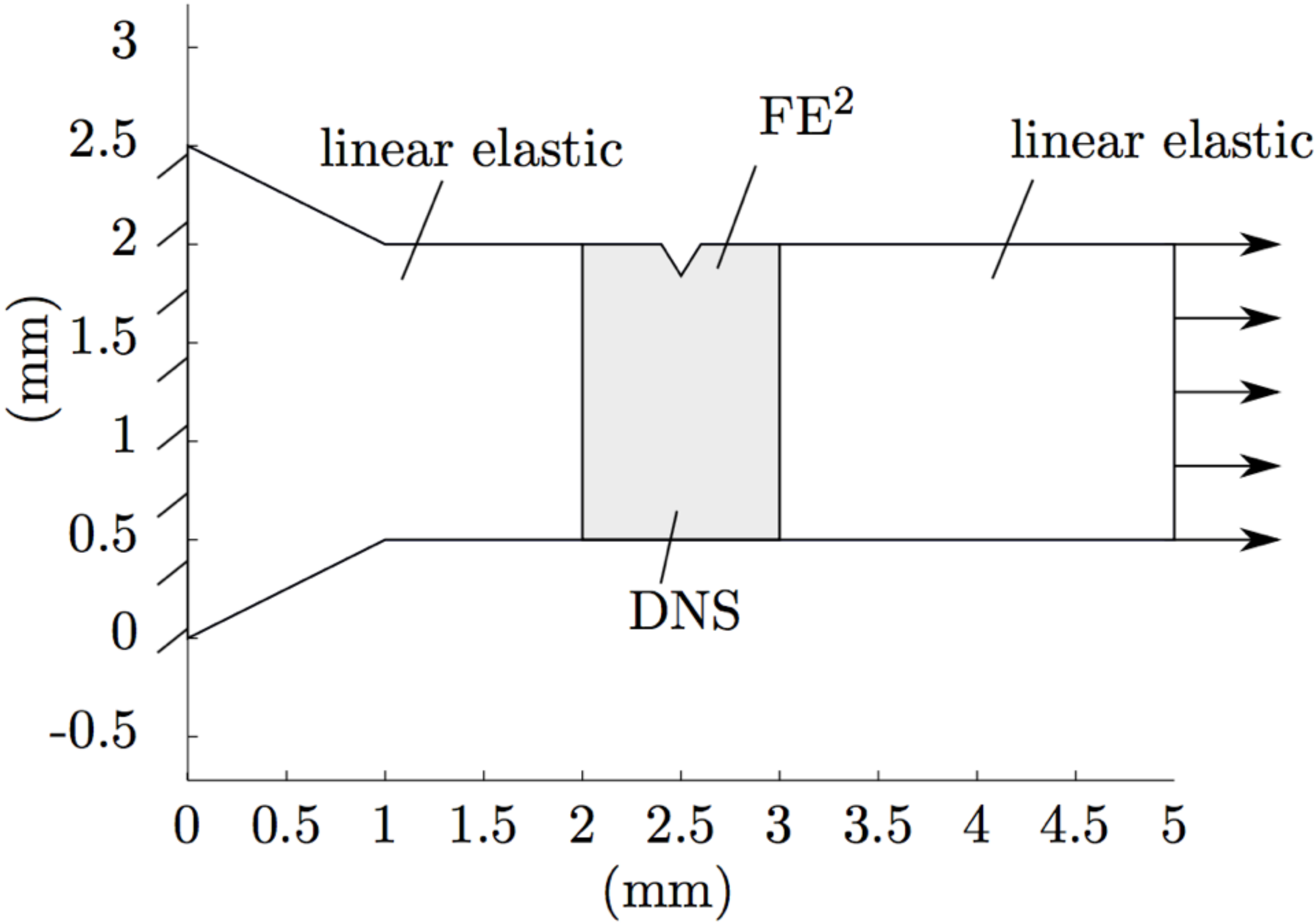

Akbari,A.; Kerfriden P.; SPAB, in Philosophical Magazine (2015)

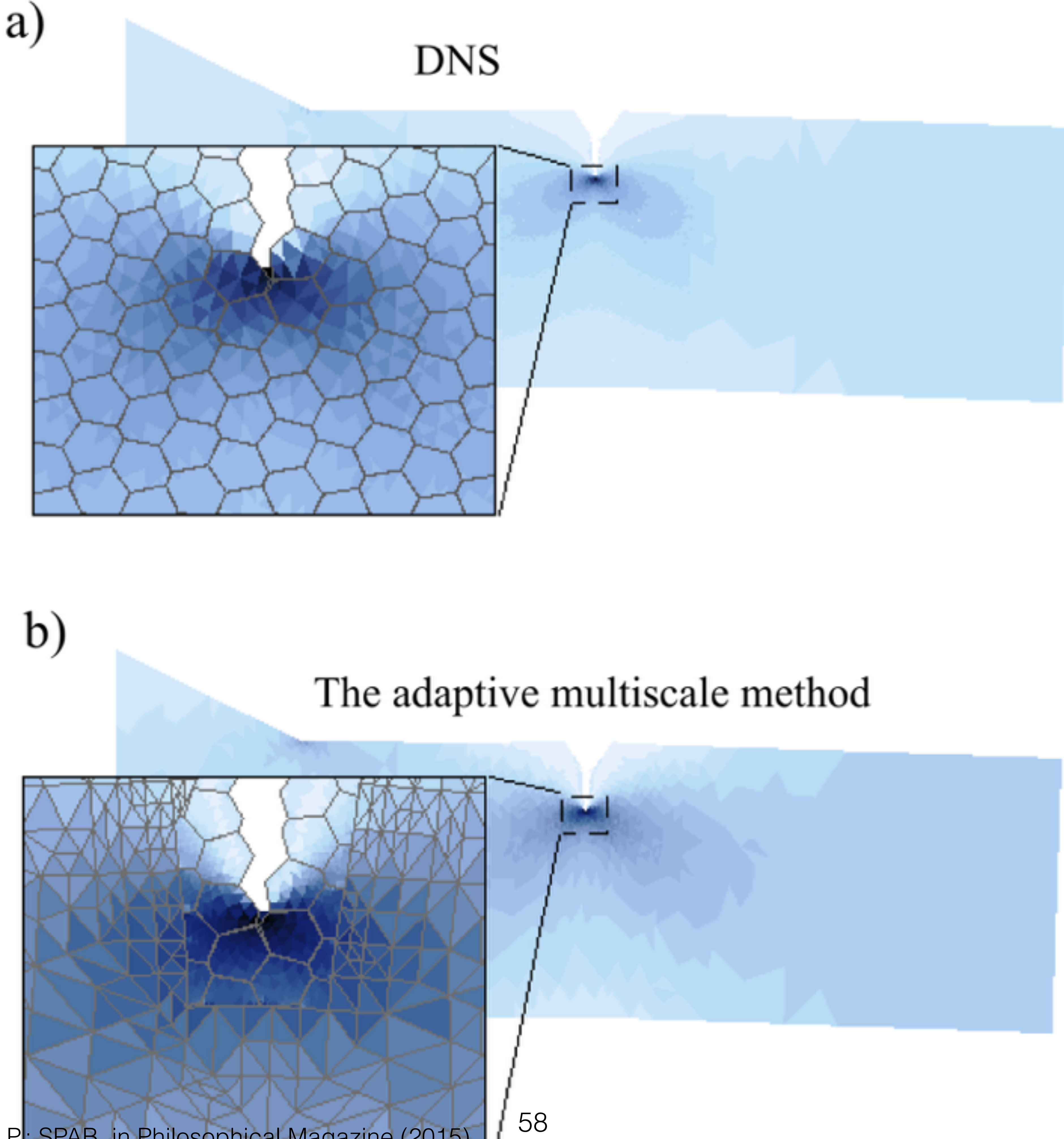

Akbari,A.; Kerfriden P.; SPAB, in Philosophical Magazine (2015)

The distribution of strain-gradient sensitivity $L_{\mathcal{V}} ||\nabla\nabla \mathbf{u}^c||_e$

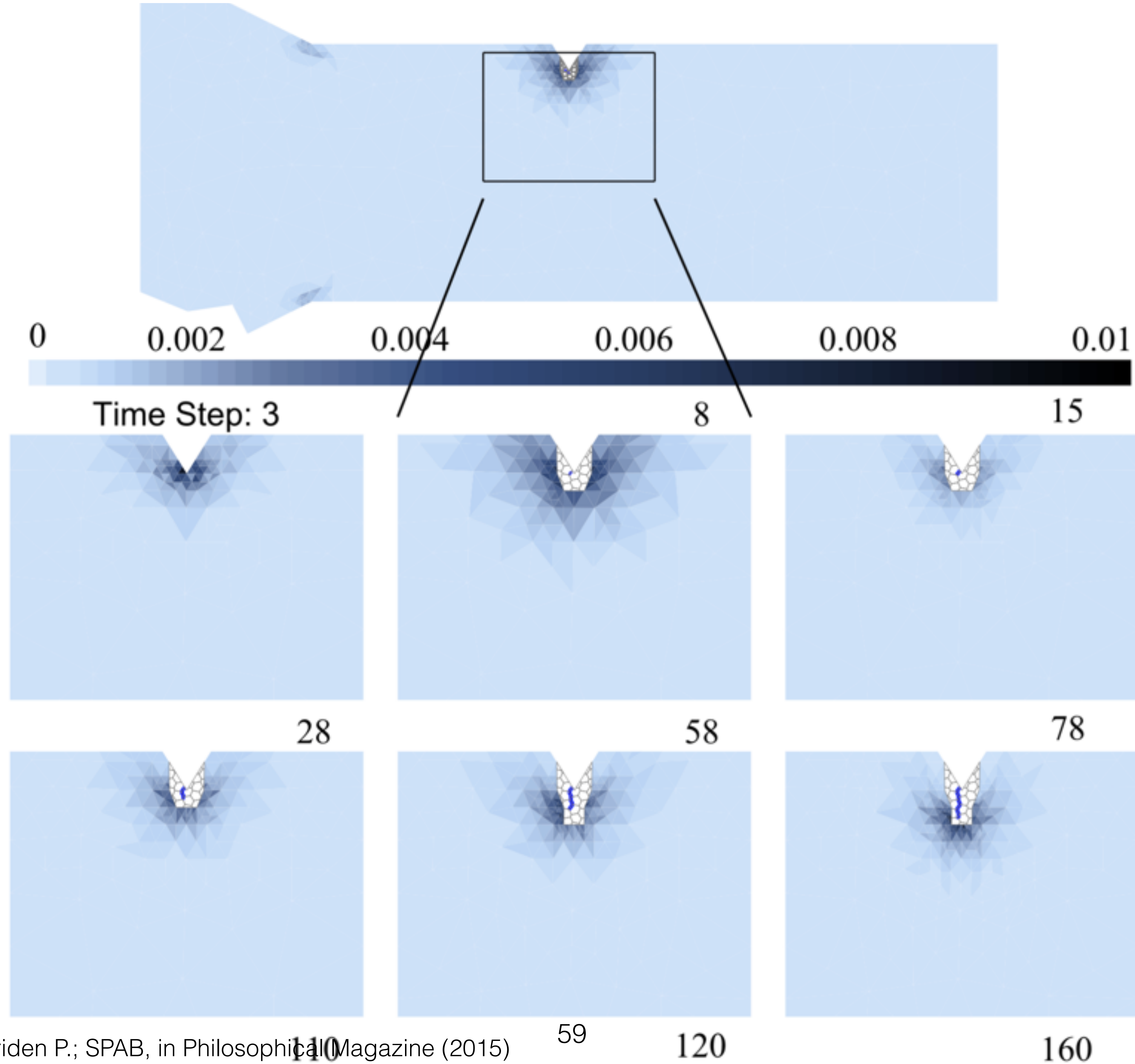

Akbari,A.; Kerfriden P.; SPAB, in Philosophical Magazine (2015)

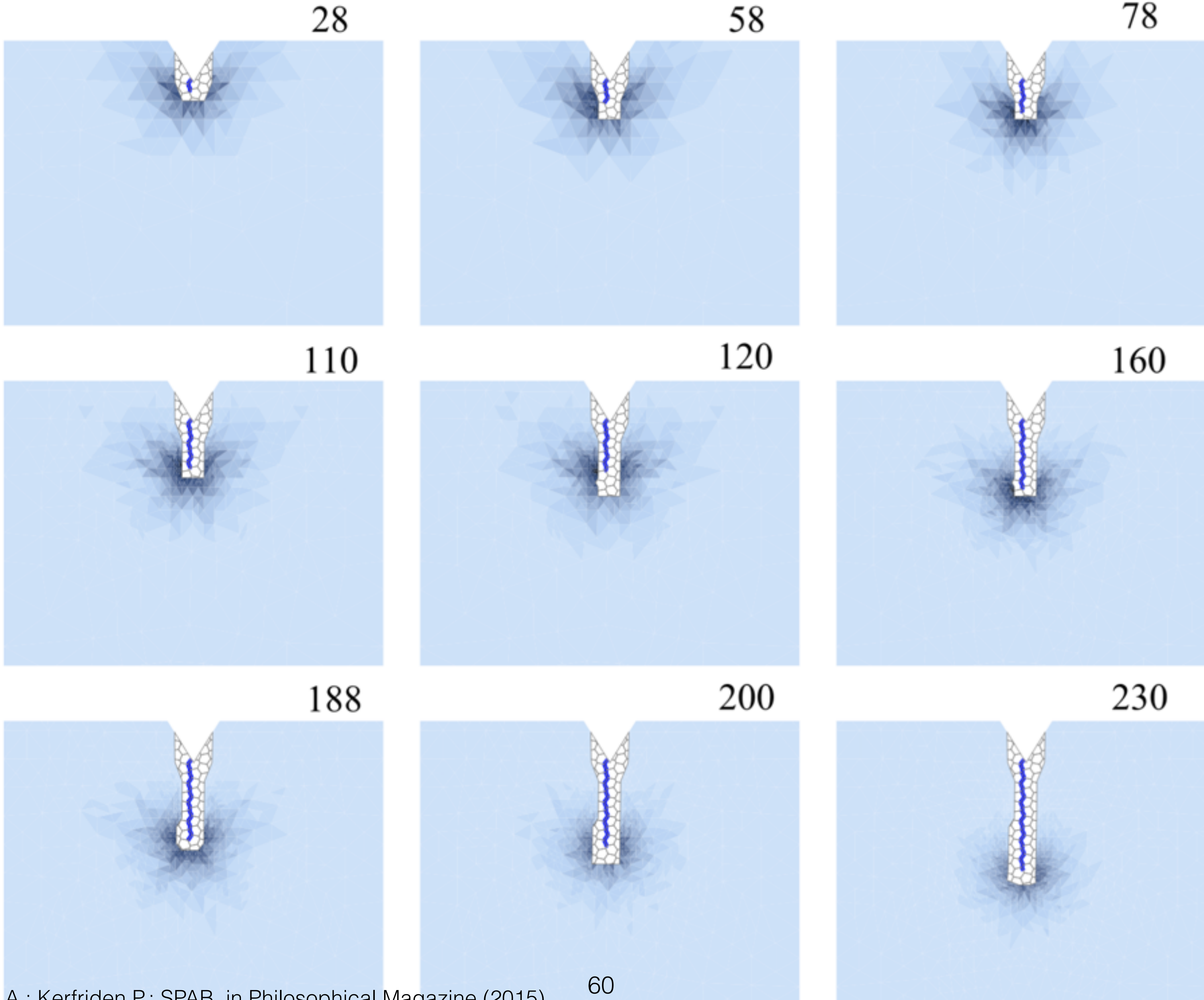

Akbari,A.; Kerfriden P.; SPAB, in Philosophical Magazine (2015)

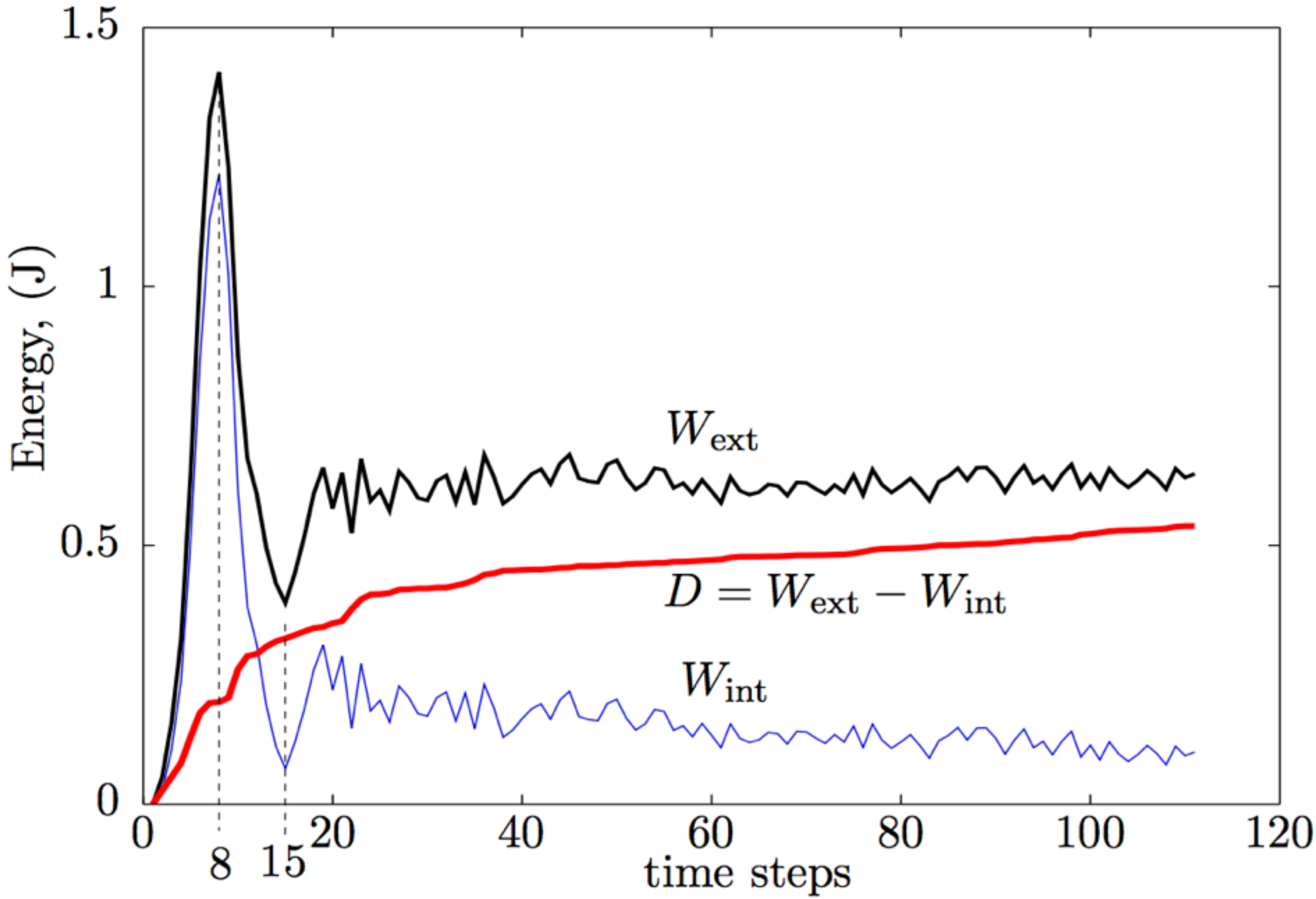

Akbari,A.; Kerfriden P.; SPAB, in Philosophical Magazine (2015)

Philosophical Magazine

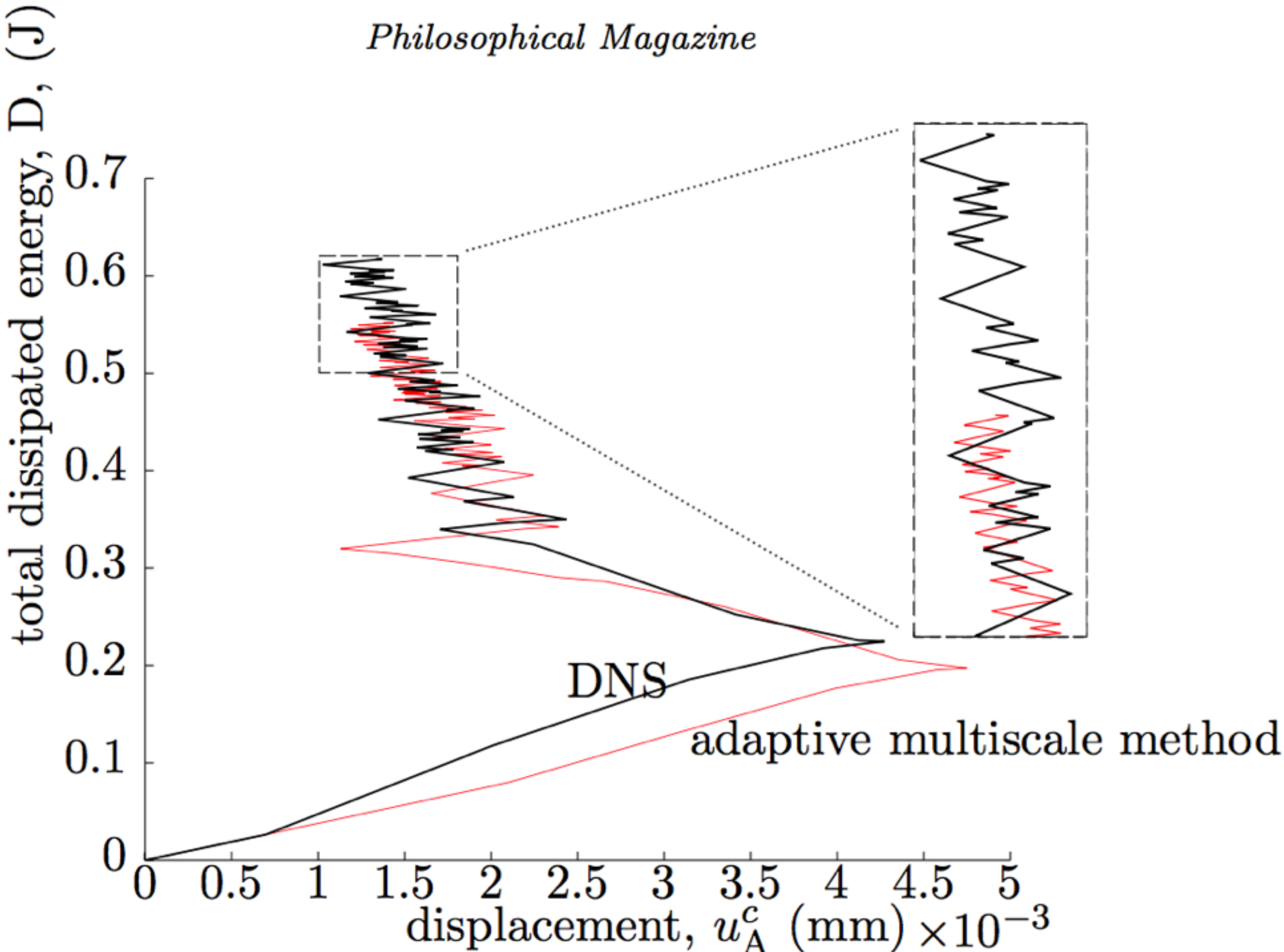

Akbari,A.; Kerfriden P.; SPAB, in Philosophical Magazine (2015)

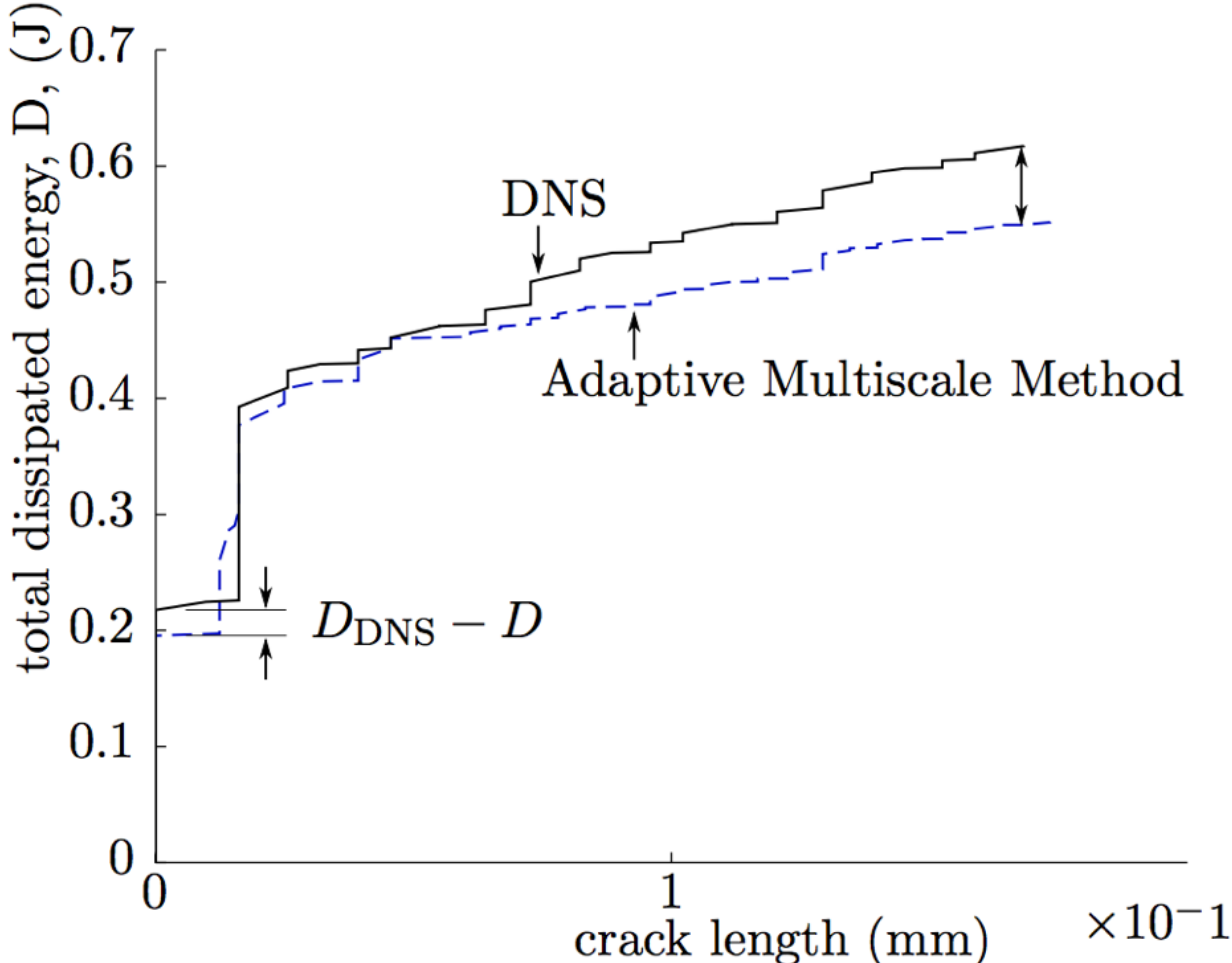

Akbari,A.; Kerfriden P.; SPAB, in Philosophical Magazine (2015)

Adaptive algebraic model order reduction

Part 1. Selective domain-based model order reduction

A partitioned model order reduction approach to rationalise computational expenses in nonlinear fracture mechanics

P. Kerfriden, O. Goury, T. Rabczuk, SPAB *Computer Methods in Applied Mechanics and Engineering*, (2013) 256:169-188.

http://orbilu.uni.lu/handle/10993/10206

Illustration of the method of separated representation

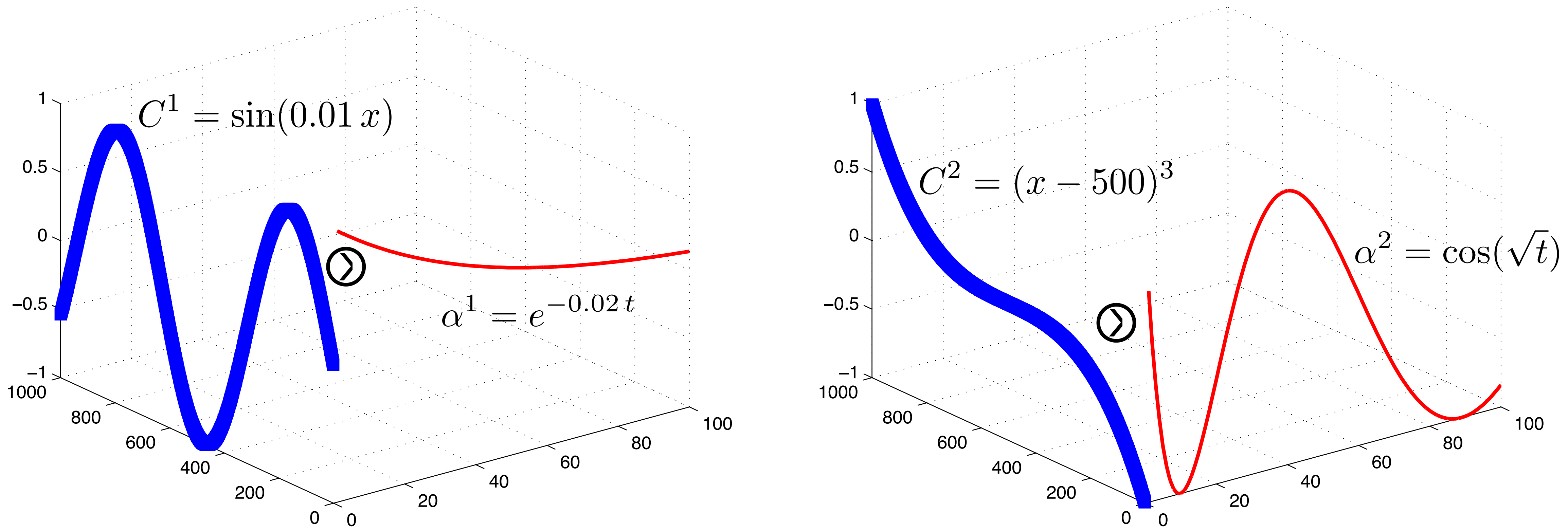

P. Kerfriden, O. Goury, T. Rabczuk, SPAB *Computer Methods in Applied Mechanics and Engineering*, (2013) 256:169-188.

Illustration of the method of separated representation

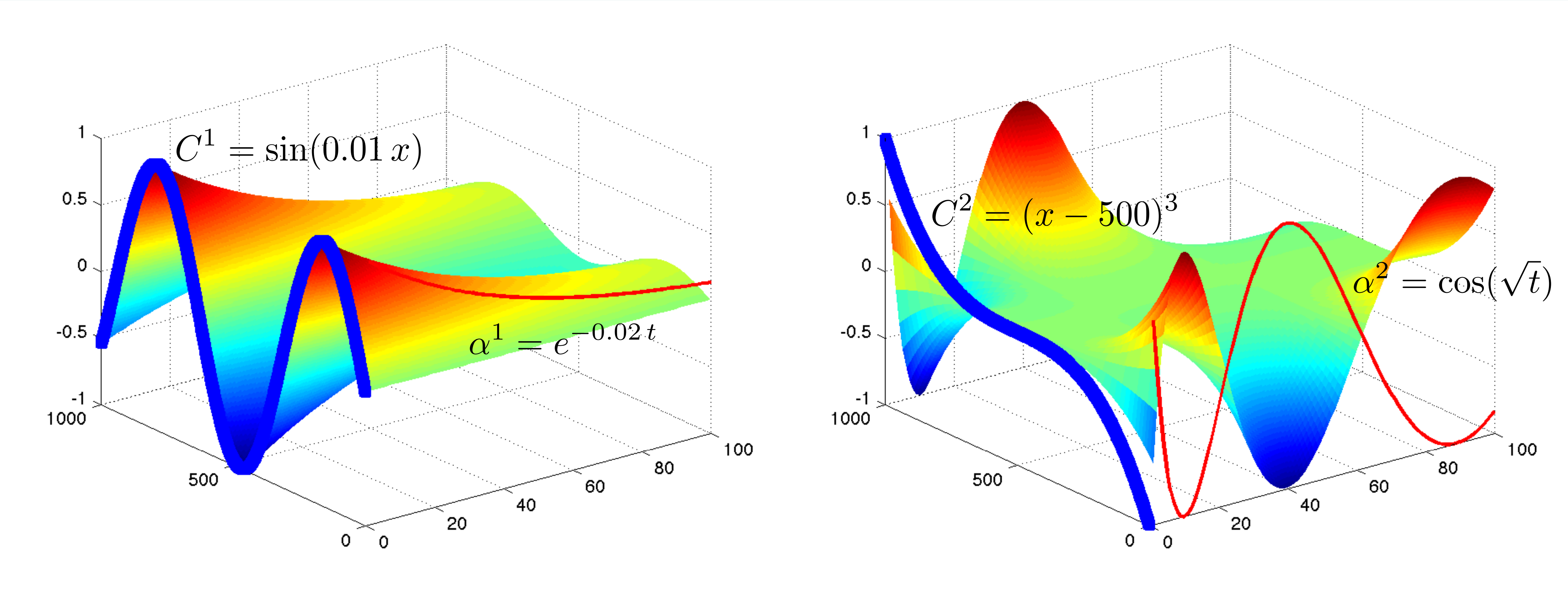

P. Kerfriden, O. Goury, T. Rabczuk, SPAB *Computer Methods in Applied Mechanics and Engineering*, (2013) 256:169-188.

Illustration of the method of separated representation

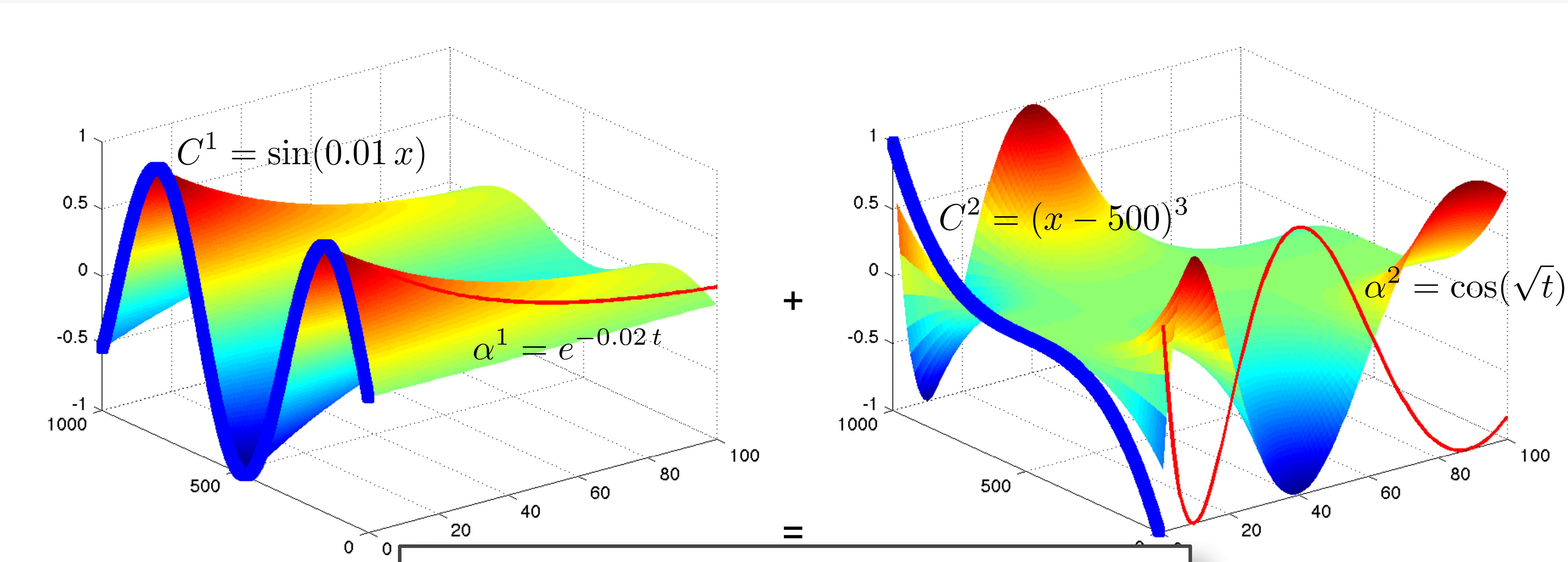

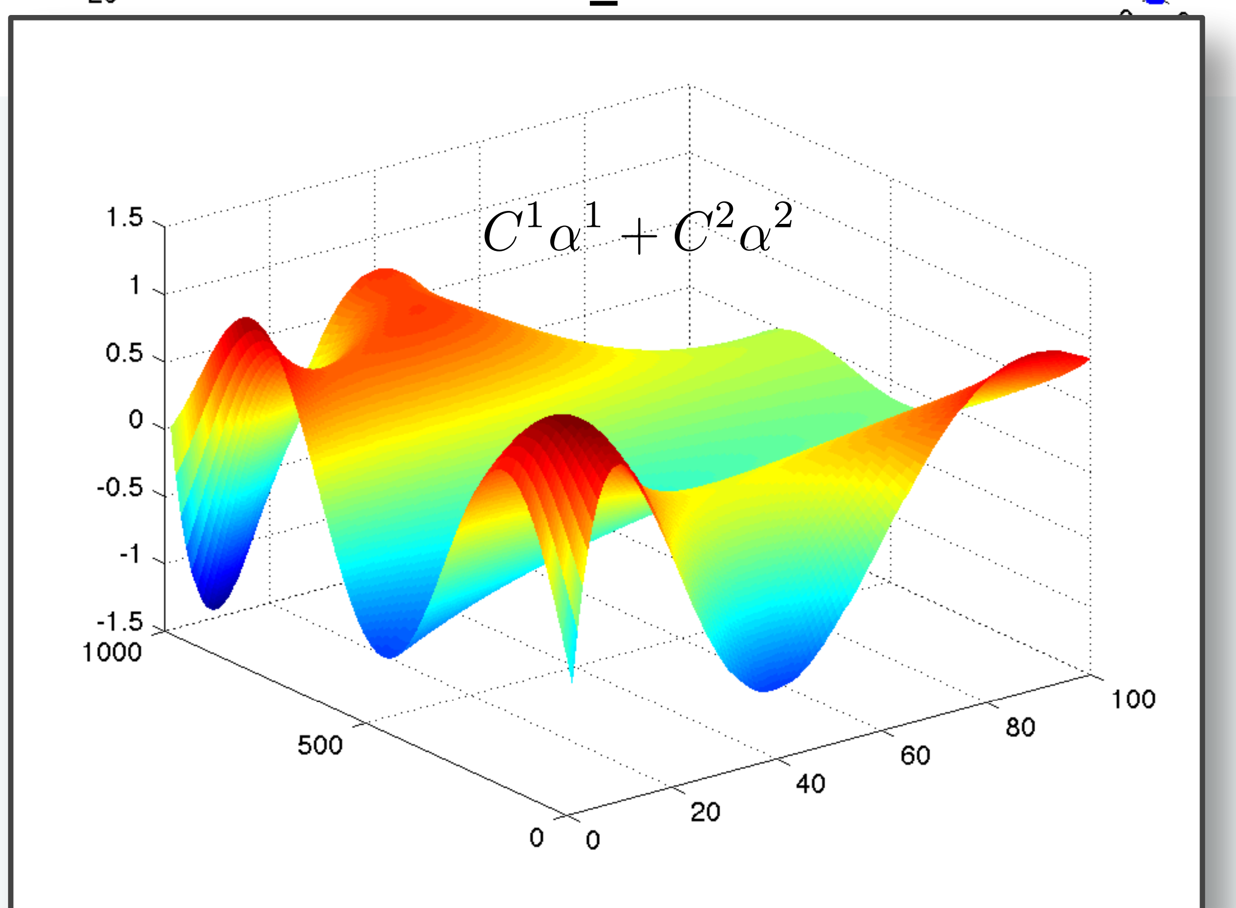

Very rich approximations!

P. Kerfriden, O. Goury, T. Rabczuk, SPAB *Computer Methods in Applied Mechanics and Engineering*, (2013) 256:169-188.

Data compression: get the nose with the POD!

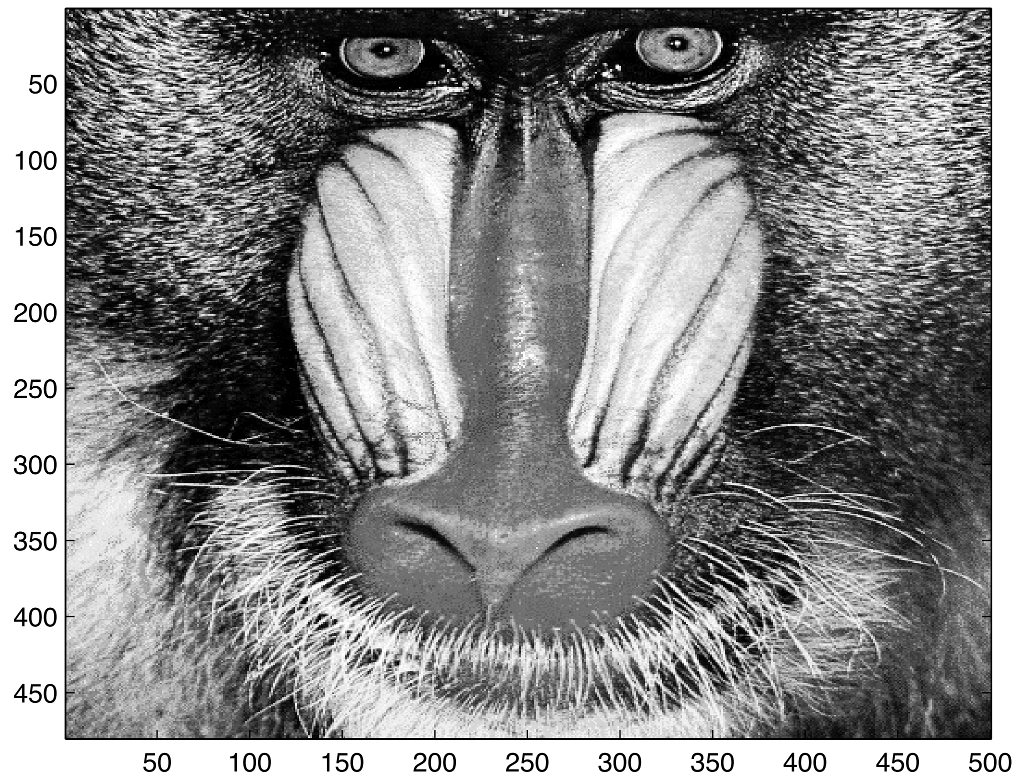

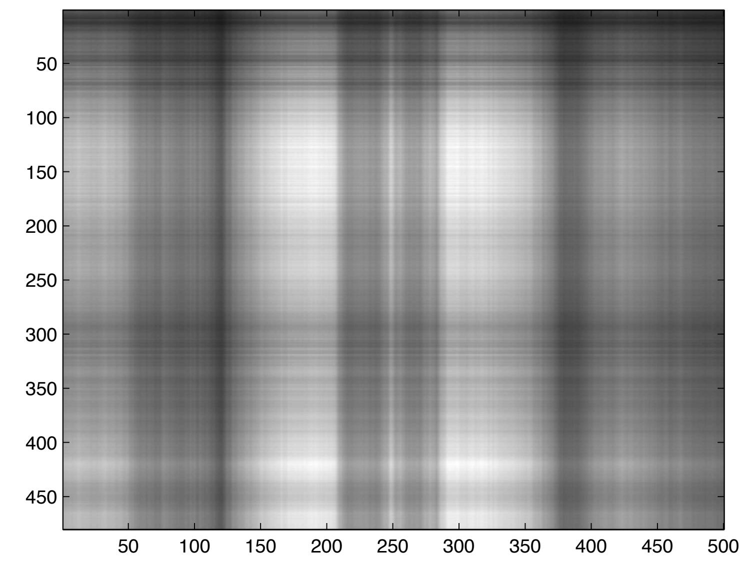

$n_c = 1$

$$\bar{u}(x_i, y_i) = \sum_{i=1}^{n_c} \underline{C}_x^i(x_i)\, \underline{C}_y^i(y_i)$$

$$(C_x^i, C_y^i)_{i \in [\![1, n_c]\!]} = \operatorname{argmin} \sum_{x_i} \sum_{y_j} \left(u(x_i, y_j) - \bar{u}(x_i, y_j)\right)^2$$

P. Kerfriden, O. Goury, T. Rabczuk, SPAB *Computer Methods in Applied Mechanics and Engineering*, (2013) 256:169-188.

Data compression: get the nose with the POD!

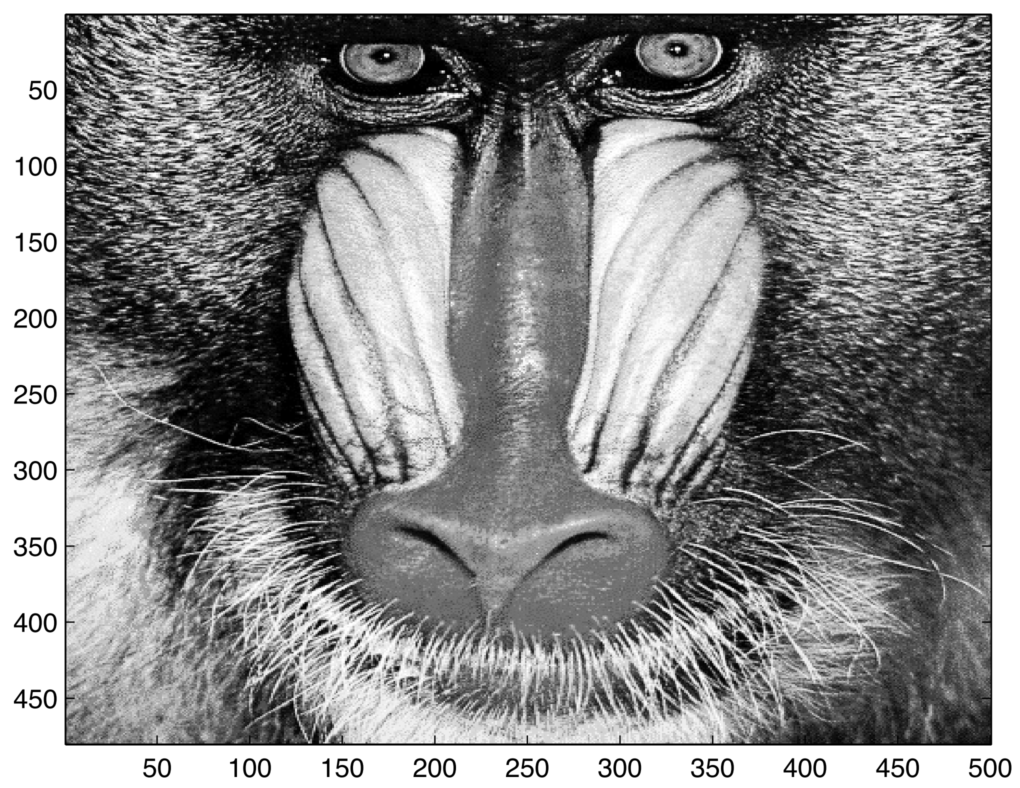

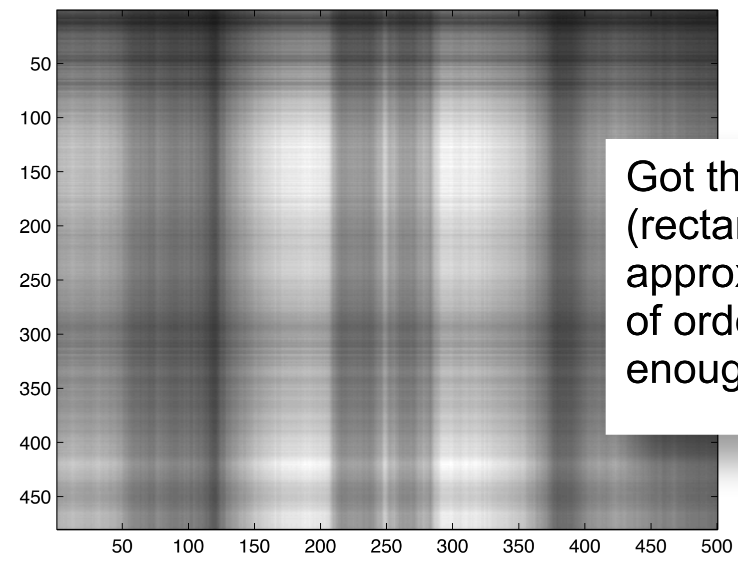

$n_c = 1$

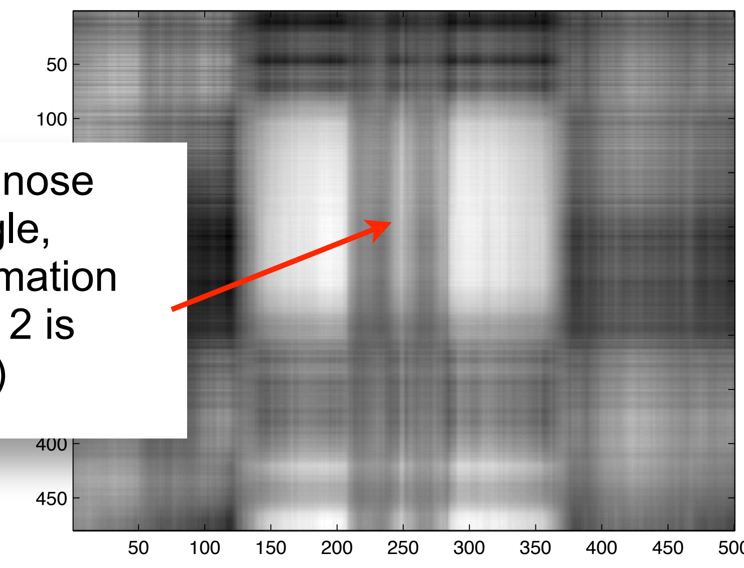

$n_c = 2$

$$\bar{u}(x_i, y_i) = \sum_{i=1}^{n_c} \underline{C}_x^i(x_i)\, \underline{C}_y^i(y_i)$$

$$(C_x^i, C_y^i)_{i \in [\![1, n_c]\!]} = \operatorname{argmin} \sum_{x_i} \sum_{y_j} (u(x_i, y_j) - \bar{u}(x_i, y_j))^2$$

P. Kerfriden, O. Goury, T. Rabczuk, SPAB *Computer Methods in Applied Mechanics and Engineering*, (2013) 256:169-188.

Data compression: get the nose with the POD!

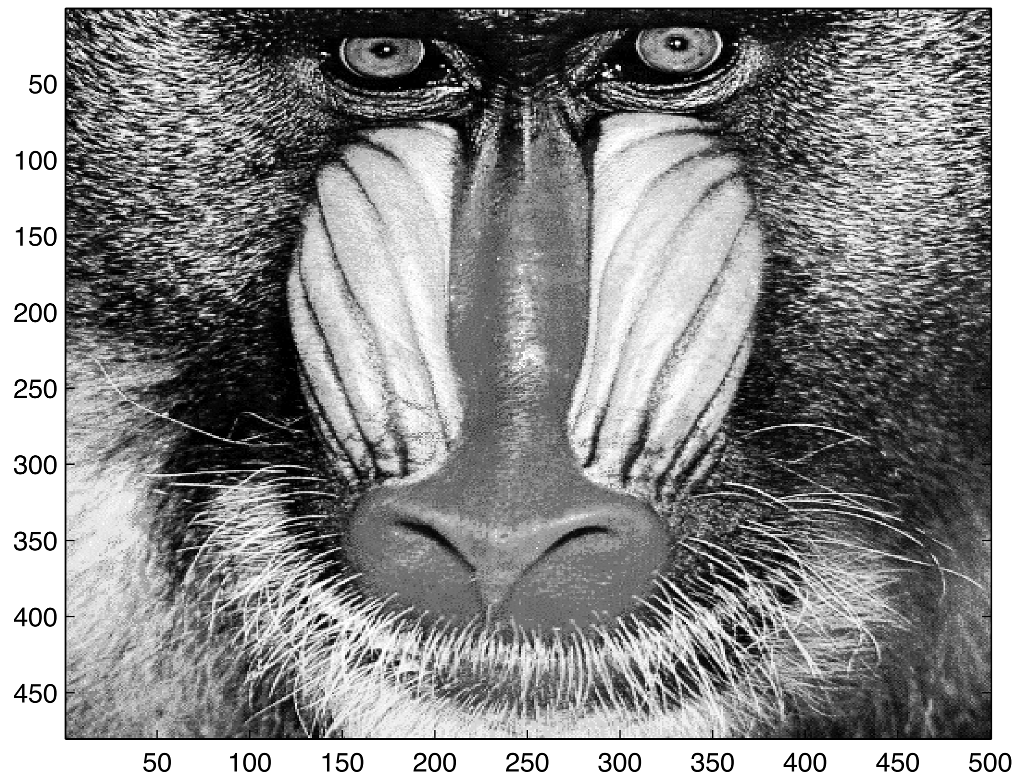

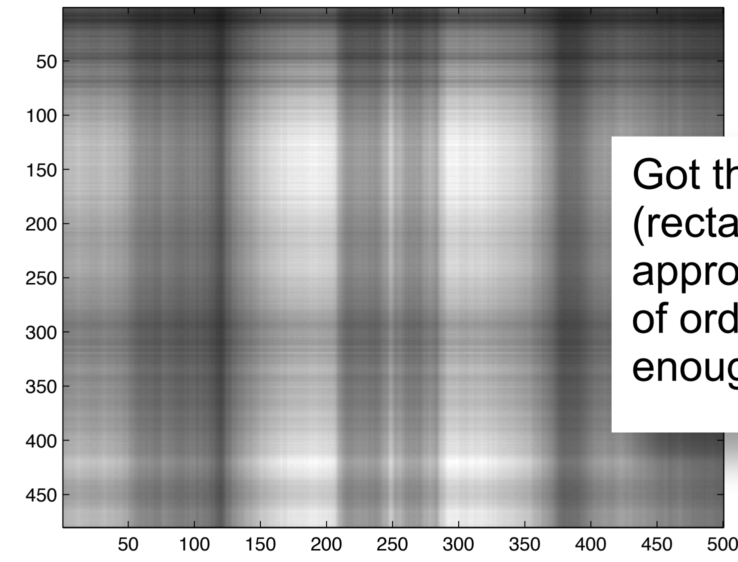

$n_c = 1$

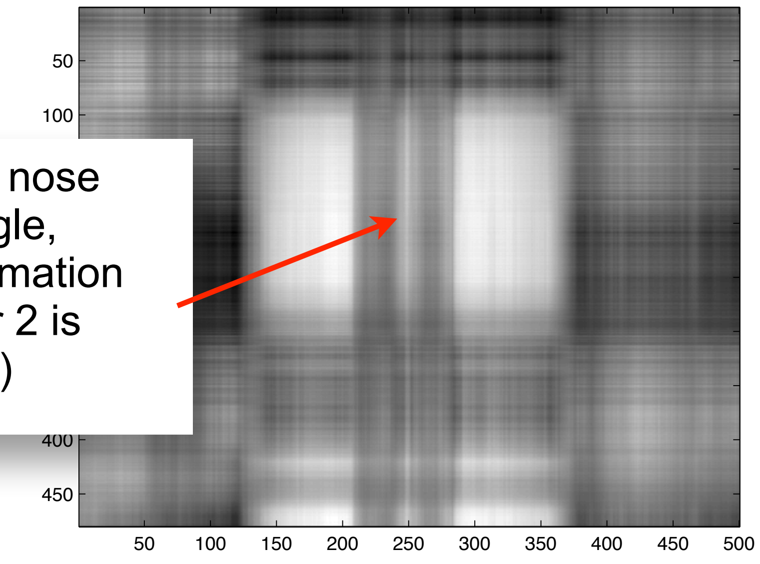

$n_c = 2$

Got the nose (rectangle, approximation of order 2 is enough)

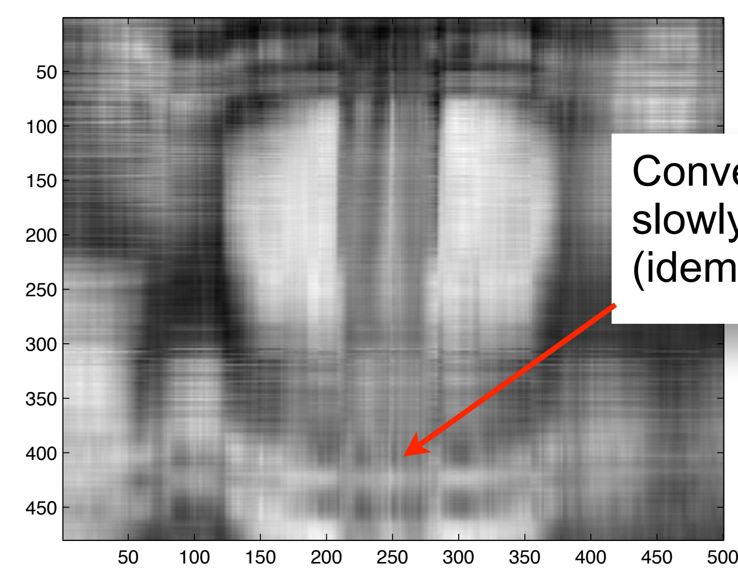

$n_c = 5$

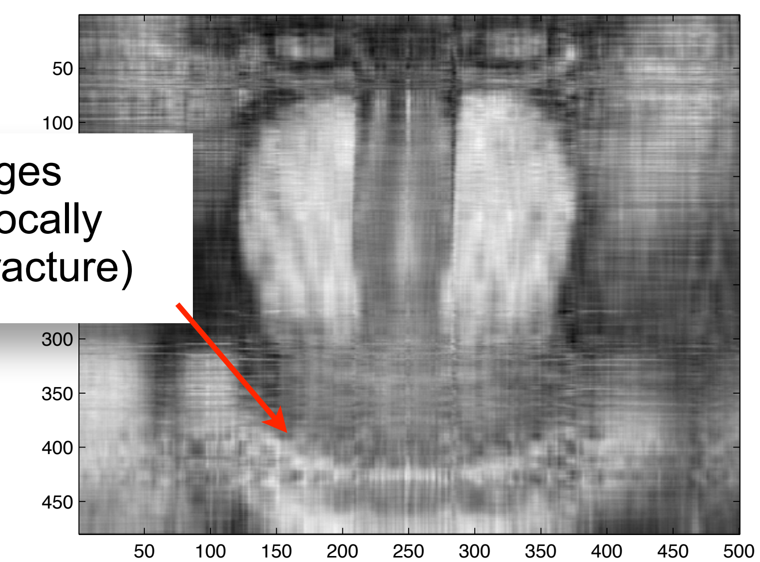

$n_c = 10$

Converges slowly locally (idem fracture)

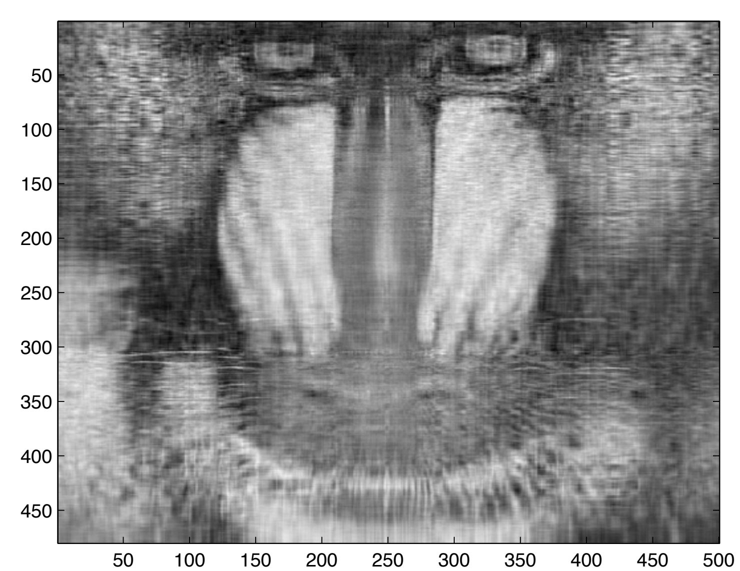

$n_c = 20$

$$\bar{u}(x_i, y_i) = \sum_{i=1}^{n_c} \underline{C}_x^i(x_i)\, \underline{C}_y^i(y_i)$$

$$(C_x^i, C_y^i)_{i \in [\![1, n_c]\!]} = \operatorname{argmin} \sum_{x_i} \sum_{y_j} (u(x_i, y_j) - \bar{u}(x_i, y_j))^2$$

P. Kerfriden, O. Goury, T. Rabczuk, SPAB *Computer Methods in Applied Mechanics and Engineering*, (2013) 256:169-188.

Method of separated representation

$$\boxed{\begin{aligned} \underline{\bar{\mathbf{U}}} : \quad & \mathcal{U}_{\text{sep}} = \mathbb{R}^n \times \mathcal{T} \times \mathcal{P} \rightarrow \mathbb{R}^n \\ & \underline{\bar{\mathbf{U}}}(t,\mu) = \sum_{i=1}^{n_C} \underline{\mathbf{C}}_i \, \beta_i(t) \gamma_i(\mu) \,, \end{aligned}}$$

$$\begin{aligned} & \underline{\mathbf{C}}^i \in \mathbb{R}^n \\ & \beta^i : \mathcal{T} \rightarrow \mathbb{R}, \quad \forall i \in [\![1, n_C]\!] \,, \\ & \gamma^i : \mathcal{P} \rightarrow \mathbb{R}, \quad \forall i \in [\![1, n_C]\!] \,, \end{aligned}$$

$\mathcal{U}_{\text{sep}}$

P. Kerfriden, O. Goury, T. Rabczuk, SPAB *Computer Methods in Applied Mechanics and Engineering*, (2013) 256:169-188.

Proper Orthogonal Decomposition (POD)

$$\underline{\underline{\mathbf{C}}} \in \mathbb{R}^{n \times n_c}, \;\; \underline{\underline{\mathbf{C}}}^T \, \underline{\underline{\mathbf{C}}} = \underline{\underline{\mathbf{I}}}_d$$

$$J_{\mathrm{POD}}(\underline{\underline{\mathbf{C}}}) = \int_{t \in \mathcal{T}} \| \underline{\mathbf{U}}(t) - \underline{\underline{\mathbf{C}}}\, \underline{\underline{\mathbf{C}}}^T \underline{\mathbf{U}}(t) \|_2^2 \, dt$$

$$\bar{J}_{\mathrm{POD}}(\underline{\underline{\mathbf{C}}}) = \int_{t \in \mathcal{T}} \underline{\mathbf{U}}(t)^T \underline{\underline{\mathbf{C}}}\, \underline{\underline{\mathbf{C}}}^T \underline{\mathbf{U}}(t) \, dt = \mathrm{Tr}(\underline{\underline{\mathbf{C}}}^T \underline{\underline{\mathbf{K}}}\, \underline{\underline{\mathbf{C}}})$$

$$\underline{\underline{\mathbf{K}}} = \int_{t \in \mathcal{T}} \underline{\mathbf{U}}(t) \, \underline{\mathbf{U}}(t) \, dt$$

$\underline{\underline{\mathbf{K}}}\, \underline{\phi}^k = \lambda^k \underline{\phi}^k$ where $(\lambda^k)_{k \in [\![0,n]\!]}$ in decreasing order

$$\underline{\underline{\mathbf{C}}} = \begin{pmatrix} \underline{\phi}^1 & \underline{\phi}^2 & \dots & \underline{\phi}^{n_c} \end{pmatrix}$$

$$\int_{t \in \mathcal{T}} \alpha^i \, \alpha^j \, dt = \delta_{ij} \, \lambda^i$$

$$J_{\mathrm{POD}}(\underline{\underline{\mathbf{C}}}) = \sum_{k=n_c+1}^{n} \lambda^k$$

P. Kerfriden, O. Goury, T. Rabczuk, SPAB *Computer Methods in Applied Mechanics and Engineering*, (2013) 256:169-188.

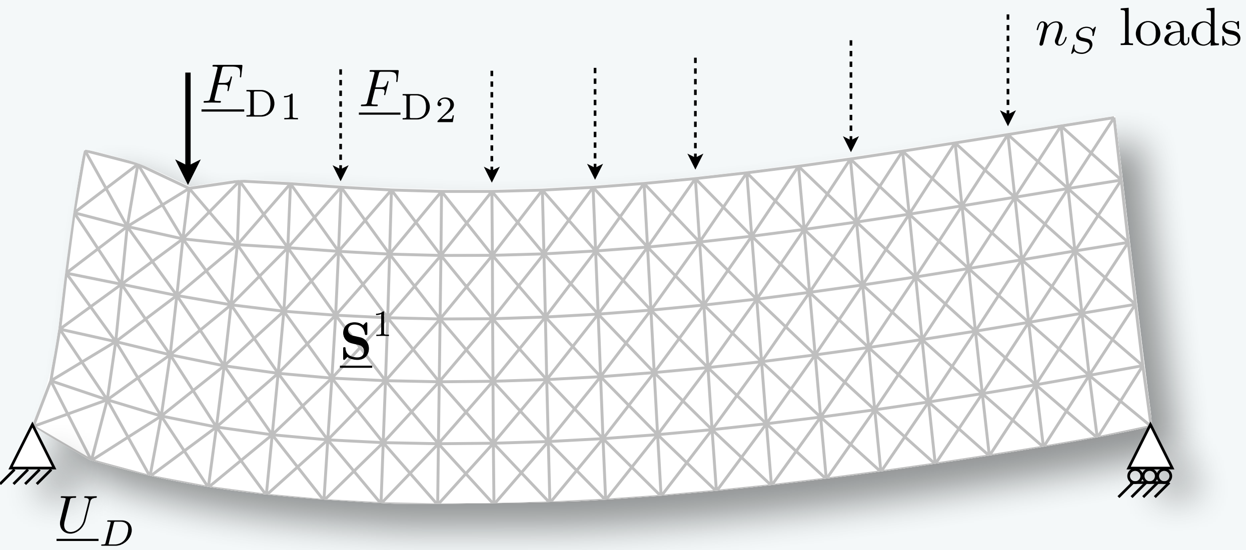

(1) Solve FINE for n_S parameters (EXPENSIVE!)

$$\underline{\underline{\mathbf{S}}} = \left(\underline{\mathbf{S}}^1 \quad \underline{\mathbf{S}}^2 \quad \dots \quad \underline{\mathbf{S}}^{n_S} \right)$$

(2) Singular value decomposition

$$\underline{\underline{\mathbf{S}}} = \underline{\underline{\mathbf{U}}}\,\underline{\underline{\mathbf{\Sigma}}}\,\underline{\underline{\mathbf{V}}}^T = \sum_{k=1}^{n_S} \Sigma^k \, \underline{\mathbf{U}}^k \, \underline{\mathbf{V}}^{k\,T}$$

n_S solutions, sorted by relevance

where $(\Sigma^k)_{k \in [\![1 \;\; n_S]\!]}$ in decreasing order

(3) Truncation

Reduced basis: family of representative solutions

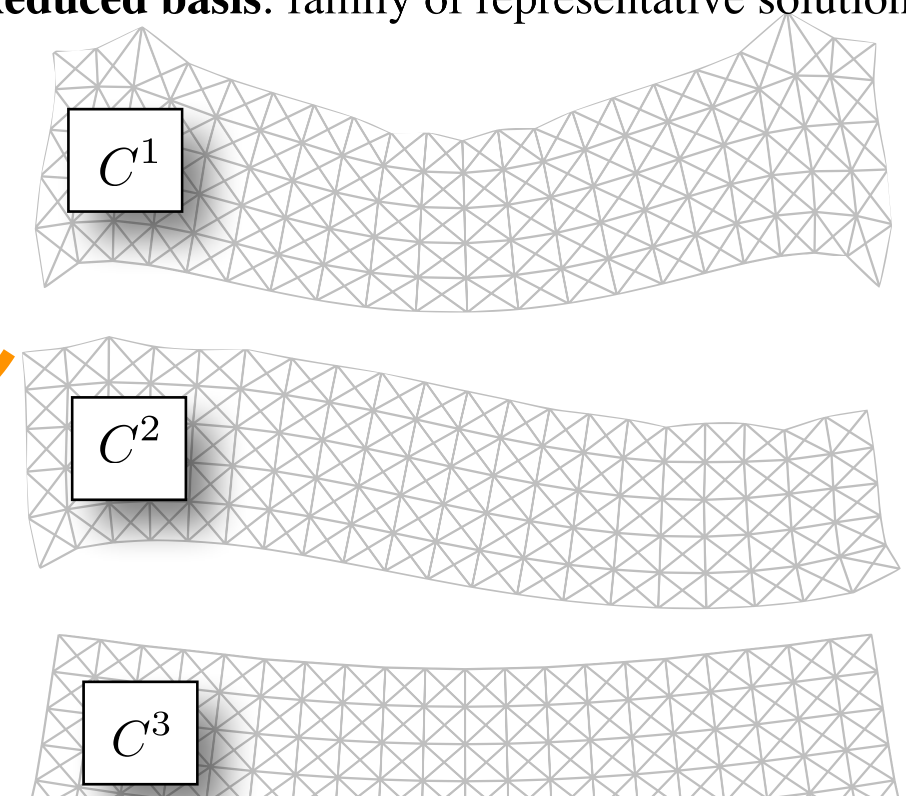

$$\underline{\underline{\mathbf{C}}} = \left(\underline{\mathbf{U}}^1 \quad \underline{\mathbf{U}}^2 \quad \dots \quad \underline{\mathbf{U}}^{n_C} \right)$$

Family of representative solutions

$$\underline{\mathbf{U}} = \underline{\underline{\mathbf{C}}}\,\underline{\alpha}$$

Solution

Coefficients

Initial set of equations

$$\underline{\mathbf{F}}_{\text{Int}}\left(\underline{\mathbf{U}}\right) + \underline{\mathbf{F}}_{\text{Ext}} = 0$$

(4) Galerkin orthogonality

$$\underline{\underline{\mathbf{C}}}^T \underline{\mathbf{F}}_{\text{int}}\left(\underline{\underline{\mathbf{C}}}\,\underline{\alpha}\right) + \underline{\underline{\mathbf{C}}}^T \underline{\mathbf{F}}_{\text{ext}} = 0$$

Approximation of the solution in a space of small dimension (n_c)

P. Kerfriden, O. Goury, T. Rabczuk, SPAB *Computer Methods in Applied Mechanics and Engineering*, (2013) 256:169-188.

Limitations: case of highly non-linear fracture mechanics pbs

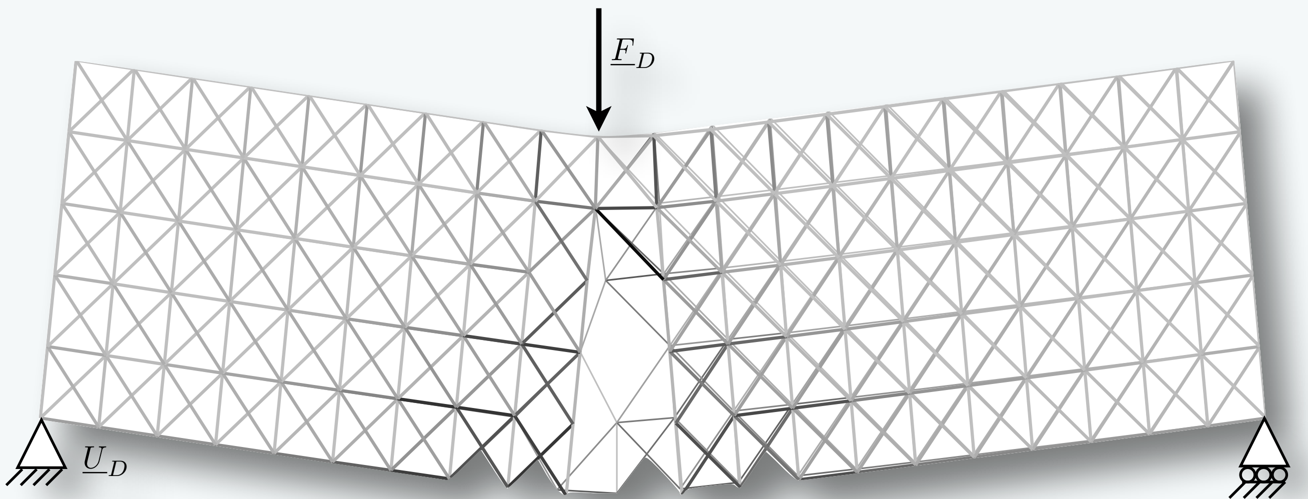

This solution is not in the snapshot !

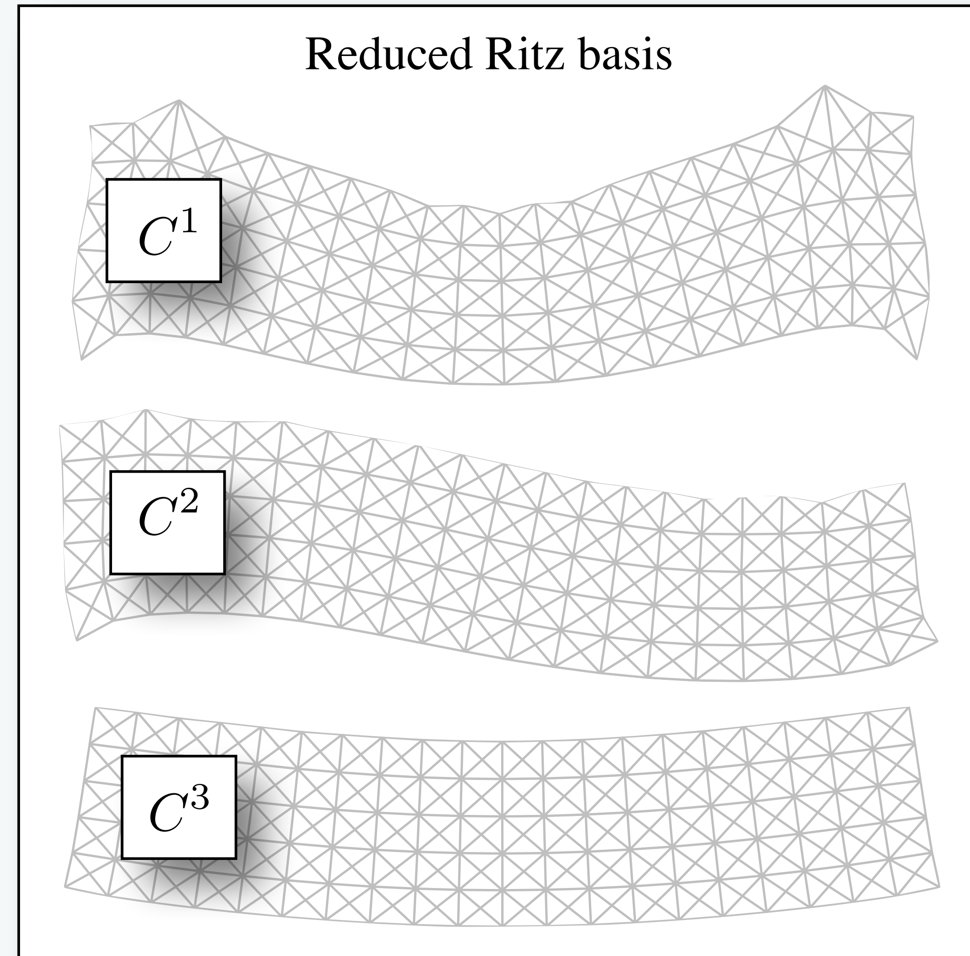

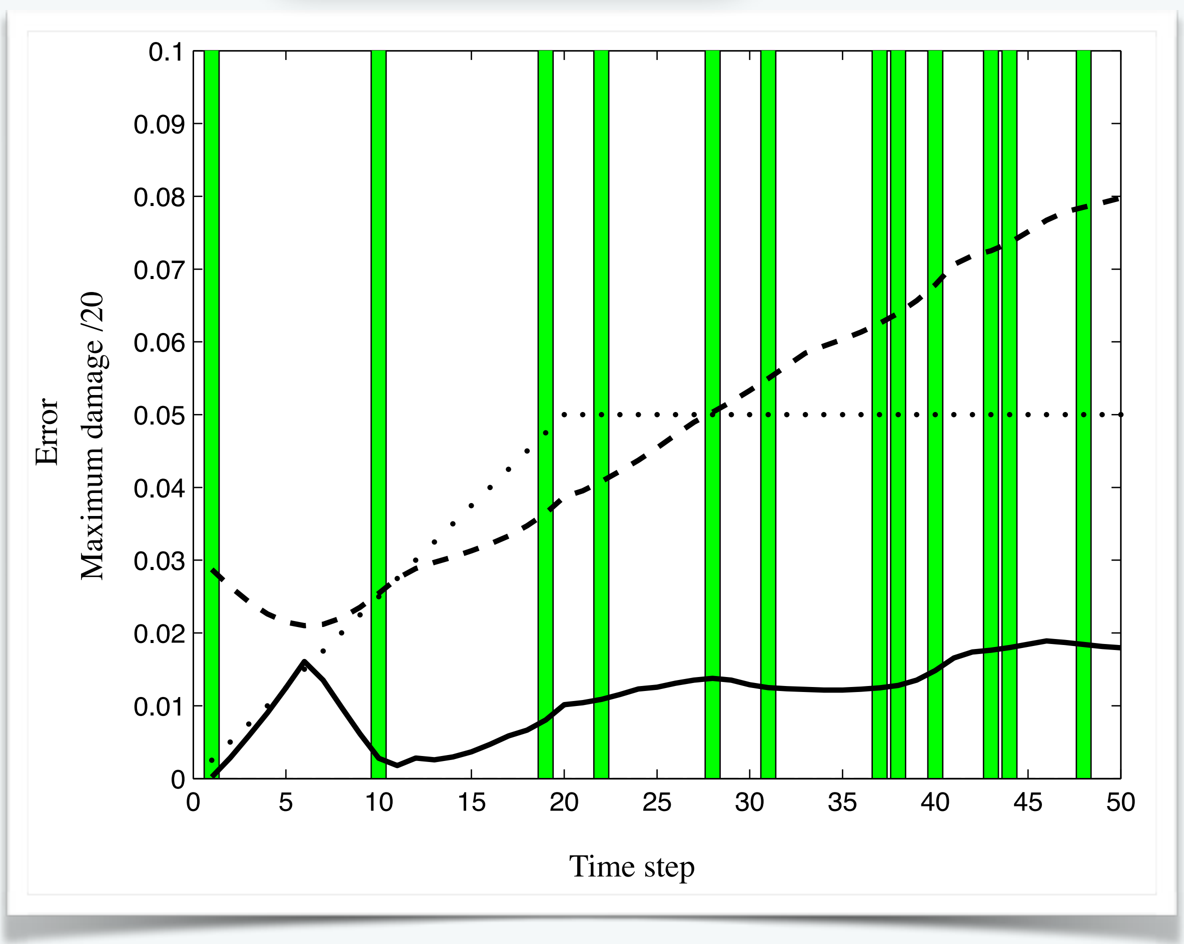

P. Kerfriden, O. Goury, T. Rabczuk, SPAB *Computer Methods in Applied Mechanics and Engineering*, (2013) 256:169-188.

Application to a parametric fracture problem

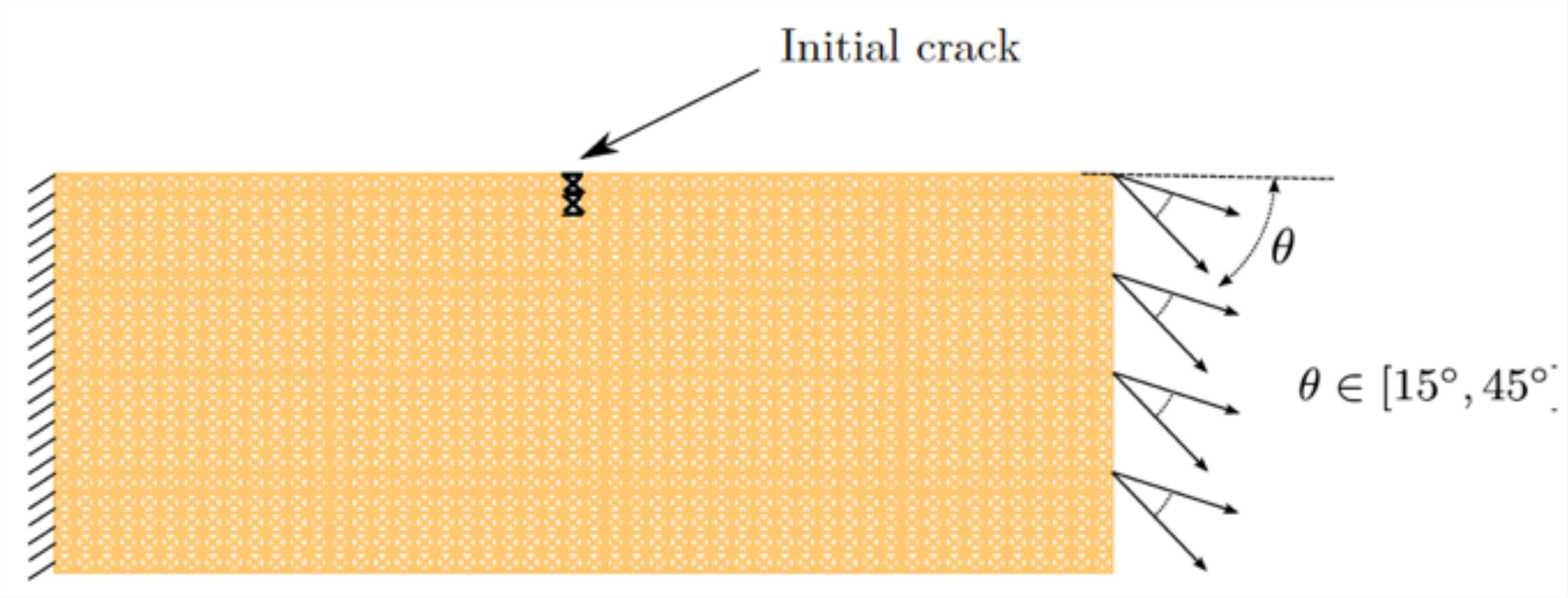

P. Kerfriden, O. Goury, T. Rabczuk, SPAB *Computer Methods in Applied Mechanics and Engineering*, (2013) 256:169-188.

Application to a parametric fracture problem

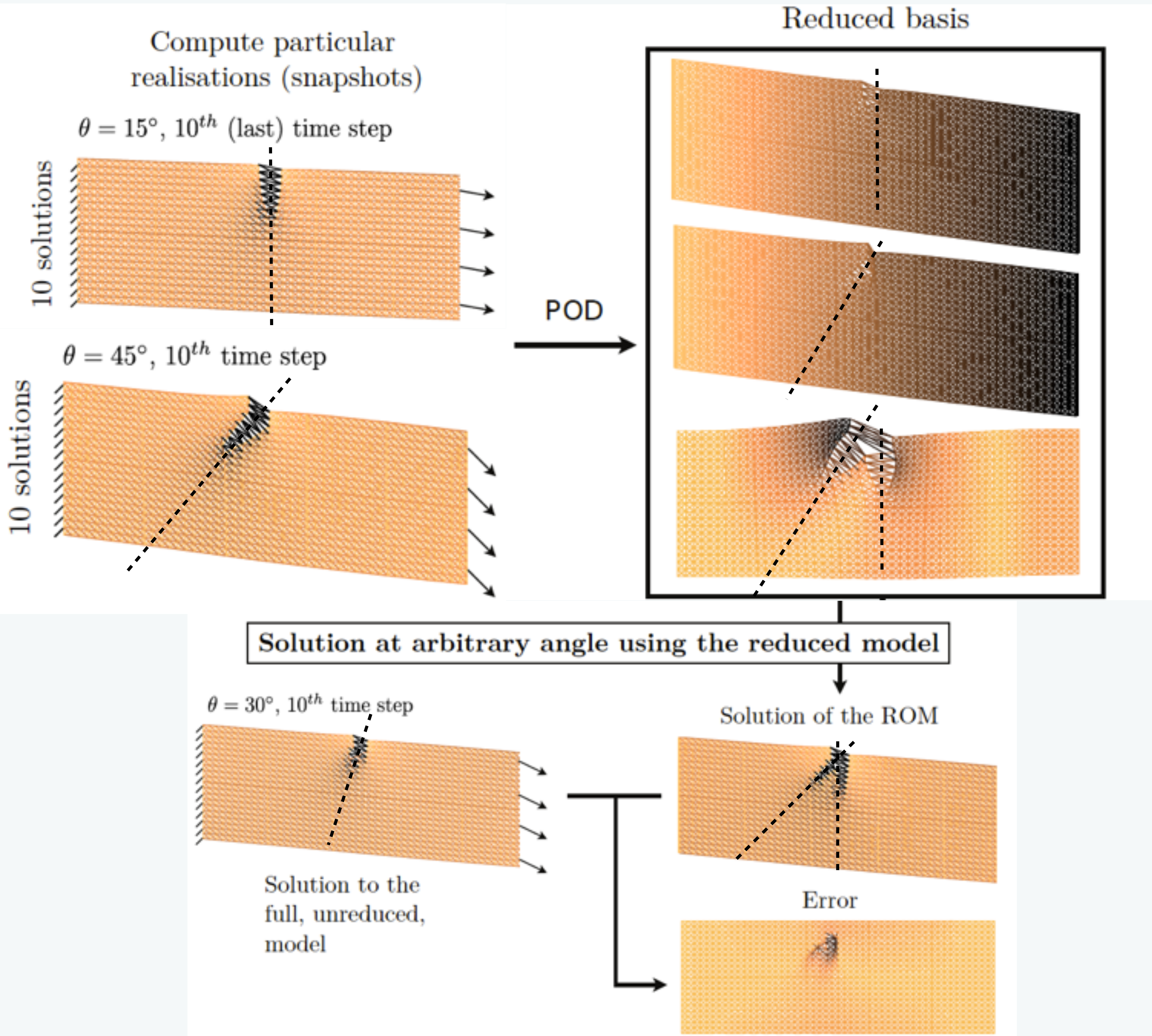

- The POD solution is not able to reproduce the solution in the cracked area
- Due to lack of correlatio introduced by crack growth
- Leads to a local projection error

Parametric / stochastic multiscale fracture mechanics

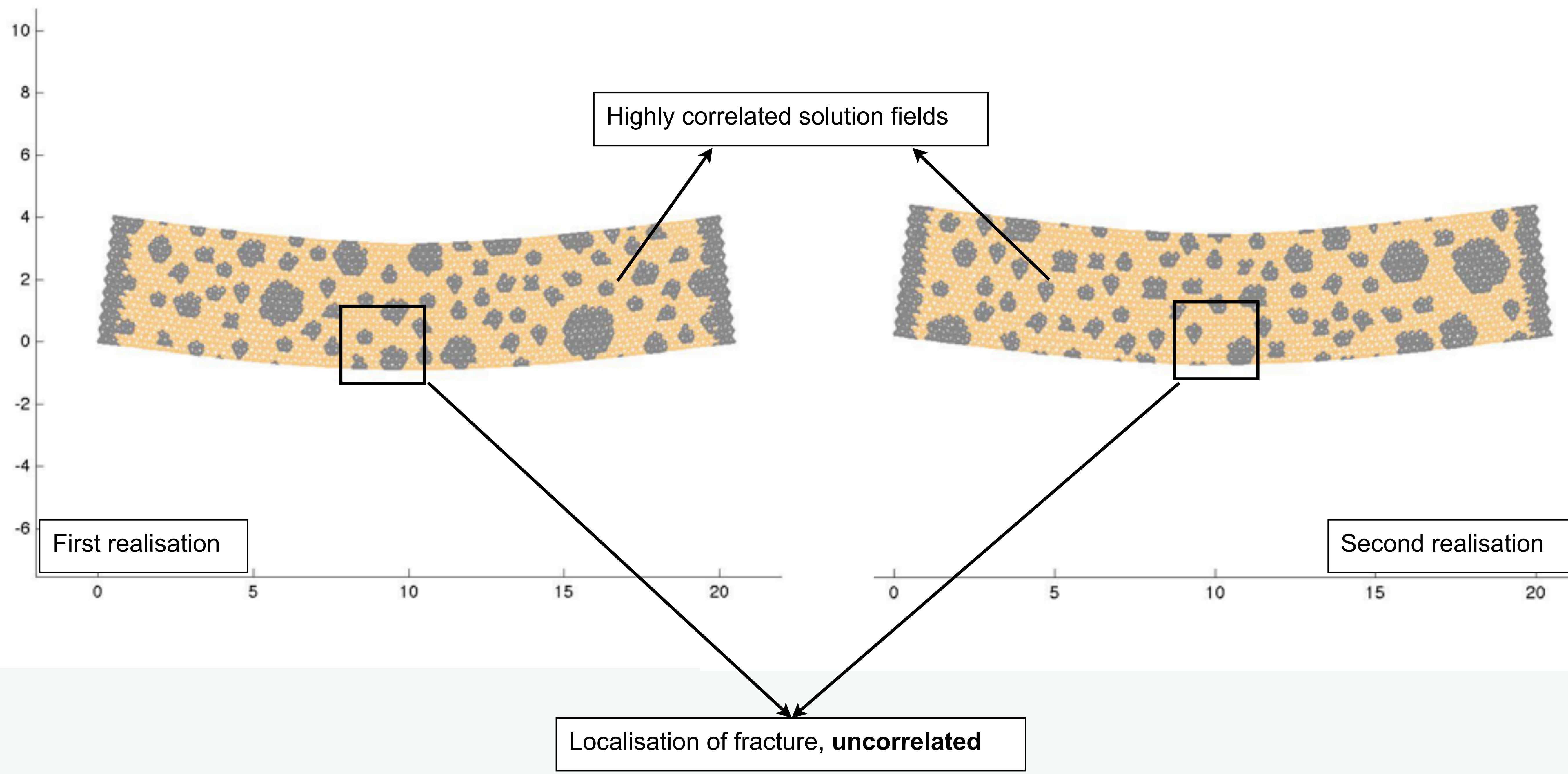

➡ Direct numerical simulation: efficient preconditioner?

➡ Reduced order modelling?

➡ Adaptive coupling?

P. Kerfriden, O. Goury, T. Rabczuk, SPAB *Computer Methods in Applied Mechanics and Engineering*, (2013) 256:169-188.

The Return of the Monkey!

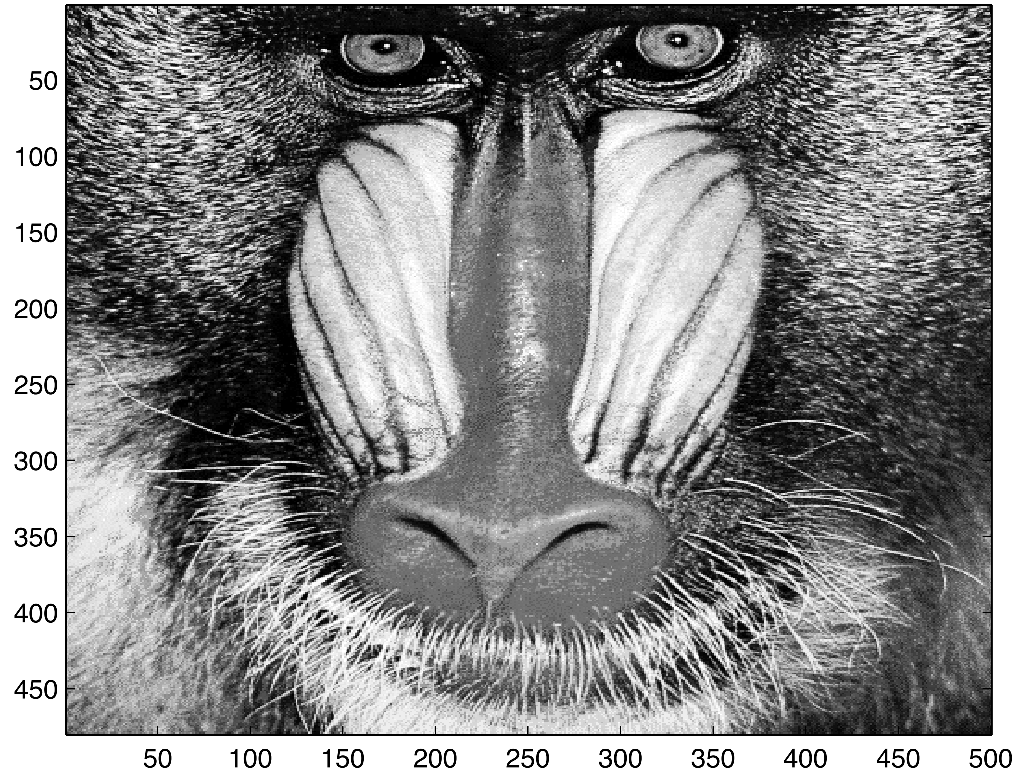

What can we do to address lack of separation of scales?

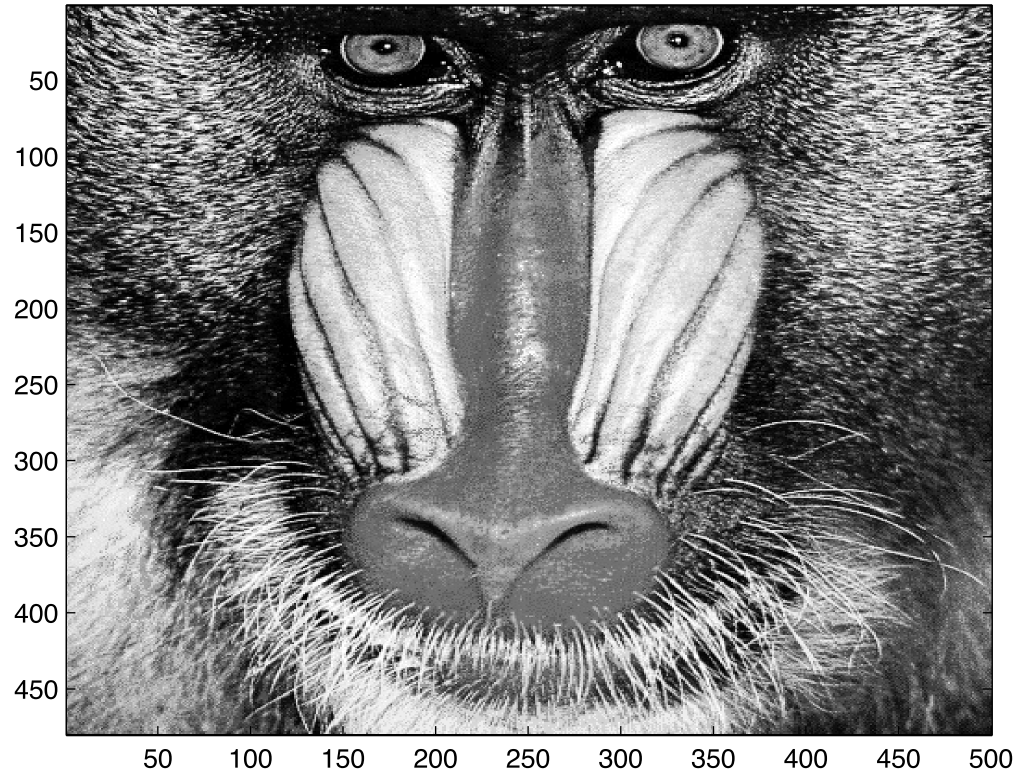

Model reduction in mechanics (non exhaustive)

- Model order reduction in a domain decomposition context
  - Craig-Bampton [Craig and Bampton ’68, Rixen et al. ’04]
  - LaTIn method / PGD [Ladevèze et al. ’03, Ladevèze et al. ’10]
  - Partitioned Component Mode Synthesis [Park and Park ’04, Markovic and Ibrahimbegovic ’09]
  - Partitioned POD [Kerfriden et al. ’11]

- Model order reduction of substructures not requiring a fine analysis *a priori*
  - Modal truncation [Barbone et al. ’03, Rickelt and Reese ’04]
  - POD [Rickelt and Reese ’06]

- Patches
  - Finite element enrichment of PGD models by VMM [Ammar et al. ’11]
  - XFEM discontinuities in soft tissues [Niroomandi et al. ’11]

- Model order reduction for heterogeneous/nonlinear materials fracture
  - *A priori* Hyperreduction for plasticity [Ryckelynck et al. ’08] and damage [Kerfriden et al. ’10]
  - Adaptive POD and morphing in the XFEM context [Galland et al. ’09]
  - Reduced model multiscale method [Yvonnet et al. ’07]
  - LaTIn method [Ladevèze et al. ’03]

How we got to this point...

P. Kerfriden, P. Gosselet, S. Adhikari, and S. Bordas. Bridging proper orthogonal decomposition methods and augmented Newton-Krylov algorithms: an adaptive model order reduction for highly nonlinear mechanical problems. *Computer Methods in Applied Mechanics and Engineering*, 200(5-8):850–866, 2011.

P. Kerfriden, J.C. Passieux, and S. Bordas. Local/global model order reduction strategy for the simulation of quasi-brittle fracture. *International Journal for Numerical Methods in Engineering*, 89(2):154–179, 2011.

P. Kerfriden, K.M. Schmidt, T. Rabczuk, and Bordas S.P.A. Statistical extraction of process zones and representative subspaces in fracture of random composites. *Accepted for publication in International Journal for Multiscale Computational Engineering, arXiv:1203.2487v2*, 2012.

http://www.ncbi.nlm.nih.gov/pmc/articles/PMC3672853/

http://orbilu.uni.lu/bitstream/10993/12454/2/presentationUSNCCM.pdf

pierre.kerfriden@gmail.com stephane.bordas@alum.northwestern.edu lars.beex@uni.lu

Data compression: fracture

Snapshot POD (snapshot space is spanned by the ensemble of solutions at all time steps)

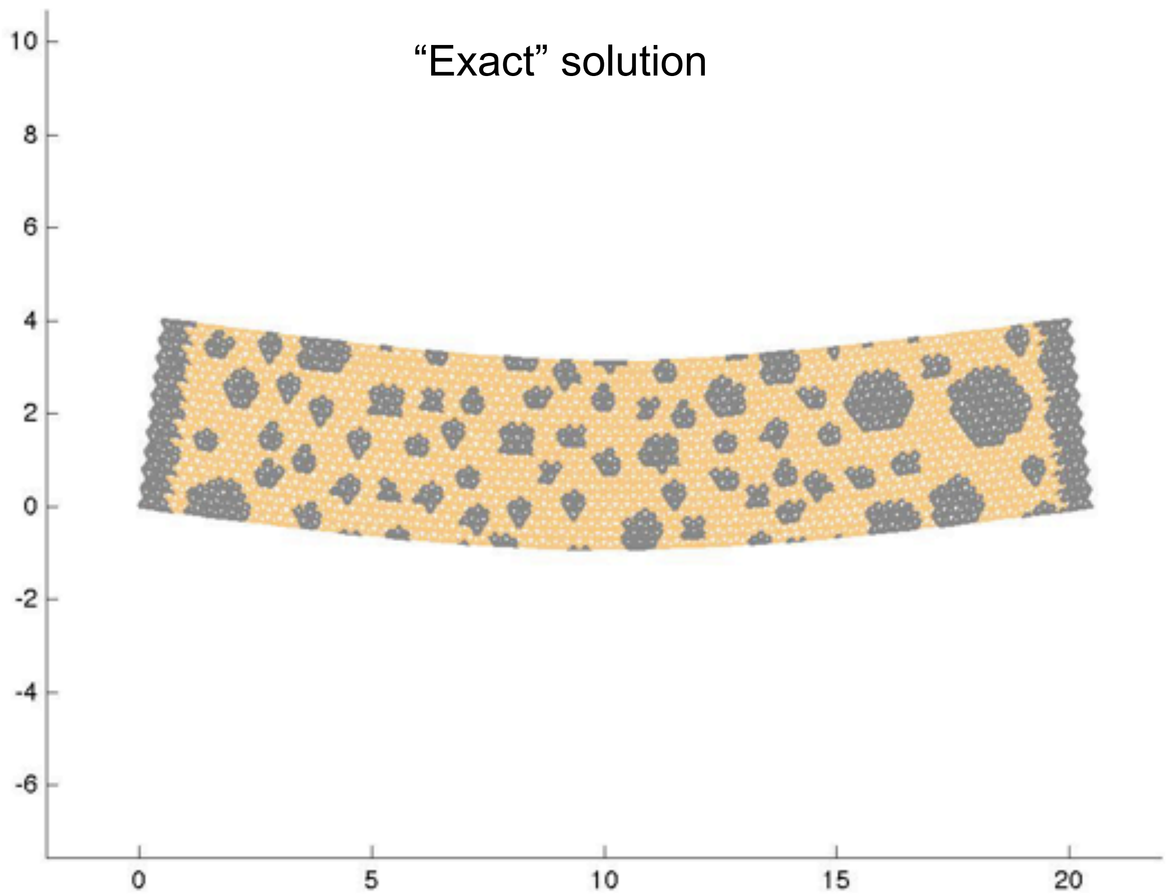

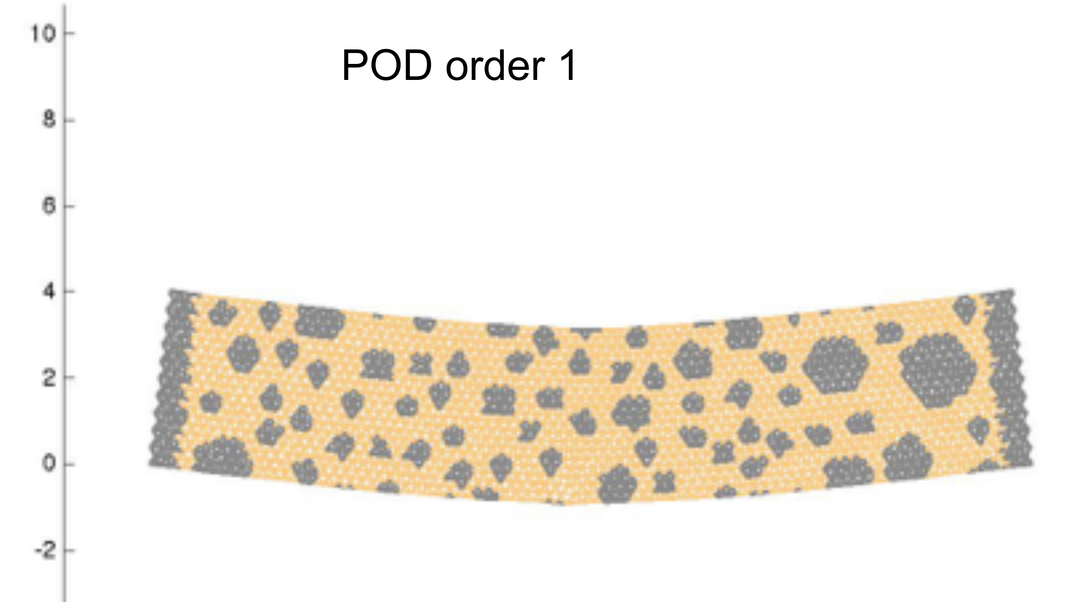

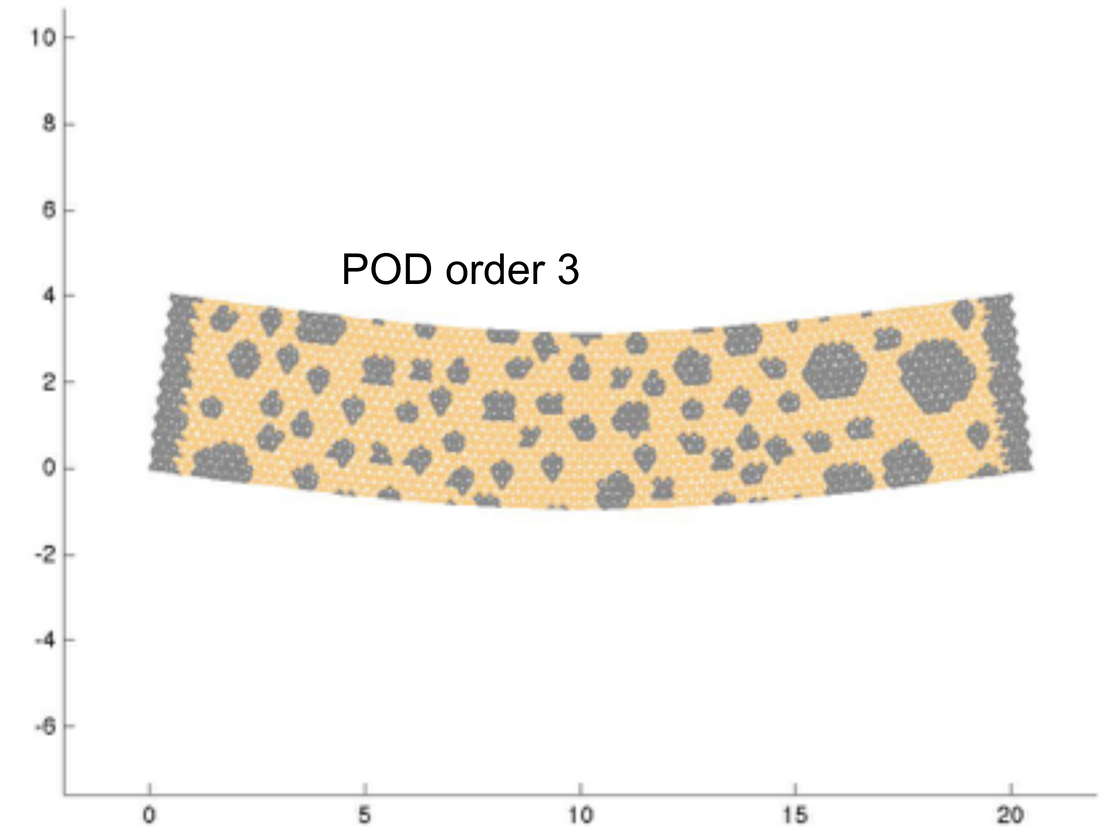

pierre.kerfriden@gmail.com stephane.bordas@alum.northwestern.edu lars.beex@uni.lu

Partitioned POD/DDM

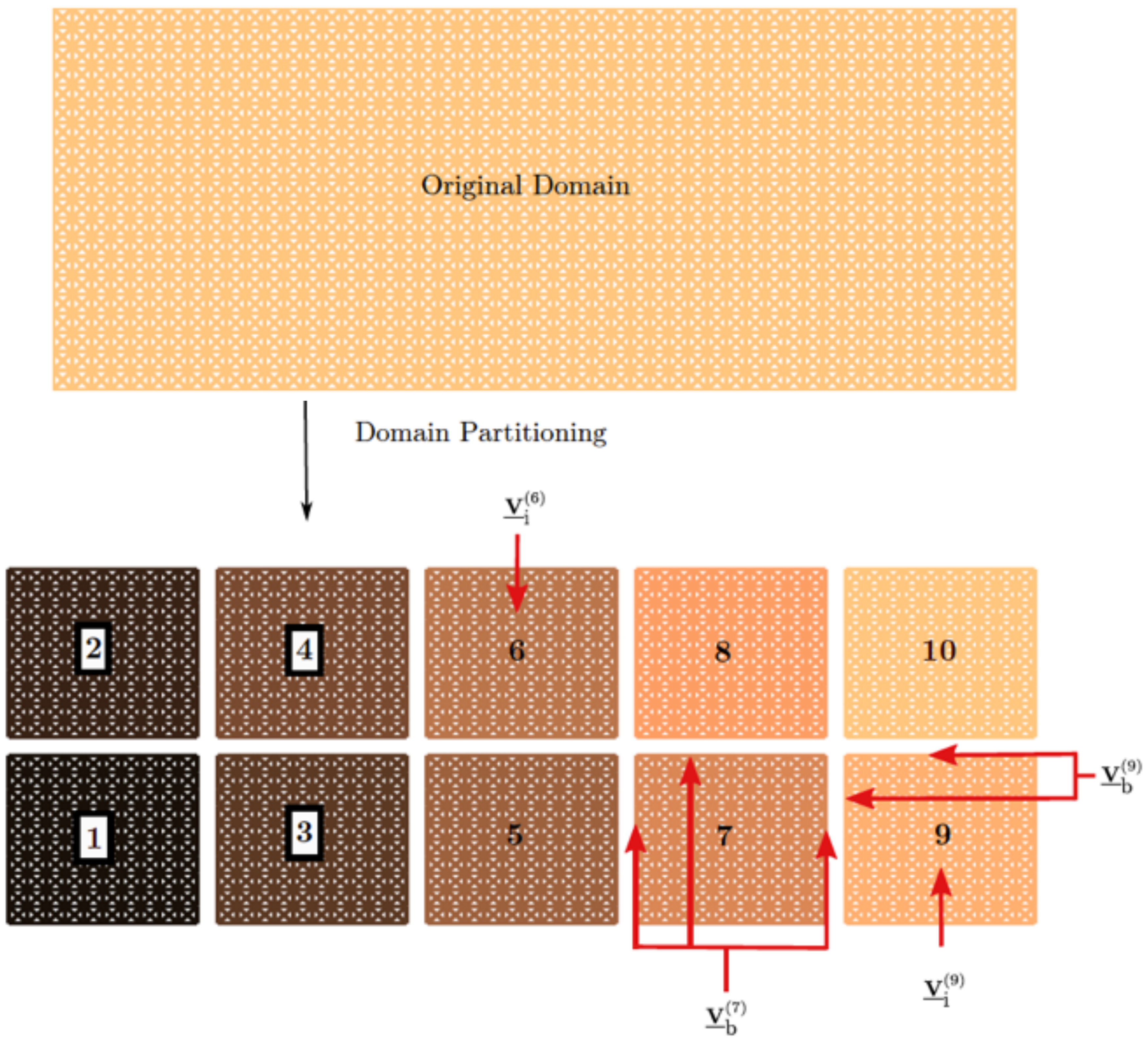

pierre.kerfriden@gmail.com stephane.bordas@alum.northwestern.edu lars.beex@uni.lu

Reduced DDM-POD

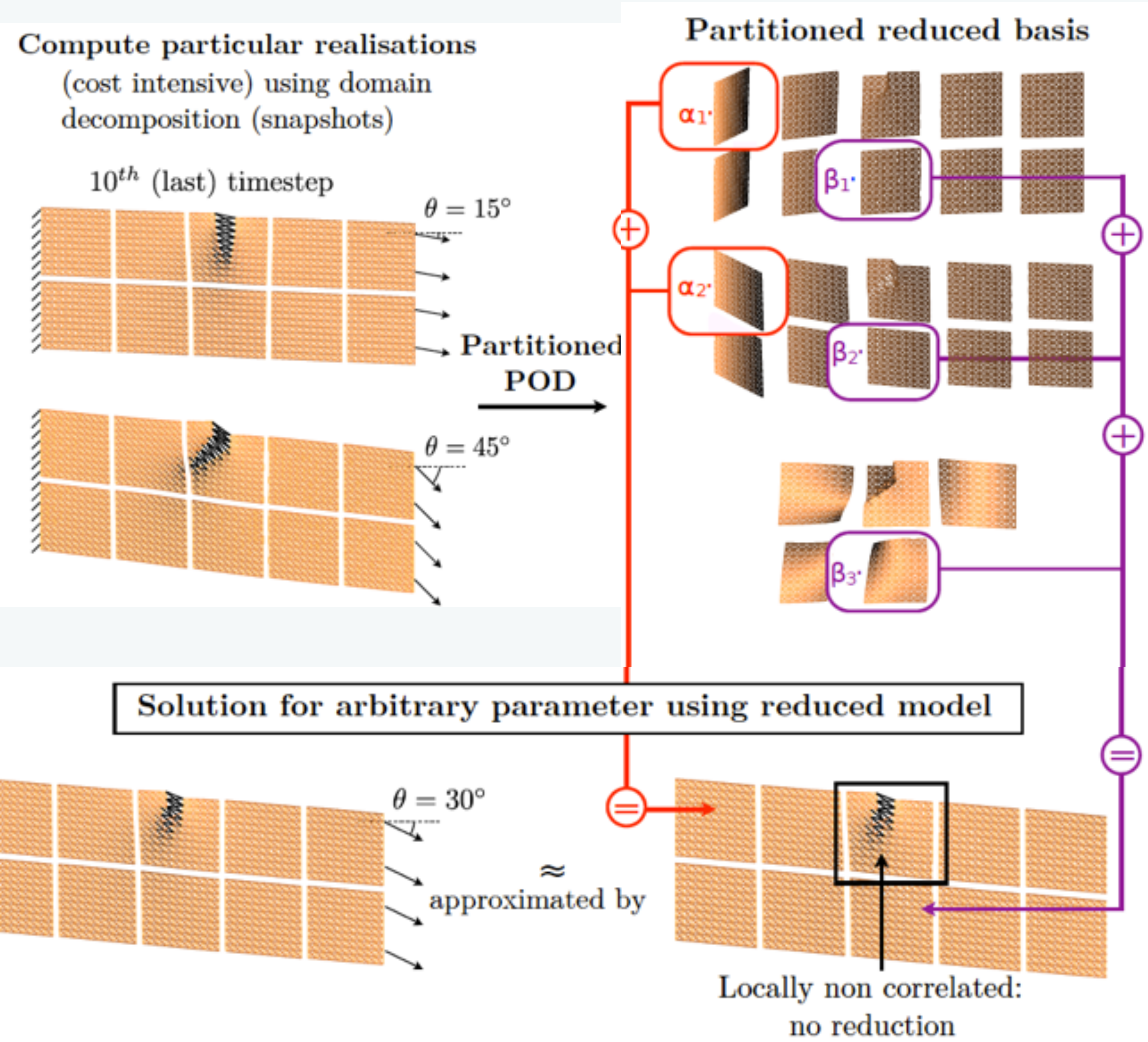

- Decompose the structure into subdomains
- Perform a reduction in the highly correlated region
- Couple the reduced to the non-reduced region by a primal Schur complement

P. Kerfriden, O. Goury, T. Rabczuk, SPAB *Computer Methods in Applied Mechanics and Engineering*, (2013) 256:169-188.

: local error estimation by “leave

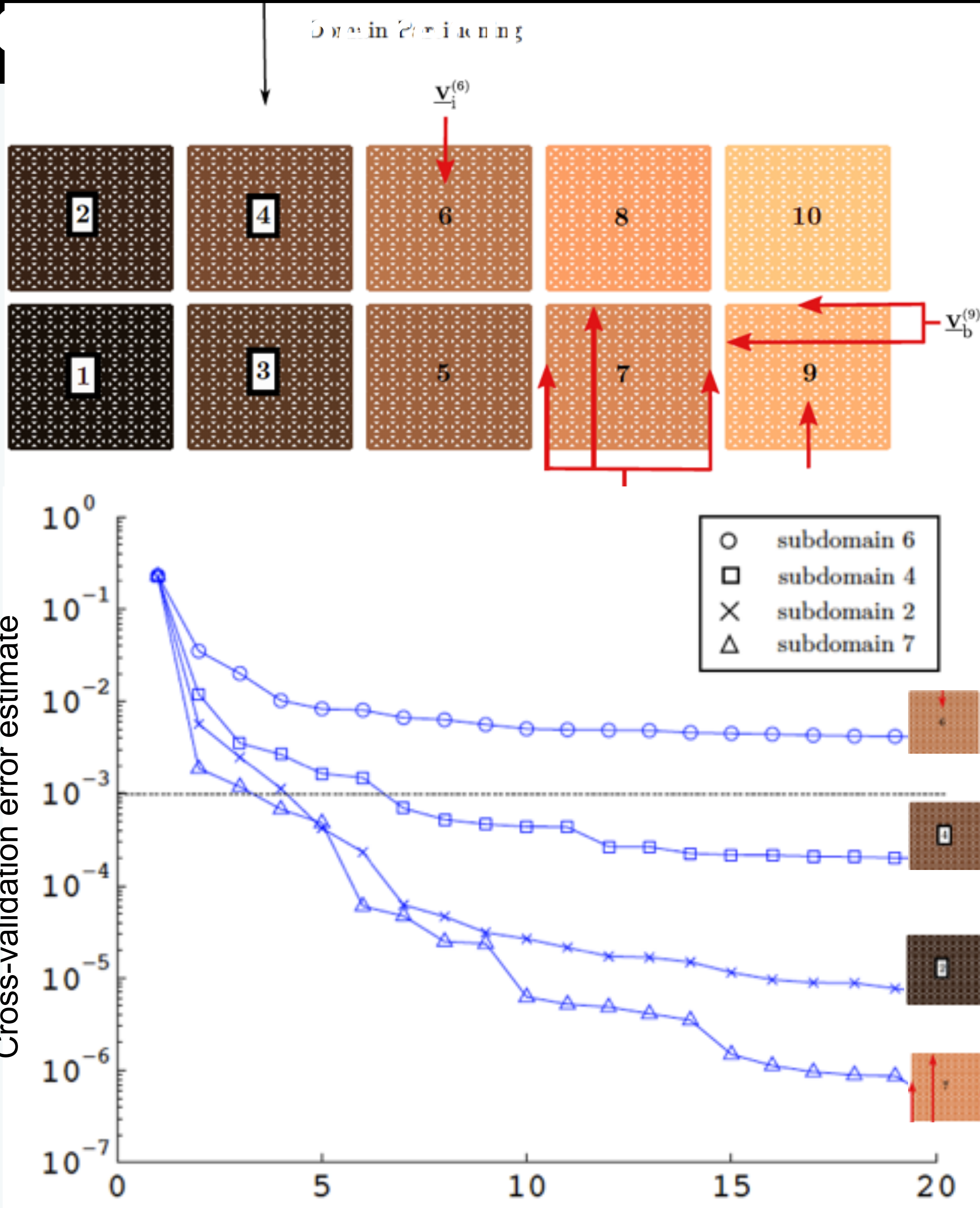

$$\left(\tilde{\nu}^{(e)}_{\text{snap}}\right)^2 = \frac{\displaystyle\sum_{\mu \in \mathcal{P}^s} \sum_{t_n \in \mathcal{T}^h} \left\| \underline{\mathbf{U}}_{\text{i}}(t_n,\mu) - \sum_{j=1}^{n_c^{(e)}} \left(\tilde{\underline{\mathbf{C}}}_{\text{i},j}^{(e),(\mu)\,T}\, \underline{\mathbf{U}}_{\text{i}}(t_n,\mu) \right) \tilde{\underline{\mathbf{C}}}_{\text{i},j}^{(e),(\mu)} \right\|_2^2}{\displaystyle\sum_{t_n \in \mathcal{T}^h} \sum_{\mu \in \mathcal{P}^s} \|\underline{\mathbf{U}}_{\text{i}}(t_n,\mu)\|_2^2}$$

P. Kerfriden, O. Goury, T. Rabczuk, SPAB *Computer Methods in Applied Mechanics and Engineering*, (2013) 256:169-188.

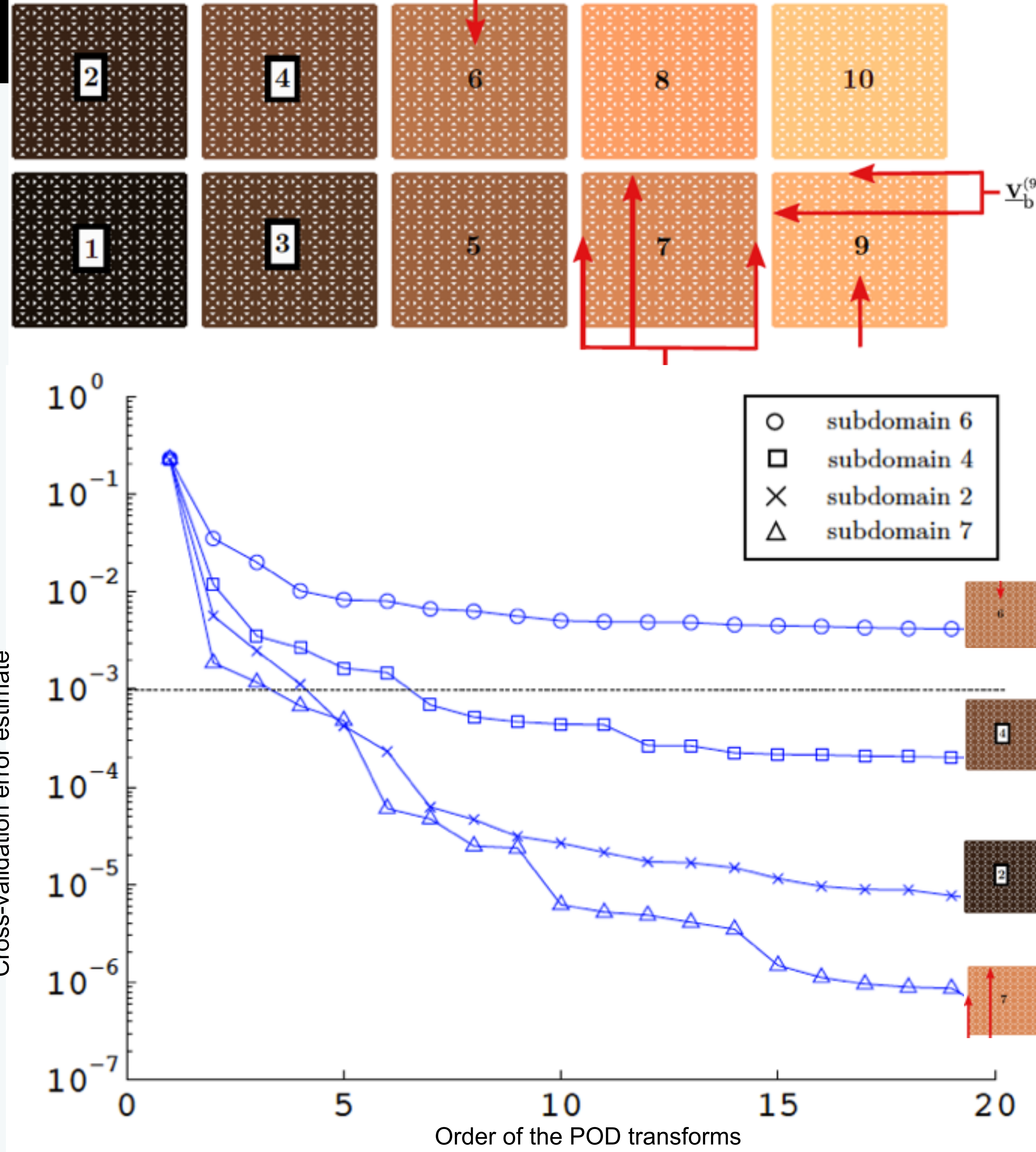
2
4
6
8
10
1
3
5
7
9
$\underline{V}_b^{(9)}$
subdomain 6
subdomain 4
subdomain 2
subdomain 7
Cross-validation error estimate
10^0
10^{-1}
10^{-2}
10^{-3}
10^{-4}
10^{-5}
10^{-6}
10^{-7}
0
5
10
15
20
Order of the POD transforms

Performance: load angle 40 | 27 - 121 nodes

$$\nu^{\mathrm{app},(\mu)}(\underline{\mathbf{U}}^{\mathrm{app}})^2 = \frac{\sum_{t_n \in \mathcal{T}^h} \|\underline{\mathbf{U}}^{\mathrm{app}}(t_n,\mu) - \underline{\mathbf{U}}^{\mathrm{ex}}(t_n,\mu)\|_2^2}{\sum_{t_n \in \mathcal{T}^h} \|\underline{\mathbf{U}}^{\mathrm{ex}}(t_n,\mu)\|_2^2}$$

40^o

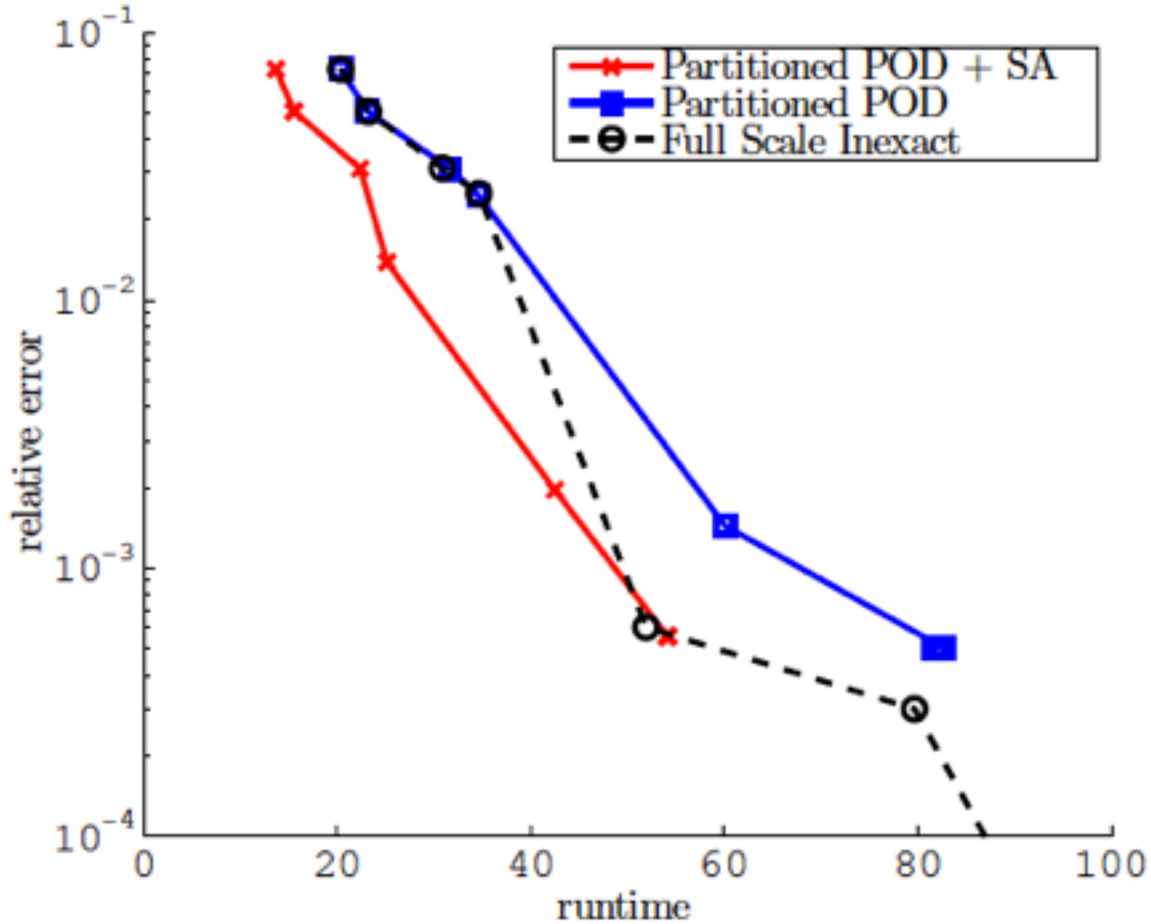

(a) Relative error for the different models using 121 nodes per subdomain

27^o

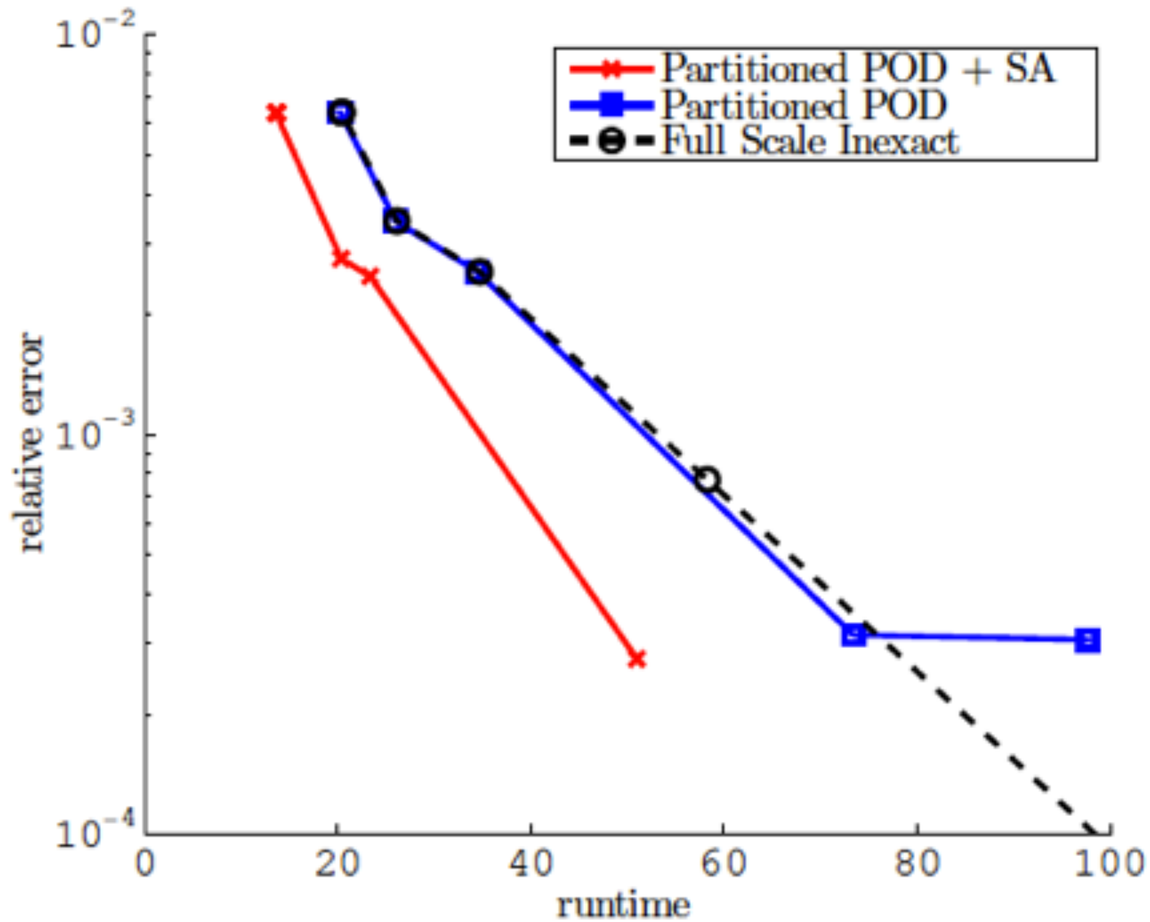

(a) Relative error for the different models using 121 no
per subdomain

P. Kerfriden, O. Goury, T. Rabczuk, SPAB *Computer Methods in Applied Mechanics and Engineering*, (2013) 256:169-188.

Performance: load angle 40 | 27 - 256 nodes

- Relative error

$$\nu^{\mathrm{app},(\mu)}\left(\underline{\mathbf{U}}^{\mathrm{app}}\right)^2 = \frac{\sum\limits_{t_n \in \mathcal{T}^h} \|\underline{\mathbf{U}}^{\mathrm{app}}(t_n,\mu) - \underline{\mathbf{U}}^{\mathrm{ex}}(t_n,\mu)\|_2^2}{\sum\limits_{t_n \in \mathcal{T}^h} \|\underline{\mathbf{U}}^{\mathrm{ex}}(t_n,\mu)\|_2^2}$$

40^o

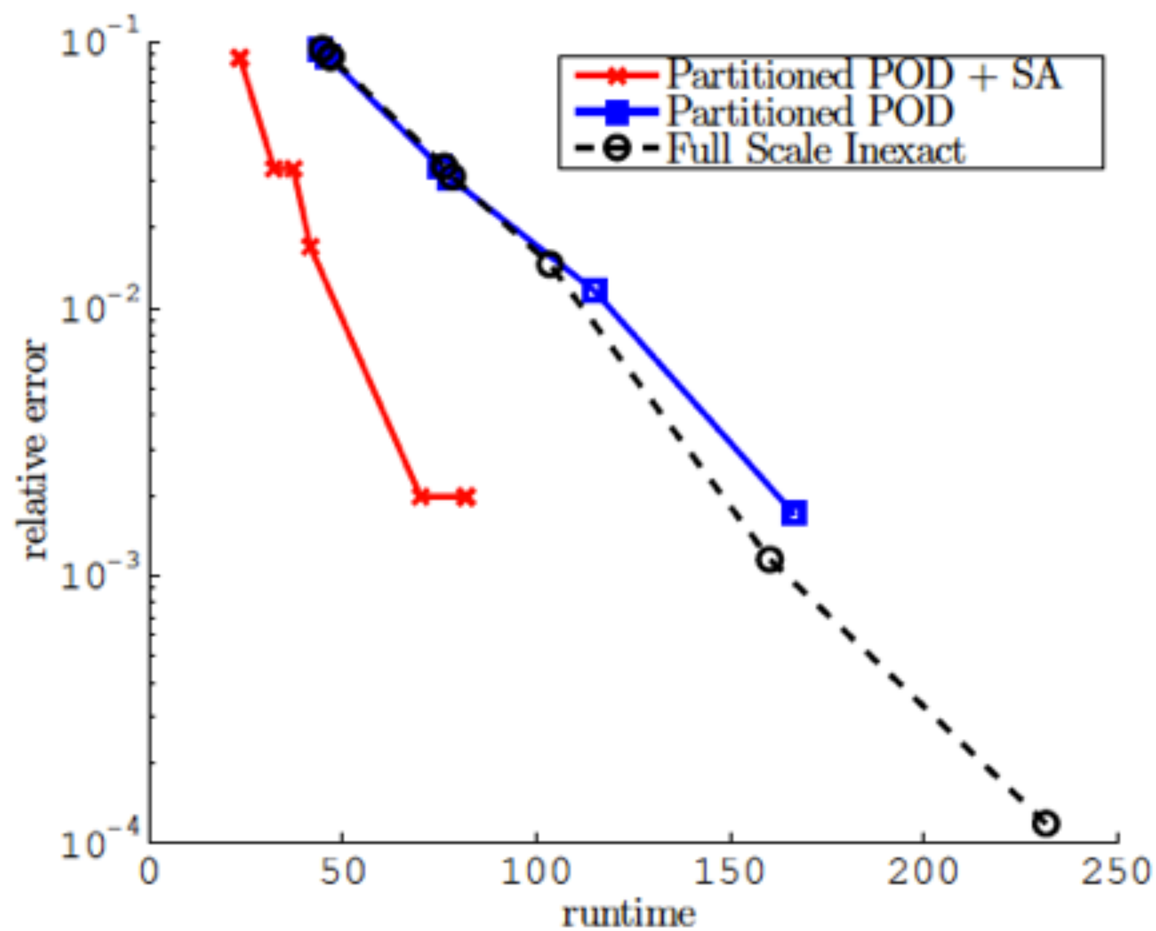

(b) Relative error for the different models using 256 nodes per subdomain

27^o

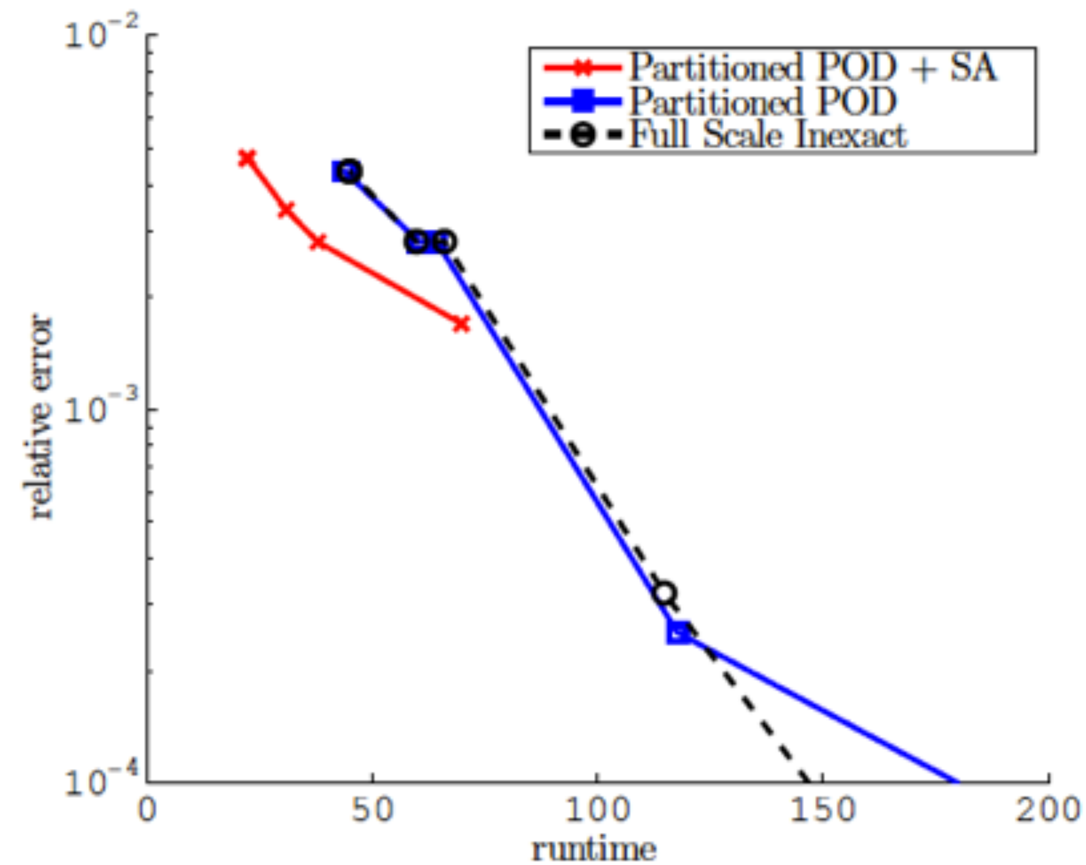

(b) Relative error for the different models using 256 nodes per subdomain

P. Kerfriden, O. Goury, T. Rabczuk, SPAB *Computer Methods in Applied Mechanics and Engineering*, (2013) 256:169-188.

Performance: load angle 40 | 27 - 441 nodes

$$\nu^{\mathrm{app},(\mu)}\left(\underline{\mathbf{U}}^{\mathrm{app}}\right)^2 = \frac{\displaystyle\sum_{t_n \in \mathcal{T}^h} \|\underline{\mathbf{U}}^{\mathrm{app}}(t_n,\mu) - \underline{\mathbf{U}}^{\mathrm{ex}}(t_n,\mu)\|_2^2}{\displaystyle\sum_{t_n \in \mathcal{T}^h} \|\underline{\mathbf{U}}^{\mathrm{ex}}(t_n,\mu)\|_2^2}$$

40^o

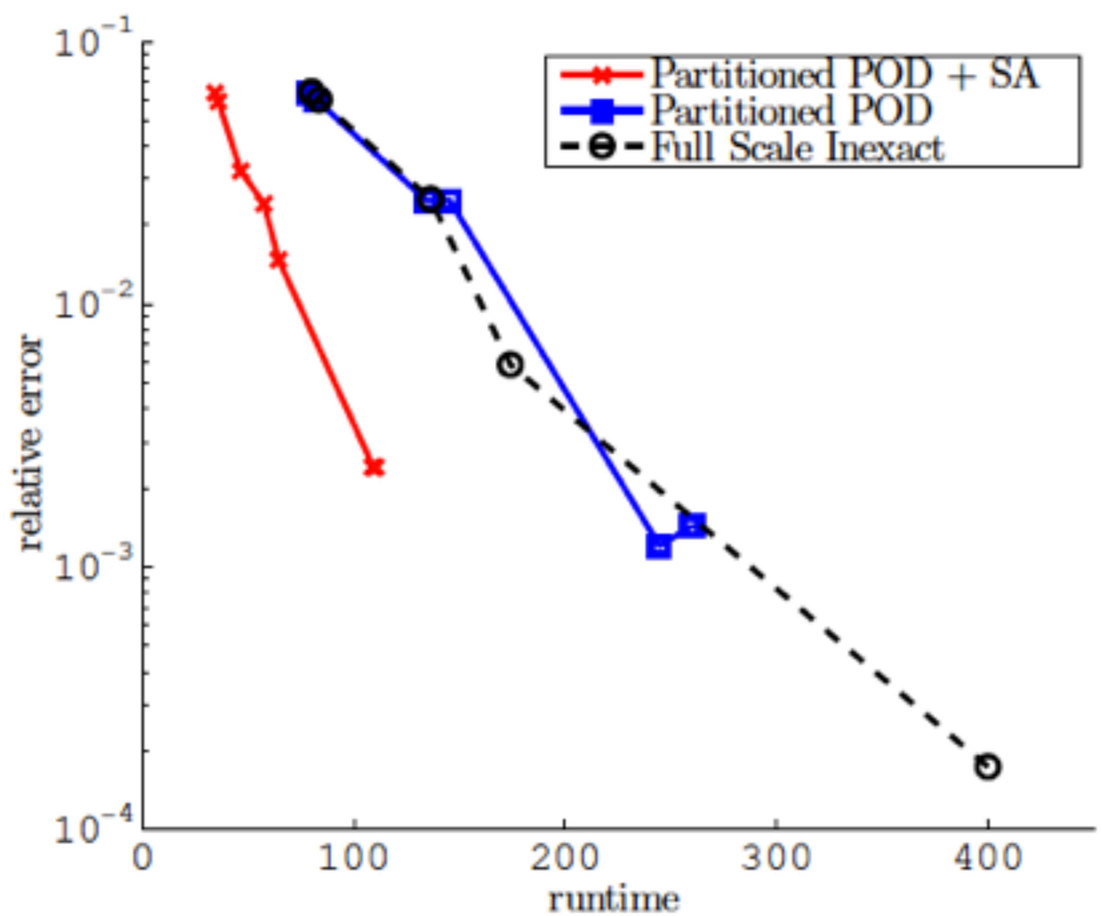

(c) Relative error for the different models using 441 nodes per subdomain

27^o

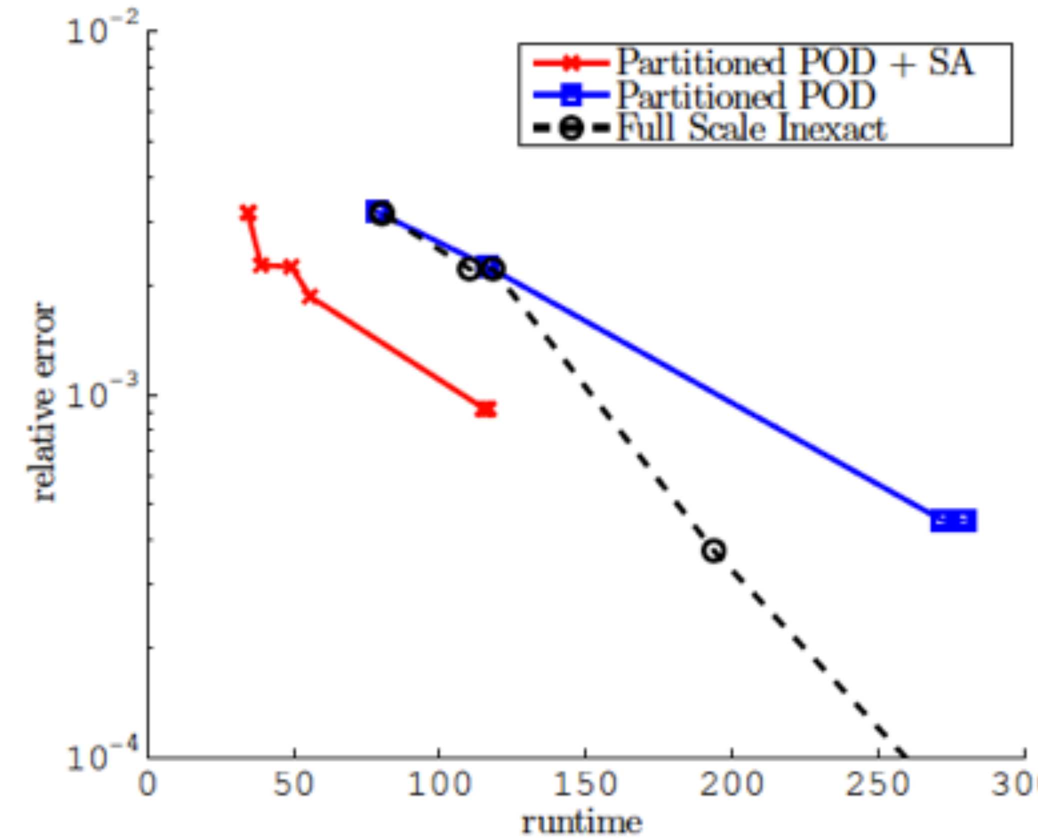

(c) Relative error for the different models using 441 nodes per subdomain

P. Kerfriden, O. Goury, T. Rabczuk, SPAB *Computer Methods in Applied Mechanics and Engineering*, (2013) 256:169-188.

Performance: load angle 40 | 27 - 961 nodes

- Relative error

$$\nu^{\mathrm{app},(\mu)}\left(\underline{\mathbf{U}}^{\mathrm{app}}\right)^2 = \frac{\sum\limits_{t_n \in \mathcal{T}^h} \|\underline{\mathbf{U}}^{\mathrm{app}}(t_n,\mu) - \underline{\mathbf{U}}^{\mathrm{ex}}(t_n,\mu)\|_2^2}{\sum\limits_{t_n \in \mathcal{T}^h} \|\underline{\mathbf{U}}^{\mathrm{ex}}(t_n,\mu)\|_2^2}$$

40^o

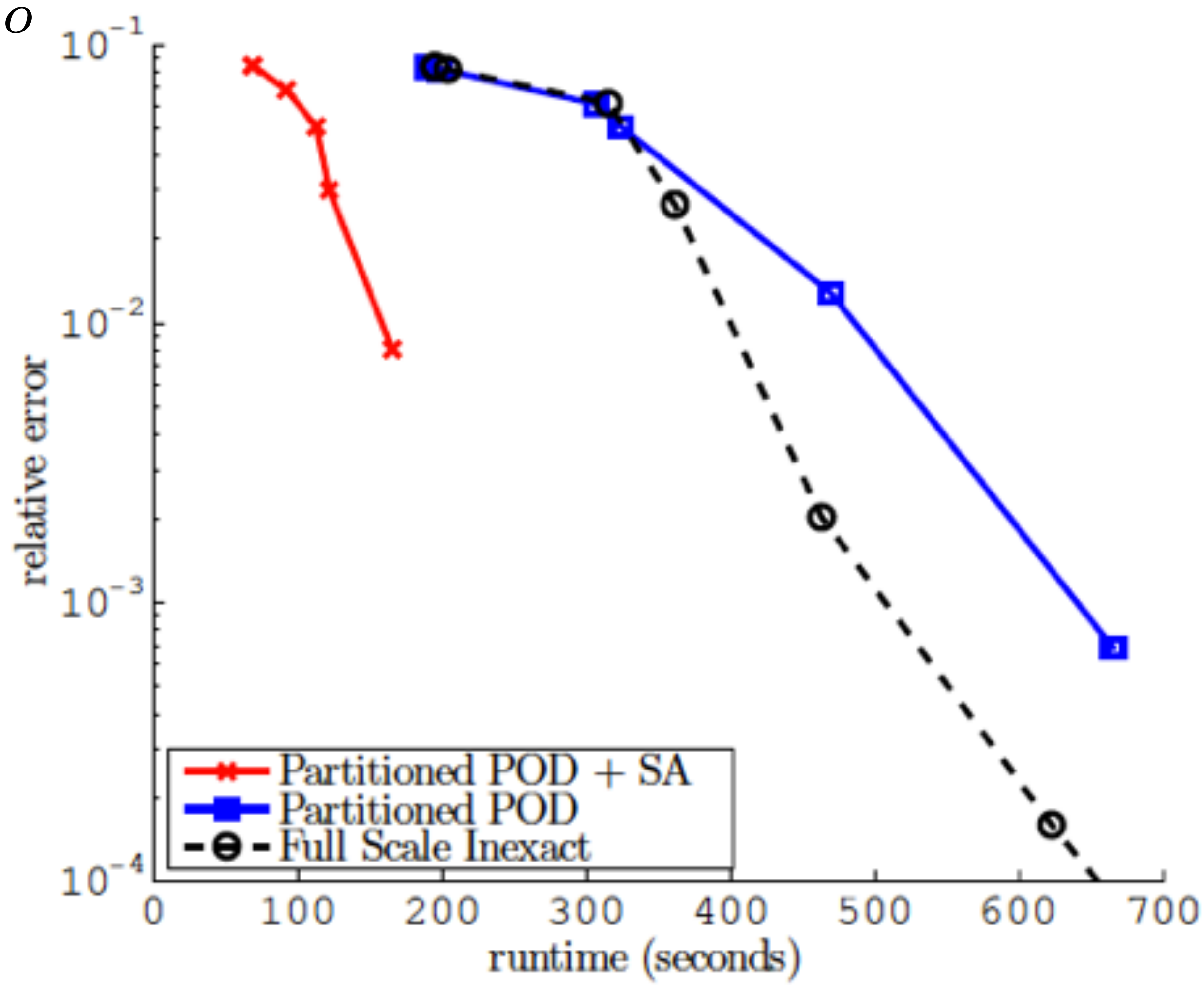

(d) Relative error for the different models using 961 nodes per subdomain

27^o

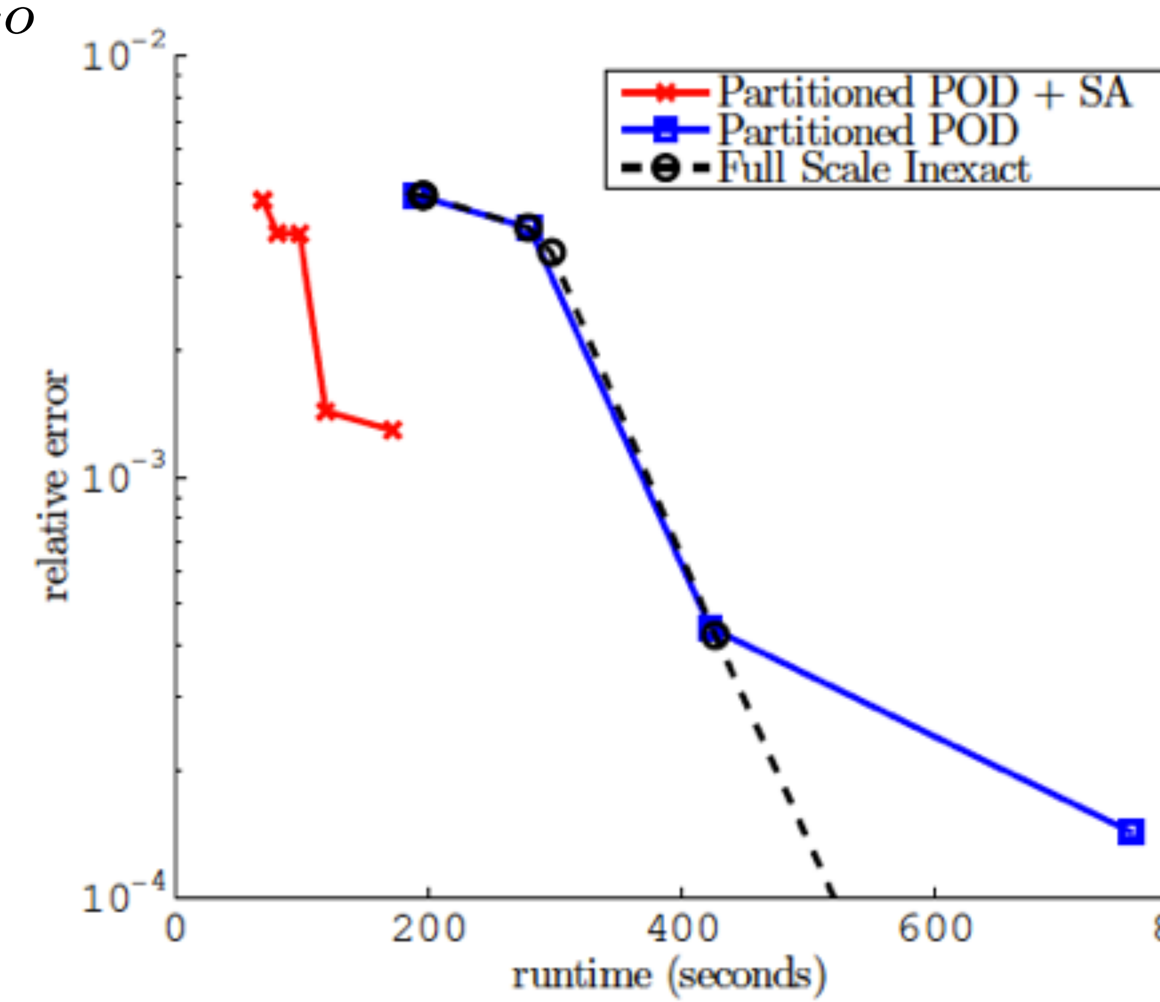

(d) Relative error for the different models using 961 per subdomain

P. Kerfriden, O. Goury, T. Rabczuk, SPAB *Computer Methods in Applied Mechanics and Engineering*, (2013) 256:169-188.

Take home message

Homogenisation reduction

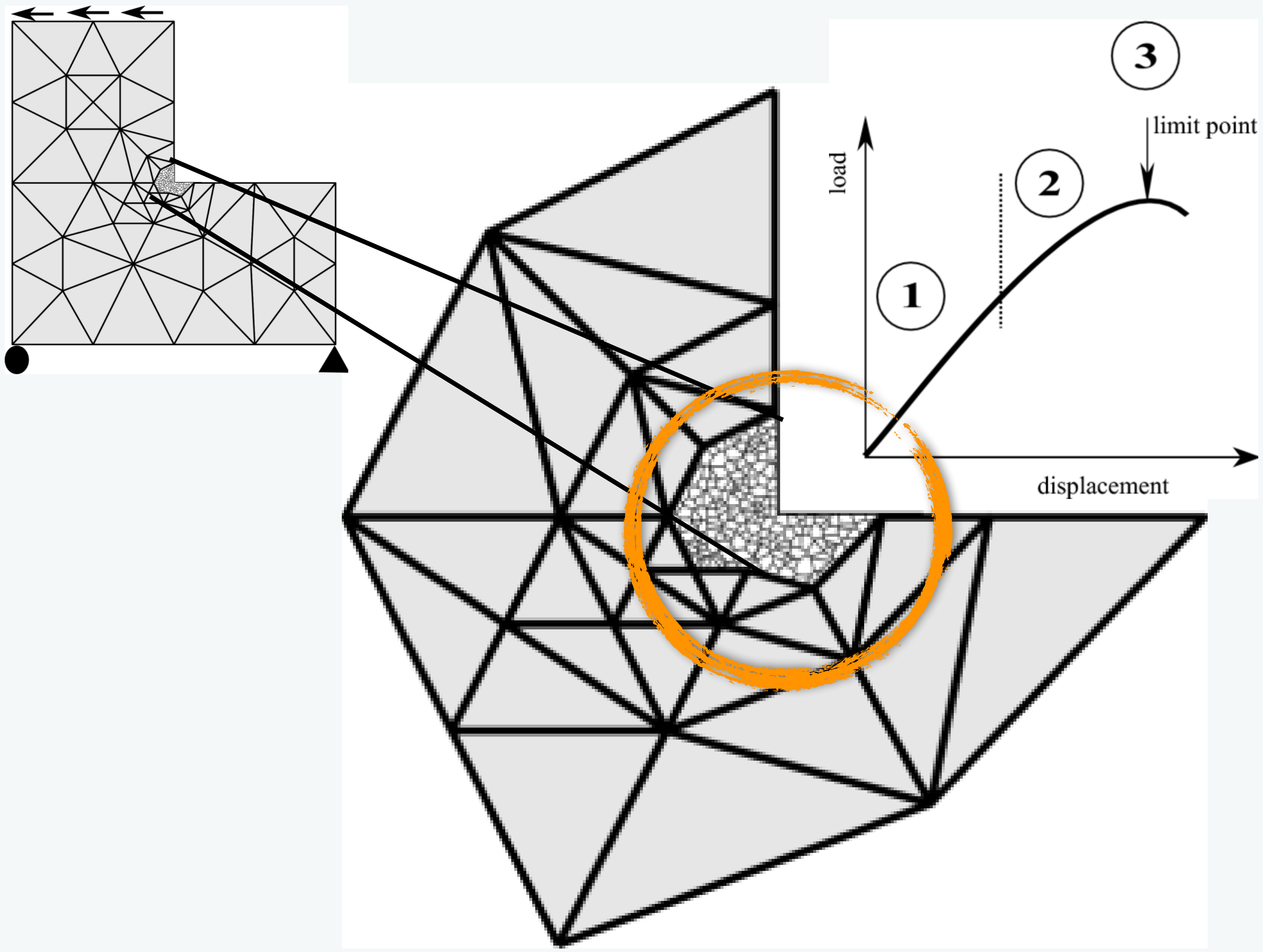

Details in Phil. Magazine, 2015,
Akbari, Kerfriden, Bordas

Algebraic reduction

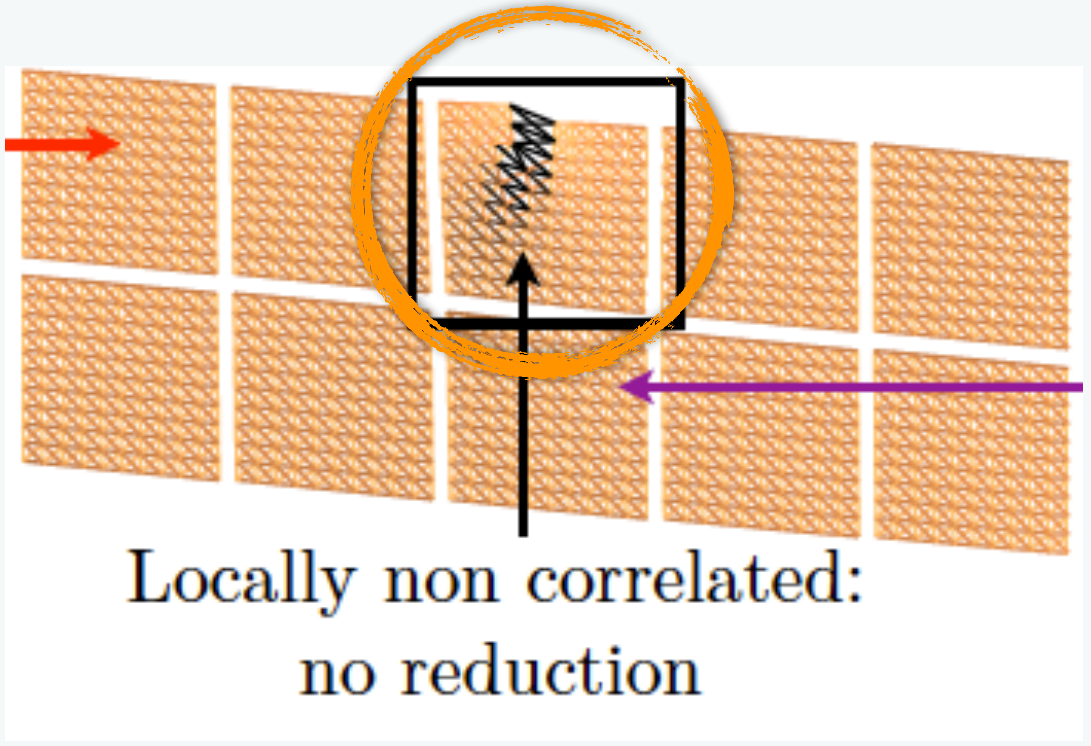

Details in CMAME, 2013,
Goury, Kerfriden, Rabczuk, Bordas

The fractured/softening regions cannot be reduced!

Adaptive algebraic model order reduction

Part 2. Quasi-Continuum Method

L. Beex, R. Peerlings, M. Geers, O. Rokos, J. Zeman, P. Kerfriden, SPAB

some other time :)

Outlook

Model learning across scales

Legato team, Frank Langbein,
Sophie Schirmer, Stephen Hallett,
Chris Bowen et al.

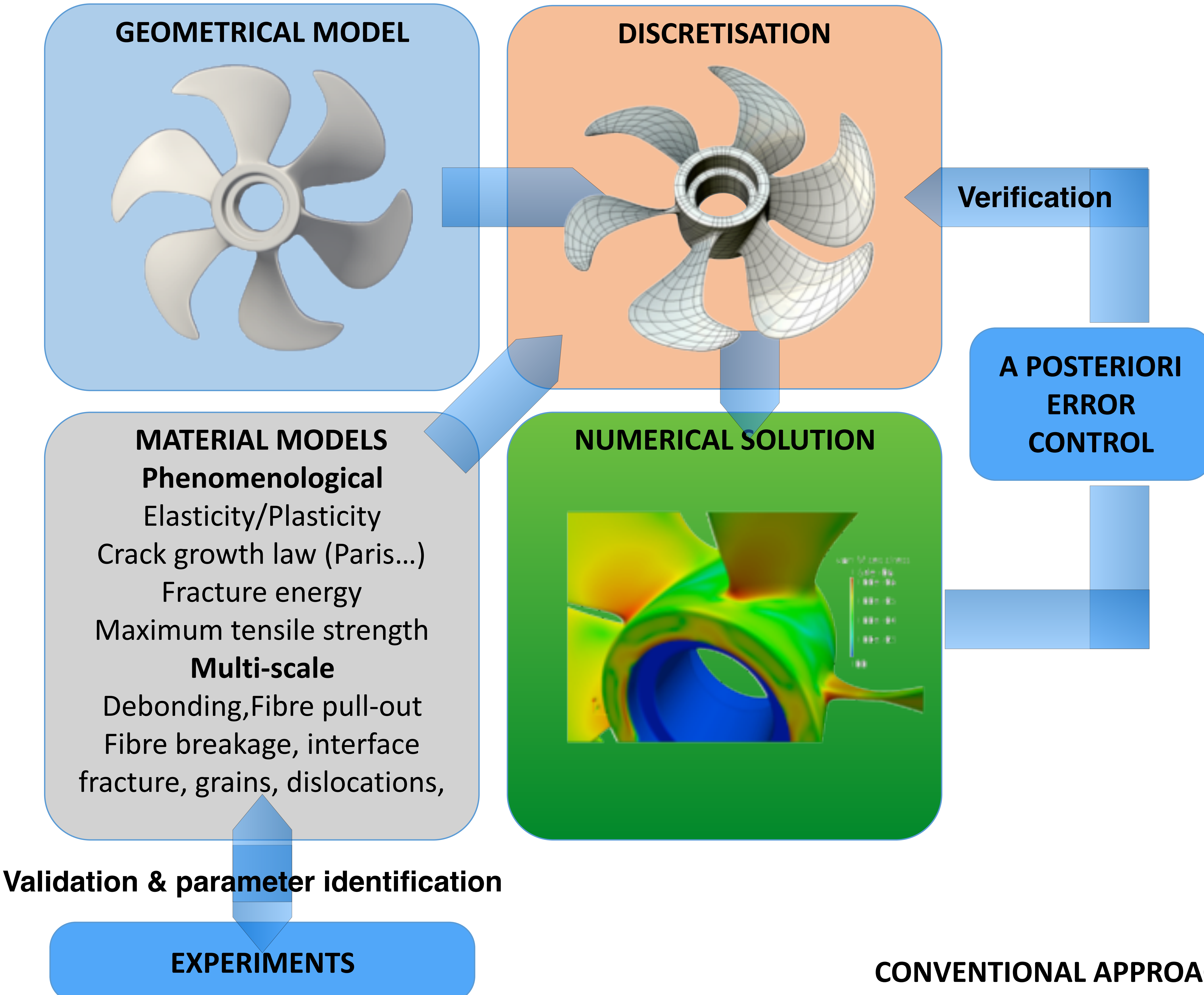

CONVENTIONAL APPROACH

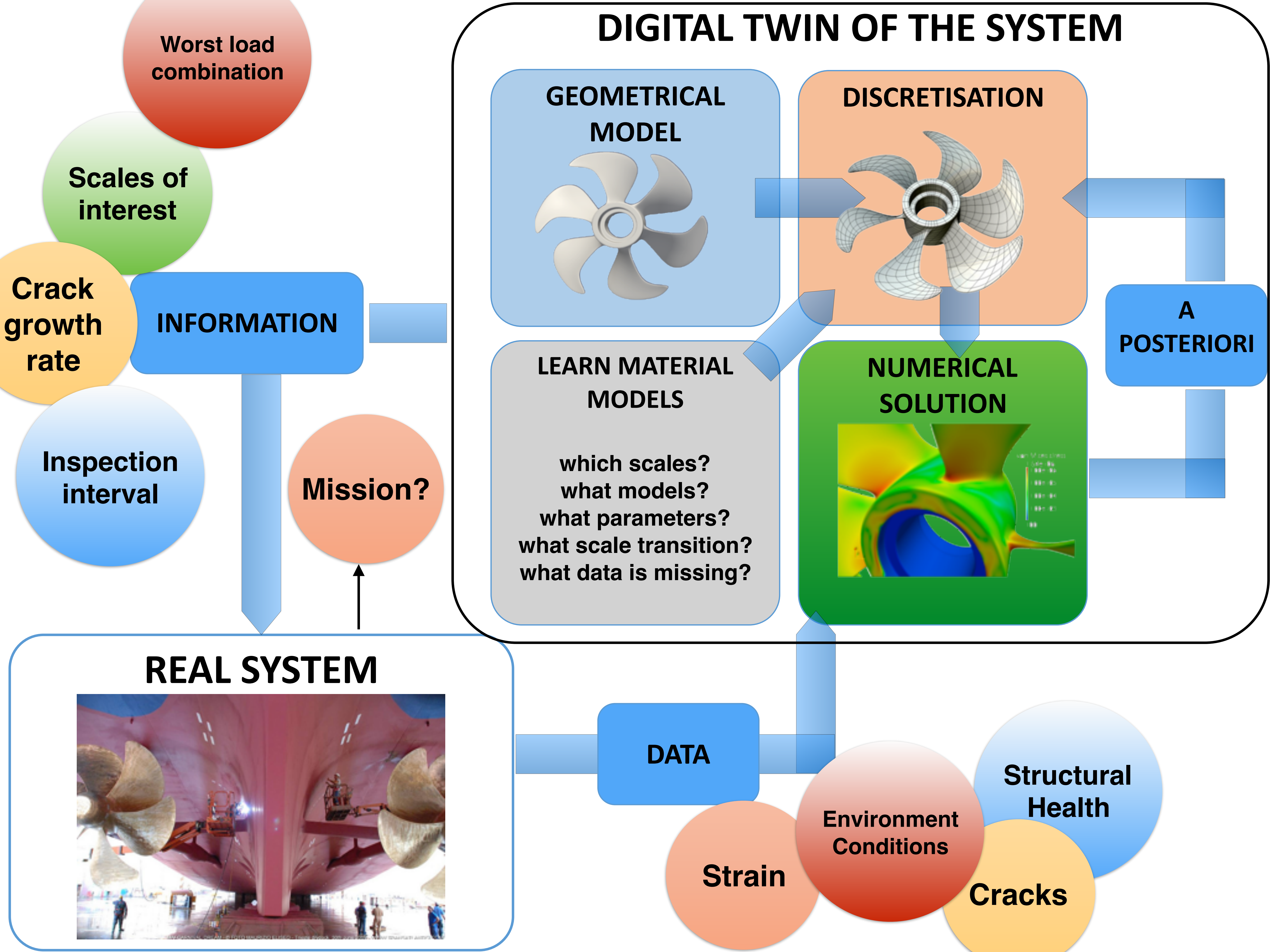

DIGITAL TWIN OF THE SYSTEM
GEOMETRICAL MODEL
DISCRETISATION
A POSTERIORI
NUMERICAL SOLUTION
LEARN MATERIAL MODELS
which scales?
what models?
what parameters?
what scale transition?
what data is missing?
Worst load combination
Scales of interest
Crack growth rate
INFORMATION
Inspection interval
Mission?
REAL SYSTEM
DATA
Structural Health
Environment Conditions
Strain
Cracks

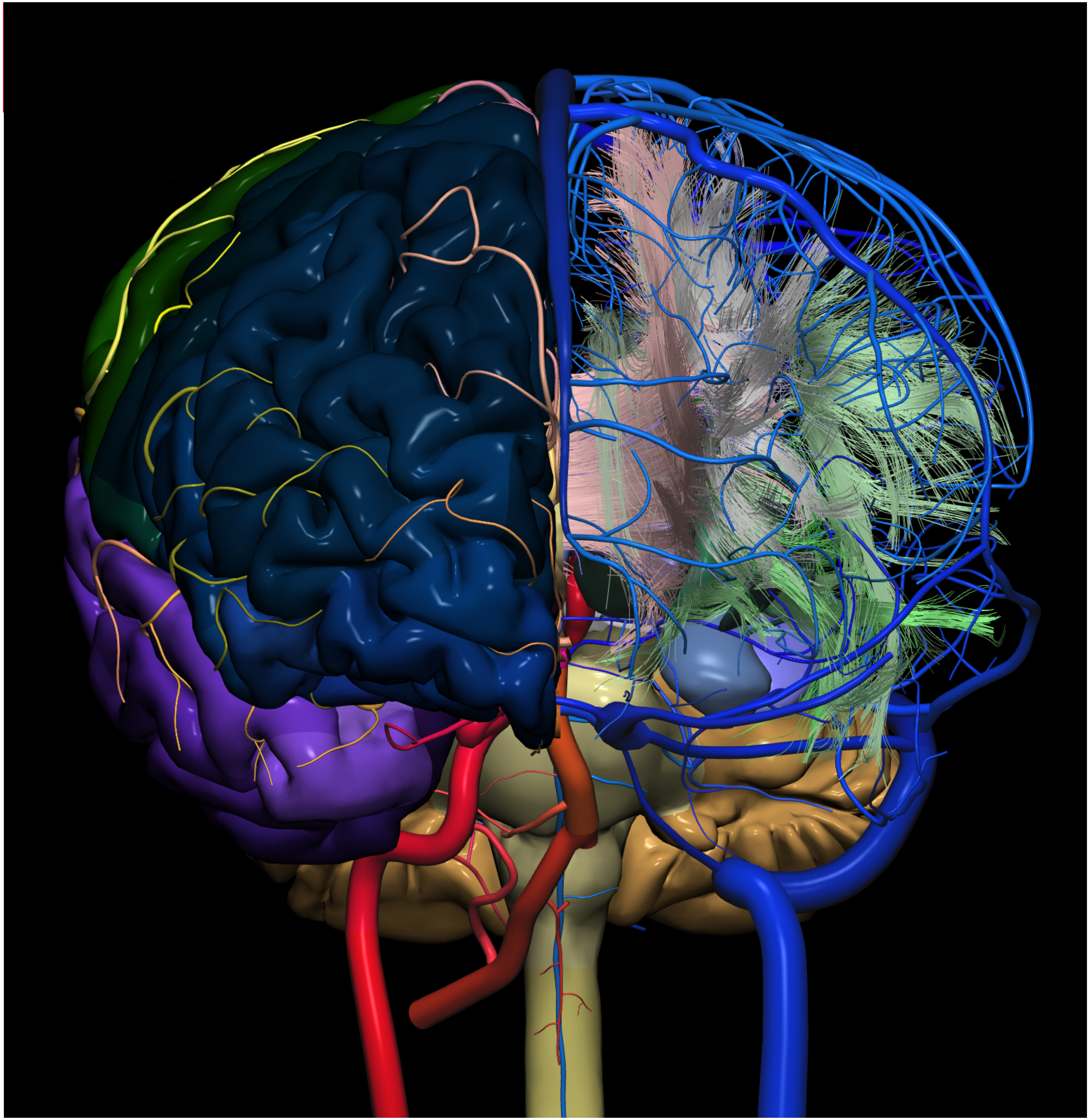

The brain is complicated…

But we only wish to compute displacements

Courtesy
Prof. Wies Nowinski,
A-Star, Singapore

Patient-specific modelling of patients

RealTcut

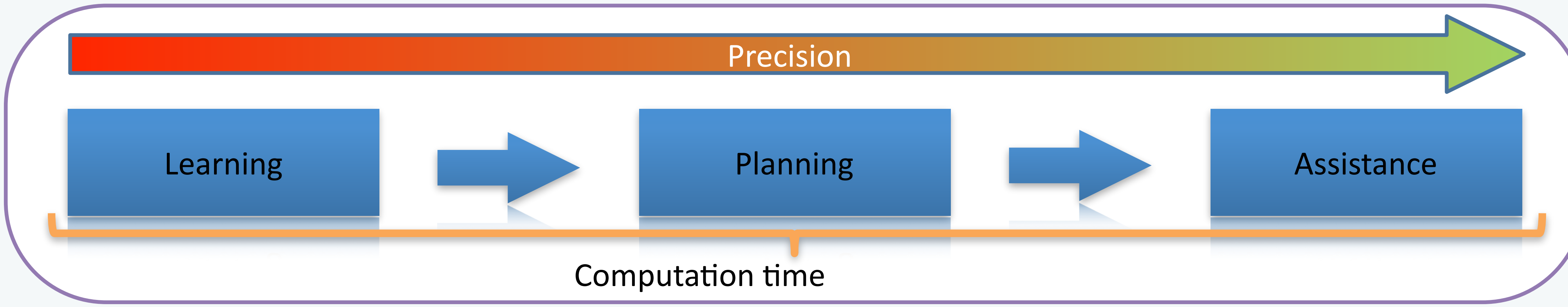

Surgical simulation (real time/interactivity)

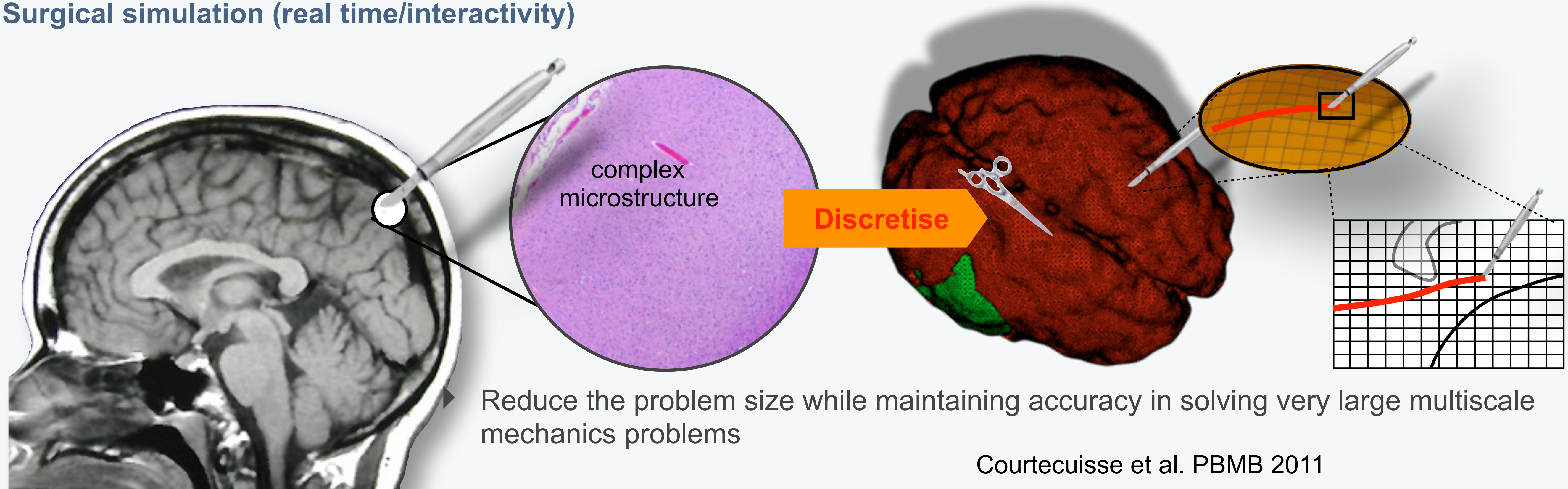

Reduce the problem size while maintaining accuracy in solving very large multiscale mechanics problems

Courtecuisse et al. PBMB 2011

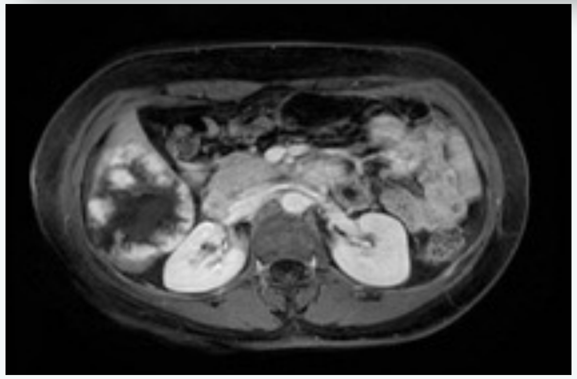

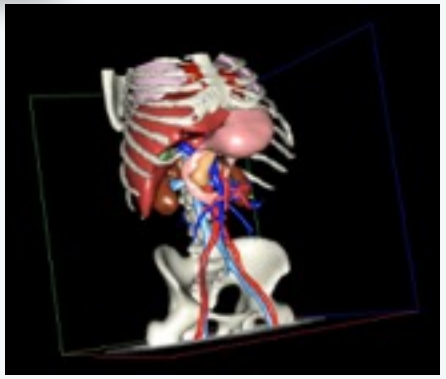

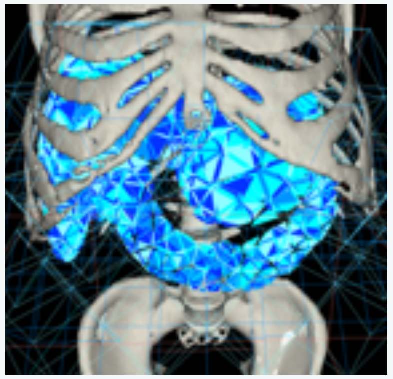

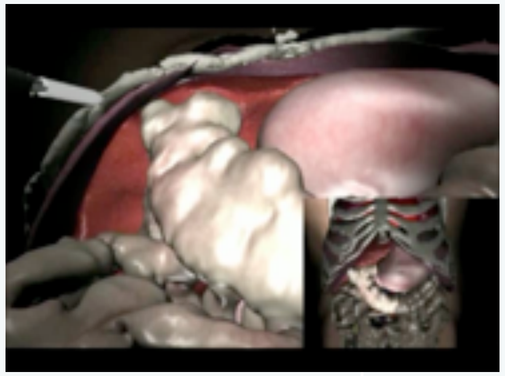

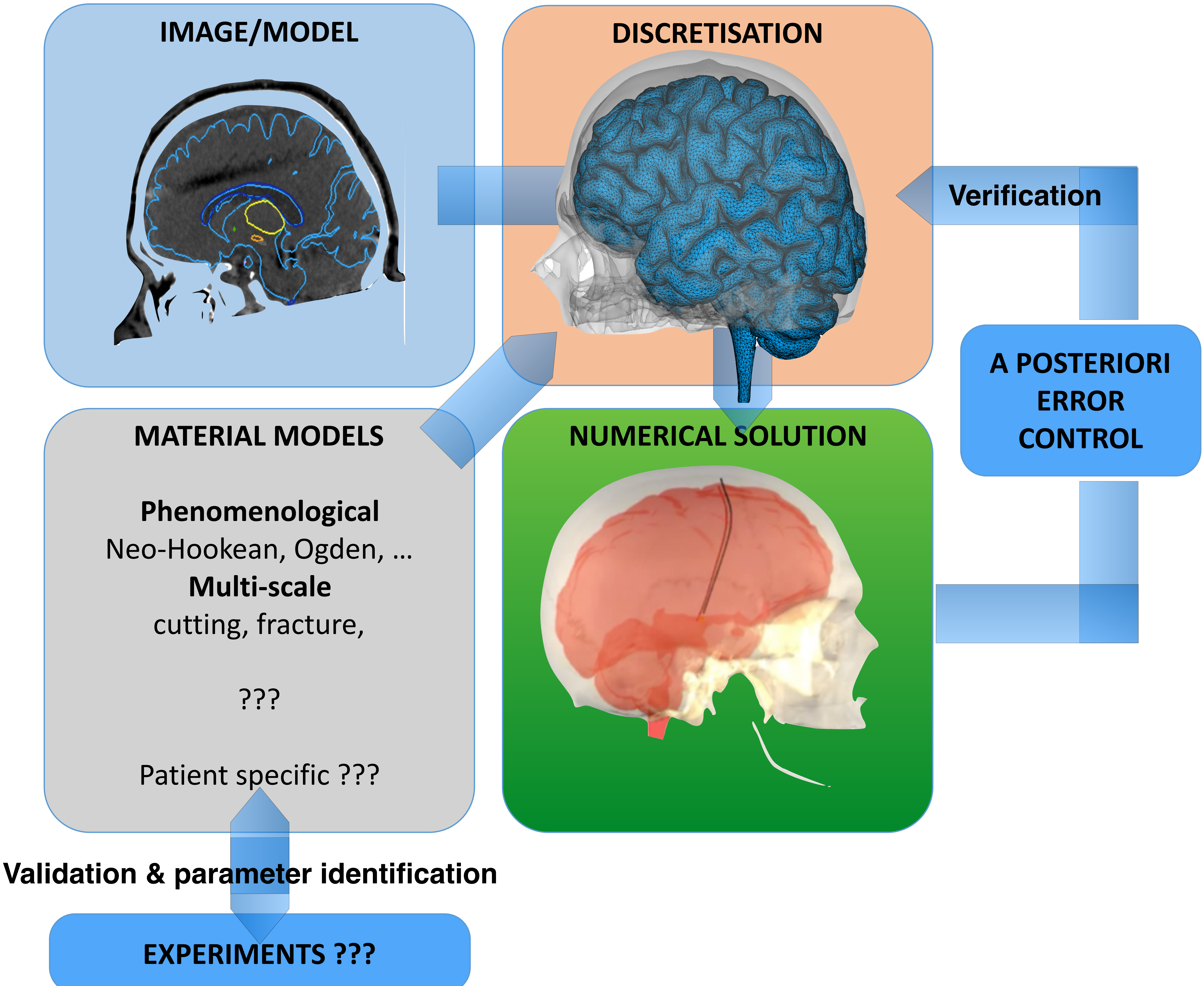
IMAGE/MODEL
DISCRETISATION
Verification
A POSTERIORI ERROR CONTROL
MATERIAL MODELS
Phenomenological
Neo-Hookean, Ogden, …
Multi-scale
cutting, fracture,
???
Patient specific ???
NUMERICAL SOLUTION
Validation & parameter identification
EXPERIMENTS ???

When the material model is not known, this conventional approach breaks down

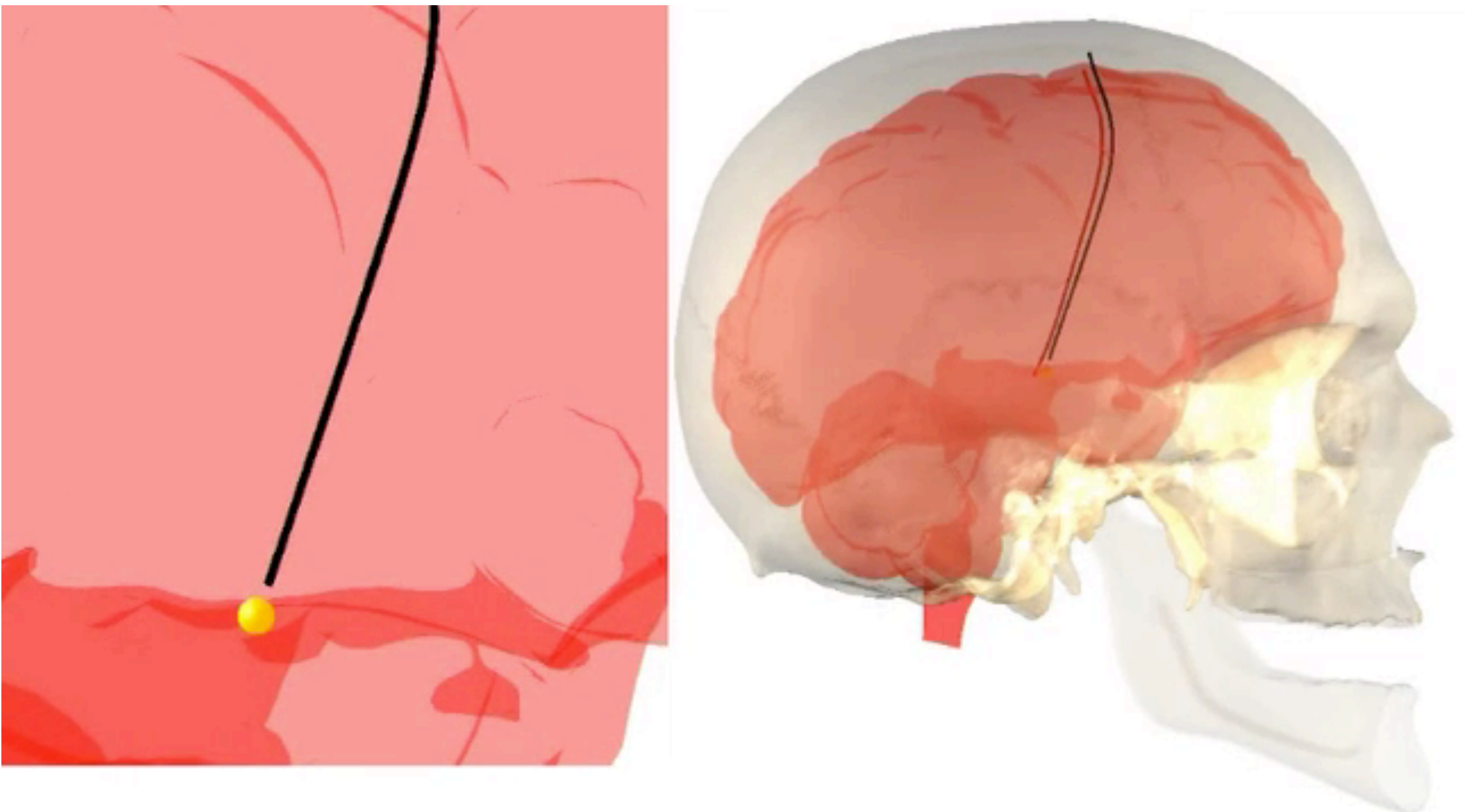

Deep-brain stimulation

Courtesy Alexandre Bilger, PhD thesis, Inria, 2014

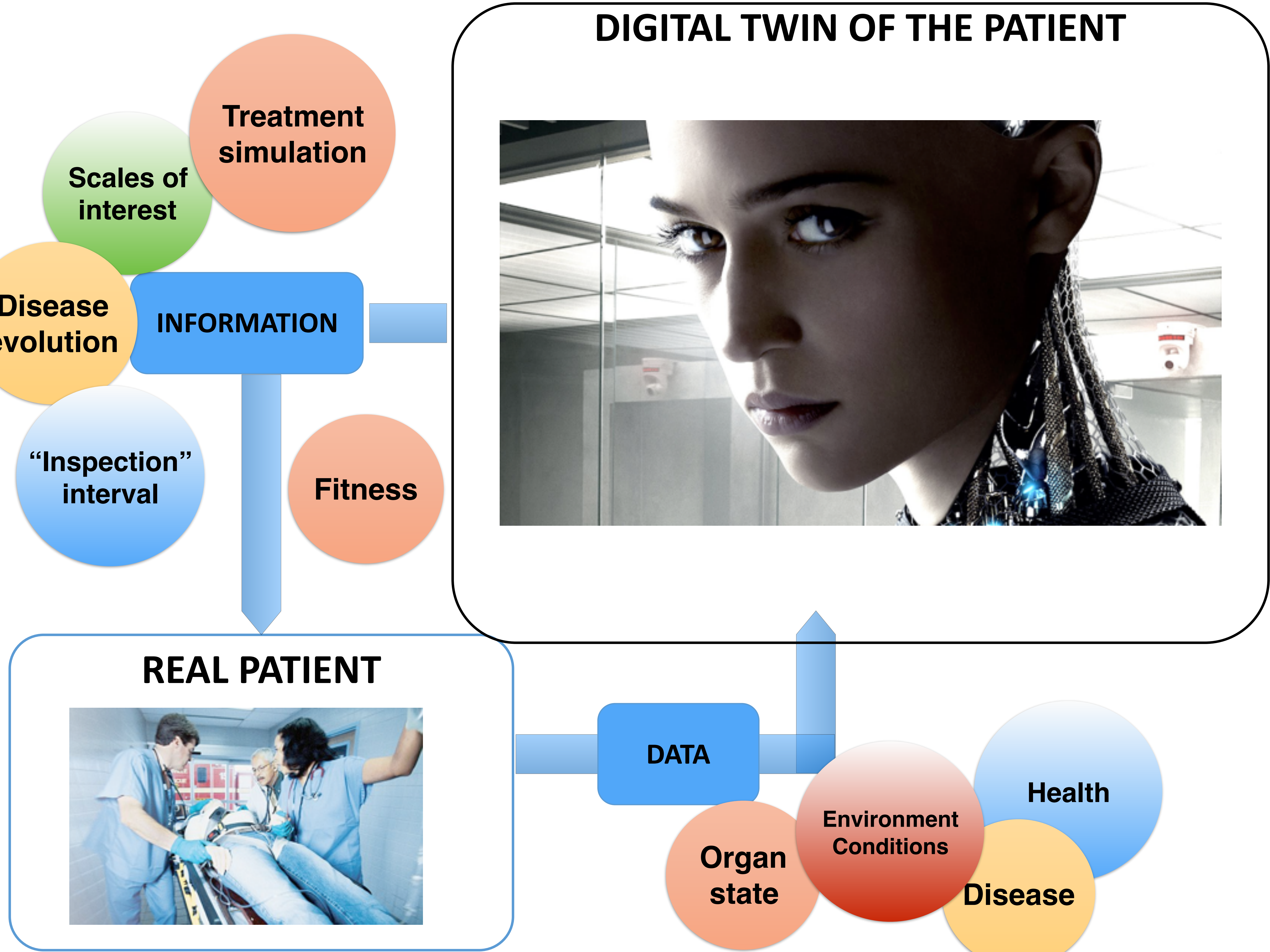
DIGITAL TWIN OF THE PATIENT
Treatment simulation
Scales of interest
Disease evolution
INFORMATION
"Inspection" interval
Fitness
REAL PATIENT
DATA
Health
Environment Conditions
Organ state
Disease

news from legato

http://legato-team.eu

Thank you for your attention!

International Centre
for Mechanical Sciences

CISM-ECCOMAS International Summer School on “Modelling, Simulation and Characterization of Multi-Scale Heterogeneous Materials” September 28, 2015 — October 2, 2015

OPEN SOURCE CODES

PERMIX: Multiscale, XFEM, large deformation, coupled 2 LAMMPS, ABAQUS, OpenMP -

MATLAB Codes: XFEM, 3D ISOGEOMETRIC XFEM, 2D ISOGEOMETRIC BEM, 2D MESHLESS
DOWNLOAD @ http://cmechanicsos.users.sourceforge.net/

COMPUTATIONAL MECHANICS DISCUSSION GROUP Request membership @
http://groups.google.com/group/computational_mechanics_discussion/about

Thank you for your attention!

International Centre
for Mechanical Sciences

CISM-ECCOMAS International Summer School on “Towards a seamless Integration of CAD and simulation” (G. Beer and S. Bordas) 2017

OPEN SOURCE CODES

PERMIX: Multiscale, XFEM, large deformation, coupled 2 LAMMPS, ABAQUS, OpenMP -

MATLAB Codes: XFEM, 3D ISOGEOMETRIC XFEM, 2D ISOGEOMETRIC BEM, 2D MESHLESS
DOWNLOAD @ http://cmechanicsos.users.sourceforge.net/

COMPUTATIONAL MECHANICS DISCUSSION GROUP Request membership @
http://groups.google.com/group/computational_mechanics_discussion/about

- Domain coupling using the primal Schur-complement domain decomposition method.
- Local subproblems have been reduced by projection in low-dimensional subspaces obtained by the snapshot POD.
- This approach permits to flexibly reduce the computational cost associated with highly nonlinear problems. In particular:
  - the **local reduced spaces are generated independently**, and have independent dimensions, which allows us to focus the numerical effort where it is most needed.
  - subdomains that are close to highly damaged zones need a richer model to account for the effect of topological changes. The local **POD transforms automatically generate local reduced spaces of larger dimension in these zones**.
  - the domain decomposition framework enables us to **switch from reduced local solvers to full local solvers** in a transparent manner. This is particularly useful for the subdomains that contain process zones, as a solution obtained by projection would be more expensive than a direct solution for a desirable accuracy.
  - the transition between ``offline'' and ``online'' computations becomes flexible. The **reduced models can be used in the zones where the local reduced spaces converge quickly** when enriching the snapshot space, while still computing snapshots and refining the reduced models via a direct local solver in the remaining subdomains.

- Further work related to domain decomposition
  - **load balancing** mismatch would occur when using such a strategy in parallel. CPUs which support domains that are not reduced, or domains for which the corresponding subproblems need to be projected in a space of relatively high dimension, would require to perform more operations. The domain partitioning itself should be performed jointly with the model reduction in order to distribute the load evenly.
  - **the interface problem itself was not reduced** here, to guarantee the interface kinematic compatibility.
    - ➡ Suboptimal reduced order model. Would generate expensive communications in parallel
    - ➡ A reduction of the interface problem using the POD can be done but is neither elegant nor easy
    - ➡ Dual Schur-complement domain decomposition method would allow the kinematic approximation of the subproblems to include the interface. However, this would only deflect the difficulty to the necessary reduction of the interface Lagrange multiplier space. This issue is our current direction of research.

Bayesian inference

Primer

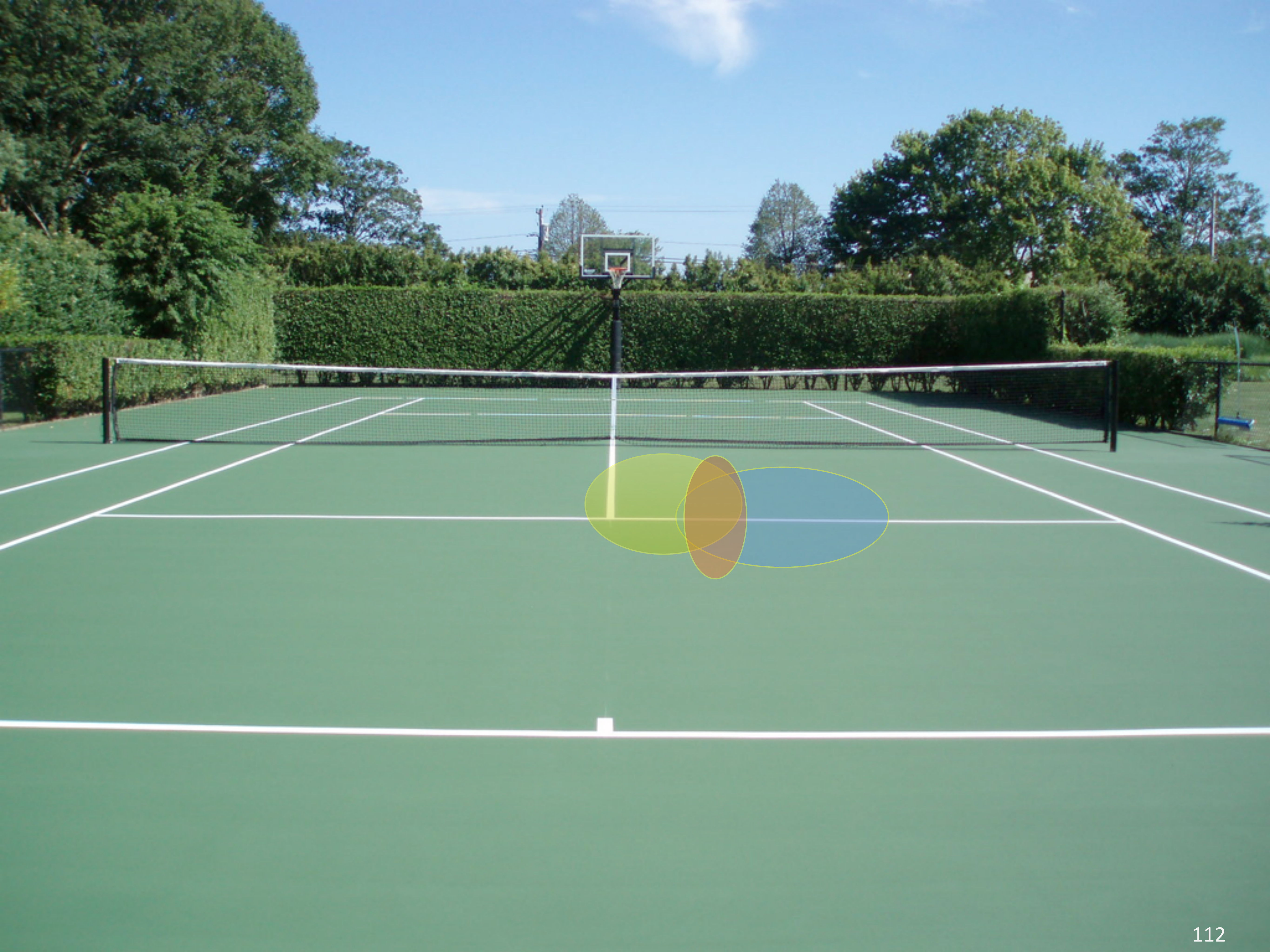

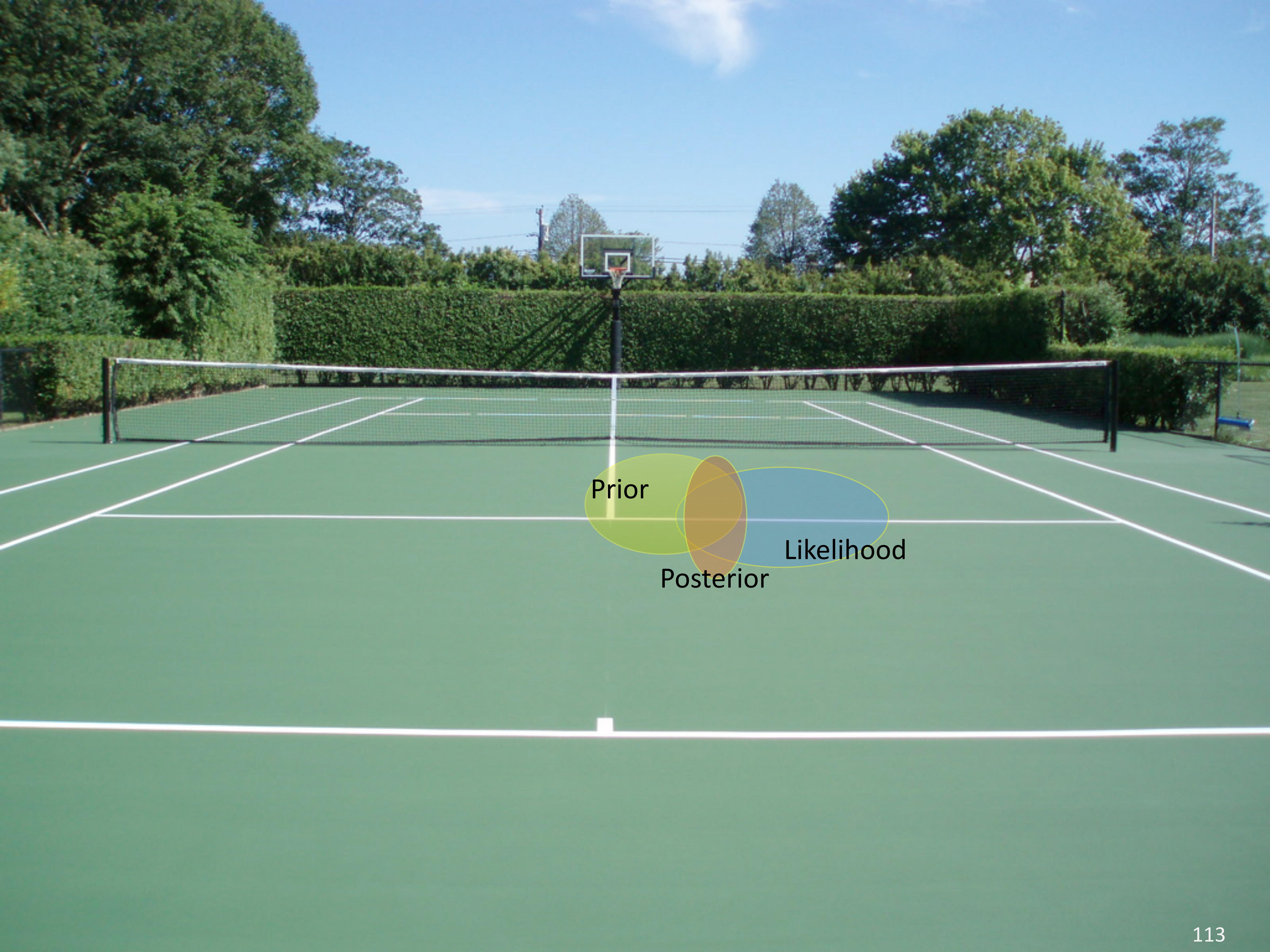
Prior
Likelihood
Posterior

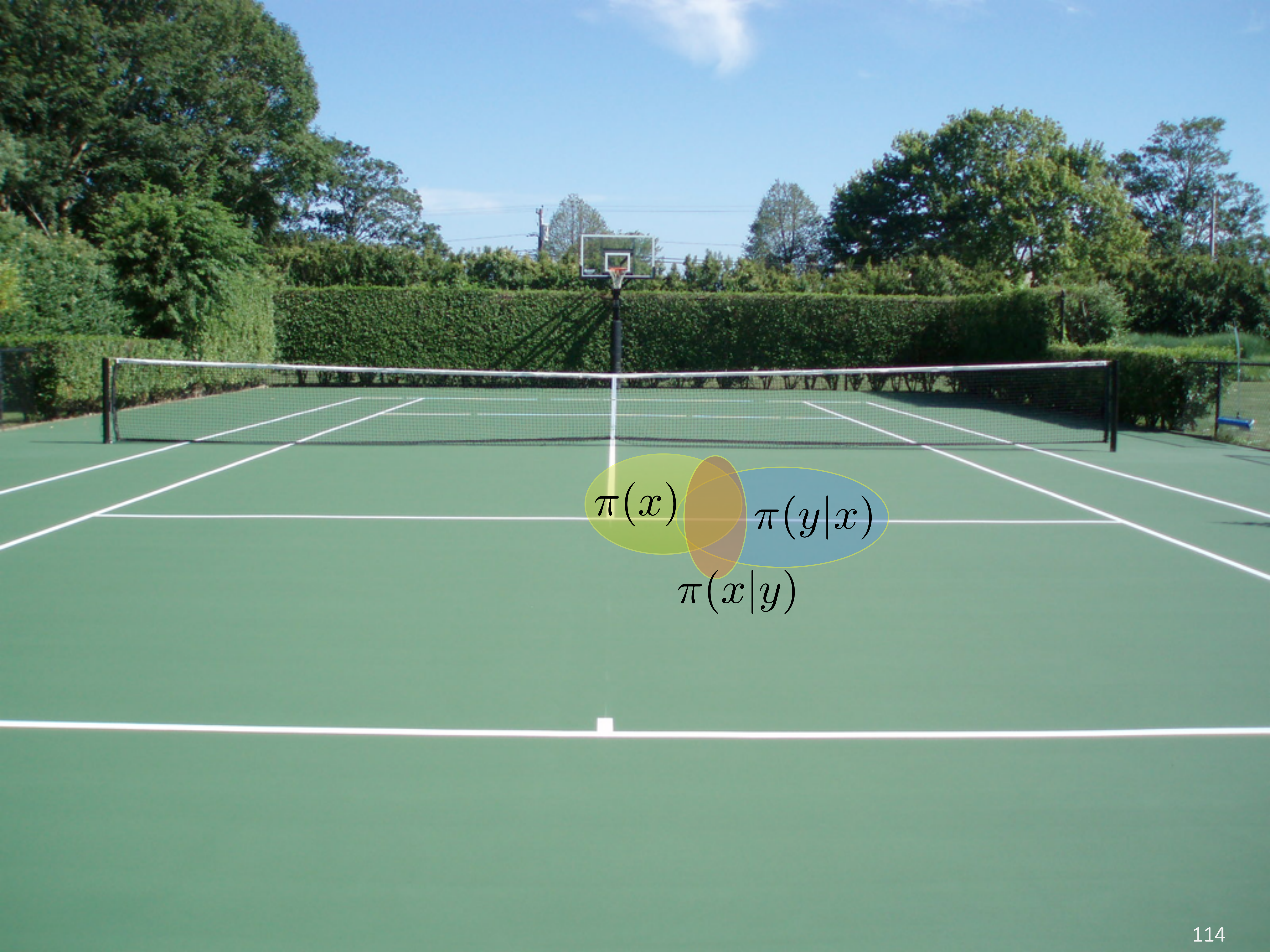
$\pi(x)$
$\pi(y|x)$
$\pi(x|y)$

Bayes' theorem

$$\text{posterior} = \frac{\text{prior} \times \text{likelihood}}{\text{evidence}}$$

$$\pi(x|y) = \frac{\pi(x)\pi(y|x)}{\int \pi(x)\pi(y|x)dx}$$

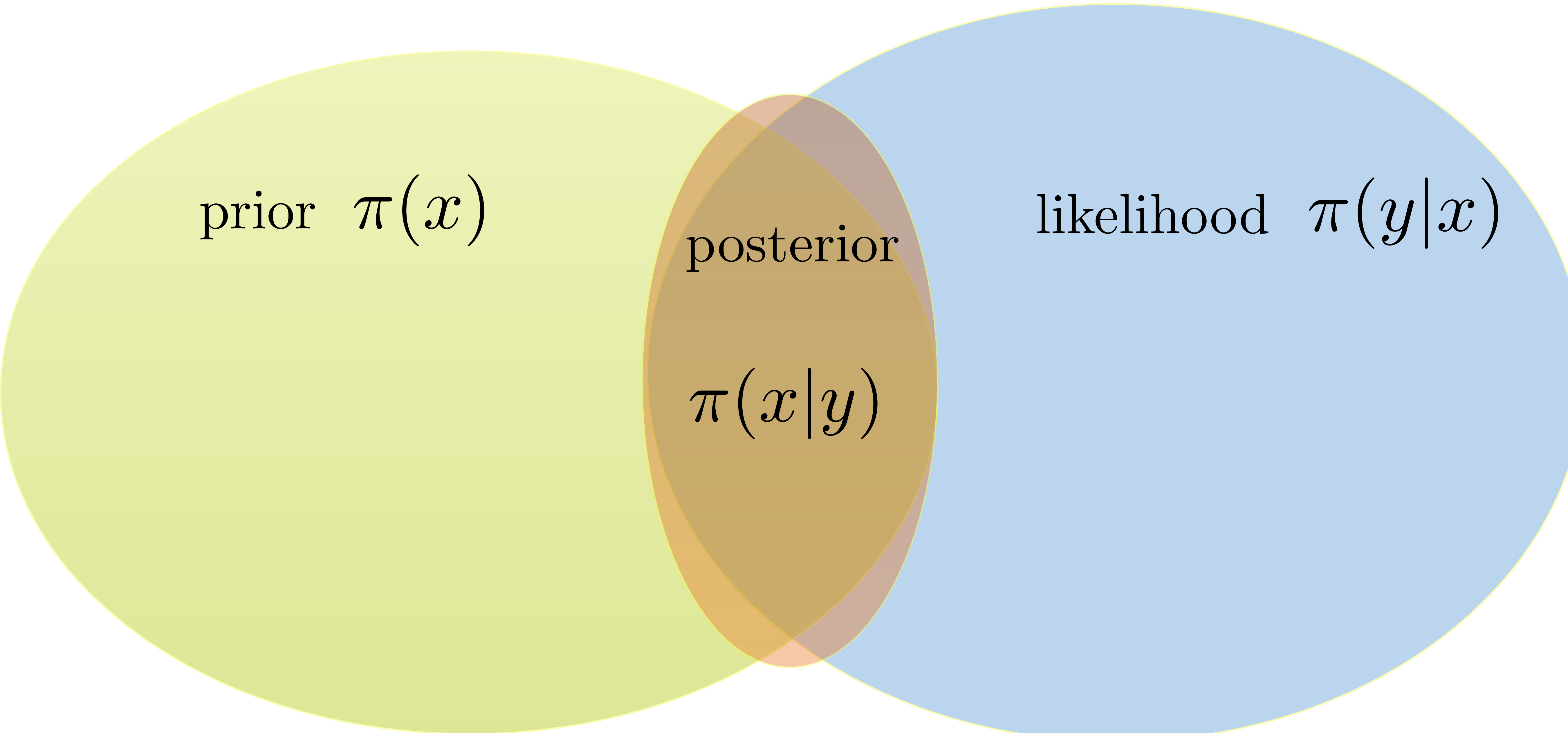

Parameter identification: Bayesian approach

Bayes' theorem

$$\pi(x|y) = \frac{\pi(x)\pi(y|x)}{\int \pi(x)\pi(y|x)dx}$$

$\pi(.)$: probability distribution function

$\pi(.|.)$: conditional probability distribution function

x : material parameter

y : observations

Parameter identification: Bayesian approach

Bayes' theorem

$$\pi(x|y) = \frac{\pi(x)\pi(y|x)}{\int \pi(x)\pi(y|x)dx}$$

Descriptive formula

$$\text{Posterior} = \frac{\text{Prior} \times \text{Likelihood}}{\text{Evidence}}$$

A discrete example of Bayes' theorem

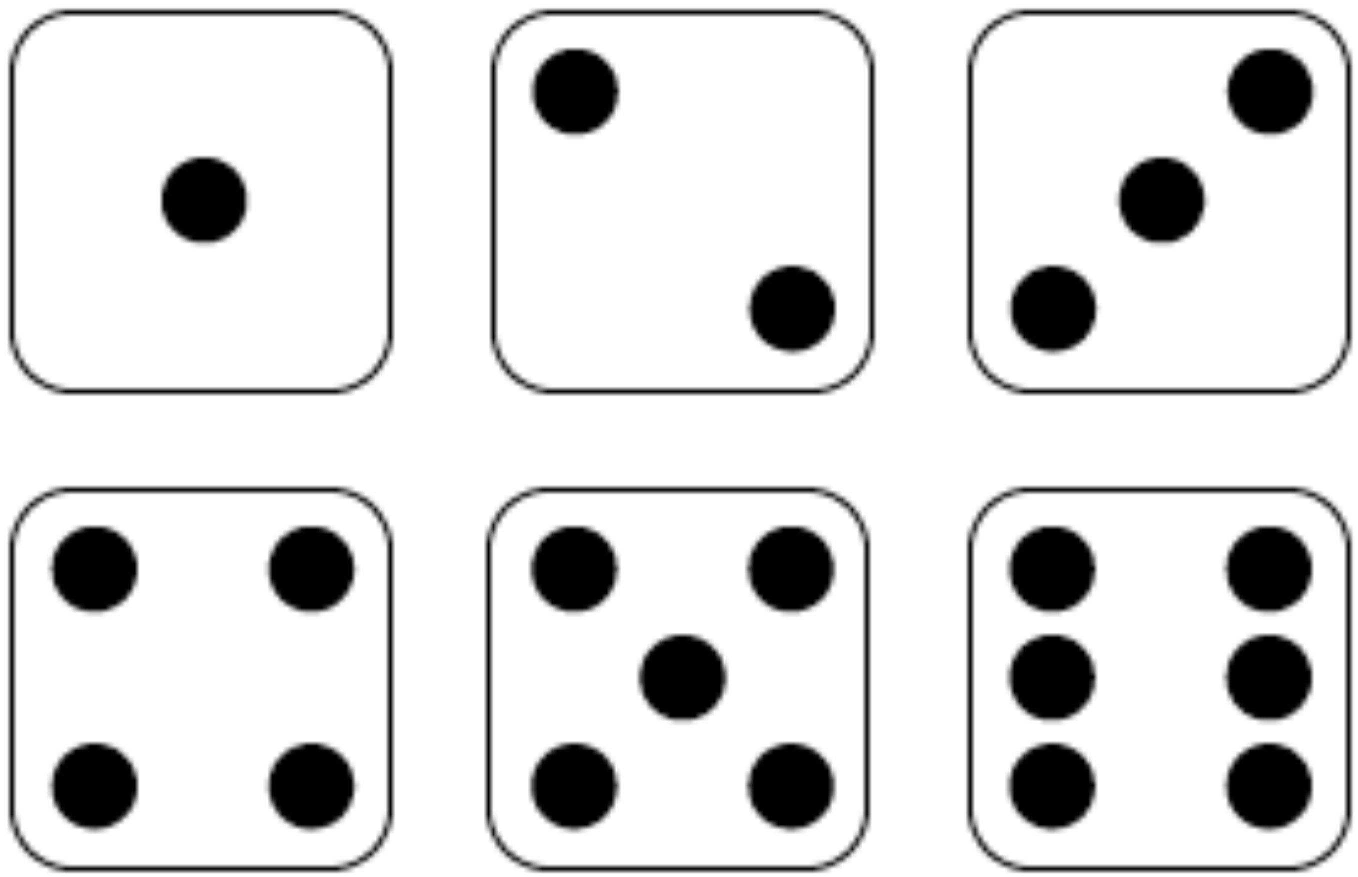

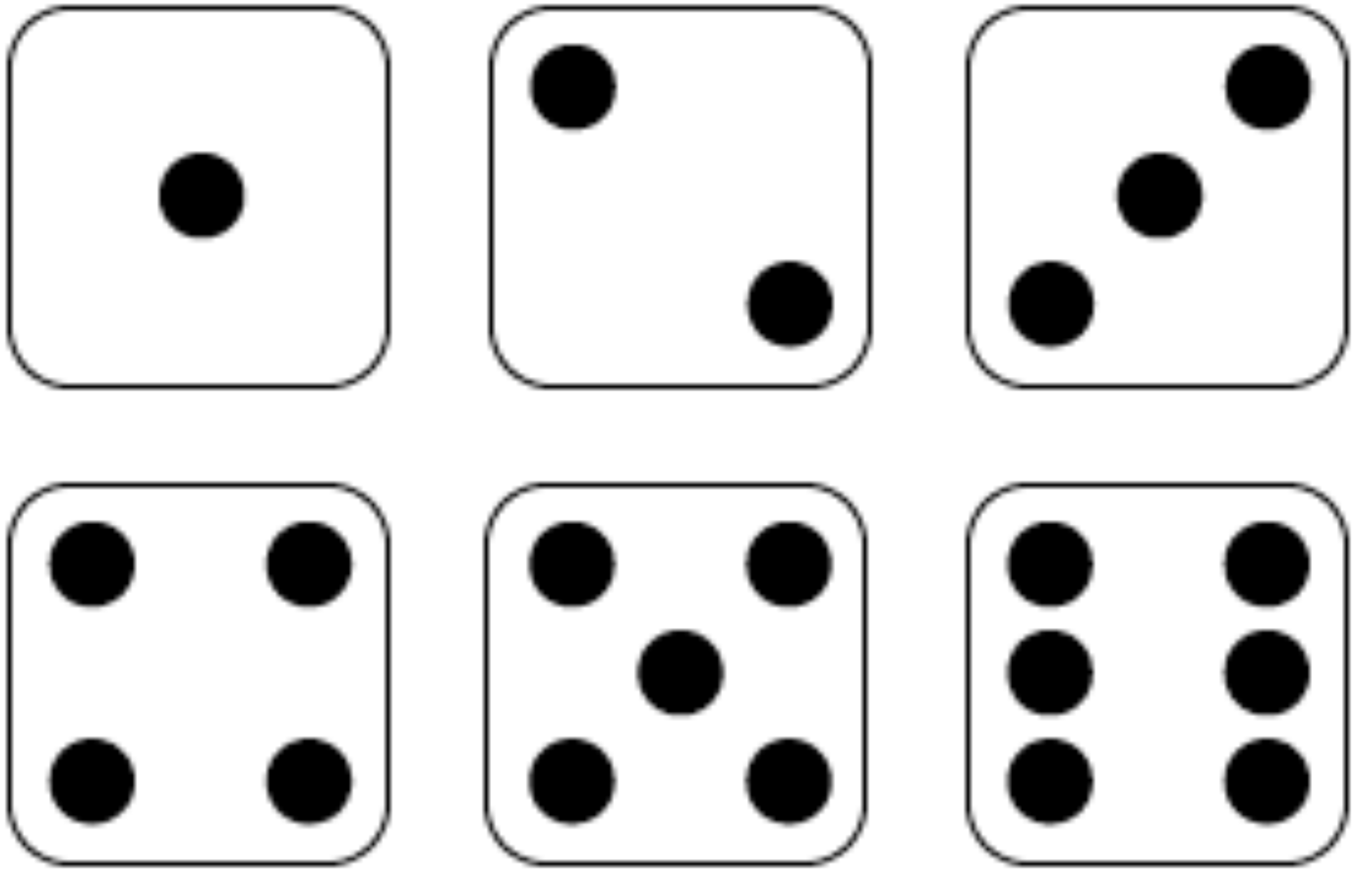

This is our prior information for the probability of each face: 1/6

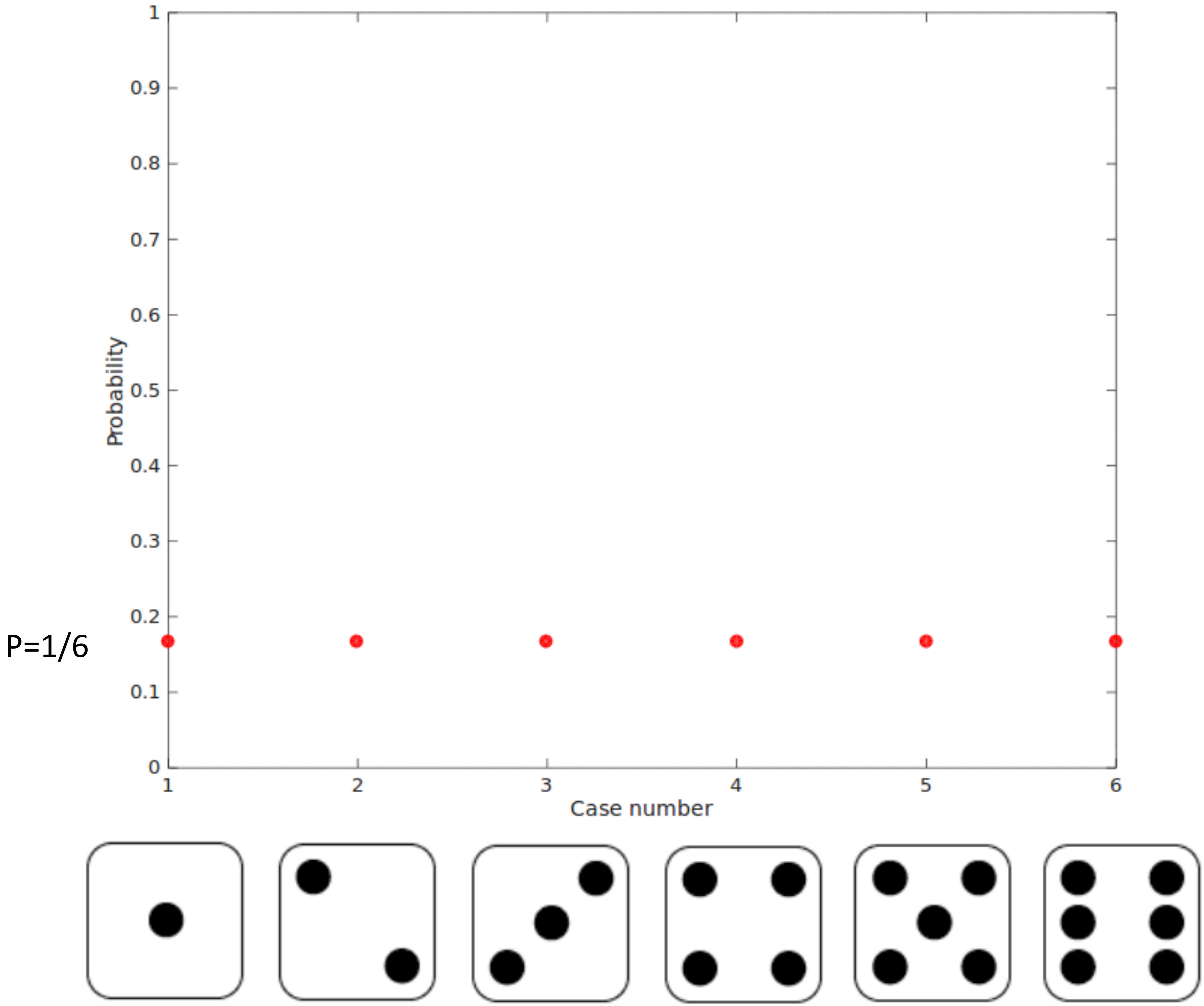
P=1/6
Probability
Case number
0
0.1
0.2
0.3
0.4
0.5
0.6
0.7
0.8
0.9
1
1
2
3
4
5
6

Assume that after throwing the dice, you see the above evidence

Goal: determine the probability of this evidence for each face of the dice

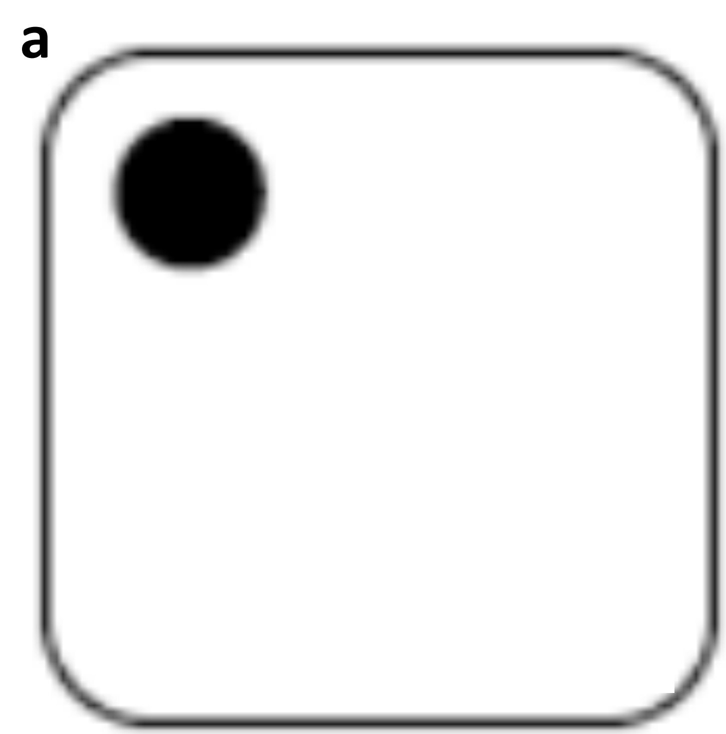
a

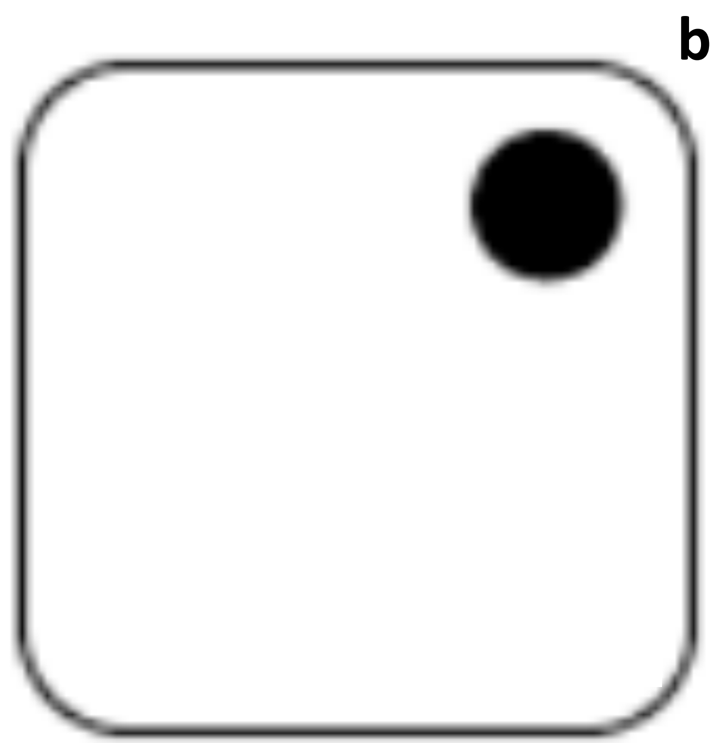
b

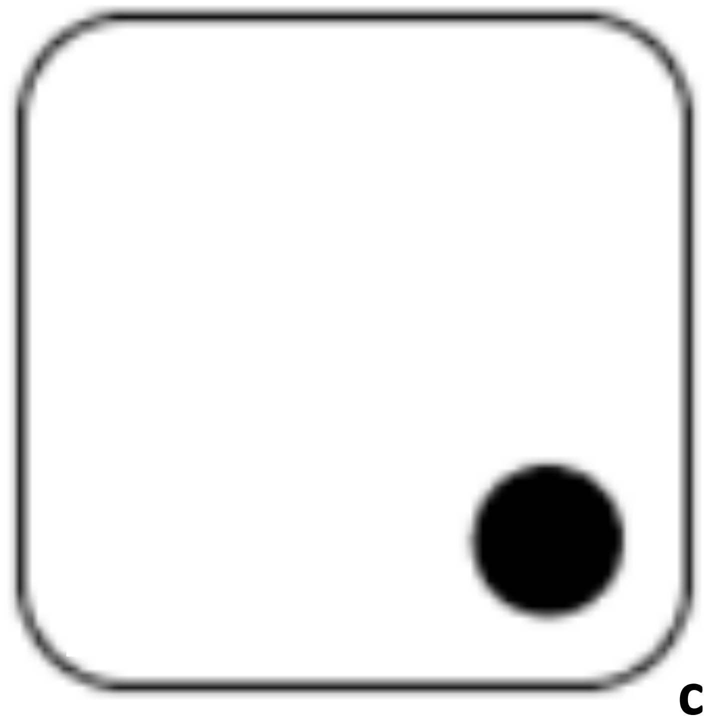
c

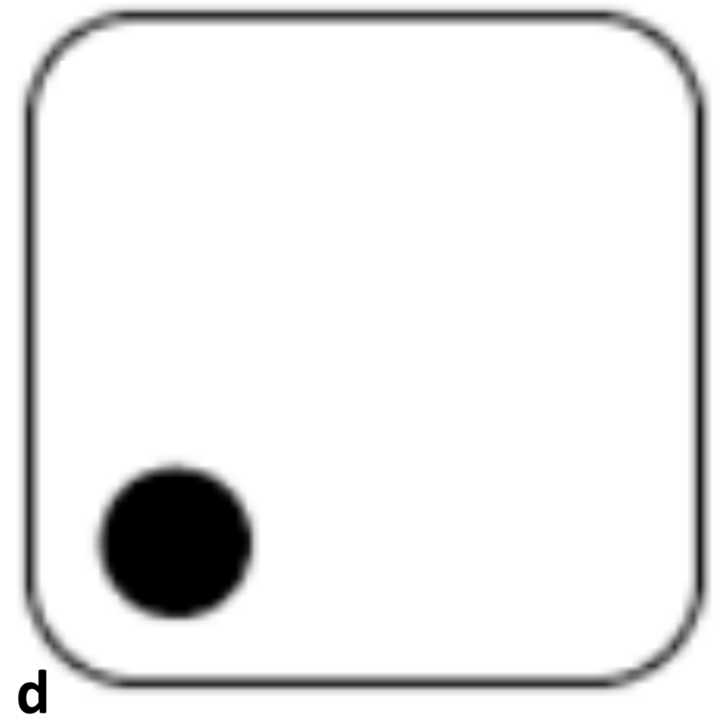
d

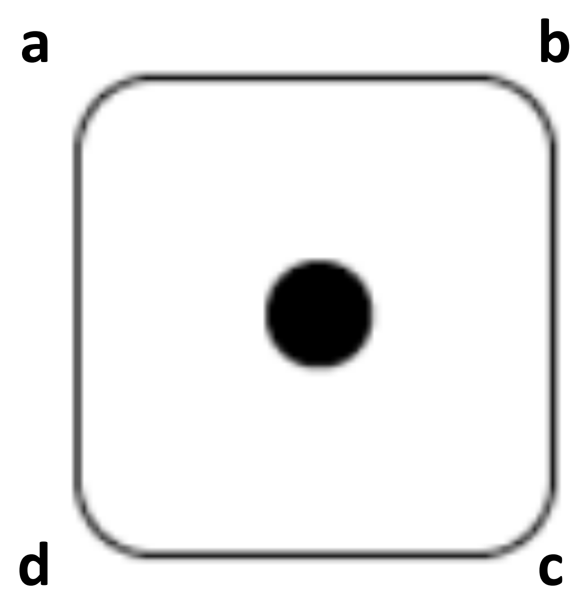
a
b
d
c

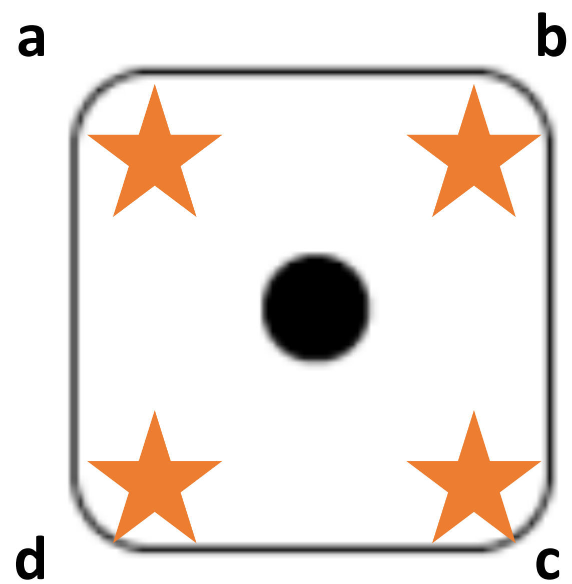
a
b
d
c

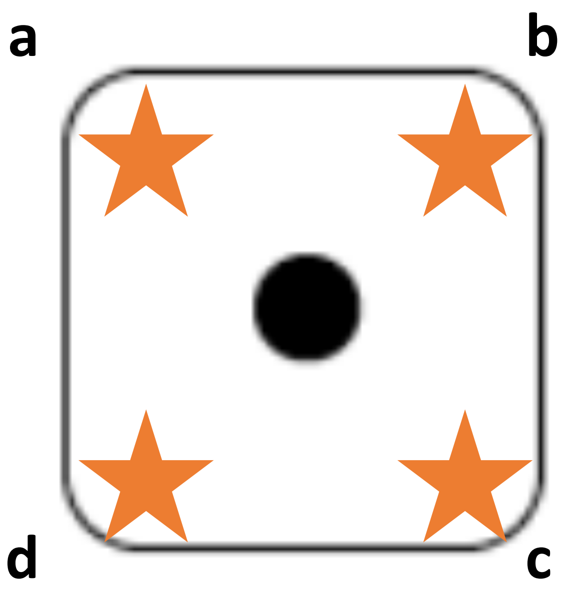

One would never see a dot at the star positions for this face
The probability of the evidence is *zero*

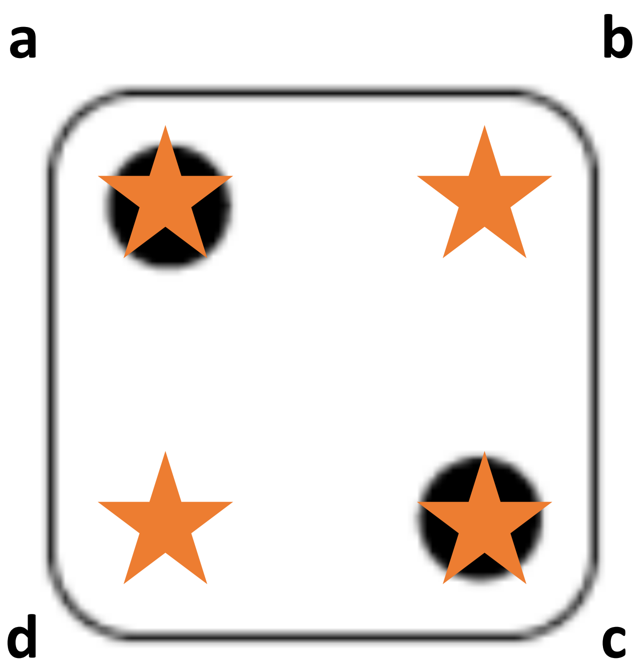

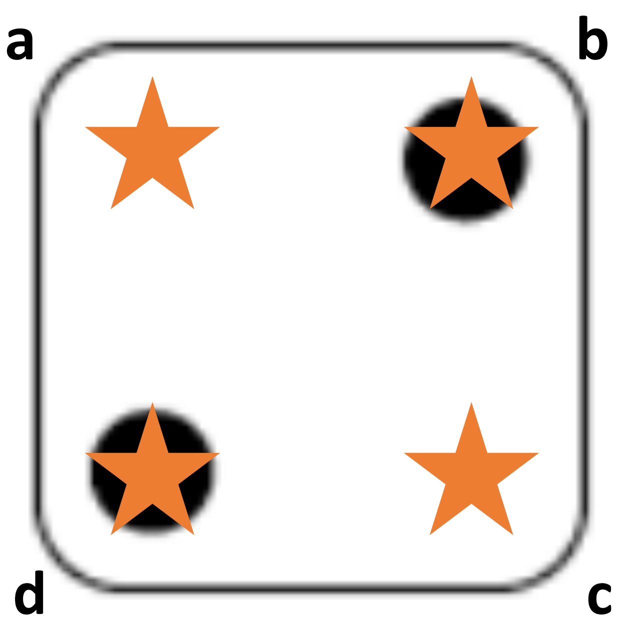

Two possibilities (a,c) and (b,d)

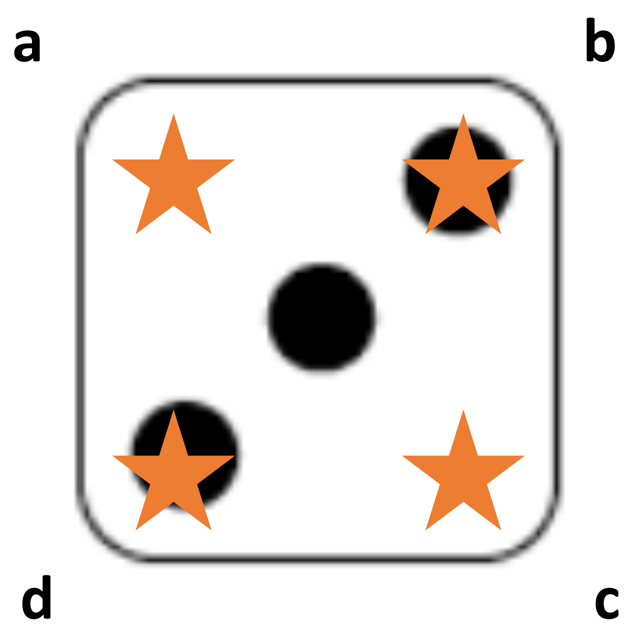

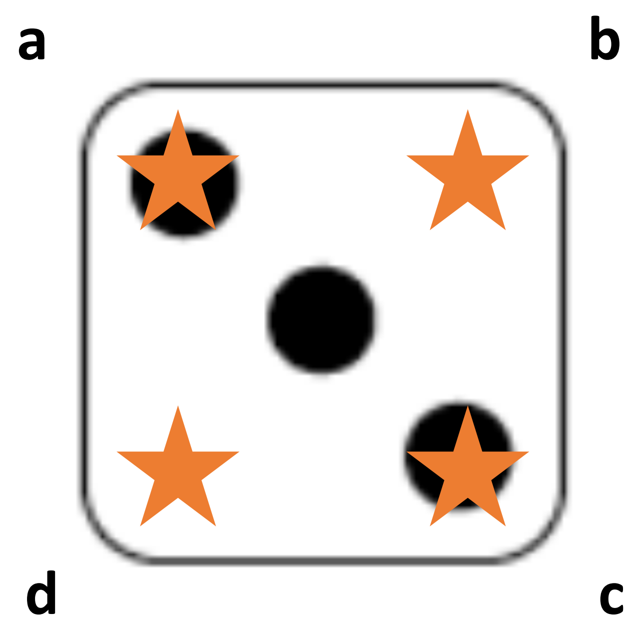

Also two possibilities (a,c) and (b,d)

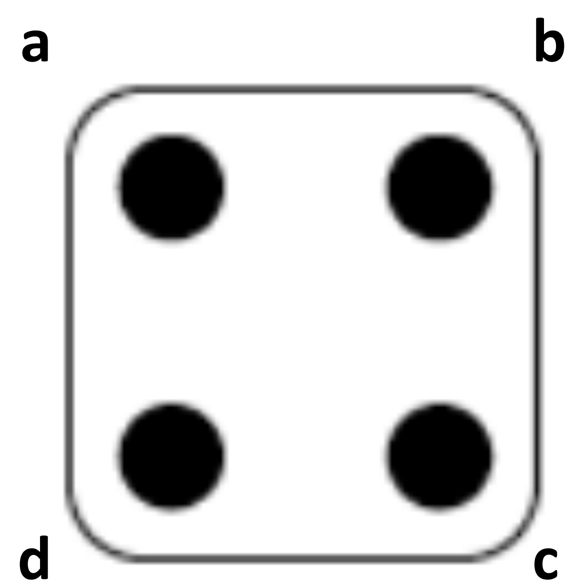
a
b
d
c

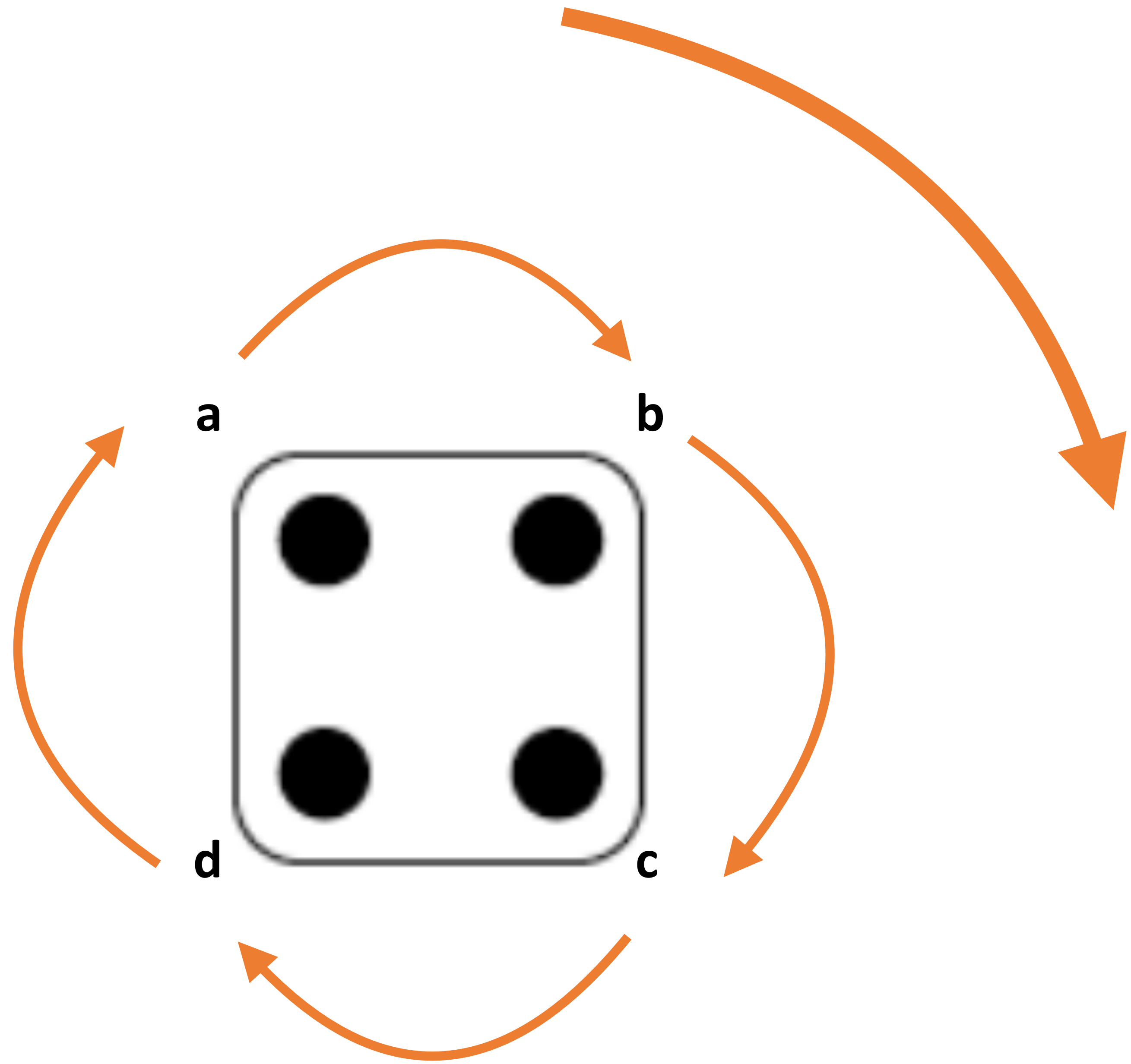
a
b
c
d

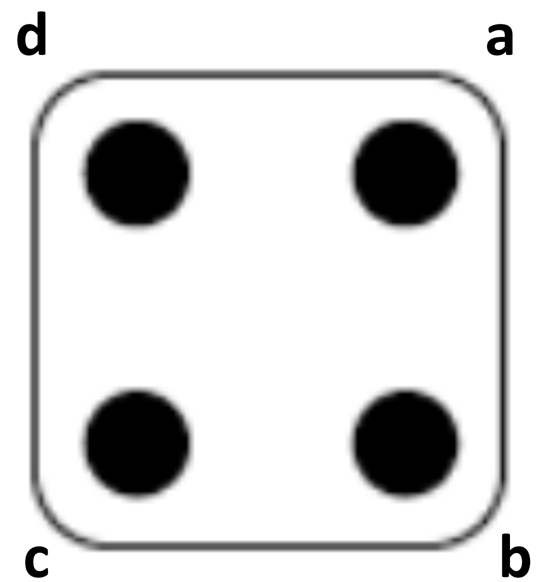
d
a
c
b

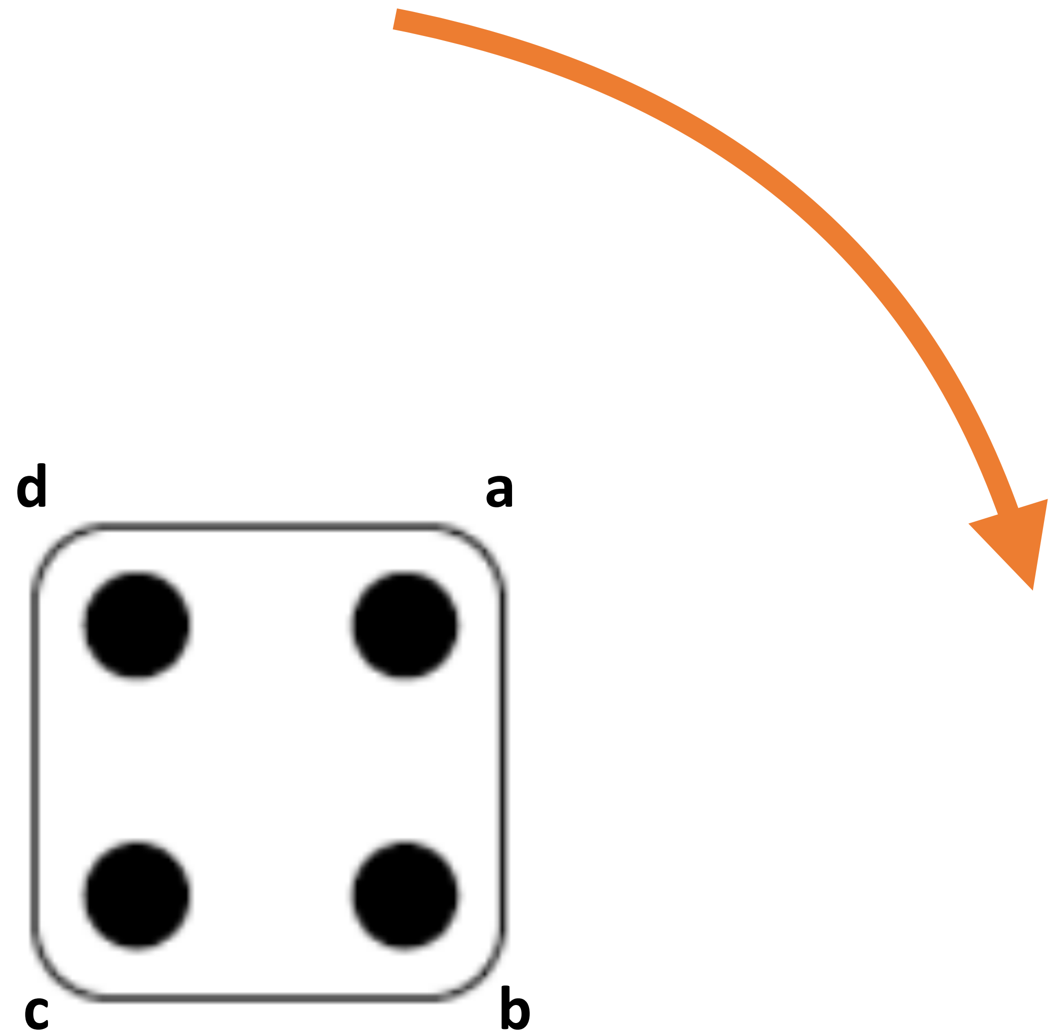
d
a
c
b

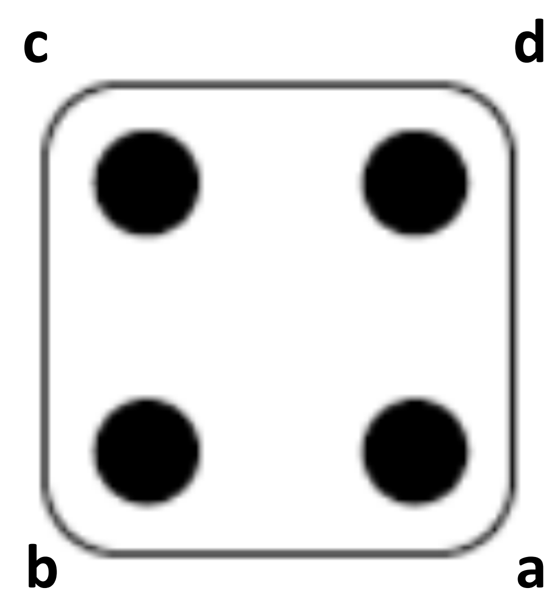
c
d
b
a

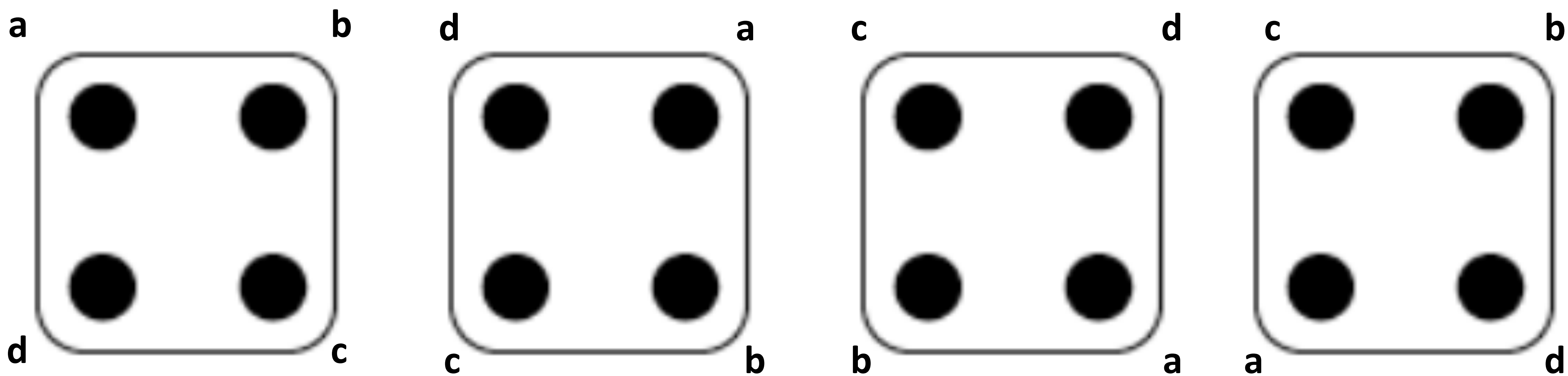
a
b
d
c
d
a
c
b
c
d
b
a
c
b
a
d

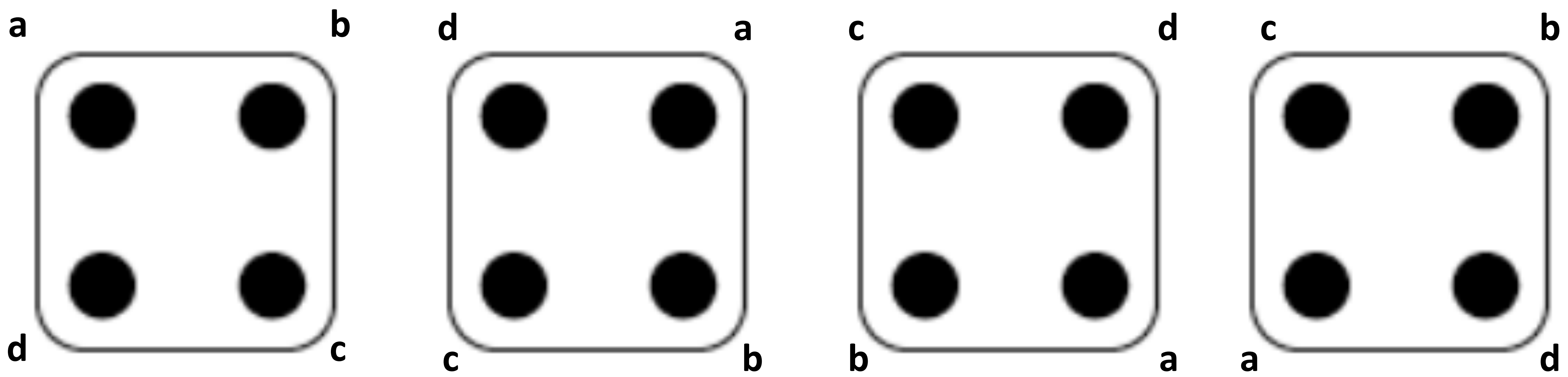

Four possibilities

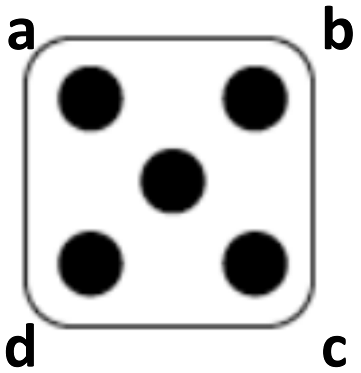

Four possibilities

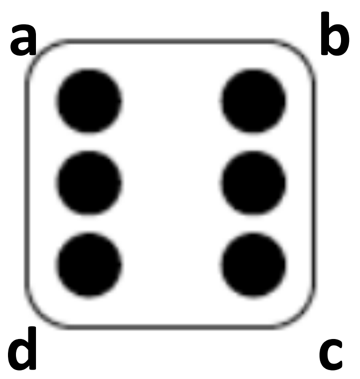

Four possibilities

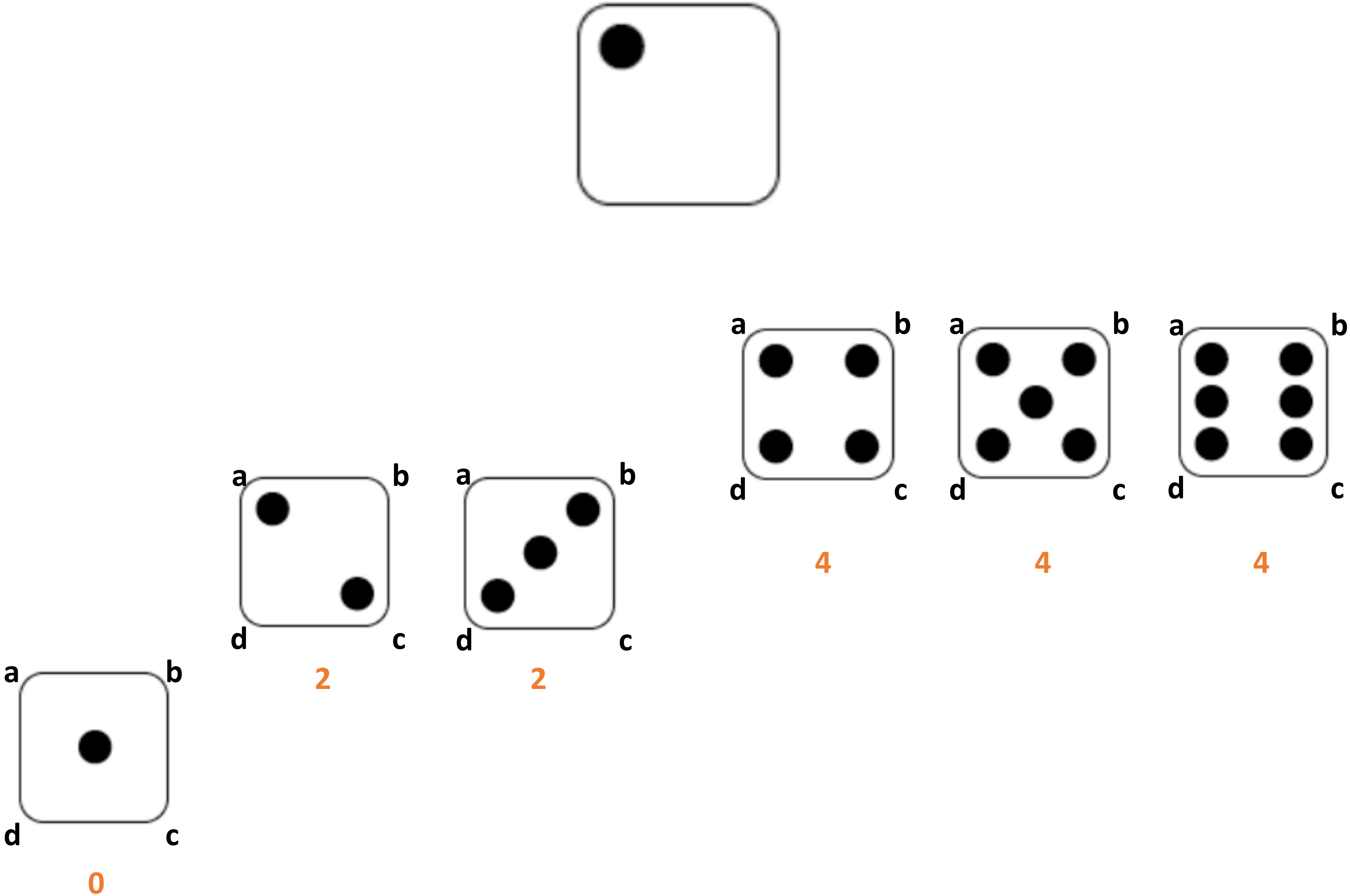
a b d c
0
a b d c
2
a b d c
2
a b d c
4
a b d c
4
a b d c
4

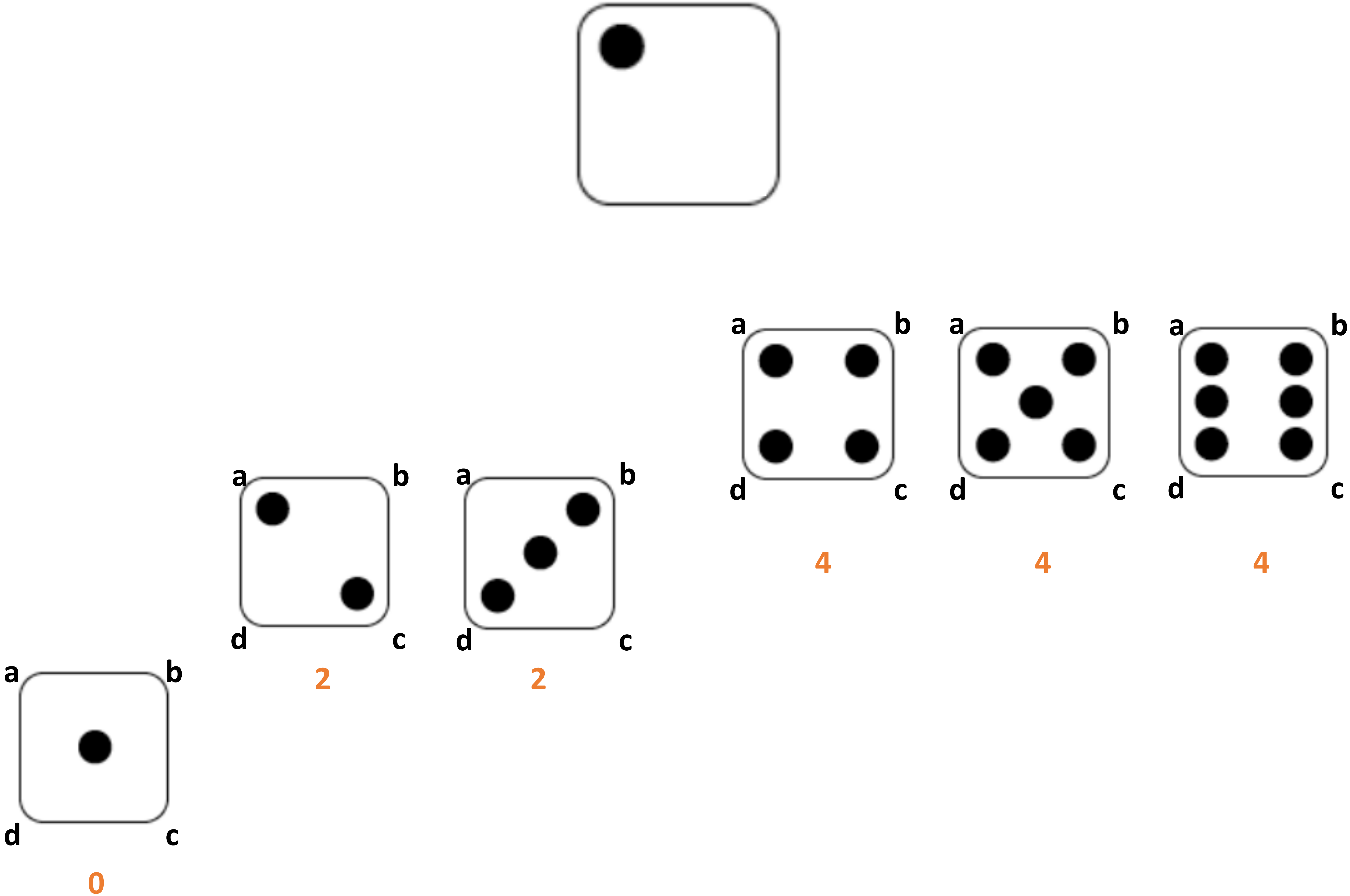

$$\pi(y) = \frac{0+2+2+4+4+4}{6 \times 4} = \frac{16}{24}$$

$$\pi(x|y) = \frac{\text{Prior} \times \text{Likelihood}}{\text{Evidence}} = \frac{\frac{1}{6} \times \frac{1}{2}}{\frac{16}{24}} = 0.125$$

Probability that 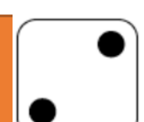 **was the face of the dice knowing**

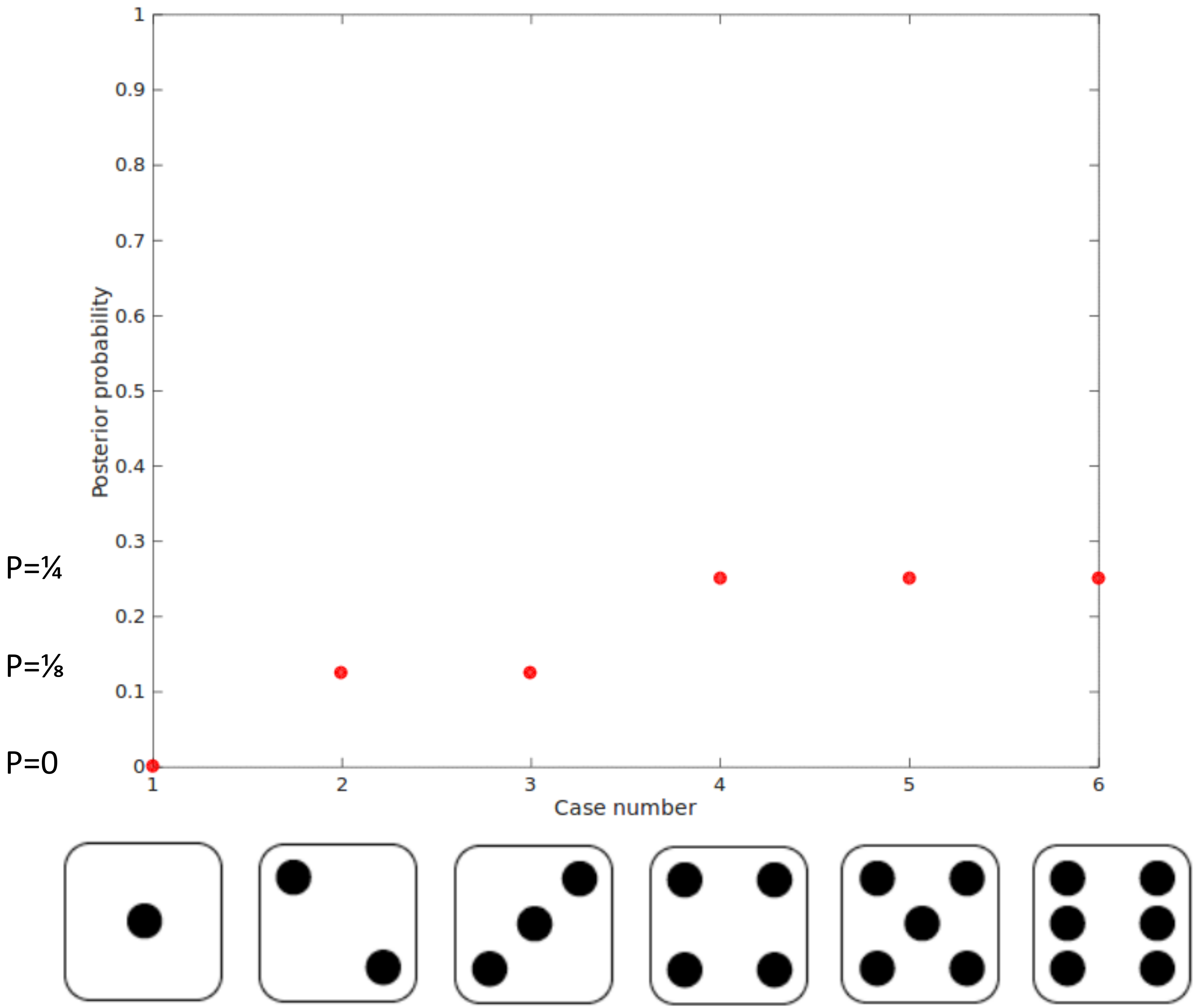
P=¼
P=⅛
P=0
Posterior probability
0
0.1
0.2
0.3
0.4
0.5
0.6
0.7
0.8
0.9
1
1
2
3
4
5
6
Case number

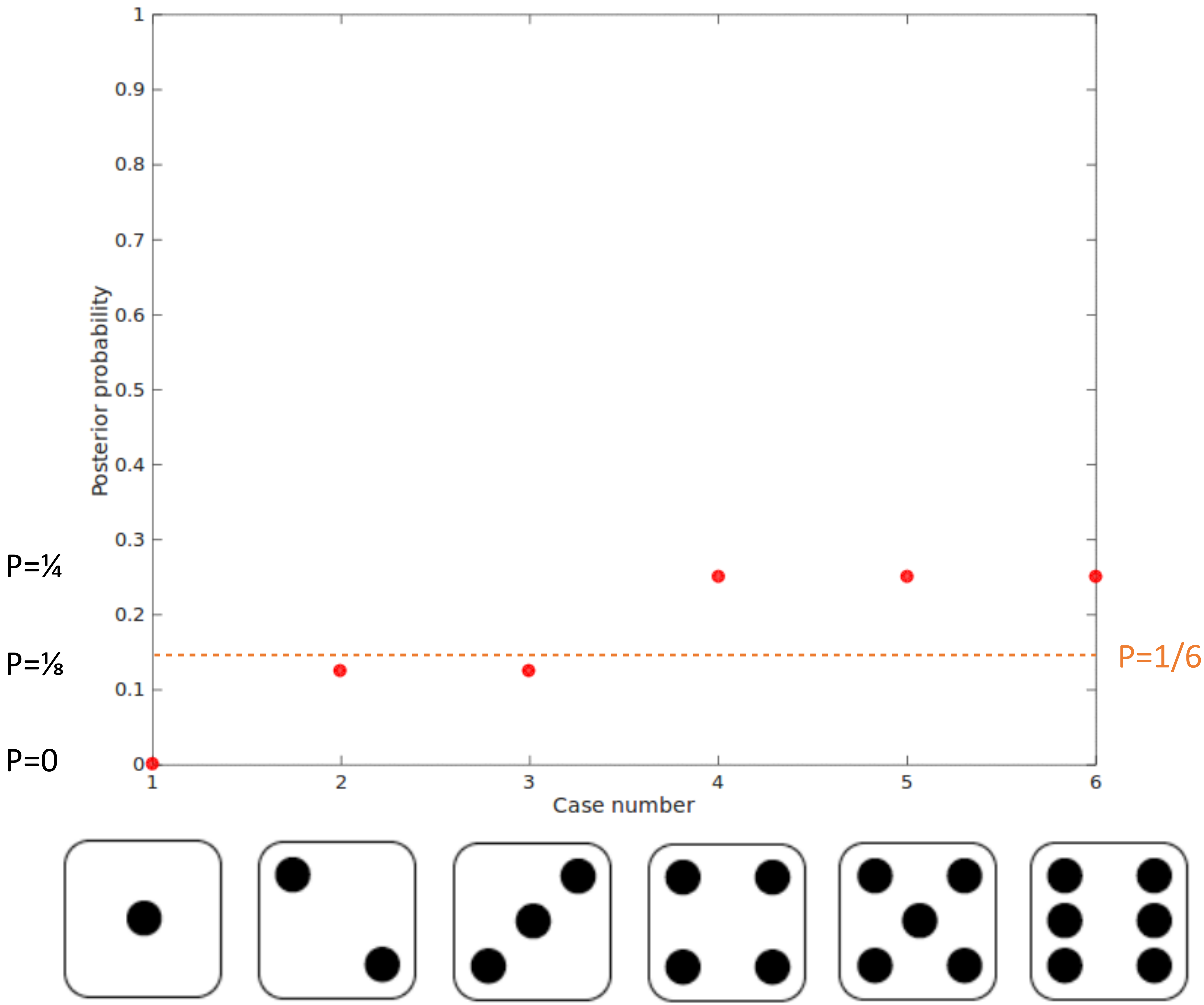
Posterior probability
0
0.1
0.2
0.3
0.4
0.5
0.6
0.7
0.8
0.9
1
1
2
3
4
5
6
Case number
P=¼
P=⅛
P=0
P=1/6

Stress-strain data

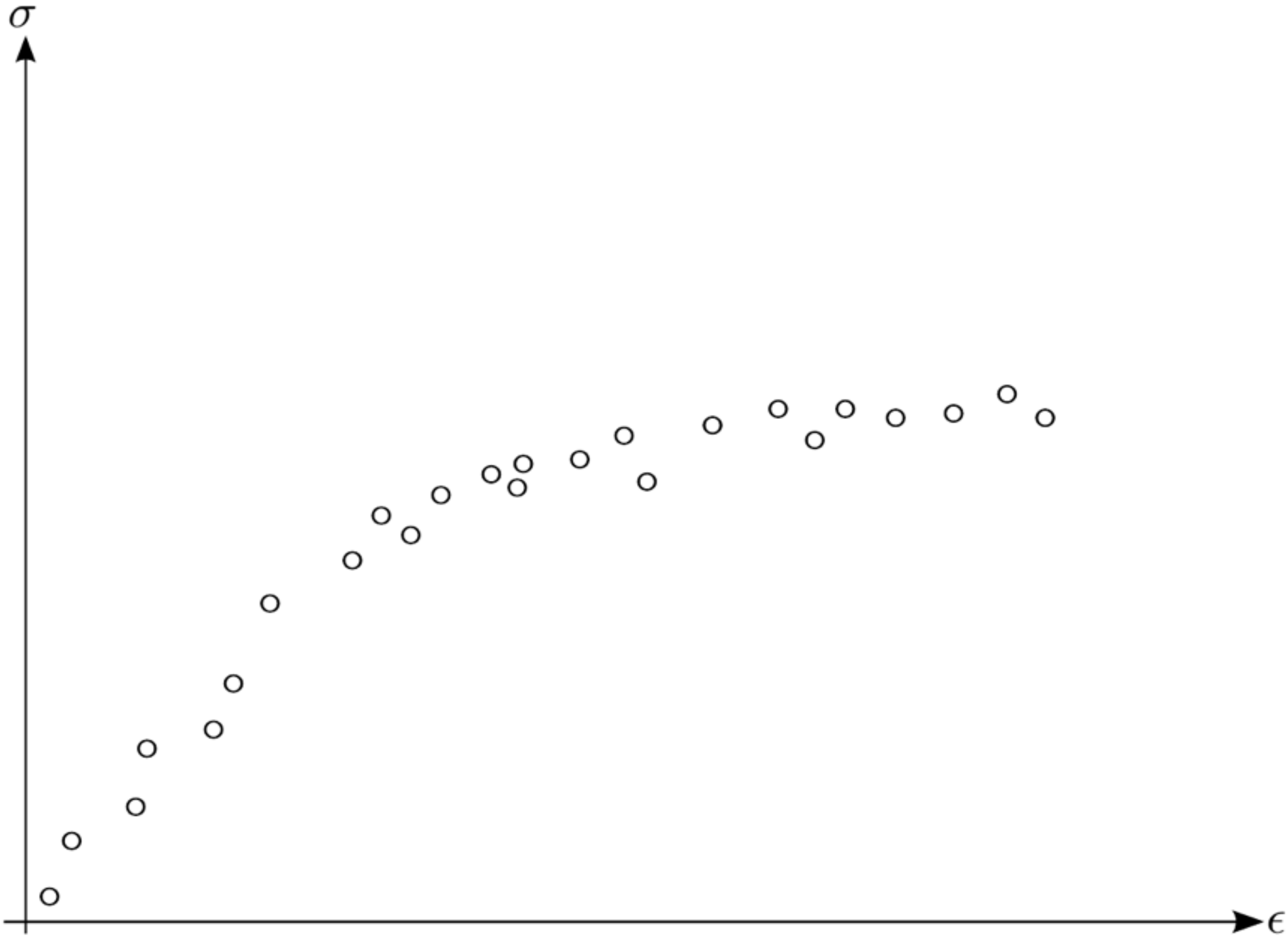

Identify the parameters

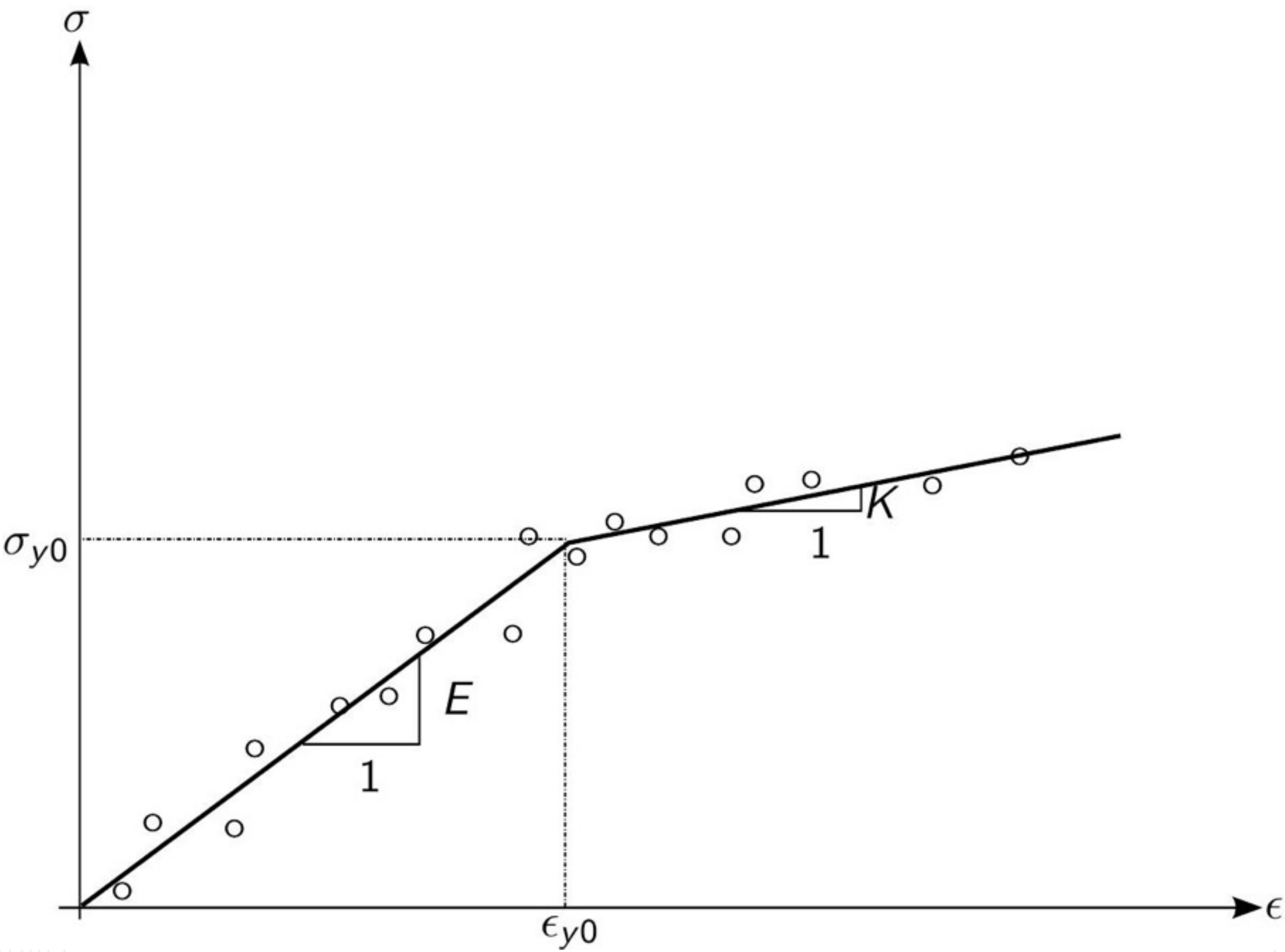

Construct the likelihood function

Model	
$Y = f(X, \Omega)$	observations=f(parameters, error)

Ω : Error

X : Material parameter

Noise model

Additive noise model

$$Y = f(X) + \Omega$$

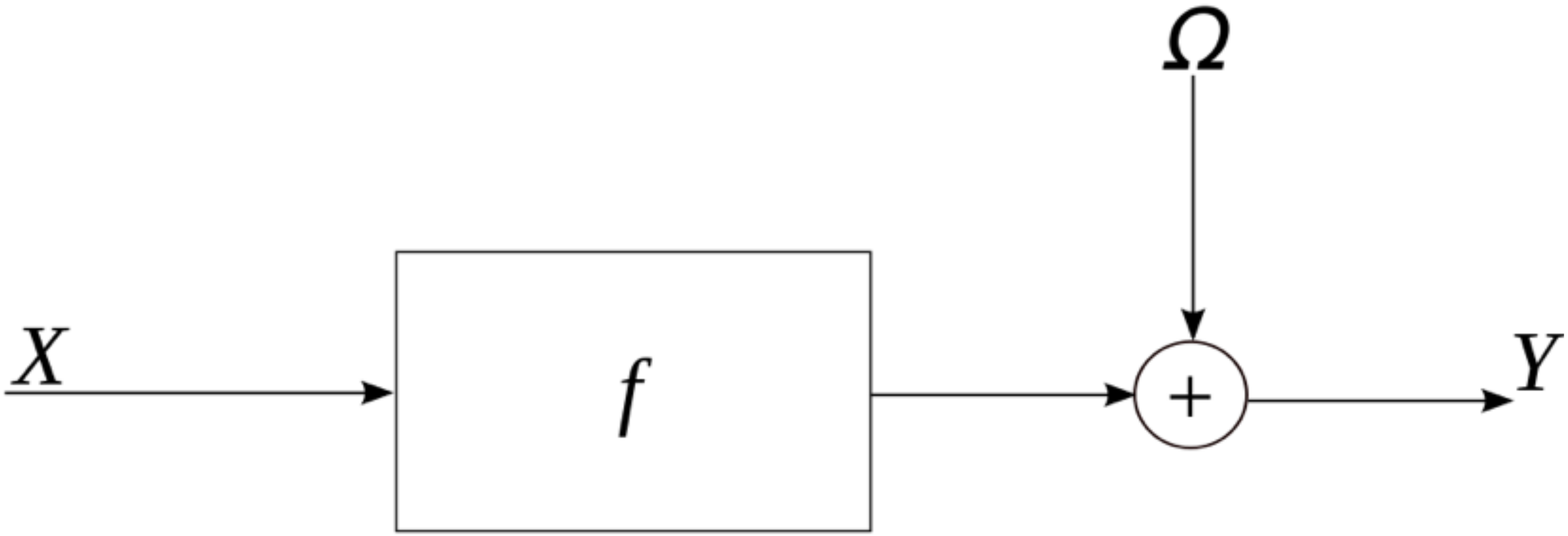

Likelihood function

Likelihood function for additive model

$$\pi(y|x) = \pi(\omega) = \pi(y - f(x))$$

$$Y = f(X) + \Omega$$

Constitutive law: linear elasticity

Constitutive model

$$\sigma = E\epsilon \text{ or } \sigma = x\epsilon$$

Observed data

$$Y = X\epsilon + \Omega$$

Prior information on Young's modulus

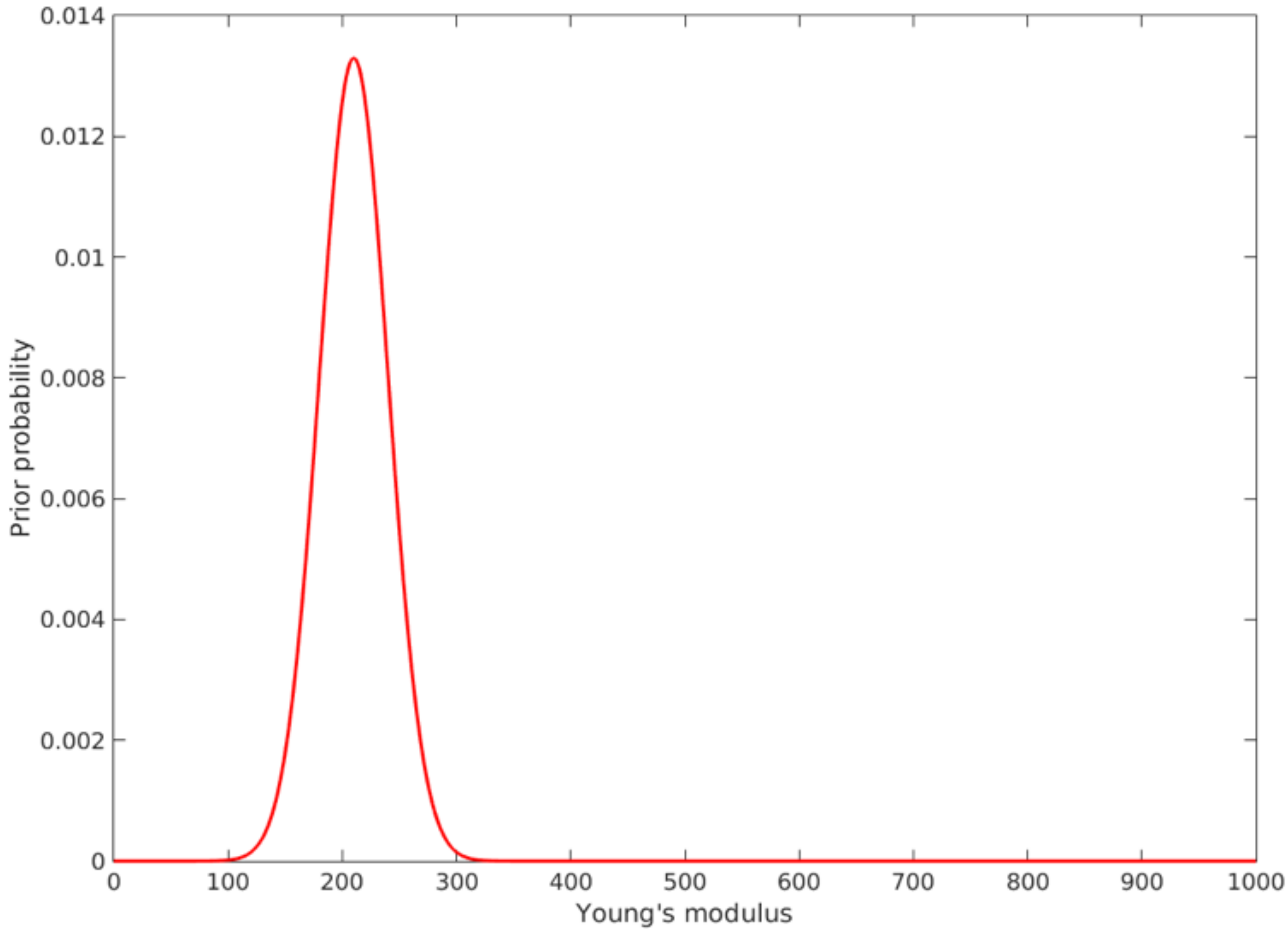

$$\pi_{prior}(x) = N(210, 900)$$

Error model (noise)

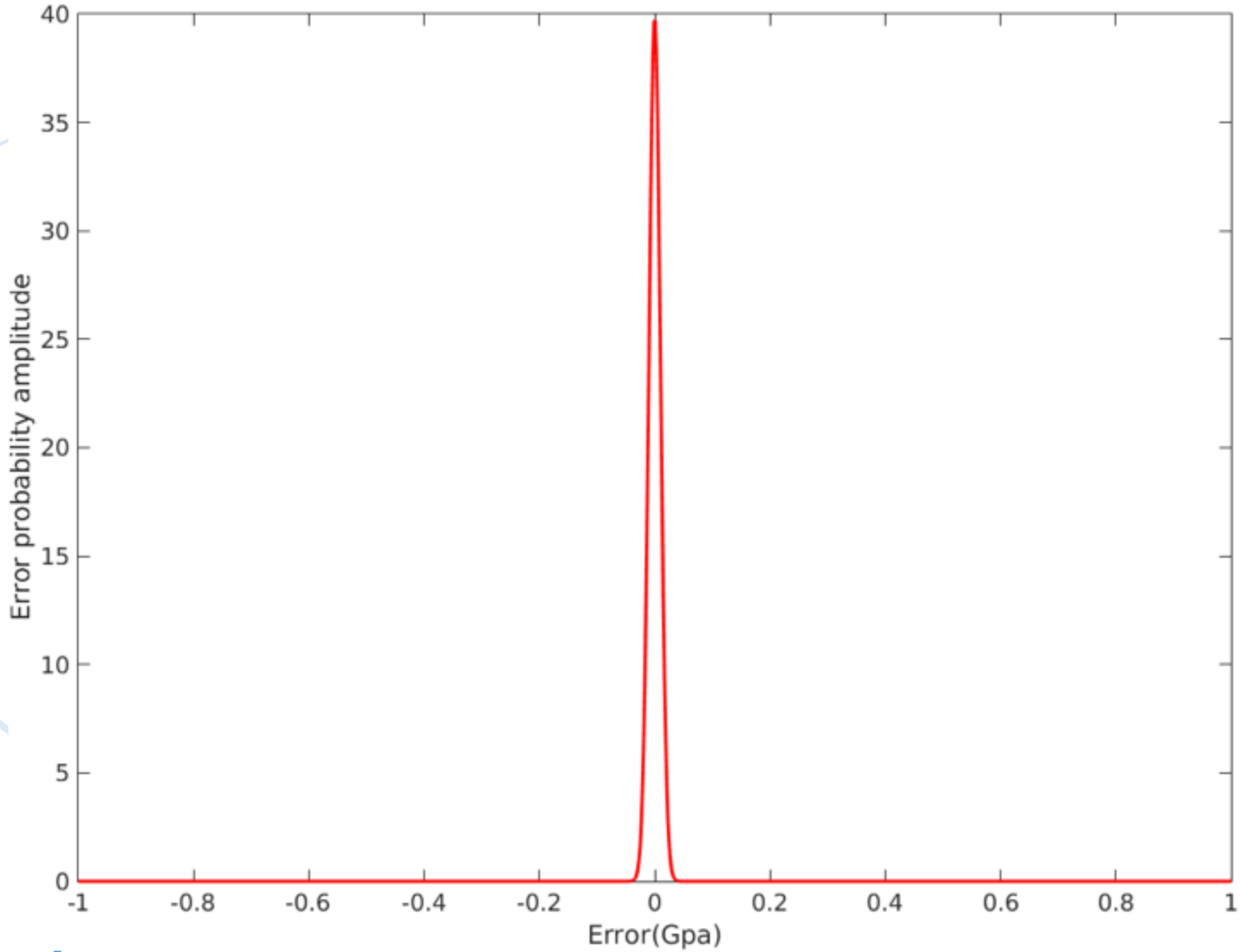

$$\pi(e)_{error} = N(0, 0.0001)$$

Likelihood function

$$\pi(y|x) = N(y - x\epsilon, 0.0001)$$

$$\pi(y|x) = \pi(\omega) = \pi(y - f(x))$$

Bayes' theorem: calculate the posterior

$$\text{posterior} = \frac{\text{prior} \times \text{likelihood}}{\text{evidence}}$$

$$\pi(x|y) = \frac{\pi(x)\pi(y|x)}{\int \pi(x)\pi(y|x)dx}$$

Bayes' theorem: calculate the posterior

$$\text{posterior} = \frac{\text{prior} \times \text{likelihood}}{\text{evidence}}$$

$$\pi(x|y) = \frac{\pi(x)\pi(y|x)}{\int \pi(x)\pi(y|x)dx}$$

prior $\pi(x)$

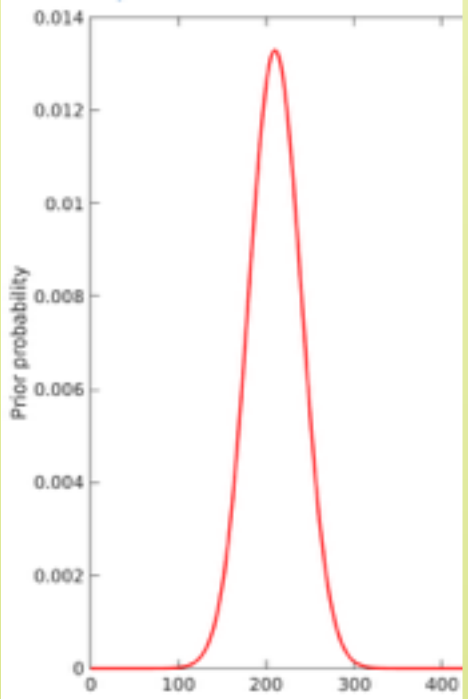

Bayes' theorem: calculate the posterior

$$\text{posterior} = \frac{\text{prior} \times \text{likelihood}}{\text{evidence}}$$

$$\pi(x|y) = \frac{\pi(x)\pi(y|x)}{\int \pi(x)\pi(y|x)dx}$$

prior $\pi(x)$

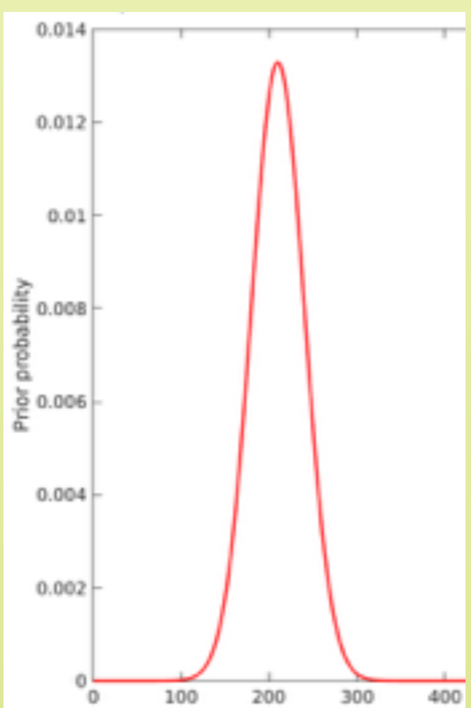

likelihood $\pi(y|x)$

$$\pi(y|x) = N(y - x\epsilon, 0.0001)$$
$$\pi(y|x) = \pi(\omega) = \pi(y - f(x))$$

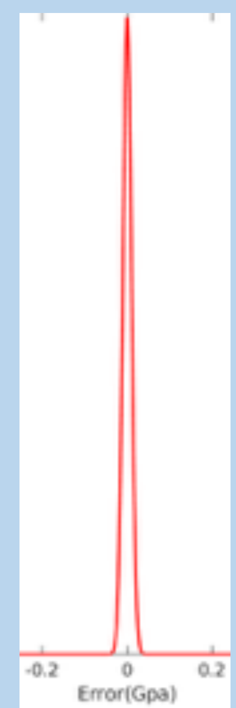

Bayes' theorem: calculate the posterior

$$\text{posterior} = \frac{\text{prior} \times \text{likelihood}}{\text{evidence}}$$

$$\pi(x|y) = \frac{\pi(x)\pi(y|x)}{\int \pi(x)\pi(y|x)dx}$$

prior $\pi(x)$

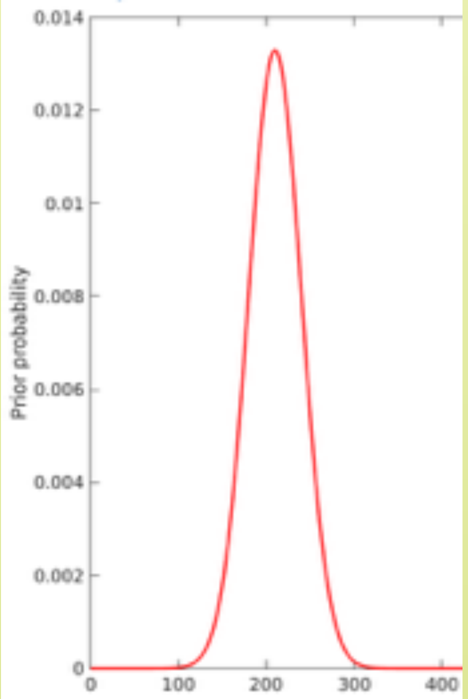

posterior

$\pi(x|y)$

likelihood $\pi(y|x)$

$$\pi(y|x) = N(y - x\epsilon, 0.0001)$$
$$\pi(y|x) = \pi(\omega) = \pi(y - f(x))$$

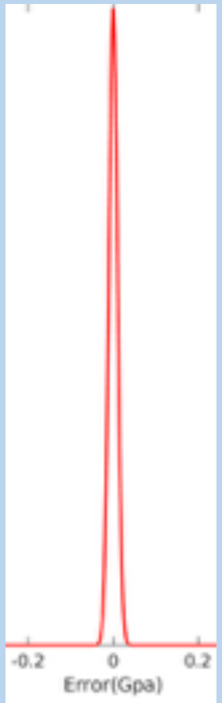

Posterior probability

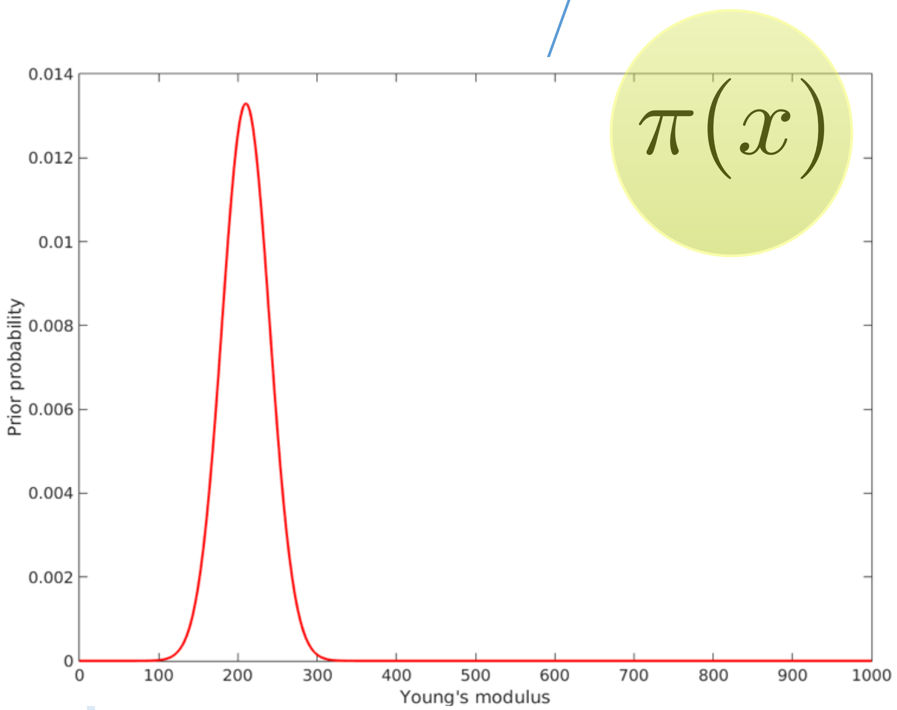

$$\pi_{prior}(x) = N(210, 900)$$

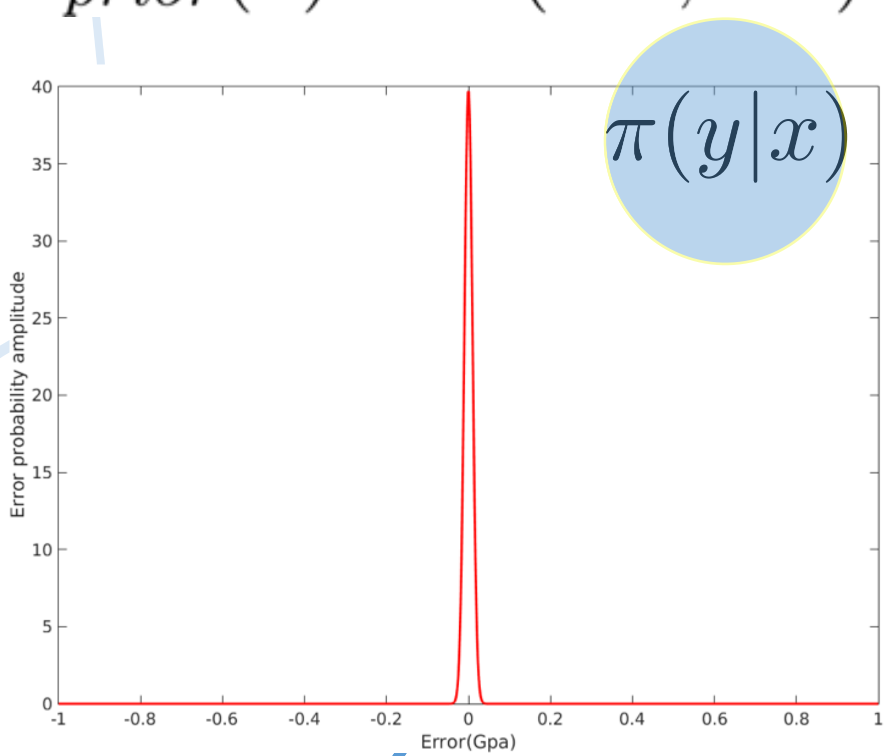

$$\pi(e)_{error} = N(0, 0.0001)$$

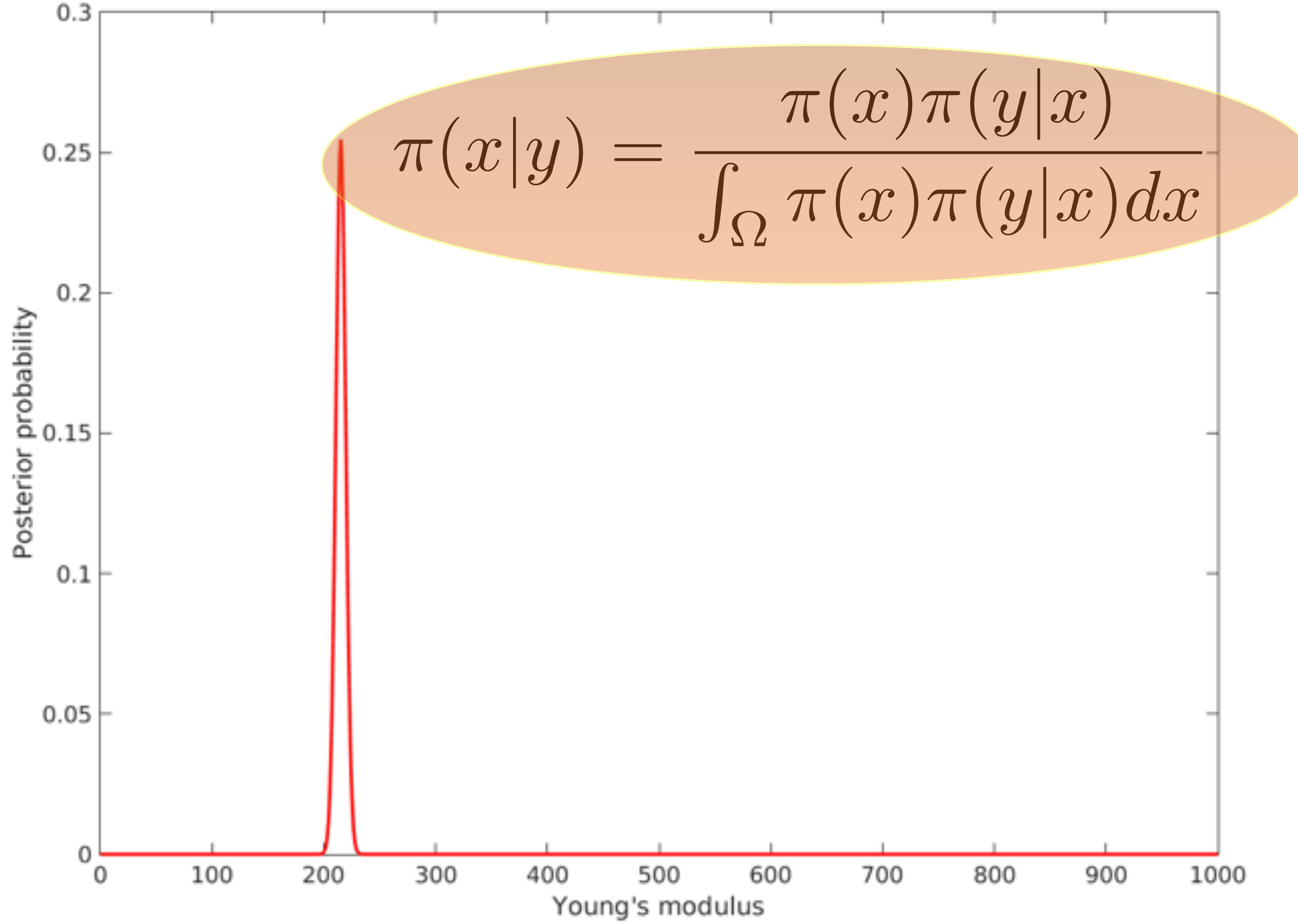

$$\pi_{posterior} = N(215.1533, 19.6168)$$

$$N_{sample} = 10$$

The 99.73% rule: observations

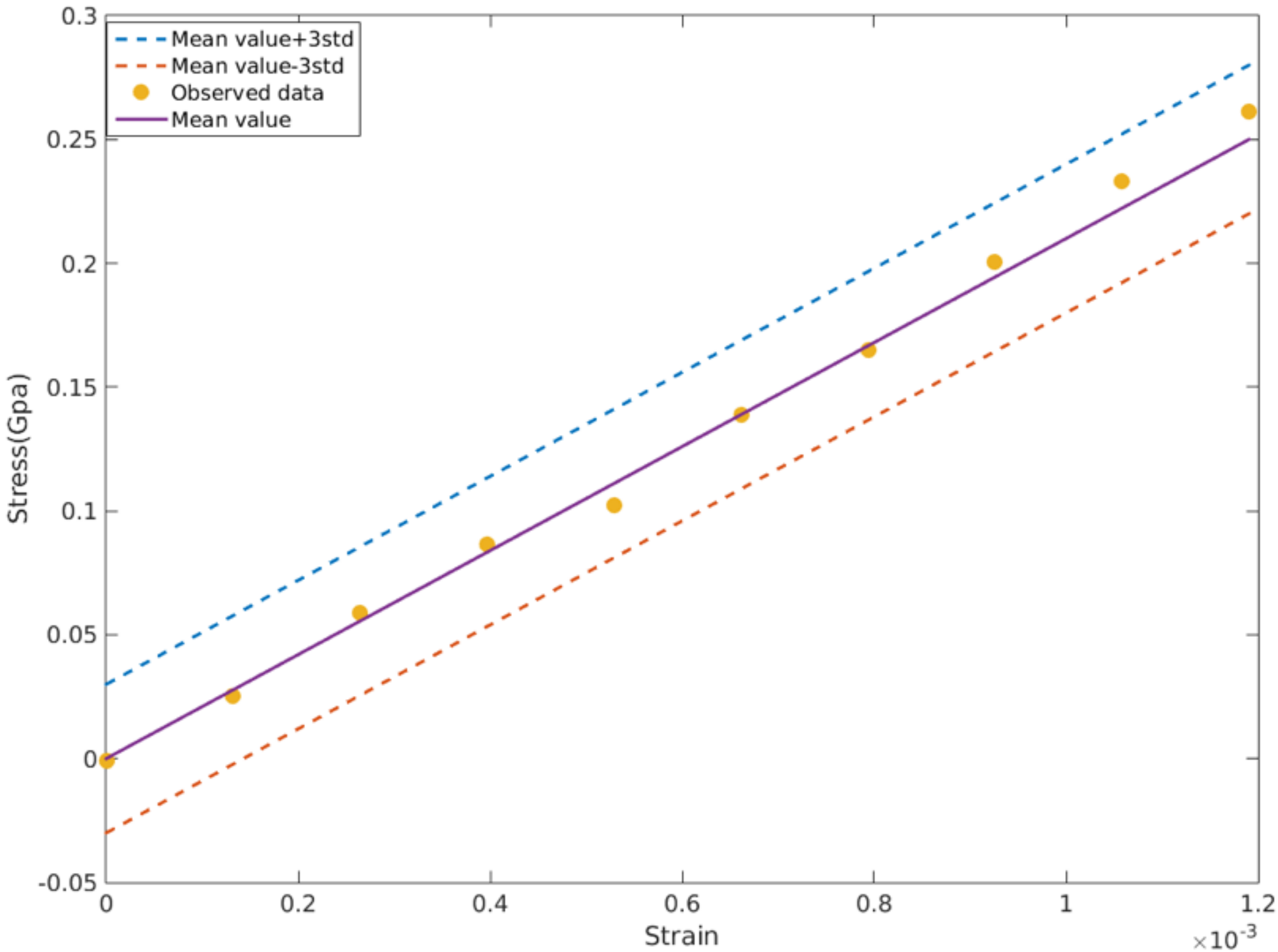

Propagation of the uncertainty to the constitutive model

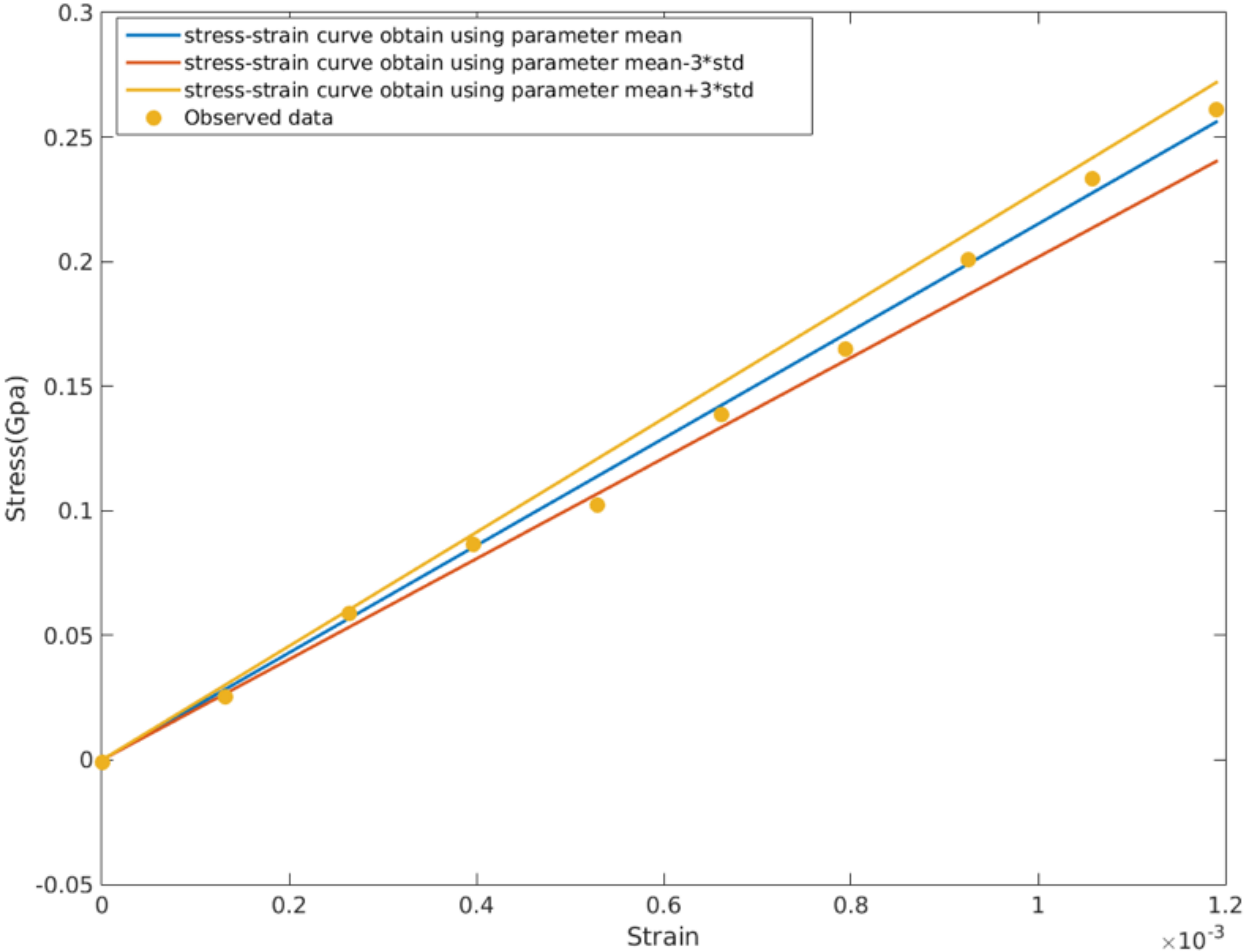

Perfect plasticity

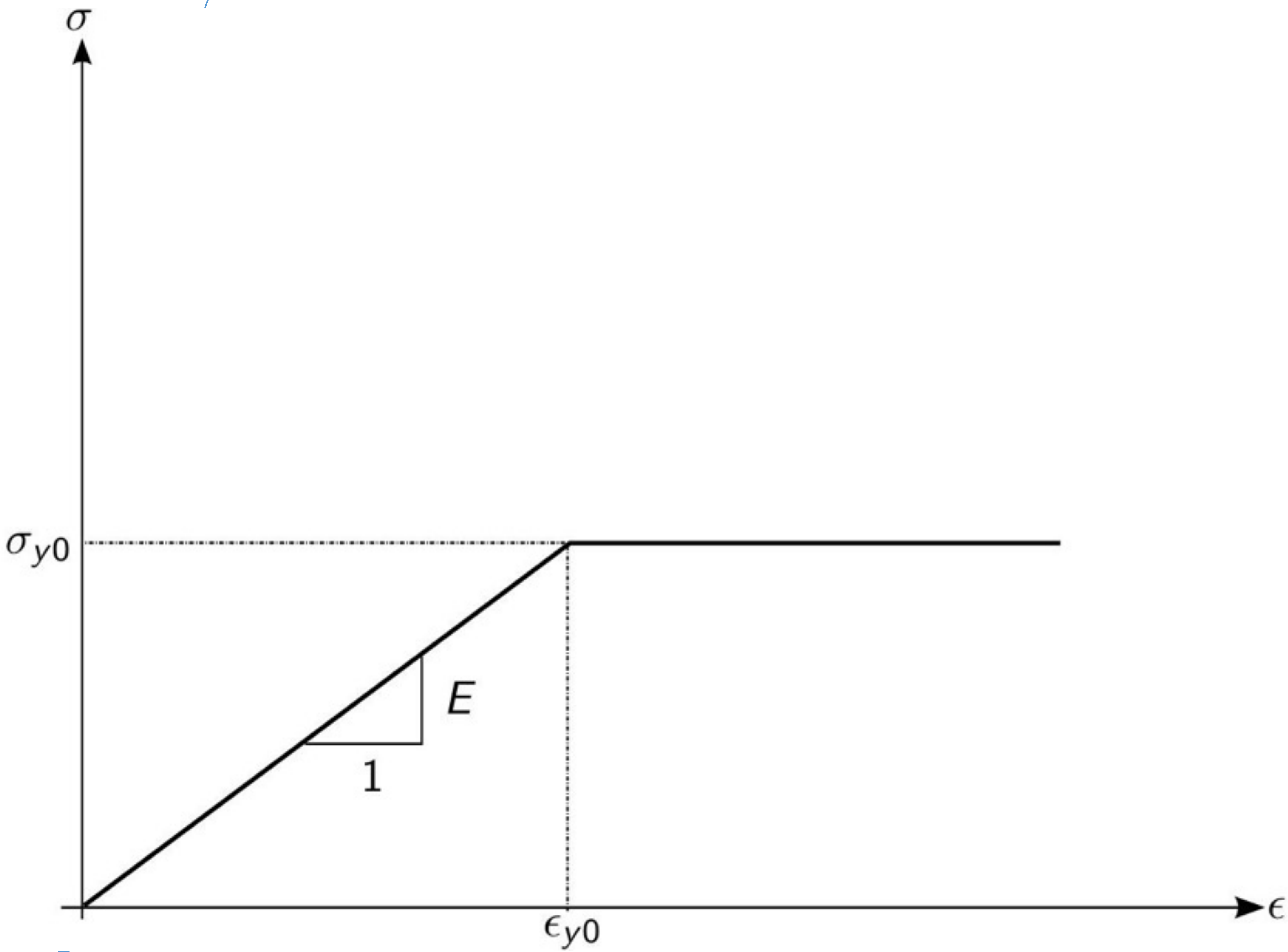

Perfect plasticity

Constitutive model

$$\sigma = \begin{cases} x(1)\epsilon & \text{if } \epsilon \leq \frac{x(2)}{x(1)} \\ x(2) & \text{if } \epsilon > \frac{x(2)}{x(1)} \end{cases} ; \; x = \left\{ \begin{array}{c} \mathrm{E} \\ \sigma_{y0} \end{array} \right\}$$

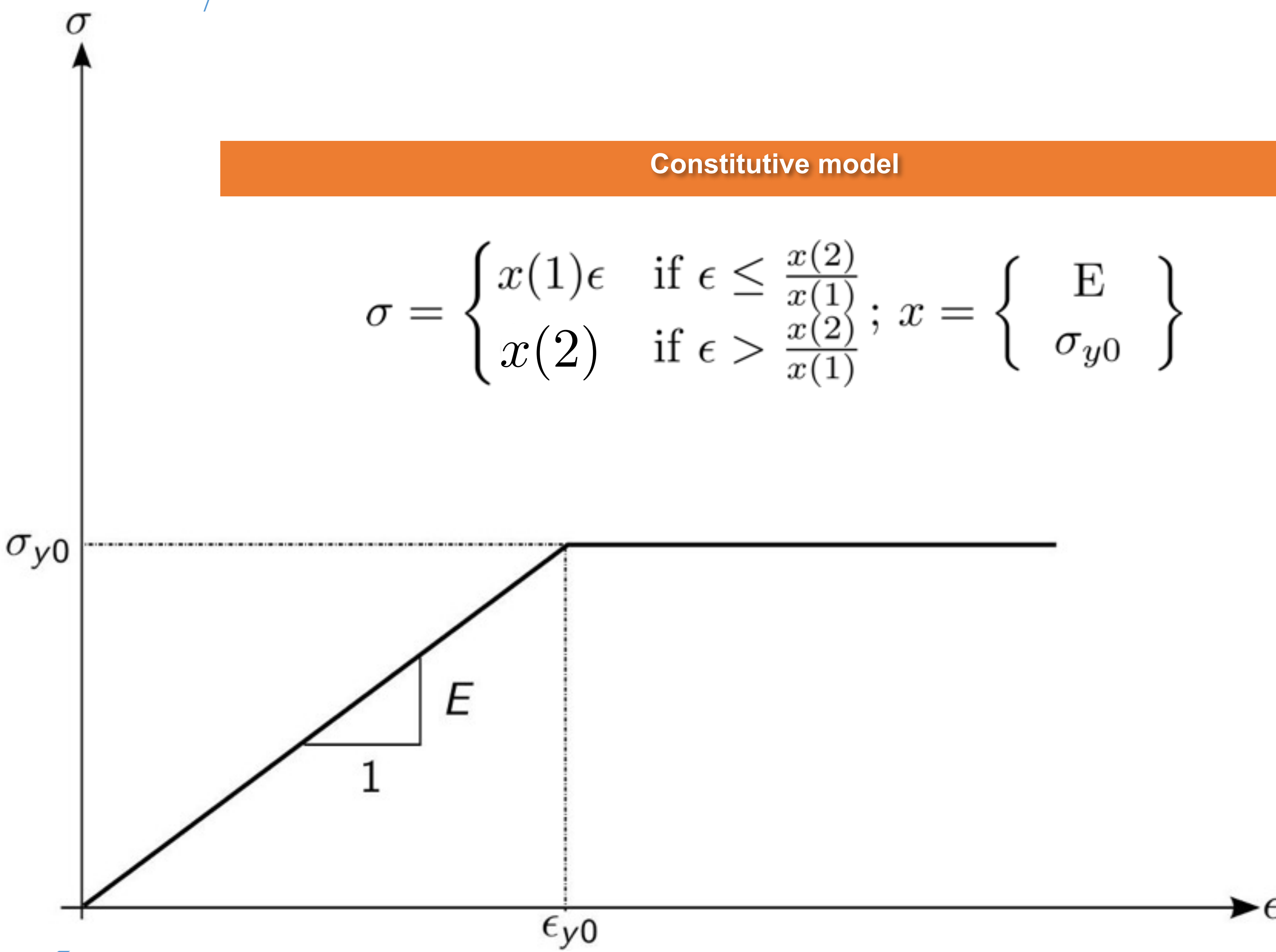

Perfect plasticity

Modified form for constitutive model

$$\sigma = x(1)\epsilon(1 - h(\sigma - x(2))) + x(2)h(\sigma - x(2))$$

$$h : \text{heaviside function}$$

Observed data

$$Y = \sigma + \Omega$$

Perfect plasticity: contour plot of prior in parameter space

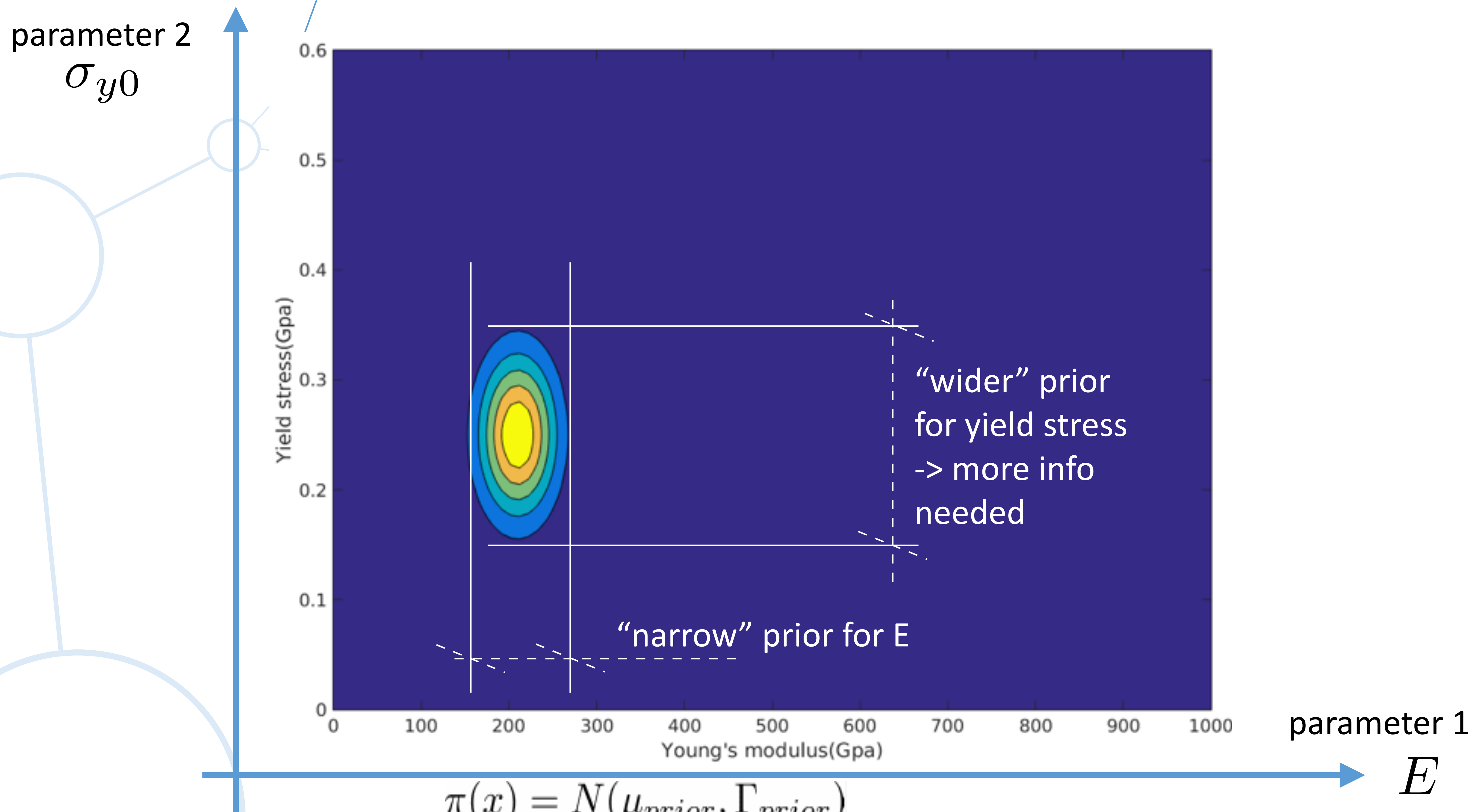

$$\pi(x) = N(\mu_{prior}, \Gamma_{prior})$$

$$\mu_{prior} = \begin{bmatrix} 210 \\ 0.25 \end{bmatrix}; \Gamma_{prior} = \begin{bmatrix} 900 & 0 \\ 0 & 0.0025 \end{bmatrix}$$

Posterior probability

$$\pi(x|y_{N_{obs}}) \propto exp\left(-\frac{1}{2}\left((x-\mu_{prior})^T\Gamma_{prior}^{-1}(x-\mu_{prior}) + \frac{\sum_{i=1}^{N_{obs}}(y_i - F_i)^2}{\sigma_\Omega^2}\right)\right)$$

σ_Ω : Error standard deviation

Posterior probability

$$(x-\mu)^2$$

$$\pi(x|y_{N_{obs}}) \propto exp\left(-\frac{1}{2}\left((x-\mu_{prior})^T\Gamma_{prior}^{-1}(x-\mu_{prior}) + \frac{\sum_{i=1}^{N_{obs}}(y_i-F_i)^2}{\sigma_\Omega^2}\right)\right)$$

σ_Ω : Error standard deviation

$$1/\sigma^2$$

likelihood for each observation

Posterior probability

stress measurement

stress model

$$(x-\mu)^2$$

$$\pi(x|y_{N_{obs}}) \propto exp\left(-\frac{1}{2}\left((x-\mu_{prior})^T\Gamma_{prior}^{-1}(x-\mu_{prior}) + \frac{\sum_{i=1}^{N_{obs}}(y_i - F_i)^2}{\sigma_\Omega^2}\right)\right)$$

σ_Ω : Error standard deviation

$$1/\sigma^2$$

likelihood for each observation

Posterior probability

stress measurement   stress model

$$(x-\mu)^2$$

$$\pi(x|y_{N_{obs}}) \propto exp\Bigg(-\frac{1}{2}\bigg((x-\mu_{prior})^T\Gamma_{prior}^{-1}(x-\mu_{prior}) + \frac{\sum_{i=1}^{N_{obs}}(y_i - F_i)^2}{\sigma_\Omega^2}\bigg)\Bigg)$$

σ_Ω : Error standard deviation

likelihood for each observation

$$1/\sigma^2$$

$$f(x|\mu,\sigma) = \frac{1}{\sigma\sqrt{2\pi}}e^{-\frac{(x-\mu)^2}{2\sigma^2}}$$

Difficult to compute the evidence probability: use MCMC

Markov-Chain Monte Carlo (MCMC) method: parameter space

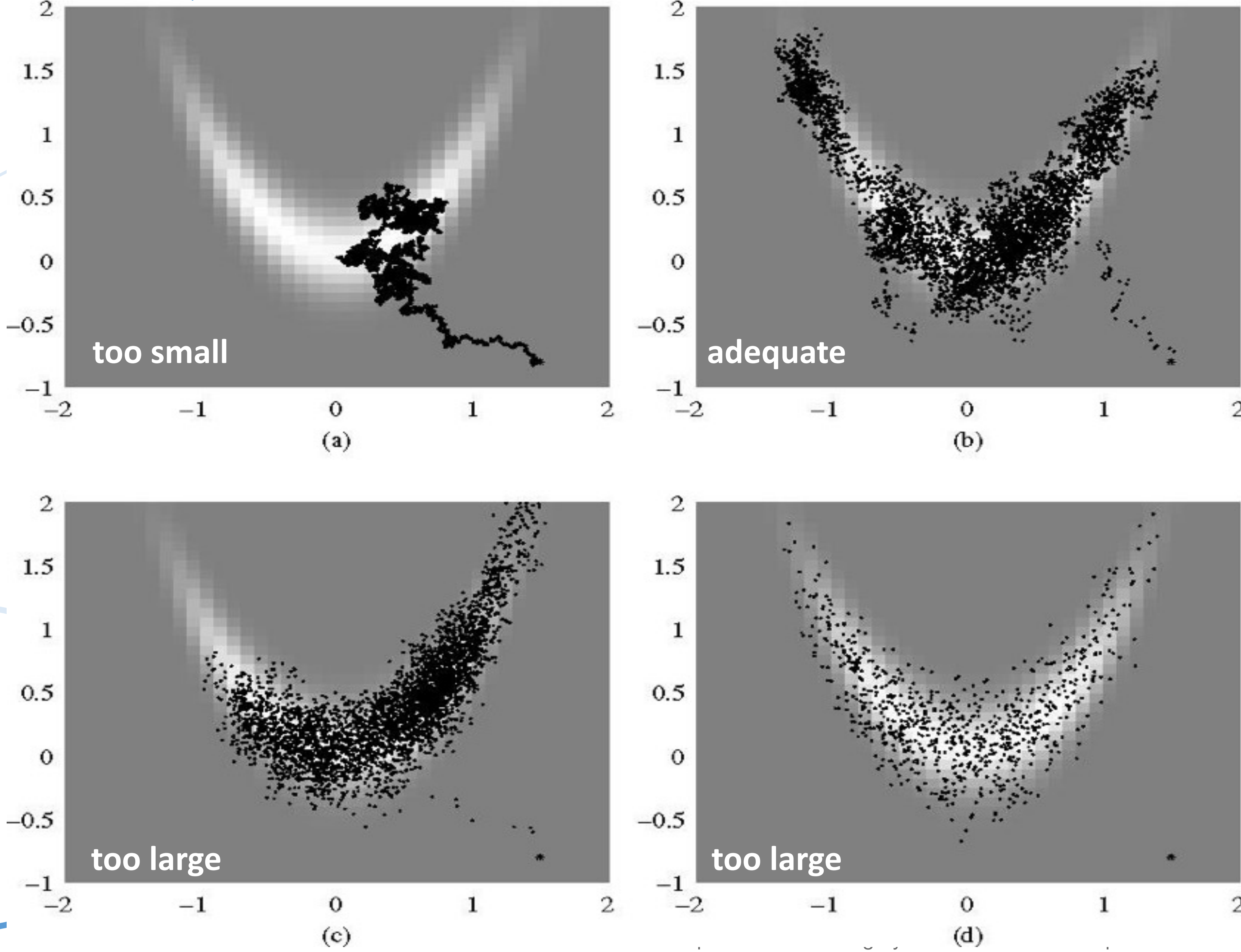

Perfect plasticity: amplitude plot

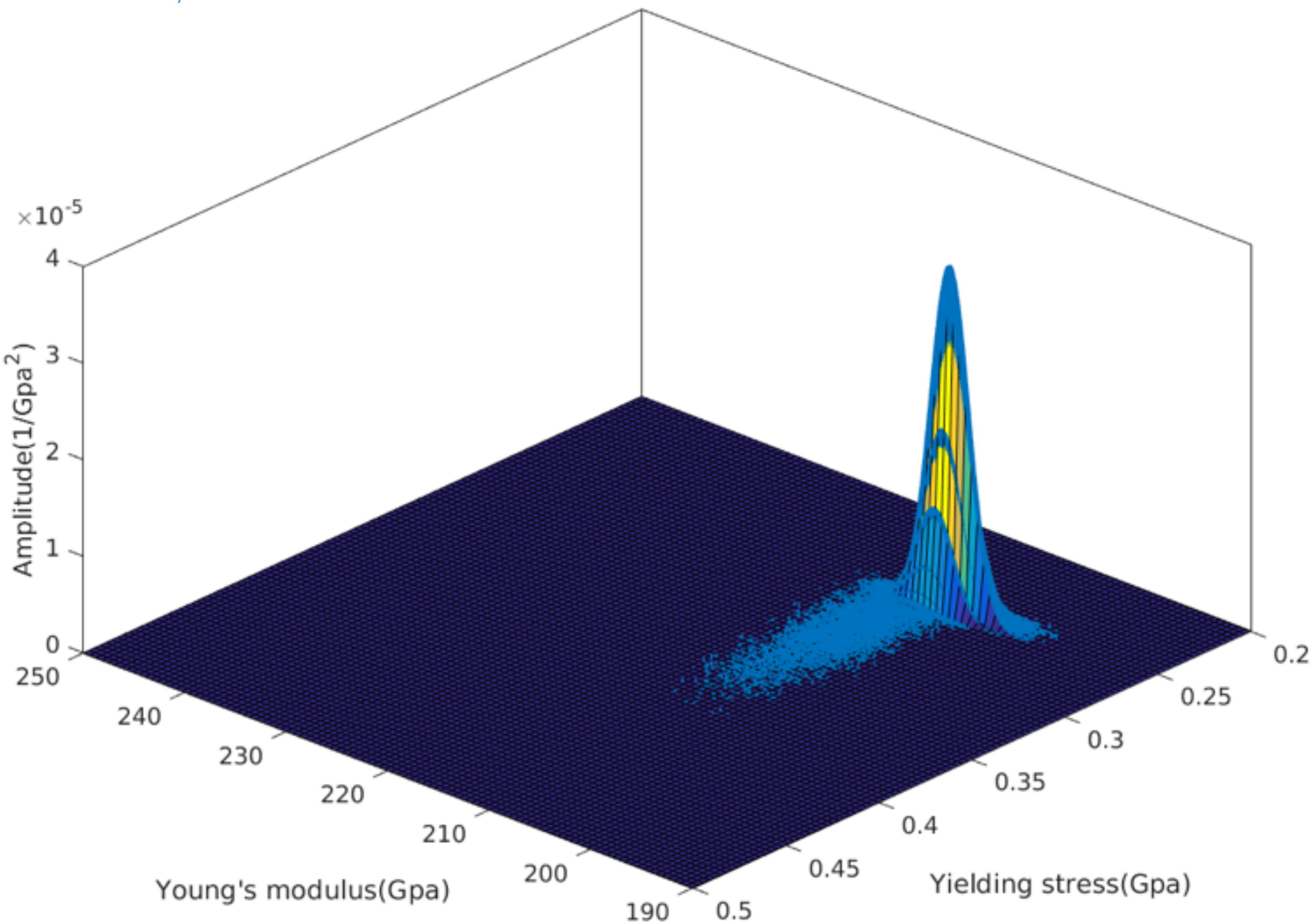

$$\mu_{posterior} = [208.6690.2603]\ ; \Gamma_{posterior} = \begin{bmatrix} 4.0918 & 0.0044 \\ 0.0044 & 0.0001 \end{bmatrix}$$

$$N_{obs} = 39$$

Application to cyst localisation

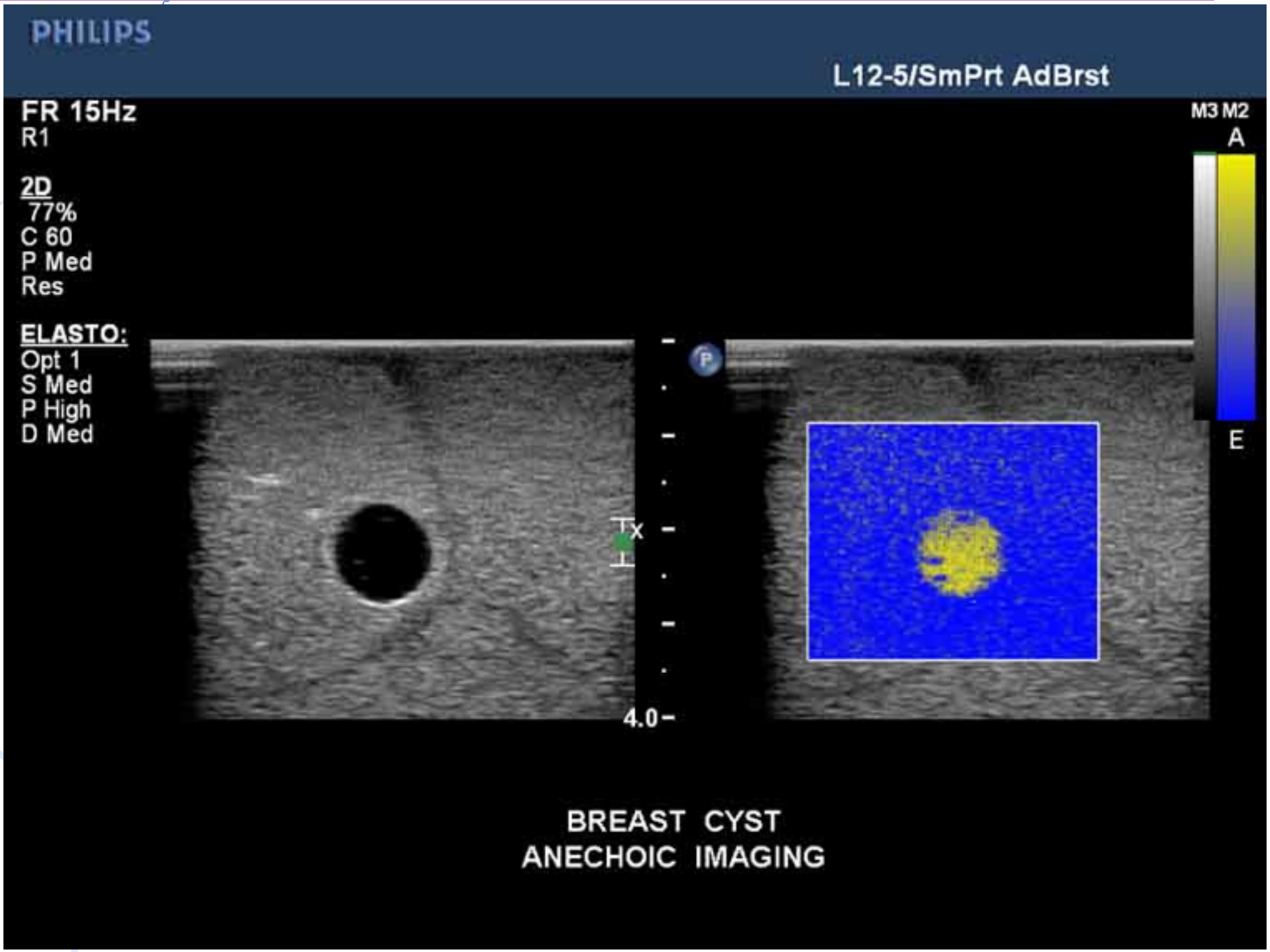

Source: Phillips

Application to cyst localisation

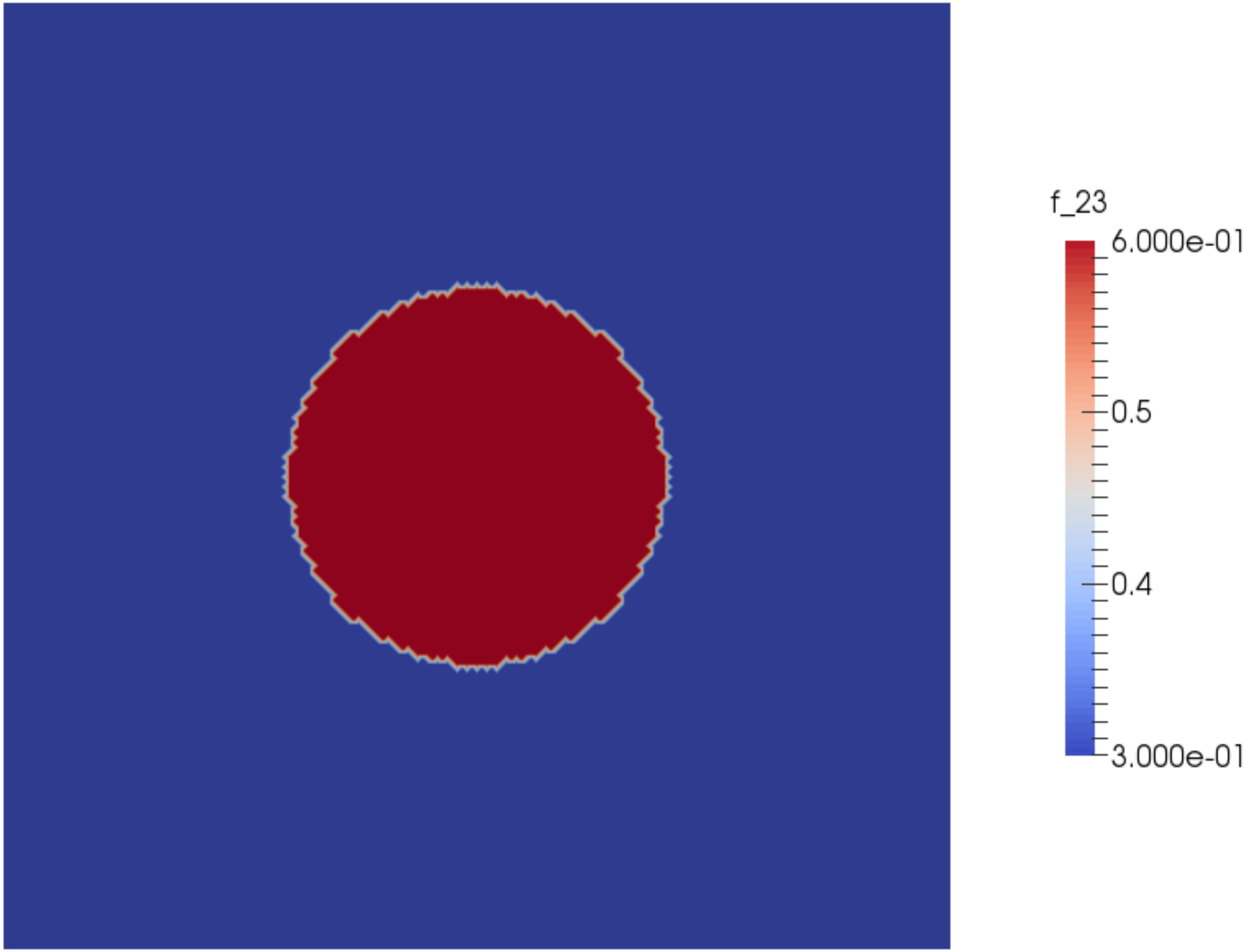

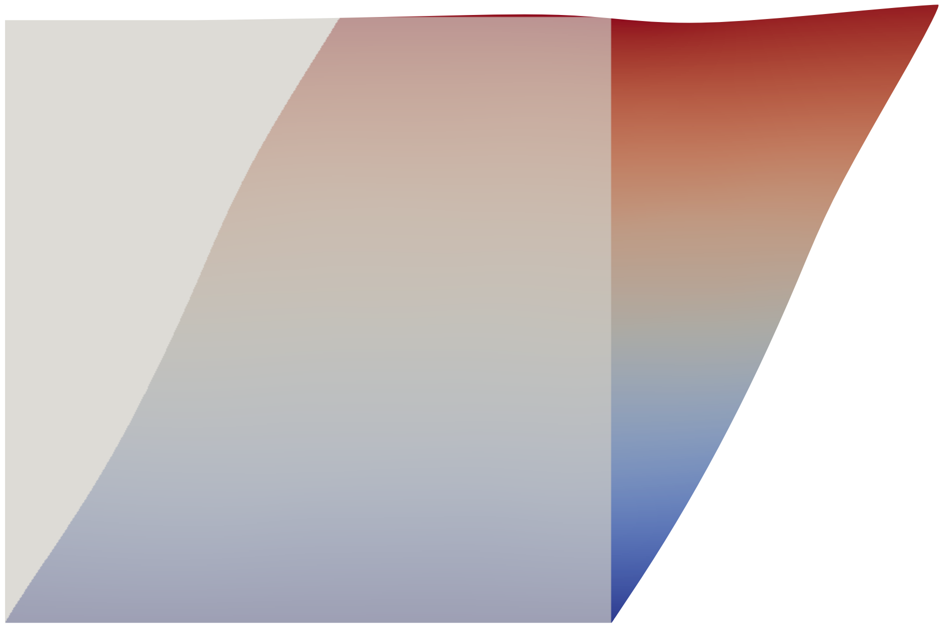

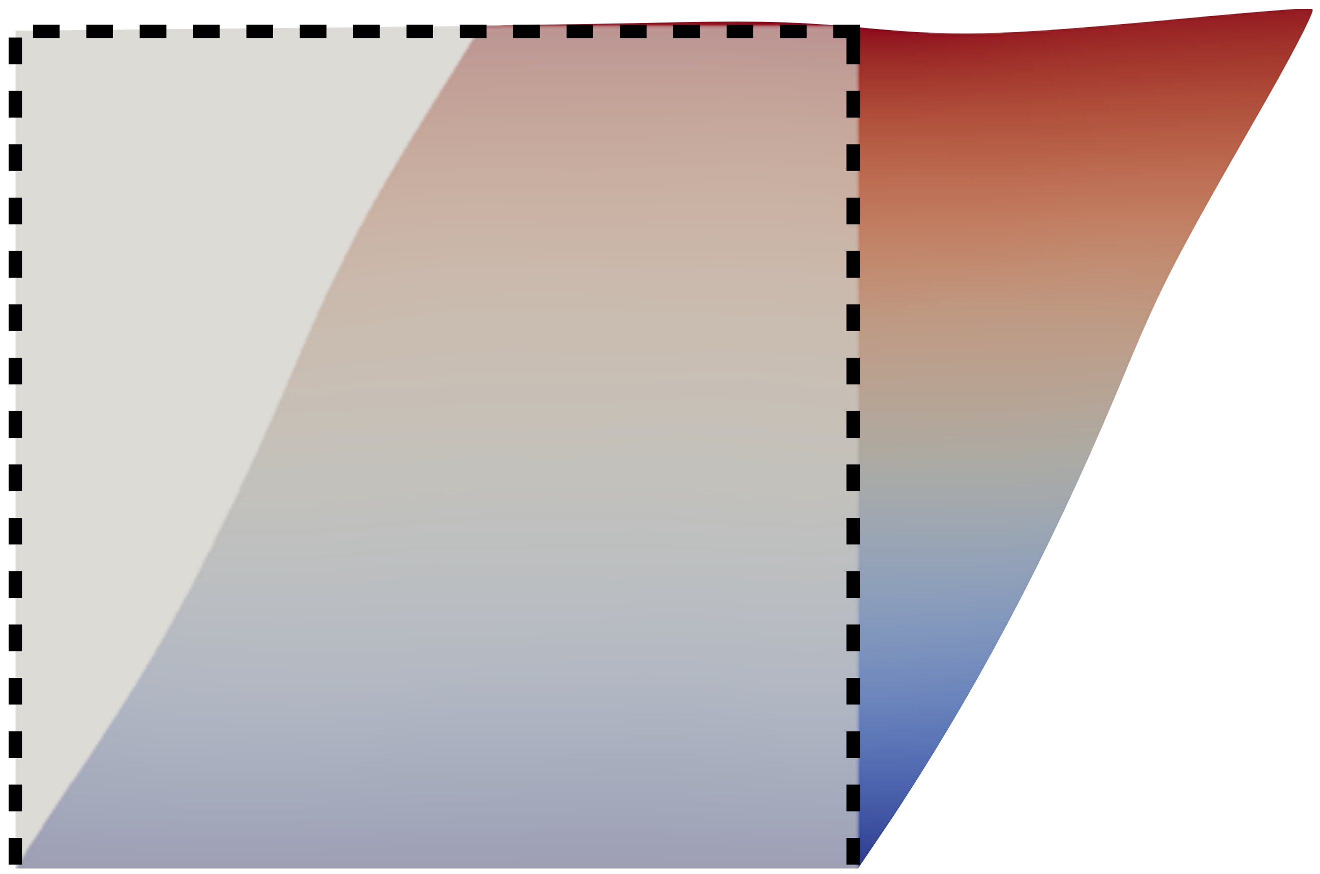

Q: What can we infer about the parameters inside the domain, just from displacement observations on the outside?

Q: Which parameters am I most uncertain about?

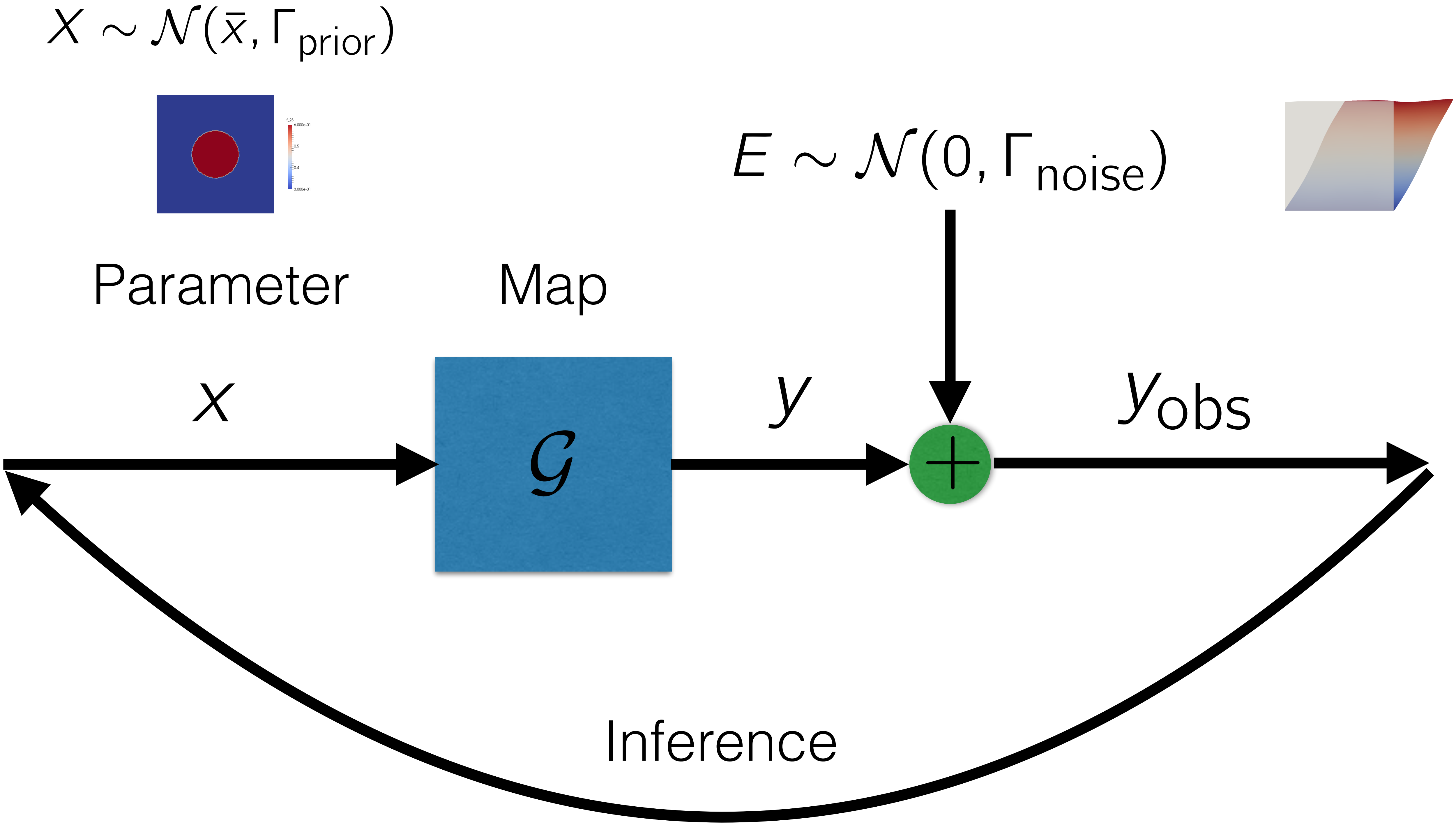

$$\pi_{\text{posterior}}(x \mid y) \propto \pi_{\text{likelihood}}(y \mid x)\pi_{\text{prior}}(x)$$

$$\pi_{\text{posterior}}(x|y) \propto \exp\left(-\frac{1}{2}||y - \mathcal{G}(u)||^2_{\Gamma^{-1}_{\text{noise}}} - \frac{1}{2}||x - \bar{x}||_{\Gamma^{-1}_{\text{prior}}}\right)$$

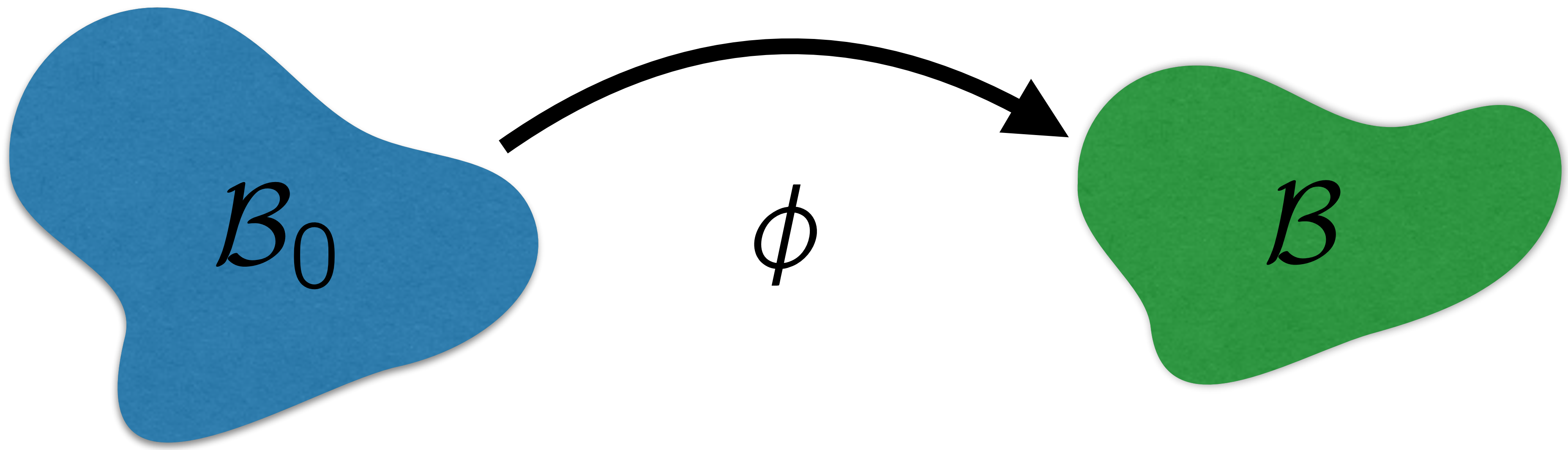

The displacements y for a given material parameter x are defined by a the minimum point of the following Lagrangian:

$$\mathcal{L}(y, x) = \int_\Omega \psi(y, x)\, dx - \int_\Gamma t \cdot y\, ds$$

where the energy density functional ψ is defined through the following equations:

$$\begin{aligned} \psi(u, x) &= \frac{x}{2}(I_C - d) - x \ln(J) + \frac{\lambda}{2} \ln(J)^2, \\ \mathbf{F} &= \frac{\partial \phi}{\partial X} = \mathbf{I} + \nabla y, \\ \mathbf{C} &= \mathbf{F}^T \mathbf{F}, \\ \mathbf{I_C} &= \mathrm{tr}(C), \\ J &= \det \mathbf{F}. \end{aligned}$$

Even once discretised (Finite Element Method)

$$\mathcal{G}_h : \mathbb{R}^n \to \mathbb{R}^m$$

$$n = 1,112,000$$

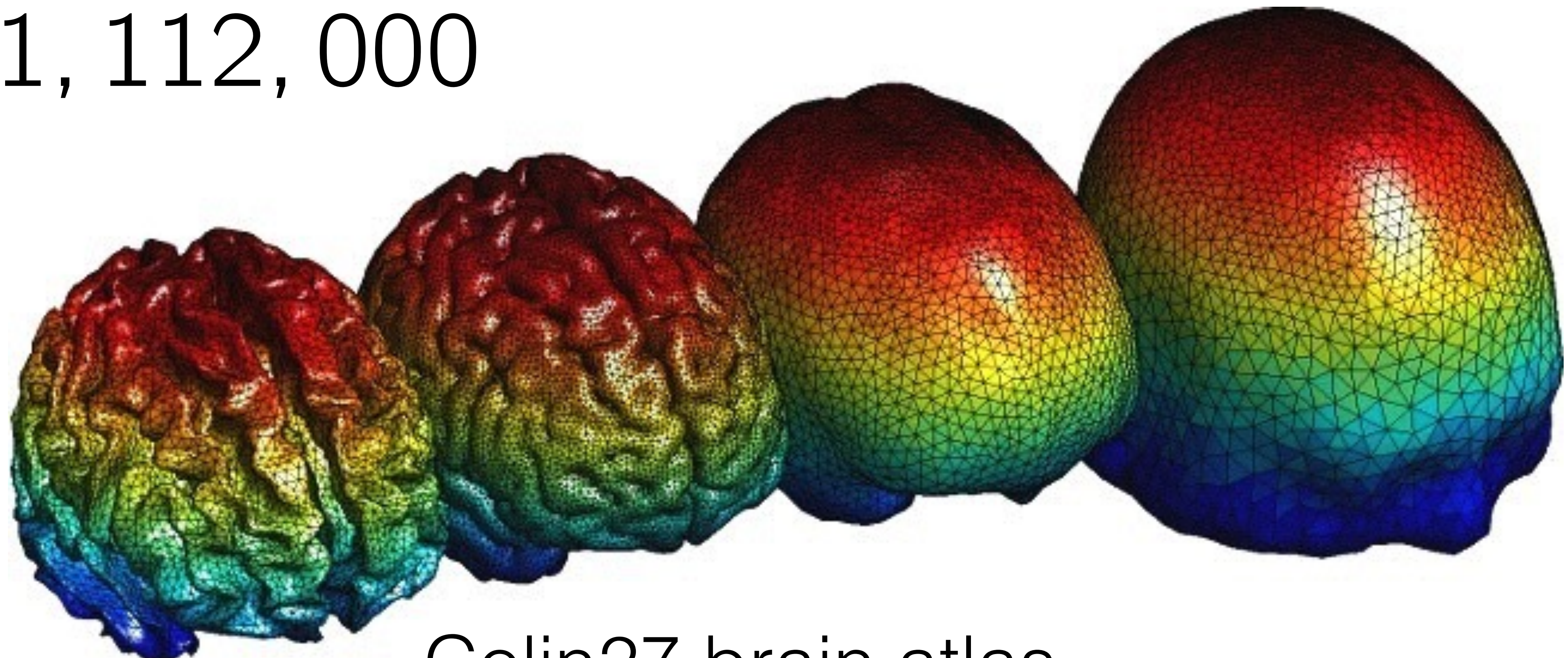

Colin27 brain atlas

20% extension test, 16 Core Xeon, 1.12 million cells, ~29 secs

on our Luxembourg Cluster

Problems

- Evaluating parameter-to-observable map is *very* expensive.
- Discretised parameter space can be *very* large.
- *Outcome:* Exploring posterior with ‘traditional sampling’ is not going to work.

Solutions

1. Connect Bayesian approach to ideas from classical optimisation. Using derivatives of posterior in parameter-space (Girolami).

2. Exploiting low-rank structure of prior to posterior covariance updates (Flath 2012, Spantini 2015).

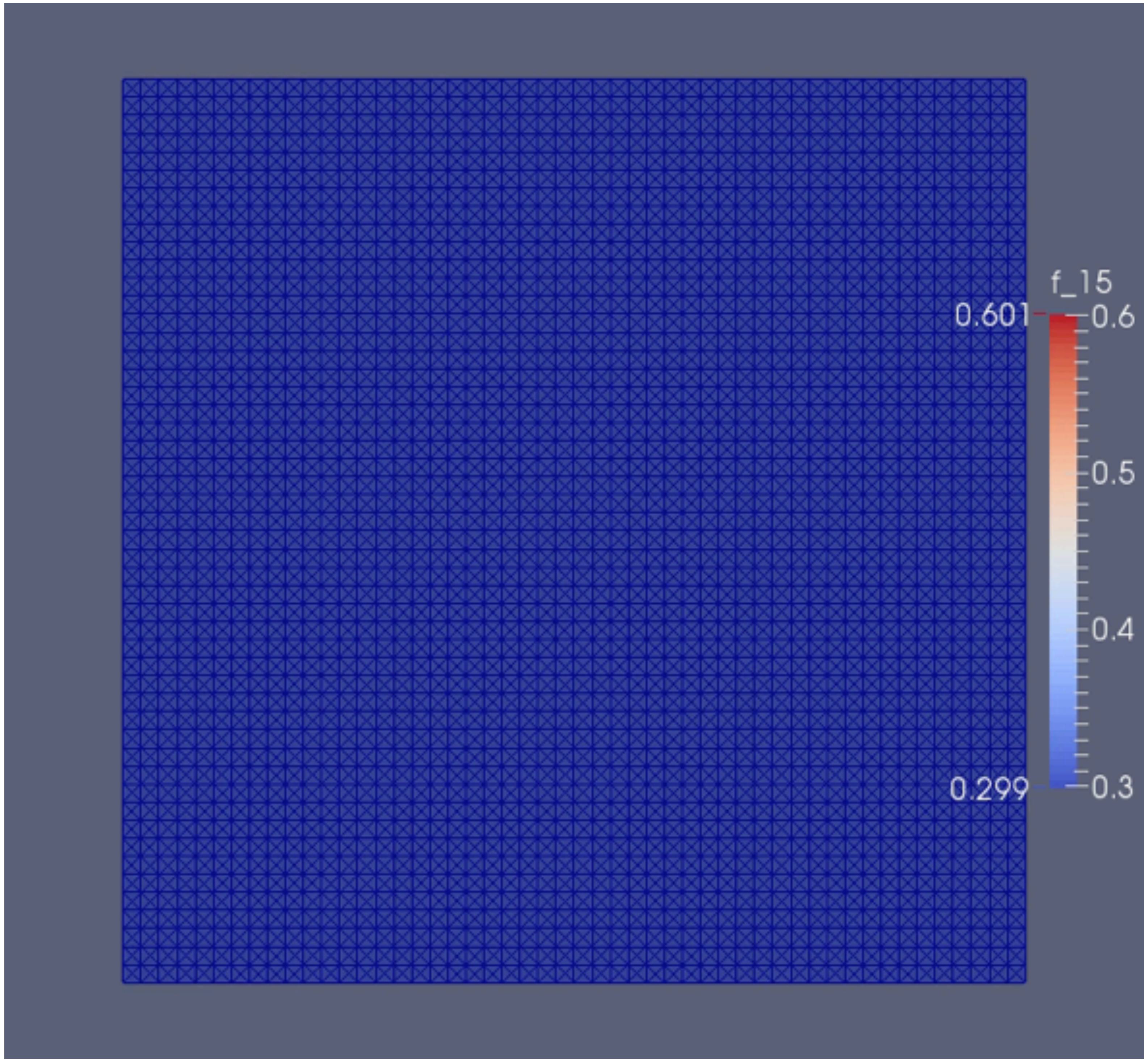

MAP estimate. Bound-constrained Quasi-Newton BLMVM with More-Thuente line search and ‘correct’ Riesz map.

Tools

- The FEniCS Project is collection of free software for the automated, efficient solution of differential equations using the finite element method.

- dolfin-adjoint automatically derives the discrete adjoint, tangent linear and higher-order adjoint models from a high-level description of the forward model.

http://fenicsproject.org

Wells, Logg, Rognes, Kirby and many, many others…

http://www.dolfin-adjoint.org

Farrell, Funke, Ham and Rognes.
2015 Wilkinson Prize for Numerical Software.

The displacements y for a given material parameter x are defined by a the minimum point of the following Lagrangian:

$$\mathcal{L}(y, x) = \int_\Omega \psi(y, x)\, dx - \int_\Gamma t \cdot y\, ds$$

where the energy density functional ψ is defined through the following equations:

$$\psi(u, x) = \frac{x}{2}(I_c - d) - x \ln(J) + \frac{\lambda}{2}\ln(J)^2,$$
$$\mathbf{F} = \frac{\partial \phi}{\partial X} = \mathbf{I} + \nabla y,$$
$$\mathbf{C} = \mathbf{F}^T\mathbf{F},$$
$$\mathbf{I_C} = \mathrm{tr}(C),$$
$$J = \det\mathbf{F}.$$

```
from dolfin import *
mesh = UnitSquareMesh(32, 32)

U = VectorFunctionSpace(mesh, "CG", 1)
V = FunctionSpace(mesh, "CG", 1)
# solution
u = Function(U)
# test functions
v = TestFunction(U)
# incremental solution
du = TrialFunction(U)
x = interpolate(Constant(1.0), V)
lmbda = interpolate(Constant(100.0), V)

dims = mesh.type().dim()
I = Identity(dims)
F = I + grad(u)
C = F.T*F
J = det(F)
Ic = tr(C)
```

```
phi = (x/2.0)*(Ic - dims) - x*ln(J) + (lmbda/
2.0)*(ln(J))**2
Pi = phi*dx
# gateaux derivative with respect to u in
direction v
F = derivative(Pi, u, v)
# and with respect to u in direction du
J = derivative(F, u, du)

u_h = Function(U)
F_h = replace(F, {u: u_h})
J_h = replace(J, {u: u_h})
solve(F_h == 0, u_h, bcs, J=J_h)
```

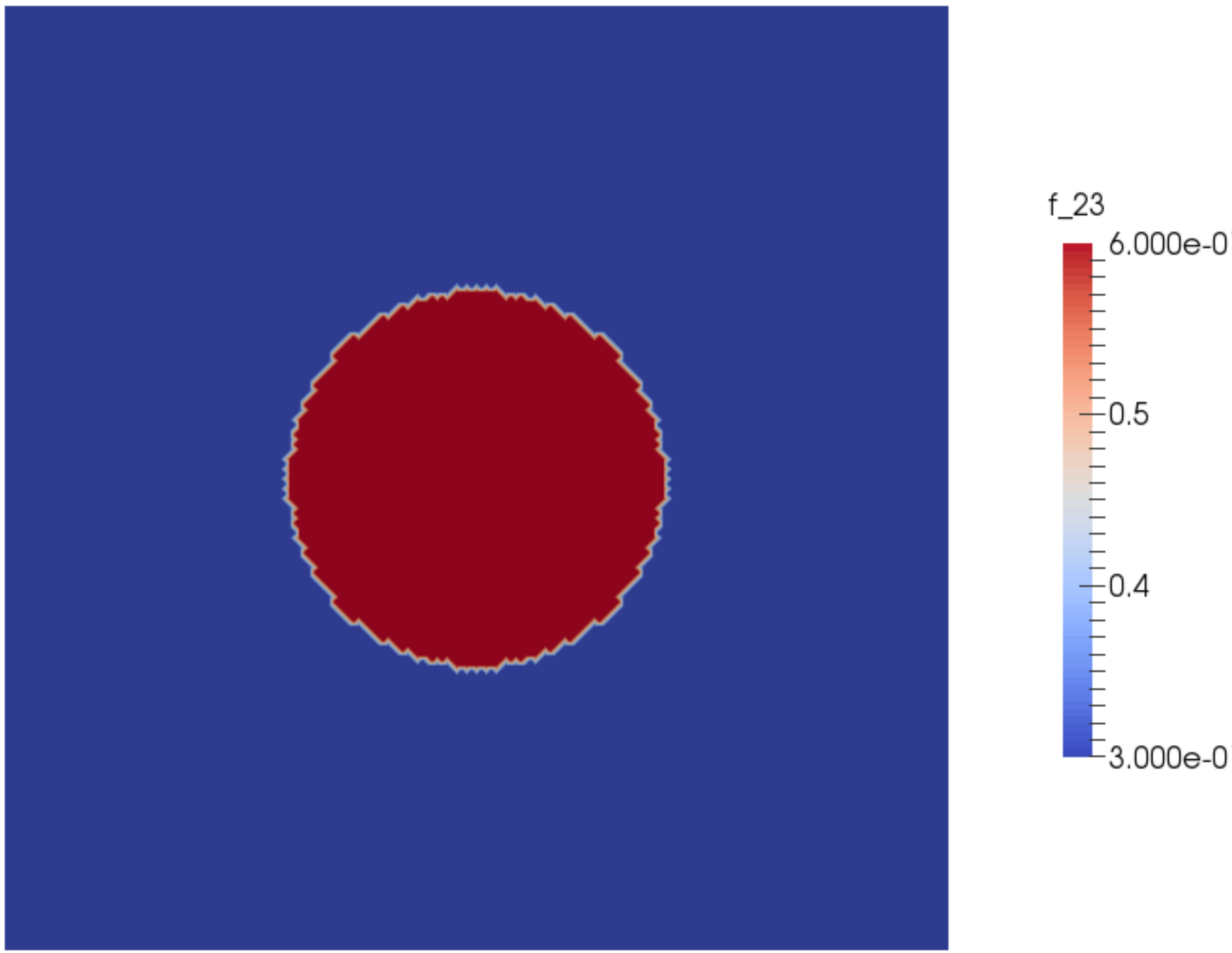
f_23
6.000e-01
0.5
0.4
3.000e-01

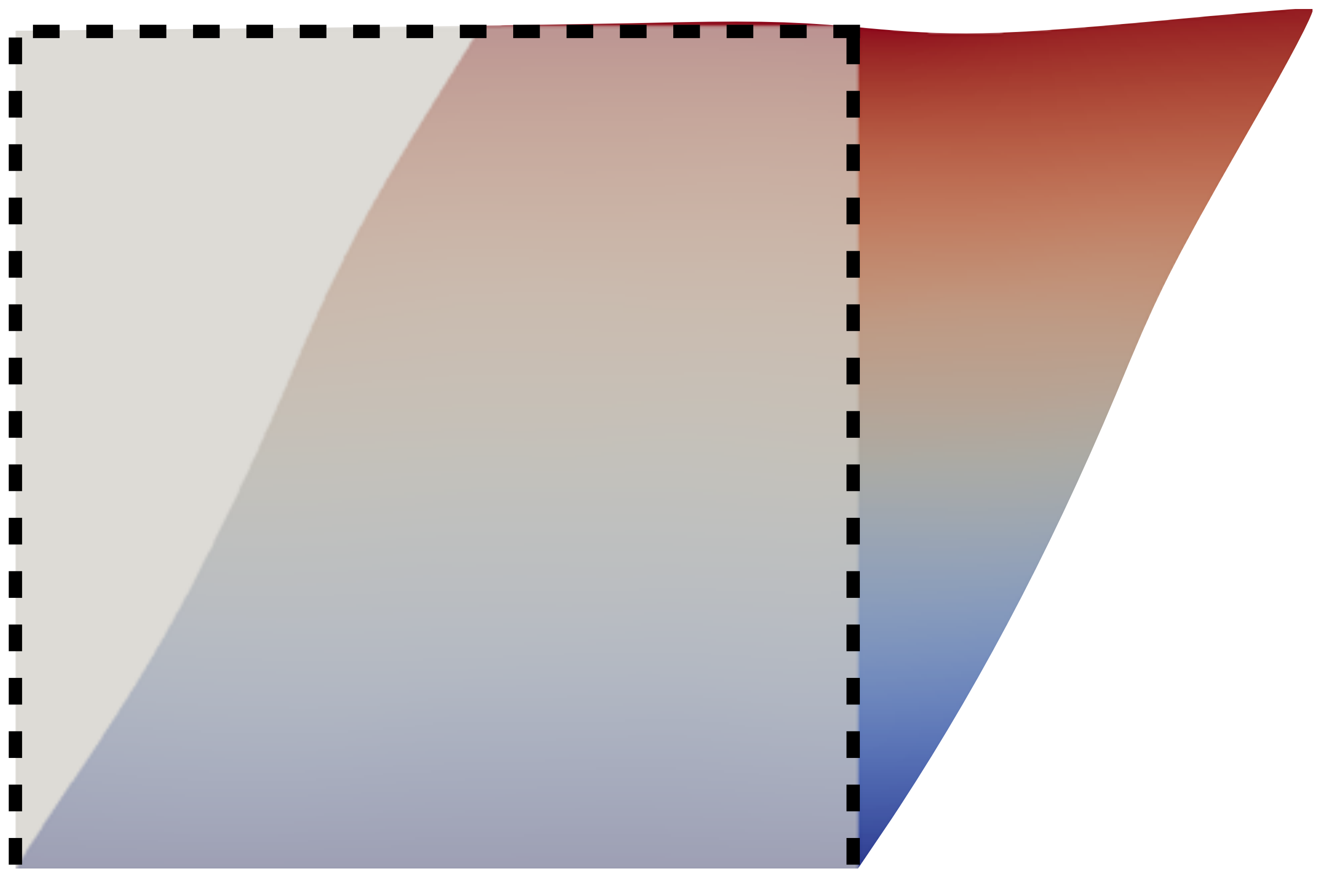

Q: What can we infer about the parameters inside the domain, just from displacement observations on the outside?

Q: Which parameters am I most uncertain about?

Trailing Eigenvector

Direction in parameter space *least* constrained by the observations

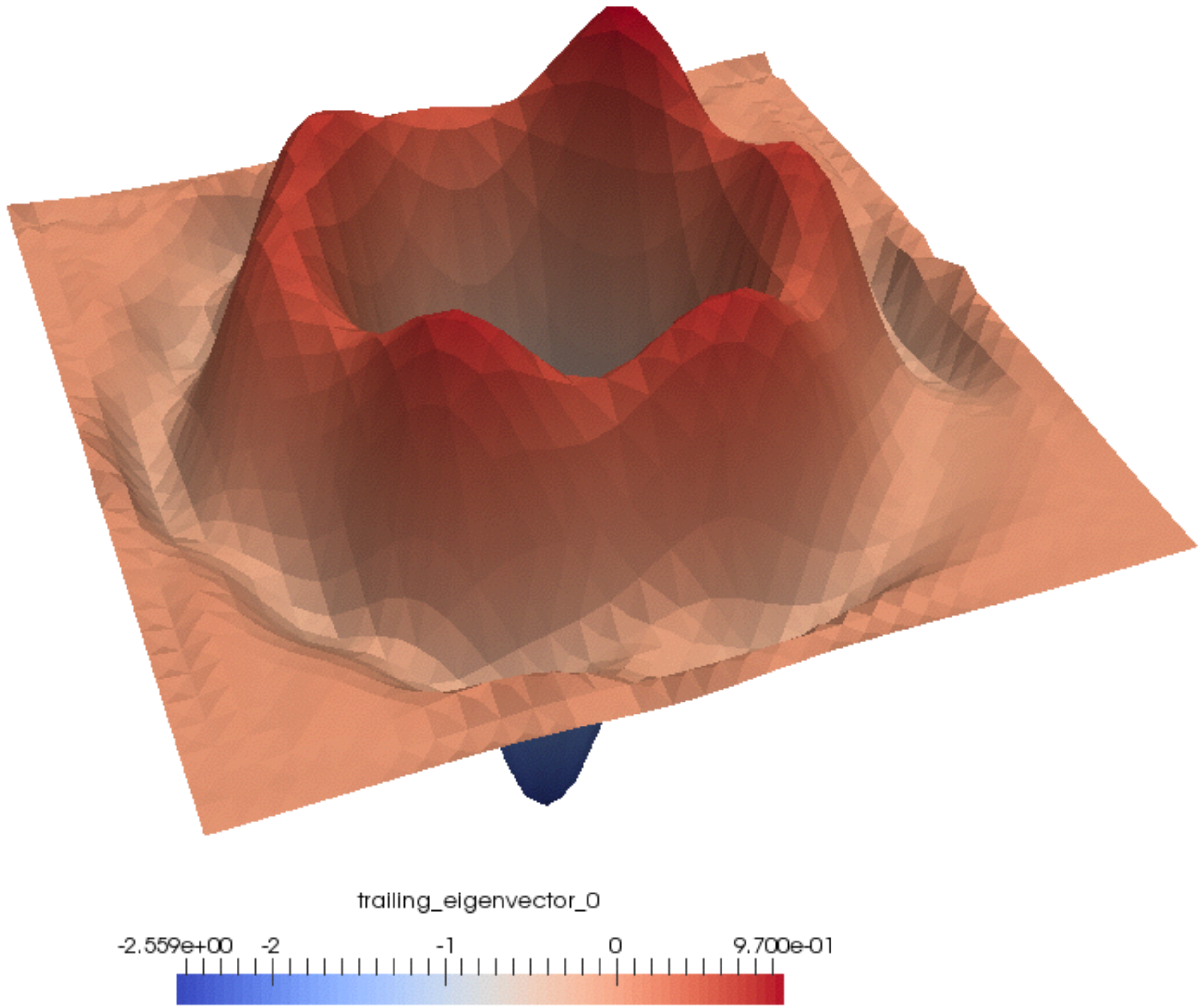
trailing_eigenvector_0
-2.559e+00
-2
-1
0
9.700e-01

Leading Eigenvectors

Direction in parameter space *most* constrained by the observations


leading_eigenvector_0
1.250e+01
10
0
-10
-1.371e+01


leading_eigenvector_1
1.405e+01
10
0
-10
-1.377e+01

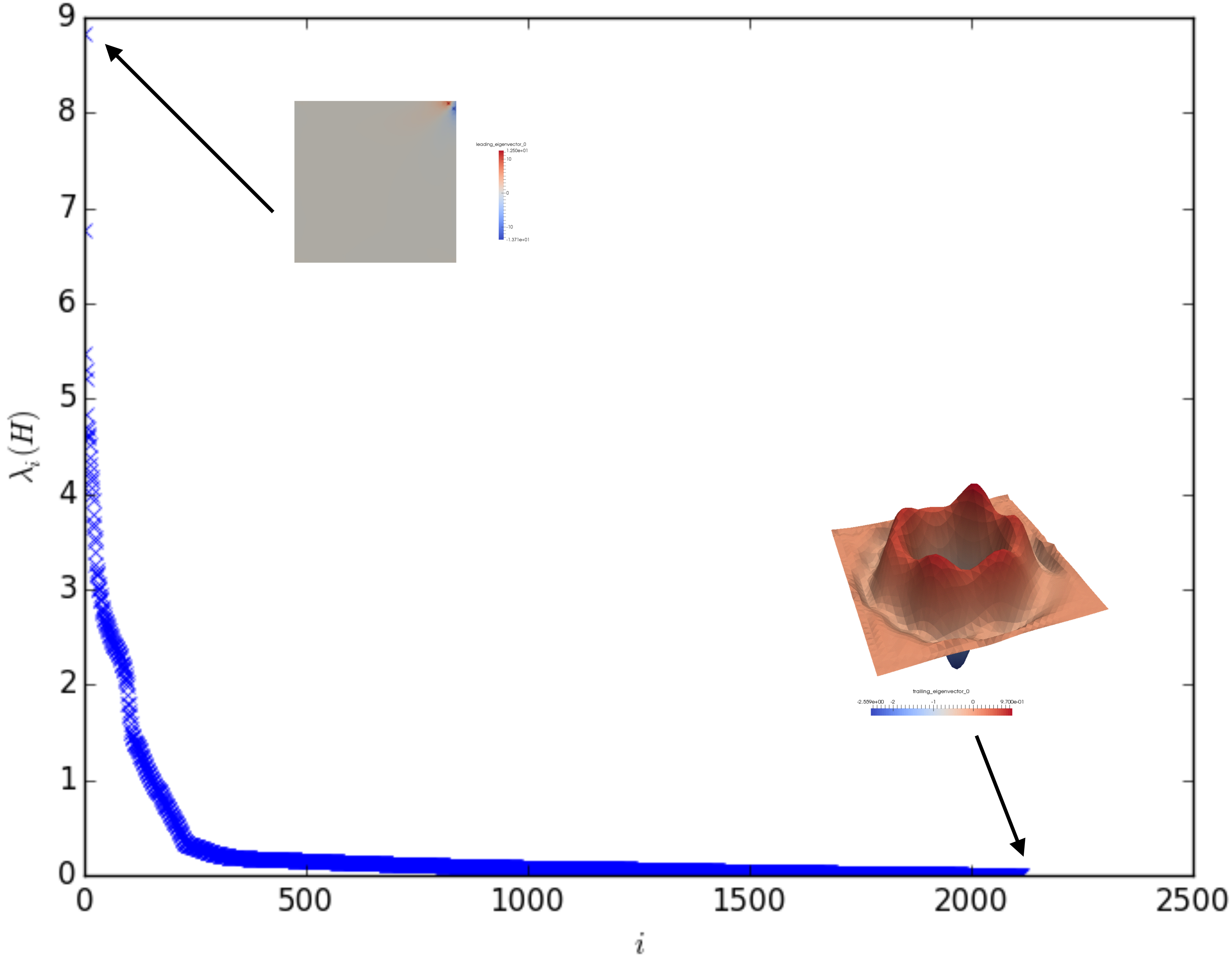

9
8
7
6
5
4
3
2
1
0
$\lambda_i(H)$
0
500
1000
1500
2000
2500
i

Full Hessian.
4000+ actions.

Low-rank update.
292 actions.

Huge savings in computational cost.
Scales with model dimension because *observations* stay the same.

Bayesian approach: summary

- Quantify and propagate uncertainties
- Select the “best” model (Bayes factor)
- Identify parameters for these models
- Assimilate experimental or other numerical data
- Which parameters are we most uncertain about?
- What additional data would reduce uncertainty?